

Co-Transport of mRNA and ER in *Saccharomyces cerevisiae*

Dissertation

der Mathematisch-Naturwissenschaftlichen Fakultät
der Eberhard Karls Universität Tübingen
zur Erlangung des Grades eines
Doktors der Naturwissenschaften
(Dr. rer. nat.)

vorgelegt von
Dipl.- Biol. Julia Fundakowski
aus Chemnitz

Tübingen
2012

Tag der mündlichen Qualifikation:

13.09.2012

Dekan:

Prof. Dr. Wolfgang Rosenstiel

1. Berichterstatter:

Prof. Dr. Ralf-Peter Jansen

2. Berichterstatter:

Prof. Dr. Doron Rapaport

Table of contents

1 Introduction.....	1
1.1 Budding yeast.....	1
1.2 Intracellular transport.....	4
1.3 mRNA localization	5
1.4 mRNA localization in yeast <i>S. cerevisiae</i>	7
1.4.1 Zipcodes - specification elements for localization processes	9
1.4.2 <i>Trans</i> -acting factors: the mRNA localization machinery.....	13
1.4.2.1 The locasome	13
1.4.2.1.1 She2p, the RNA-binding protein	15
1.4.2.1.2 Myo4p, the motor protein.....	17
1.4.2.1.3 She3p, adaptor and RNA-binding protein.....	18
1.4.2.2 Puf6p, Khd1p, Loc1p	19
1.5 Inheritance of cortical endoplasmic reticulum in <i>S. cerevisiae</i>	21
1.5.1 Function of the ER	21
1.5.2 Inheritance of the ER	23
1.6 Reticulons	27
1.7 Indications for the co-transport of mRNA and ER in <i>S. cerevisiae</i>	29
1.8 Aim of this work including experimental background.....	33
1.8.1 Visualization of mRNPs.....	34
1.8.2 mRNAs of interest.....	34
2 Results.....	37
2.1 ER morphology of yeast mutants	37
2.2 Myo4p as control protein used for studying mutants affecting mRNP transport	41
2.3 Deletion of <i>AUX1</i> affects localization of <i>WSC2</i> , <i>IST2</i> , <i>SRL1</i> and <i>EAR1</i> mRNAs but not <i>ASH1</i> mRNA	44
2.4 Deletion of J-domain of Aux1p affects mRNP localization.....	51

Table of contents

2.5 Deletion of <i>Slf2p</i> and <i>Scs2p</i> only perturbs localization of a subset of mRNAs	54
2.6 Deletion of <i>Ptc1p</i> has no effect in mRNP localization of <i>EAR1</i> , <i>IST2</i> , <i>MID2</i> , <i>SRL1</i> and <i>WSC2</i> mRNA	57
2.7 Localization of early expressed mRNAs requires tubular ER transport and the exocyst component <i>Sec3p</i>	58
2.8 Knockout of <i>YOP1</i> together with <i>RTN1</i> or <i>SEY1</i> leads to affected RNP transport while single knockout has no effect	61
2.9 Loss of <i>Yop1p</i> alters RNP localization efficiency at early stages of cell growth	63
2.10 Co-visualization of ER structures and mRNPs	65
2.11 RNP particle localization of <i>WSC2</i> is independent of its translation	69
2.12 Biochemical analysis	70
2.12.1 Oligomerization of <i>She2p</i> is required for ER association	70
2.12.2 Characterization of the association of <i>She2p</i> and ER	76
3 Discussion	81
3.1 New model for mRNP trafficking in yeast - early versus late transport strategies	92
4 Materials	98
4.1 Chemicals	98
4.2 Equipment	100
4.3 Commercially available kits	101
4.4 Enzymes	101
4.5 Oligonucleotides	101
4.6 Plasmids	104
4.7 <i>Escherichia coli</i> (<i>E. coli</i>) strains	105
4.8 Yeast strains	105
4.9 Antibodies	112
5 Methods	113

Table of contents

5.1 Basic methods.....	113
5.1.1 Agarose gel electrophoresis and gel extraction	113
5.1.2 Restriction digest and dephosphorylation	113
5.1.3 Blunting of DNA fragments.....	114
5.1.4 Ligation of DNA fragments	114
5.2 <i>E. coli</i> -specific techniques	114
5.2.1 Preparation of chemical competent <i>E. coli</i> cells.....	114
5.2.2 Preparation of plasmid-DNA	115
5.2.3 Transformation of competent <i>E. coli</i> cells	115
5.2.4 Long term storage of bacteria	115
5.3 <i>S. cerevisiae</i> -specific techniques	115
5.3.1 Cell density of yeast cultures	115
5.3.2 Culture of <i>S. cerevisiae</i>	116
5.3.3 Polymerase chain reaction.....	117
5.3.3.1 Standard analytical PCR	117
5.3.3.2 Tagging PCR.....	118
5.3.3.3 Yeast colony PCR	118
5.3.4 Transformation of yeast cell.....	119
5.3.4.1 One-step transformation with plasmids	119
5.3.4.2 High efficiency yeast transformation.....	119
5.3.5 Preparation of genomic DNA from yeast.....	120
5.3.5.1 Mechanical lysis of yeast cells	120
5.3.5.2 Chemical lysis of yeast cells	121
5.3.6 Whole cell extracts	121
5.3.6.1 WCE preparation	121
5.3.6.2 WCE preparation using a Retsch® MM400 cell grinder	122
5.4 Genomic tagging of mRNAs with MS2L	122
5.5 Preparation for microscopy	125

Table of contents

5.5.1 Growth of yeast cells on plate	125
5.5.2 Growth of yeast cells in fresh liquid culture	126
5.5.3 Imaging	126
5.5.4 Time lapse experiments	126
5.5.5 Tracking	126
5.5.6 Z-stack experiments.....	127
5.5.7 Statistical procedures and measurements	127
5.6 Genomic deletion via homologous recombination.....	127
5.7 Plasmid generation and site directed mutagenesis	128
5.8 ER visualization.....	128
5.9 Sequencing and analysis	129
5.10 Long term storage of yeast strains	129
5.11 SDS-PAGE and Western blot.....	129
5.11.1 SDS-PAGE	129
5.11.2 Staining of polyacrylamid gels.....	130
5.11.2.1 Coomassie staining.....	130
5.11.2.2 Silver staining	130
5.11.3 Western blot.....	130
5.12 Purification of recombinant She2p and She2p mutants from <i>E. coli</i>	131
5.12.1 Purification of TEV protease	131
5.12.2 Recombinant expression in <i>E. coli</i>	132
5.12.3 Lysis of cells.....	132
5.12.4 Affinity purification	133
5.13 Subcellular fractionation experiments.....	133
5.13.1 Spheroplasting of yeast and cell lysis	133
5.13.2 Velocity gradient centrifugation on discontinuous sucrose gradients	134
5.13.3 Protein precipitation by TCA from sugar containing samples.....	135

Table of contents

5.13.4 <i>In vitro</i> binding assay: Velocity gradient centrifugation with whole cell extracts and recombinant protein.....	135
5.14 <i>In vitro</i> binding assay with flotation purified ER membranes	136
5.14.1 Preparation of yeast microsomal membranes.....	136
5.14.2 Protease treatment of purified microsomal membranes.....	137
5.14.3 Flotation purification of ER membranes	137
5.14.4 <i>In vitro</i> binding assay	137
6 Summary	139
7 References	141
8 Abbreviations.....	149
9 Acknowledgement	152
10 Curriculum Vitae	154
11 Publication.....	155

1 Introduction

1.1 Budding yeast

Besides *Drosophila melanogaster* (*D. melanogaster*), *Xenopus laevis* (*X. laevis*), *Danio rerio* (*D. rerio*) and *Caenorhabditis elegans* (*C. elegans*) the baker's yeast *Saccharomyces cerevisiae* (*S. cerevisiae*) is one of the most important model organisms for genetic and molecular biological sciences. This organism has the ability to be propagated as stable haploid and diploid stages and the environmental-influenced capability to alternate between a filamentous and single-cellular growth. *S. cerevisiae* is used as model organism because it is a fast growing and easy to cultivate eukaryotic organism. Additionally, this yeast is designated to be one of the simplest eukaryotic organisms with many essential cellular processes that are conserved between yeast and human.

In case of sufficient nutrient supply the vegetative growth of *S. cerevisiae* occurs by budding. A daughter cell is generated at a specific location of the mother cell. The specific site where the bud growth is initiated is regulated by several gene products (Chant J., 1999) like the transmembrane protein Bud10p (Axl2p) that is required for guiding the budding machinery in haploid cells towards the correct position. Together with Bud3p and Bud4p these are proteins that are required for the axial budding pattern (Chant J. and Herskowitz I. 1991; Fujita A. *et al.*, 1994; Halme A. *et al.*, 1996; Roemer T. *et al.*, 1996), while in case of diploid cells Bud8p and Bud9p assign the site of polarization and therefore regulate the bipolar pattern (Zahner J.E. *et al.*, 1996). Bud1p, Bud2p and Bud5p are required for both the axial and the bipolar pattern (Bender A. and Pringle J.R. 1989; Chant J. and Herskowitz I. 1991). These gene products are involved in the proper bud site selection and polarized cell growth.

The initiation of budding starts during late G1-phase (Pryne D. and Bretscher A., 2000) and is mediated by three classes of regulatory proteins; GTPase activating proteins (GAPs), guanine-nucleotide exchange factors (GEFs) and guanine-nucleotide dissociation inhibitors (GDIs; Gulli M.P. and Peter M., 2001). During S-phase (synthesis) components are delivered to the bud e.g. for the segregation of endoplasmic reticulum (ER) and DNA replication. This occurs until the cell enters G2-phase. During this phase between S-phase and mitosis the cell continues growing until it reaches almost the size of the mother cell and then the bud separates from the

mother cell by cytokinesis at the end of M-phase (mitosis). During M-phase the chromosomes are segregated while the nuclear envelope (NE) remains intact. After division the daughter cell can be distinguished from the mother by its smaller size. It therefore passes through a longer G1-phase to form a new bud and then enter into S-phase (Figure 1).

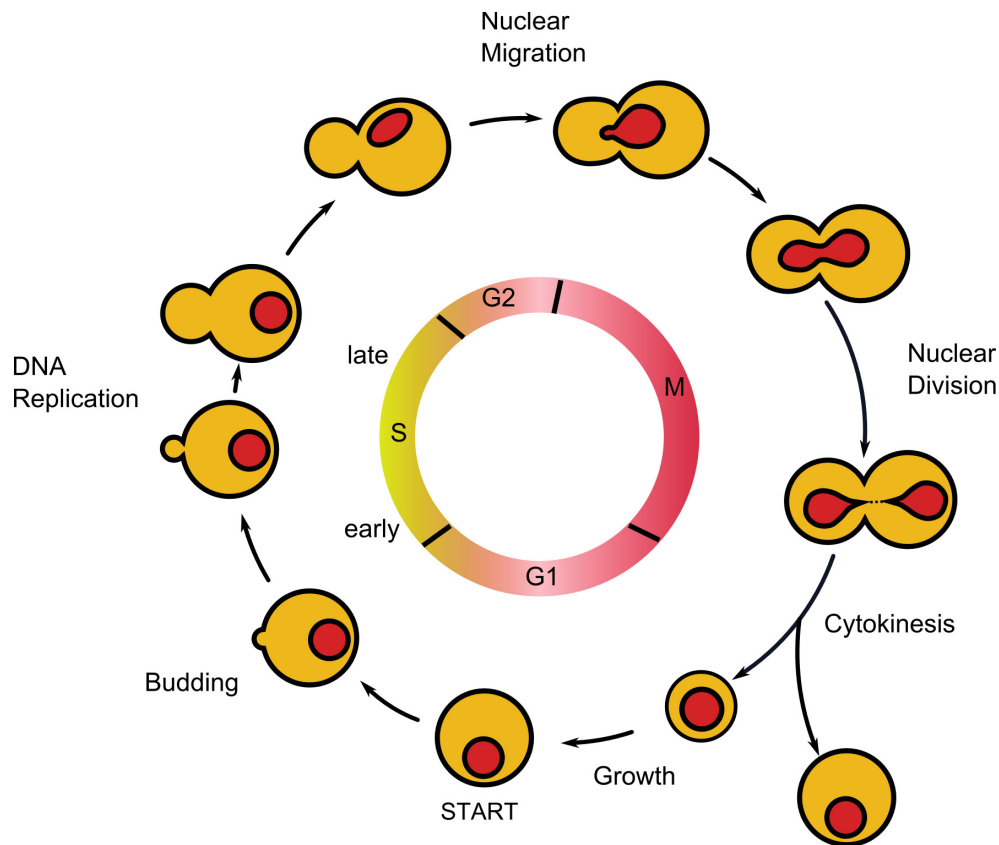


Figure 1 | Cell cycle of baker's yeast *S. cerevisiae*. Scheme of the cell cycle of *S. cerevisiae* modified from Lodisch H. *et al.*, 1999. The mother cell forms a bud during late G1-phase that reaches almost the size of the mother cell and then the new daughter cell separates from the mother cell by cytokinesis. During mitosis the NE remains intact. Comparing with the mother cell the daughter cell is smaller and therefore passes through a longer G1-phase to form a new bud and then enter into S-phase.

In case of nutrient deficiency a diploid cell sporulates and forms four haploid spores after meiosis. The quartet of spores (called tetrad) has different mating types (a and α) and germinate in case of good nutrient supply followed by further cell cycles and budding. An alternative pathway is also shown in Figure 2 where two spores of different mating types can conjugate to a diploid zygote.

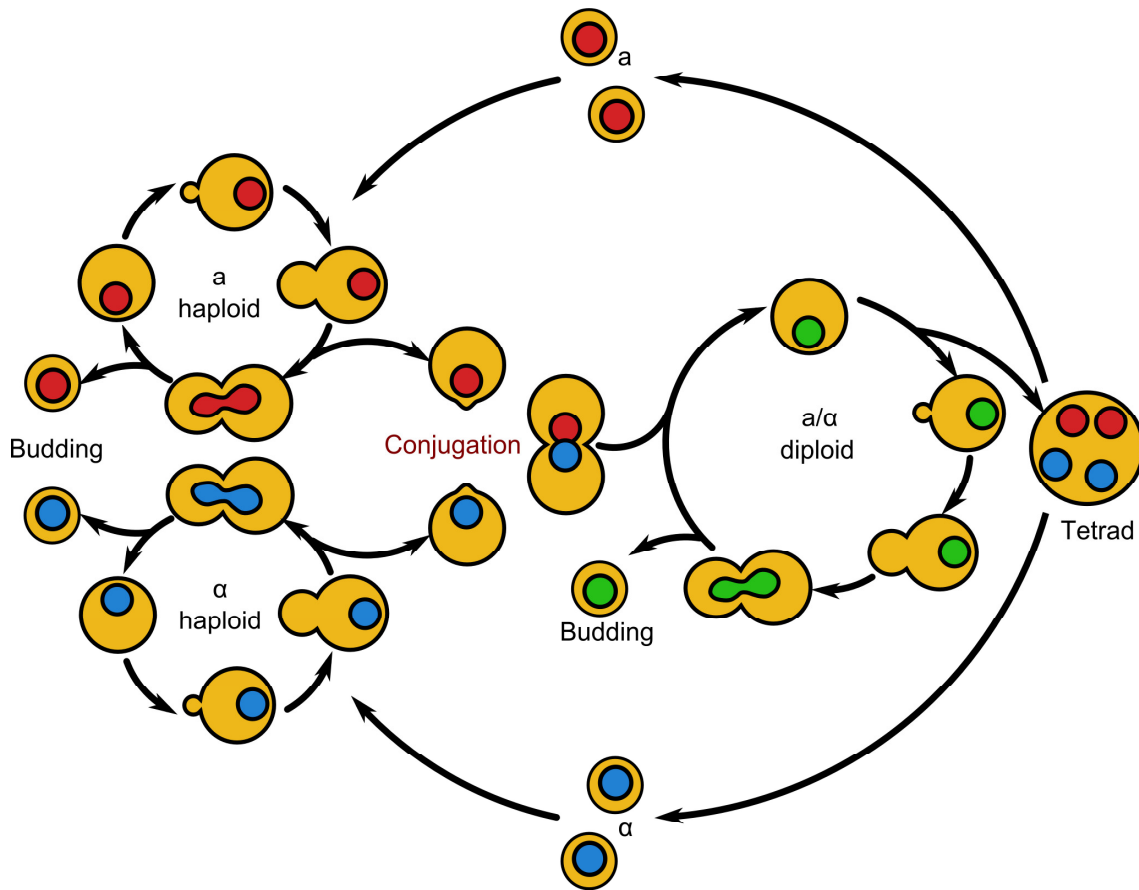


Figure 2 | Cell cycle of baker's yeast *S. cerevisiae*. In case of a good nutrient supply the yeast *S. cerevisiae* grows vegetative under diploid conditions while in case of nutrient deficiency the diploid cell germs by sporulation and forms four haploid permanent spores in a tetrad. Two of these spores have mating type a and the other two have mating type α . In case of good nutrient conditions the spores germinate either vegetative (Figure 1) or mate by conjugation with a spore of the opposite mating type and thus become diploid.

The possibility to change from a diploid to a haploid cell stage and the return to a diploid stage is achieved by the mating of two haploid cells with the opposite mating type a (*Mat a*) or α (*Mat α*). To facilitate mating yeast has implemented mating type switching. Resulting from asymmetric expression of the *HO* endonuclease mating type switching is exclusive for the mother cell and therefore the mother and daughter cell have the opposite mating types after their separation. The transcription of the endonuclease *HO* is controlled by Ash1p that is specifically localized to the nuclei of the presumptive daughter cell during late M-phase of the cell cycle and therefore inhibits *HO* transcription in the following G1-phase. This process ensures the formation of diploid cells through the mating process (Darzacq X. *et al.*, 2003).

1.2 Intracellular transport

Asymmetric cell division like in yeast requires specific adaptations to the segregation of cellular compartments. During the process of reproduction genetic information in form of mRNA and DNA, as well as organelles like the vacuole, post-Golgi secretory vesicles, peroxisomes, the Golgi network and mitochondria have to be transported from the mother cell to the new daughter cell.

But how does this transport occur? How does the cell know when, how and what kind of compartments have to be delivered from one cell to its progeny? A lot of the molecular mechanisms have been understood by studying the transport machinery of yeast proliferating by budding. As I already mentioned, bud initiation occurs during late G1-phase. This process is mediated by GAPs and GEFs that specify bud site selection, establishment of a polar axis and polarized cytoskeleton structures. Cell polarity is maintained by actin filaments that are necessary to overcome the long distance between mother cell and bud during growth of the yeast cell from late G1- to mitotic phase (DeRosier D.J. and Tilney L.G., 2000). Two different forms of filamentous actin are known. First, actin that is randomly spread at the cortex of the cell and the second, actin filaments that originate from the bud and form bud-associated actin cables (Pon L. *et al.*, 2001). These bud-associated actin filaments are anchored at the specific location of the bud neck (Bnr1p) and the bud tip (Bni1p) and therefore assemble at or associate with these positions (Pryne D. *et al.*, 2004). Bundles of actin form actin cables that are distributed in yeast cells that are not entering the process of dividing, but are oriented along the mother-bud axis and therefore elongate at the periphery and affiliating new material by attachment at their anchor site. The transport of a plenty of material along actin filaments is powered by the motor proteins Myo2p and Myo4p of the myosin V family that are moving from the mother cell along these actin filaments to the tip of the new bud. While Myo2p is responsible for transporting cellular material like vacuole, post-Golgi secretory vesicles, peroxisomes, the Golgi network and microtubule plus ends Myo4p transports ribonucleoprotein particles (RNPs) to the bud and is also required for the inheritance of cortical ER (cER).

In principle, mRNAs are localized as part of messenger ribonucleoprotein particles (mRNP). During the transport from perinuclear areas the transcripts are translationally silenced until they reach their peripheral destination and the protein

synthesis occurs (Besse F. and Ephrussi A., 2008; Martin K.C. and Ephrussi A., 2009). In brief, protein synthesis consist of transcription, RNA processing, translation and co-or post-translational modifications (Cooper G.M. 2000). Because translation initiation is the rate-limiting step it is therefore a primary control target. The initiation itself consists of a sorted multistage process that involves a bunch of translation factors and adapter proteins that provides the recruiting of the ribosome to the mRNA.

1.3 mRNA localization

mRNA molecules that are transcribed in the cell nucleus are transported into the cytoplasm. Either the transcripts are stored, translated to produce proteins or are guided to areas specific for their translation or distribution. The latter case results in the asymmetric distribution of some cytoplasmic proteins and supports embryonic development or localization activities in polarized cells.

Previous studies have shown that the localization process in different eukaryotic organisms often requires nuclear RNA binding proteins (RBPs) that associate with the mRNA. In some cases the coating of mRNA by RBPs is essential for its transport. The localization process itself is predicated on so-called zipcodes (Shav-Tal, Y. and Singer R.H., 2005). The specific regulatory sequences are located mainly in the 3' untranslated region (3'UTR) and belong to *cis*-acting elements. Zipcodes affect features of RNA in form of translation efficiency and stability (Jackson R.J., 1993, Martin K.C. and Ephrussi A., 2009). After packaging by RBPs the localized mRNA is transported actively with the help of kinesin, dynein and motor proteins of the myosin families (Shav-Tal, Y. and Singer R.H., 2005).

The until now three best studied models of mRNA localization are shown in Figure 3.

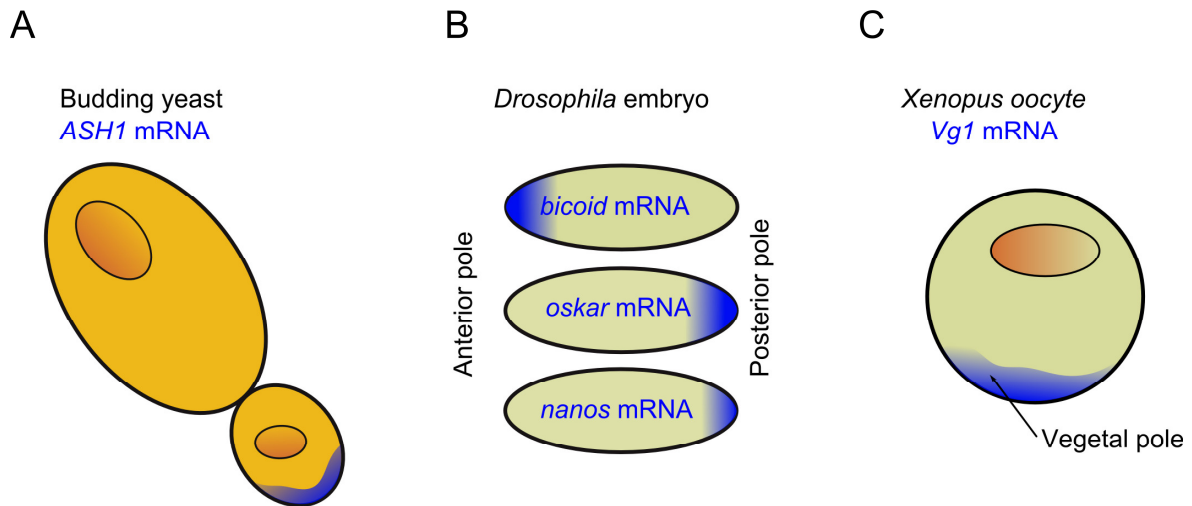


Figure 3 | Examples of localized mRNA. Scheme of classic examples for localized mRNAs in different organisms is shown. (A) In budding yeast the *ASH1* mRNA localizes to the bud tip. (B) In *Drosophila* embryos *bicoid* mRNA localizes to the anterior pole; *oskar* and *nanos* mRNAs to the posterior pole. (C) In *Xenopus* oocytes (stage IV) *Vg1* mRNA localizes to the vegetal pole. Figure modified and text adapted from Martin K.C. and Ephrussi A., 2009.

This Figure displays the *ASH1* mRNA of the budding yeast *S. cerevisiae* that inhibits mating type switching and has to be transported from the mother to the daughter cell. In *D. melanogaster* oocytes the localization of *bicoid*, *oskar* and *nanos* mRNA leads to a spatial developmental pattern of the embryos. The *Vg1* mRNA in *X. laevis* oocytes is localized to the vegetal pole and after its later activation causes induction of meso- and endodermal cell fates in the early embryo (Martin K.C. and Ephrussi A., 2009).

In case of the transport and the growth of the mother cell in *S. cerevisiae* it is indispensable that the aforementioned mating type switching is repressed in the daughter cell. This ensures that an isolated spore can form diploids and guarantees the production of an offspring with different genetic patterns for multicellular development. The repression of mating type switching is controlled by Ash1p that encodes beside a cell fate determinant for a transcriptional repressor of the endonuclease *HO* (Jansen R.P. *et al.*, 1997). The transport of this mRNA from the mother cell to the bud tip is attended by the repression of the *HO* endonuclease that has the ability to cut the active MAT locus and therefore change the mating type (Darzacq X. *et al.*, 2003).

1.4 mRNA localization in yeast *S. cerevisiae*

In addition to the aforementioned *ASH1* mRNA that ensures the repression of the *HO* endonuclease and therefore inhibits mating type switching in the daughter cell 23 other localized mRNAs are known in *S. cerevisiae* (Aronov S. *et al.*, 2007; Oeffinger M. *et al.*, 2007; Shepard K.A. *et al.*, 2003). These 24 transcripts (Table 1) were identified by co-immunoprecipitation with the transport machinery (see below) and are actively transported to the bud tip (Shepard K.A. *et al.*, 2003; Takizawa P.A. *et al.*, 2000).

Shepard K.A. et al, 2003					
mRNA	Cell cycle regulation	Protein Localization	Cellular compartment of the encoded protein	signal peptide	predicted Transmembrane domain
<i>ASH1</i>	M	bud nucleus	nucleus	-	-
<i>BRO1</i>	None	punctae on vacuole	cytoplasm, endosomes, membranes	-	-
<i>CLB2</i>	M	nuclei, spindle pole	nucleus	-	-
<i>CPS1</i>	None	cytoplasmic punctae	vacuole	Yes	1 TMD
<i>DNM1</i>	S	mitochondrial periphery	outer mitochondrial membrane	-	-
<i>EGT2</i>	M	membranes , large bud enriched	cell wall	Yes	GPI anch.
<i>ERG2</i>	M	ER	ER	Yes	1 TMD
<i>IST2</i>	None	bud plasma membrane	plasma membrane, cell periphery	-	8 TMDs
<i>MID2</i>	None	cell periphery , mother-bud junction	plasma membrane, cell periphery	Yes	1 TMD
<i>MMR1</i>	M	bud sites&tips, mother-bud junction	outer mitochondrial membrane	-	-
<i>SRL1</i>	G1	periphery of small buds	cell wall	Yes	-
<i>TPO1</i>	M	bud plasma membrane	ER, cell periphery, bud	-	12 TMD
<i>WSC2</i>	S	membranes , bud enriched	cell periphery	Yes	1 TMD
<i>TAM41</i>	None	mitochondria	mitochondria	-	-
<i>IRC8</i>	M	membranes , bud enriched	bud, membrane	Yes	4 TMD
<i>YLR434C</i>	None	mitochondria	no localisation data	-	-
<i>TCB3</i>	G2	membranes , bud enriched	cell periphery	-	1 TMD
<i>EAR1</i>	None	ER	endosomes	Yes	1 TMD
<i>TCB2</i>	None	membranes , bud enriched	cell periphery	-	1 TMD
<i>KSS1</i>	None	not defined	cytoplasm, nucleus	-	-
<i>LCB1</i>	None	ER	ER	-	-
<i>MET4</i>	None	Nuclei	nucleus	-	-
<i>MTL1</i>	None	not defined	plasma membrane	Yes	1 TMD
<i>RGL1</i>	None	not defined	bud neck	unknown	unknown

Table 1 | Overview of all 24 localized mRNAs in yeast *S. cerevisiae*. This table gives an overview of 24 localized mRNAs in yeast *S. cerevisiae* and their important characteristics (table modified from Schmid M. Dissertation, 2008). Reddish cells of the table mark mRNAs encoding membrane or secreted proteins. The mRNAs marked in tall bold letters were used for this work.

Interestingly, although mRNA distribution is highly asymmetric in all 24 cases only eight of the encoded proteins show a bud specific localization while 16 are found in the mother cell and the bud.

From these listed 24 mRNAs only eleven are expressed during specific stages of the cell cycle and since encoded proteins have manifold functions some are involved in general processes that belong to plasma membrane and cell wall synthesis, stress signaling and response pathways in yeast (Shepard K.A. *et al.*, 2003). Examples are the *ASH1* mRNA that is expressed only during mitotic phase or in case of *WSC2*

mRNA that is expressed only in S-phase of the cell cycle and encodes a sensor-transducer of the stress-activated *PKC1-MPK1(SLT2)* signaling pathway which is involved in the maintenance of cell wall integrity (Verna J. *et al.*, 1997).

Intriguingly, 16 of these mRNAs marked by the reddish cells in Table 1 are coding for membrane associated or membrane proteins like *IST2* or *EAR1* mRNA which encodes an endosomal specificity factor required for Rsp5p-dependent ubiquitination and sorting of specific cargo proteins at the multivesicular body (Giaever G. *et al.*, 2002; Terashima H. *et al.*, 2002; Leon S. *et al.*, 2008). Another example is the *MID2* mRNA that codes for a plasma membrane protein acting as a sensor for cell wall integrity signaling (Philip B. and Levine D.E., 2001; Green R. *et al.*, 2003) and *SRL1* mRNA that encodes a mannoprotein required for cell wall stability (Terashima H. *et al.*, 2002; Hagen I. *et al.*, 2004).

Besides the different types of mRNAs that have to be transported during budding of the mother cell the transport itself seems to be disordered. Normally an energetic, fast and successful transport of cargo would be characterized by the fact that it expires directly by using the shortest distance and fastest connection between the starting point and its destination. Instead, the transport seems to be chaotic by the first point of view. But this is only the first presumption by having a cursory look at live cell imaging observations (shown in Figure 4) of moving mRNPs from the mother cell to the bud. Previous studies (Bertrand E. *et al.*, 1998) of three dimensional (3D) tracking of mRNPs (*ASH1-MS2*) were able confute this first assumption by showing that the movement can be classified in different types of motion. Thus, motion itself must be organized directly.

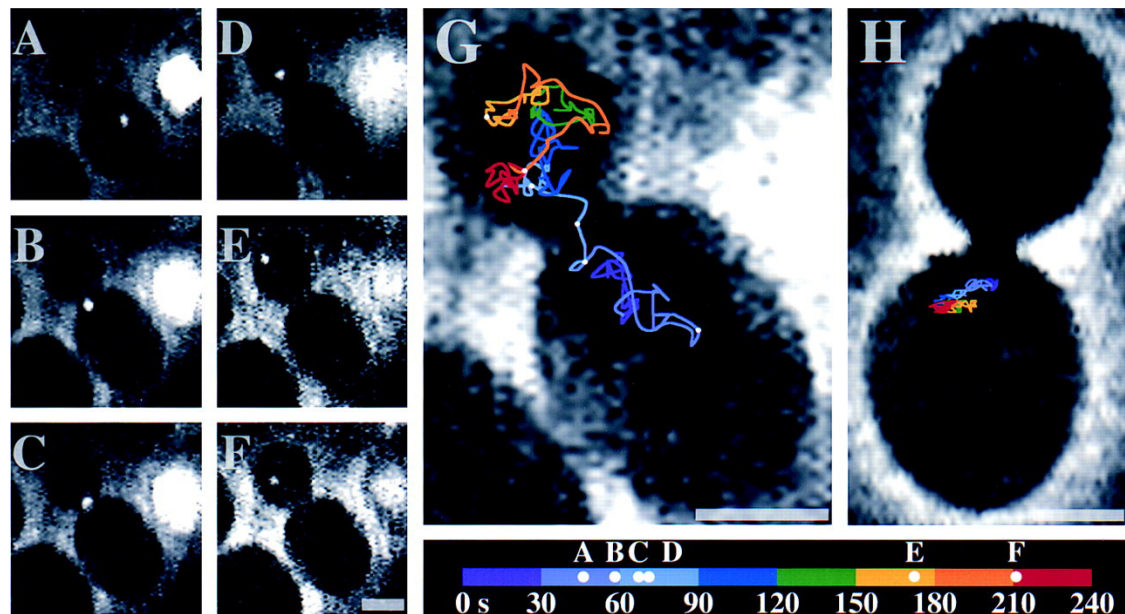


Figure 4 | Analysis of particle movement. (A–G) Wild type yeast strain expressing both the *ASH1* reporter and the GFP-MS2 protein were observed. Movement of the particle was recorded. (A–F) Movement of the particle from the mother to the bud is shown. The mRNA particle was analyzed over a period of 4 min during which it moved a net linear distance of 4.4 μm in a time of 128 sec, over a total path length of 23 μm . Coordinated transport of *ASH1* mRNA and *IST2* mRNA in *S. cerevisiae*. Figure adapted and text modified from Bertrand E. *et al.*, 1998.

The movement of the mRNP towards the yeast bud starts first with a unidirectional pattern and periods of diffusion in specific regions of the cell. Later on, when the bud growing achieves a bigger volume the mRNP particle shows a more corralled diffusion movement.

Nevertheless, the transport itself is yet not completely understood and therefore additional studies using live cell imaging to follow-trafficking mRNPs in wild type and mutated cells like it was done in this study are necessary.

1.4.1 Zipcodes - specification elements for localization processes

The localization process itself depends on elements that target the RNAs that have to be delivered and thus differentiate between localized and unlocalized RNAs. Localized RNAs are recognized by so-called zipcodes that are *cis*-acting elements. Zipcodes can be found in the 5'UTR or in the coding sequence, but they are mainly present in the 3'UTR (Martin K.C. and Ephrussi A., 2009). These specific sequence elements are forming secondary and tertiary structures that act as recognition sites for RNA-binding proteins like She2p. Thus, zipcodes determine mRNA localization in

the cytoplasm (Chabanon H. Mickleburgh I. and Hesketh J., 2004) by having the ability to bind specific RNA-binding proteins (RBP; Martin K.C. and Ephrussi A., 2009) that direct the transport.

Identified by affinity purification, fluorescent *in situ* hybridization (FISH) or genetic screens zipcodes play a critical role by regulating and directing the localization of mRNAs (Martin K.C. and Ephrussi A., 2009). Since zipcodes cannot easily be identified by bioinformatics tools it is very difficult or even impossible to screen for zipcodes. Therefore, the best method to identify these *cis*-acting elements is e.g. the monitoring of subcellular distributions of fragments originated from localized RNAs fused to reporter transcripts (Jambhekar and DeRisi, 2007). Zipcodes itself are highly variable in structure, length and complexity. They range from short single motifs like in mammalian *Methallothionein-I* that has 40 nt in length (Chabanon H. Mickleburgh I. and Hesketh J., 2004) to multi-component units with hundreds of nucleotides like the zipcode of *Drosophila nanos* mRNA with 547 nt or the zipcode for *bicoid* mRNA with 625 nt in length. In case of the yeast *S. cerevisiae* *ASH1* mRNA more than one element exists. These are E1, E2a and E2b that are positioned in the coding sequence or E3 that is positioned at the end of the coding sequence, the 3'UTR. Zipcodes that are made of multiple elements can either act together or independently underlining the complexity of the localization mechanism and RNA-protein interactions. Structural analyses of some zipcodes showed that their secondary structures might be more conserved than consensus sequences (Olivier C. *et al.*, 2005). These analyses also showed that there is coherence between structure and functionality that is organism-comprehensive (Chabanon H. Mickleburgh I. and Hesketh J., 2004).

In case of *S. cerevisiae* the *ASH1* mRNA zipcodes E1, E2a, E2b and E3 are predicted to form loop-stem-loops secondary structures while in one of the loops a CGA triplet and in the other loop a conserved single cytosine exists (Figure 5).

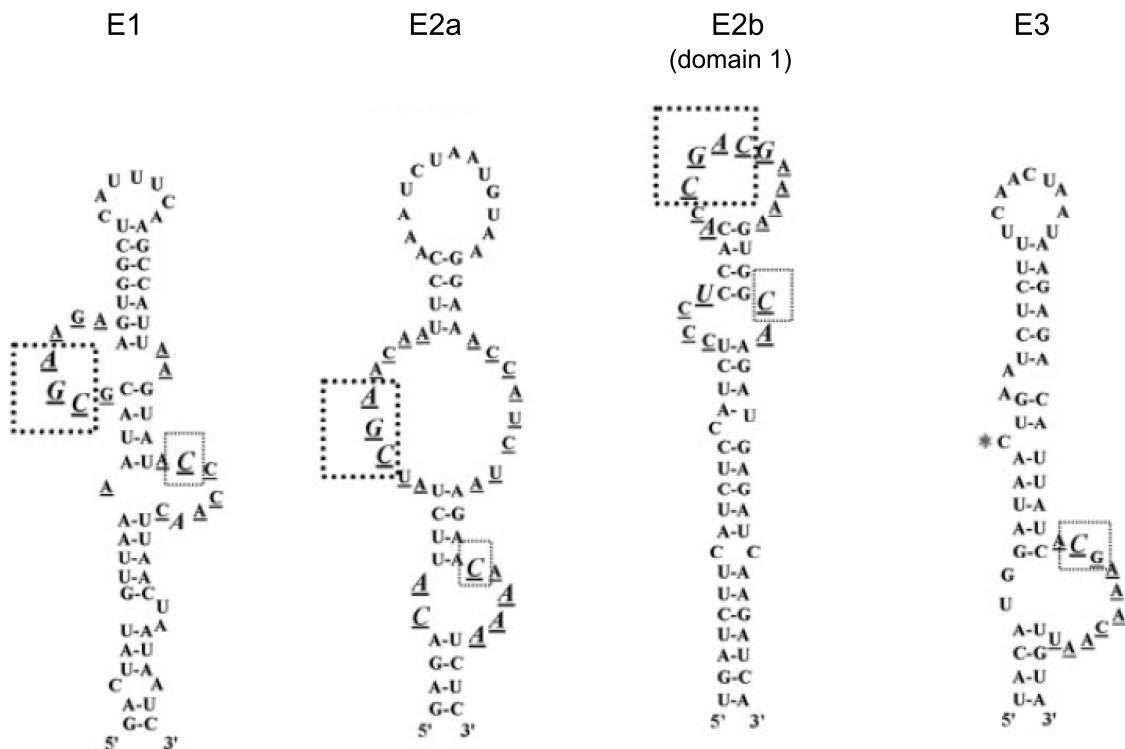


Figure 5 | The *ASH1* mRNA zipcodes in *S. cerevisiae*: E1, E2a, E2b and E3. Diagram of the four *ASH1* mRNA zipcodes is shown. Nucleotides conserved in 95% of the clones are indicated in capital letters and italicized. The conserved CGA sequence is boxed with large dotted lines whereas the conserved cytosine in E1, E2a and E2b (domain 1) is boxed with small dotted lines. A cytosine at an analogous position on the element E3 is indicated by an asterisk. Figure and text modified from Olivier C. *et al.*, 2005.

By mutating these two characteristics (CGA triplet and the conserved single cytosine) the localization of a reporter mRNA fused to the corresponding zipcode failed because the binding of the zipcode to its RNA-binding protein was not longer possible. Therefore, the CGA triplet and the cytosine can be defined as binding domain. Because this motif was also identified in two other mRNAs, *EAR1* and *IST2* which are localized to the bud the importance of this sorting motif was approved (Olivier C. *et al.*, 2005).

Additionally, each of these four individual motifs must have the right secondary structure and the right distance between the two cytosines (Olivier C. *et al.*, 2005) to ensure sufficiently the assembly of the mRNP that continues with the localization to the bud (Bertrand E. *et al.*, 1998; Chartrand P. *et al.*, 1999). Typically, a localized mRNA has more than one zipcode (Bashirullah A. *et al.*, 1998), but in case of the *ASH1* mRNA in yeast (Figure 6) each single of the four zipcode elements is sufficient for the RNA localization that suggests that the transport efficiency is altered by the

presence of more than one localization element (Martin K.C. and Ephrussi A., 2009; Gonsalvez G.B. *et al.*, 2005).

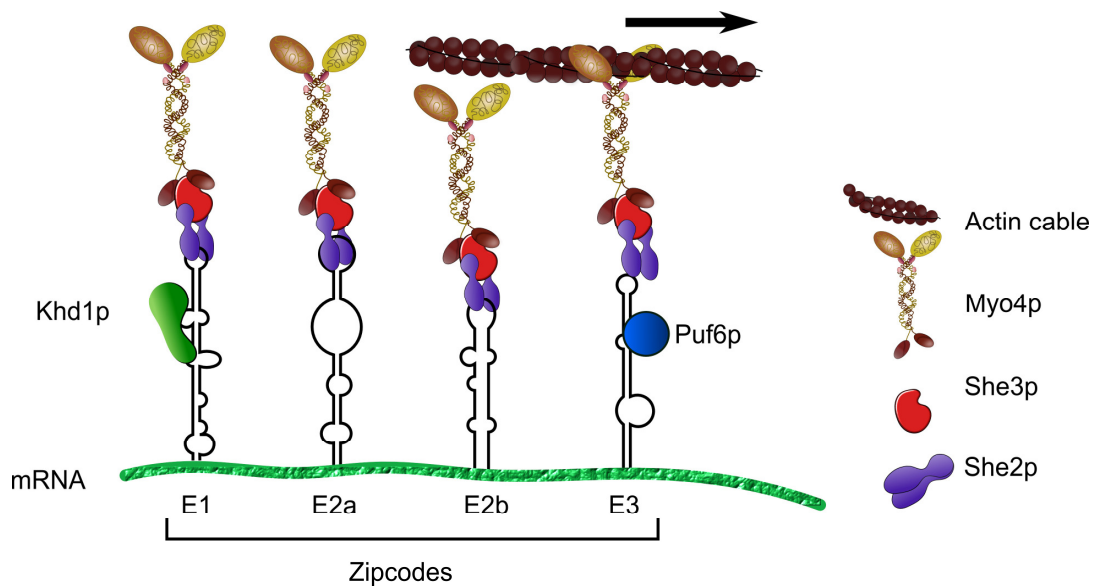


Figure 6 | Four *ASH1* mRNA zipcodes interact with the RNA-binding protein She2p. Schematic drawing of the four zipcodes E1, E2a, E2b and E3 of the *ASH1* mRNA that interact with the RNA-binding protein She2p is shown. She2p binds to the motor protein Myo4p via the adapter protein She3p. Myo4p (She1p) is a Type V myosin and transports the mRNA and ER from the mother to the daughter cell while She3p as an adapter links Myo4p with She2p-*ASH1* mRNA. Myo4p, She3p and She2p are components of the core locasome (chapter 1.4.2.1.). The zipcodes E1, E2a, E2b and E3 of the *ASH1* mRNA are able to bind to locasomes individually. When the locasome is bound to actin cables the transport occurs from the mother cell to the daughter cell. E1 is also bound to Khd1p that is essential for anchoring and translational regulation of *ASH1* mRNA illustrating that *ASH1* mRNA is translational repressed during its transport to the bud of the daughter cell. In case of E3 the protein Puf6p is bound. Puf6p is also a RNA-binding protein like Khd1p that in this case is responsible for the translational regulation and localization of *ASH1* mRNA (Gonsalvez G.B. *et al.*, 2005).

Besides the *cis*-acting factors (zipcodes) that are necessary for the cytoplasmic localization of mRNAs (Chabanon H. Mickleburgh I. and Hesketh J., 2004) and represent binding sites for RBPs, so-called *trans*-acting factors that bind to the zipcodes are essential for the transport machinery. In the following chapter I will focus on the yeast transport machinery.

1.4.2 *Trans-acting factors: the mRNA localization machinery*

Not only the mRNA signal but also the proteins that are interacting with these regions are necessary to form the localization complex and therefore facilitate localization (Chabanon H. Mickleburgh I. and Hesketh J., 2004). By studying the *ASH1* mRNA associated RNA-binding proteins in yeast a big insight into the mechanism and role of *trans-acting* factors has been achieved (Paquin N. and Chartrand P., 2008). The proteins that are required for the *ASH1* mRNA localization include Myo4p and the two RNA-binding proteins She2p and She3p (Elson S.L. *et al.*, 2009; Müller M. *et al.*, 2011). Each of the aforementioned zipcodes of the *ASH1* mRNA is recognized by the RNA-binding protein She2p (Darzacq X. *et al.*, 2003) which shuttles between the nucleus and the cytoplasm. In the cytoplasm it recruits She3p that acts as an adapter and therefore links the motor protein Myo4p with She2p-*ASH1* mRNA (Martin K.C. and Ephrussi A., 2009). She3p together with Myo4p are exclusively cytoplasmic proteins (Darzacq X. *et al.*, 2003) while She3p was recently also identified to be able to bind to a subset of mRNAs (Elson S.L. *et al.*, 2009; Müller M. *et al.*, 2011).

All together these three proteins, originally identified by a genetic screen that selects for mutants defective in the *HO* endonuclease asymmetric expression (Jansen R.P. *et al.*, 1996), are forming a complex that is called locasome that mediates the trafficking of the *ASH1* mRNA along actin filaments (Martin K.C. and Ephrussi A., 2009).

1.4.2.1 The locasome

The locasome is a complex of unknown stoichiometry and the three factors She2p, She3p and Myo4p (She1p; Figure 7) are forming its core complex. They are co-localizing with each other *in vivo* and with the transported *ASH1* mRNA (Böhl F. *et al.*, 2000; Gonsalvez G.B., Urbinati C.R. and Long R.M., 2005).

While She2p was recognized to bind weakly but specifically and directly to all four *ASH1* mRNA zipcodes (Böhl F. *et al.*, 2000; Long R.M. *et al.*, 2000; Darzacq X. *et al.*, 2003), Myo4p is able to associate with the N-terminal domain of She3p. The C-terminal domain of She3p is in turn able to associate with She2p (Böhl F. *et al.*, 2000). The locasome is formed (Figure 7) and thus mRNAs are localized (see below)

on polarized actin cables to the bud (Gonsalvez G.B., Urbinati C.R. and Long R.M., 2005).

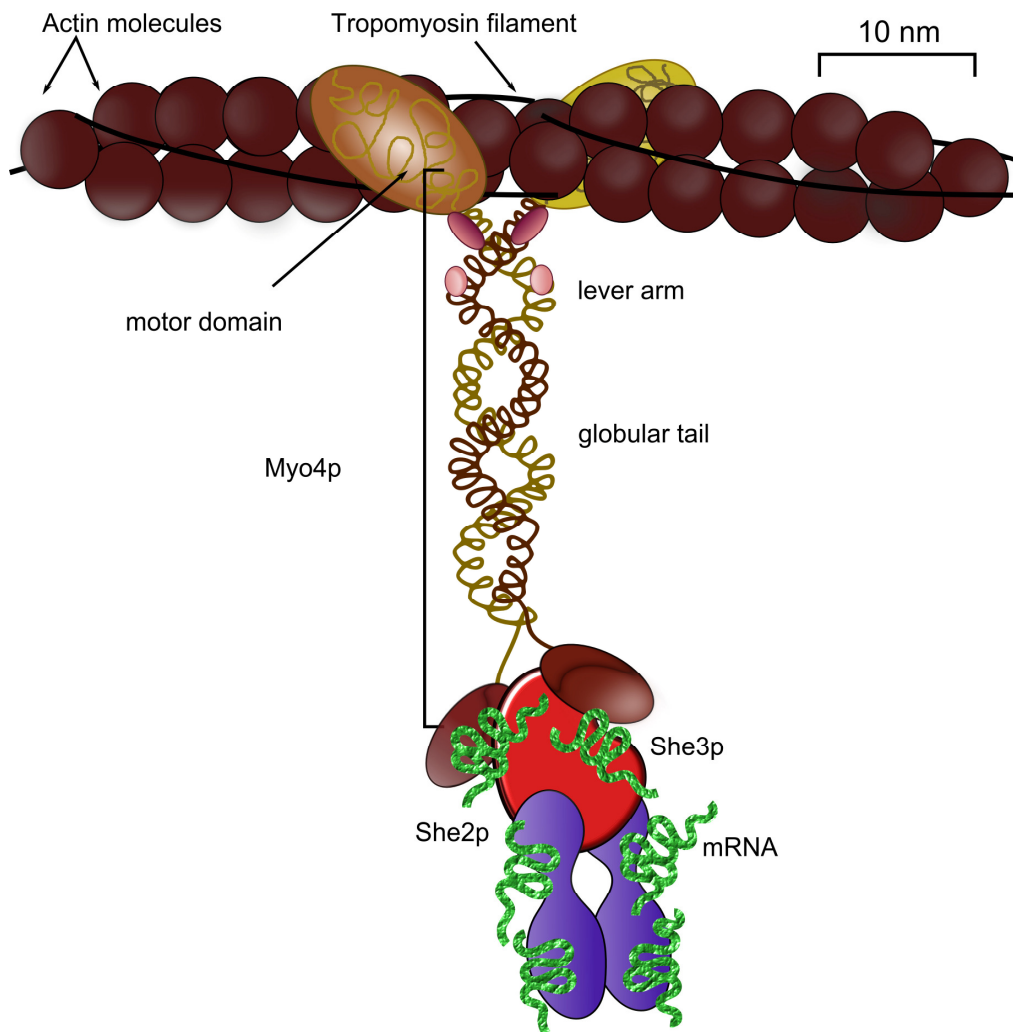


Figure 7 | The yeast core locosome consisting of She2p, She3p and Myo4p (She1p) is moving towards the bud on polarized actin filaments. The schematic drawing of the central transporting machinery is shown. It is essential for the localization of mRNAs (green) towards the bud. The core locosome consists of the mRNA-binding protein She2p (blue), the adaptor protein She3p (red) that is also able to bind to mRNAs and the motor protein Myo4p. The mRNA binds to She2p by its *cis*-acting elements (zipcodes). She2p is then associated to Myo4p via She3p that acts as an adapter. The motor protein Myo4p, a member of the type V myosin family that can dimerize, consists of two motor domains, each attached to a lever arm that forms the globular tail. The mRNP is transported towards the barbed ends of actin cables consisting of actin molecules and tropomyosin filaments located at the bud tip. How the single components are assembled stoichiometrical to each other is not yet completely clear.

1.4.2.1.1 She2p, the RNA-binding protein

The RNA-binding protein She2p (28 kDa) is responsible for the trafficking of mRNPs (Böhl F. *et al.*, 2000; Chartrand P. *et al.*, 2001; Niessing D. *et al.*, 2004). Besides She3p that is another protein of the *SHE* gene family, She2p was discovered primarily to bind RNA. Its binding is weakly with an affinity in the nanomolar range (Böhl F. *et al.*, 2000; Long R.M. *et al.*, 2000; Darzacq X. *et al.*, 2003; Niessing D. *et al.*, 2004).

As the key player for the mRNA localization She2p binds localized mRNAs by binding to the zipcodes. This binding occurs already in the nucleus during transcriptional elongation (Shen Z. *et al.*, 2010) and even if the other *SHE* genes were deleted (Böhl F. *et al.*, 2000 and Takizawa P.A. *et al.*, 2000). However, the presence of She3p seems to enhance the binding of She2p to localized mRNAs (Böhl F. *et al.*, 2000). She2p then escorts the mRNAs out from the nucleus to the cytoplasm (Du T.G. *et al.*, 2008; Shen Z. *et al.*, 2009) followed by the binding of the primary mRNP complex to protein She3p that in turn associates with the motor protein Myo4p (Böhl F. *et al.*, 2000; Hodges A.R. *et al.*, 2008; Heuck A. *et al.*, 2010).

Besides the functionality of She2p being part of mRNA localization machinery (Böhl F. *et al.*, 2000; Shepard K.A. *et al.*, 2003), binding of She2p to *ASH1* mRNA is also required for the translational repression (Martin K.C. and Ephrussi A., 2009) and thus She2p represents a protein that acts both in the translational regulation of localized mRNAs and directed trafficking (Martin K.C. and Ephrussi A., 2009).

The RNA-binding protein She2p has structural homology only in other yeasts (Niessing D. *et al.*, 2004). It is a nearly exclusive α -helical protein. Initial experiments suggest that She2p is a homodimer and forms stable dimers in solution determined by X-ray crystallography and analytical equilibrium ultracentrifugation (Niessing D. *et al.*, 2004). Later on, it was shown by Müller M. *et al.*, 2009; Chung S. and Takizawa P.A., 2010 and Kremntsova E.B. *et al.*, 2011 that She2p has a tetrameric structure and thus the previous results did not fully represent the functional unit of She2p.

If the dimeric structures were disrupted by a mutation as in case of the amino acid exchange in S120Y (Figure 8) the dimerization capability of She2p is affected and thus She2p cannot bind mRNAs *in vivo* efficiently and does not localize *ASH1* mRNA in yeast cells correctly anymore (Niessing D. *et al.*, 2004). It has also been shown

that deletions in the hydrophobic core of each monomer of She2p within the pentacle arranged bundle of five α helices lead to a disrupted mRNA transport *in vivo* (Gonsalvez G.B. *et al.*, 2003; Niessing D. *et al.*, 2004).

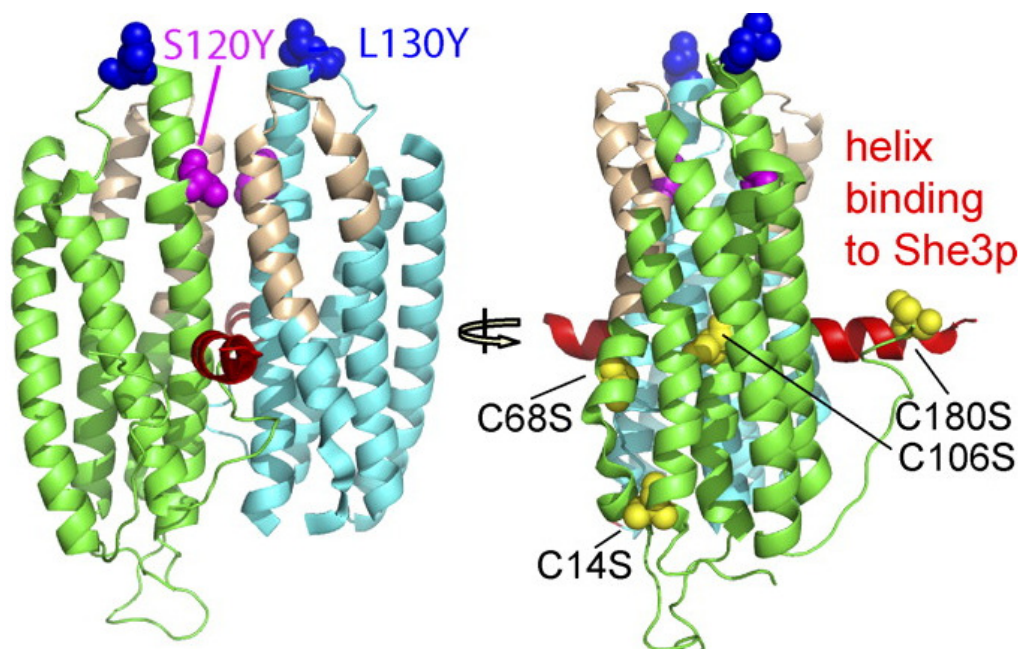


Figure 8 | The crystal structure of She2p. Crystal structure of She2p (Protein Data Bank accession no. 1XLY) is shown. The two chains of the dimer are shown in green and cyan. The location of the two point mutants, S120Y and L130Y are shown in space-filling representation. S120Y is at the interface of the crystallographic dimer, whereas L130Y is at the proposed interface for tetramer formation (Müller M. *et al.*, 2009). The Cys to Ser mutations were made to prevent formation of higher oligomers of She2p. A single α helix that protrudes from the side of She2p (red) is identified as all or part of the binding site for She3p. The mRNA-binding site is indicated in light brown. Figure and text adapted from Kremontsova E.B. *et al.*, 2011.

The formation of two globular She2p monomers to a symmetric homodimer is essential for its function. It is also described that She2p forms a helical hairpin motif that consists of amino acids that are positively charged. These amino acids are located onto two co-terminal anti-parallel α helices. The RNA binding occurs at the surface patch on She2p that is positively charged and is allocated to the basic helical hairpin motif (Müller M. *Et al.*, 2007). Mutations at this surface patch by amino acid exchanges of leucine 130 to tyrosine (L130Y; Figure 8) lead to a reduced binding activity of She2p to RNAs *in vitro* (Niessing D. *et al.*, 2004). These results were supported with data that show that in case of an amino acid exchange of leucine 130 to serine (L130S) this mutant was also impaired in localization of *ASH1* mRNA (Gonsalvez G.B. *et al.*, 2003)

Since in case of dimerization these hairpin motifs are located at the opposite sites on the She2p surface, the idea came up that each monomer can bind to zipcodes independently. This would imply that dimerization is possibly not required for the binding of mRNAs. Thus, mutations of She2p were generated that only produce monomers. The results show that She2p monomers weren't able to bind mRNAs and therefore demonstrated that the dimerization of She2p is essential for its proper functionality (Niessing D. *et al.*, 2004).

By comparing the structure of She2p and its novel protein fold with other proteins it seems that She2p is an unconventional RNA-binding protein with no analogous proteins outside the *Saccharomyces* clade (Schmid M. Dissertation 2008).

1.4.2.1.2 Myo4p, the motor protein

For Myo4p, also known as She1p it has been shown in previous studies that it directly transports substrates along microfilaments in living yeast (Reck-Peterson S.L. *et al.*, 2001). The dependency of the mRNA transport on an intact actin cytoskeleton was demonstrated previously by generating mutants that prevent bundling of actin cables or using drugs that disrupt actin filaments. Both resulted in the loss of targeting *ASH1* mRNA (Long R.M. *et al.*, 1997; Takizawa P.A. *et al.*, 1997). Additionally, actin also plays a role in the anchoring process at the bud tip of localized *ASH1* mRNA (Beach D.L. *et al.*, 1999) as shown by experiments that result in a disruption of the cortical actin at the bud tips leading to changes in the *ASH1* mRNA localization (Takizawa P.A. *et al.*, 1997; Beach D.L. *et al.*, 1999). Besides yeast the actin cytoskeleton is also necessary for the anchoring of messages in other organisms like the aforementioned *Vg1* mRNA in *X. laevis* oocytes (Yisraeli J.K. *et al.*, 1990) or *bicoid* mRNAs in the oocytes and embryos of *D. melanogaster* (Weil T.T. *et al.*, 2008).

Myo4p represents one of two type V myosin motors that are involved in the actin-based cargo transport. The protein is required for the mRNA transport and also assisting the movement and growth of ER tubular structures to the bud along actin cables together with She3p (Jansen R.P. *et al.*, 1996; Münchow S. *et al.*, 1999) while Myo4p is associated with the N-terminal domain of She3p (Böhl F. *et al.*, 2000).

In contrast to Myo4p that acts as the molecular motor and thus is necessary for the mRNA trafficking (Paquin N. and Chartrand P. 2008), but is not essential (Jansen

R.P. *et al.*, 1996) the essential Myo2p is required for the polarized delivery of the vacuole, secretory vesicles, late Golgi elements, the mitotic spindle, mitochondria and peroxisomes (Altmann *et al.*, 2008; Pruyne D. *et al.*, 2004). Both Myo4p and Myo2p are motor proteins with a very low processivity (Reck-Peterson S.L. *et al.*, 2001). The presence of multiple binding sites on a presumptive cargo like multiple zipcodes within a localized mRNA might ensure the processive cargo transport (Darzacq X. *et al.*, 2003).

Previous studies show that Myo4p does not move to the bud tip in the absence of She3p suggesting that Myo4p has to be associated with its adapter She3p or with the cargo that has to be transported (Jansen R.P. *et al.*, 1996).

1.4.2.1.3 She3p, adaptor and RNA-binding protein

She3p that is recruited by She2p (Darzacq X. *et al.*, 2003) and links the motor protein Myo4p with She2p-*ASH1* mRNA (Martin K.C. and Ephrussi A., 2009) represents the typical characteristics for an adaptor protein. While She3p is able to associate with the RNA-binding protein She2p via its C-terminal domain (Böhl F. *et al.*, 2000), She3p is also able to associate with its N-terminal to the C-terminal tail of Myo4p and its coiled-coil. This results in the linkage between She2p and Myo4p and thus the formation of the locosome (Gonsalvez G.B., Urbinati C.R. and Long R.M., 2005).

While Myo4p is able to associate with the N-terminal domain of She3p the C-terminal domain of She3p is in turn able to associate with She2p (Böhl F. *et al.*, 2000, Long R.M. *et al.*, 2000; Heuck A. *et al.*, 2007; Takizawa P.A. *et al.* 2000) and thus forms the locosome (Gonsalvez G.B., Urbinati C.R. and Long R.M., 2005). Together with Myo4p, She3p is an exclusively cytoplasmic protein (Darzacq X. *et al.*, 2003).

She3p was also identified to be able to bind to specific mRNAs. In the previous study of Elson S.L. *et al.*, 2009 using the yeast *Candida albicans* as model organism immunoprecipitation of She3p-mRNA revealed its association with a set of mRNAs. This binding occurs independent of She2p which is absent in this organism. Another study (Müller M. *et al.*, 2011) showed that She3p is able to bind independently on She2p to zipcode elements of both *ASH1* and *EAR1* mRNAs. Thus, in both studies the RNA-binding protein She3p was identified and therefore the RNA-binding ability in the core complex of the locosome is no more “exclusive” for She2p.

1.4.2.2 Puf6p, Khd1p, Loc1p

Besides She2p, She3p and Myo4p that are the core components of the locasome other proteins affecting the localization of *ASH1* mRNA were identified. These proteins (Table 2) are playing other roles during the trafficking process supported by the fact that their deletion affects processes like translation, motor-driven motility and cell polarization (Darzacq X. *et al.*, 2003).

Protein	Alternative names	Function	Role in <i>ASH1</i> mRNA localization	Locasome association	Subcellular association	Δ phenotype bud/bud tip
She1p	Myo4p	Unconventional myosin V type motor	Locasome molecular motor	Yes	C, bud enriched	Abolished
She2p		RNA-binding	Binds <i>ASH1</i> mRNA zipcodes	Yes	N/C, bud enriched	Abolished
She3p		Myosin binding protein	Molecular link in between She2p and She1p	Yes	C, bud enriched	Abolished
She4p	Dim1p	Endocytosis Enhance association of Myo3p and Myo5p to the actin network Interacts with She1p	Enhance association of She2p to the actin network?	Yes	C, bud enriched	nd/nd bud neck
She5p	Bn1p, Ppf3p	Actin filament polymerisation at the bud tip Bud growth Establishment of cell polarity	Polarization and growth of the actin network Interacts with Bud6p (Two-hybrid and synthetic lethality)	No	C, bud tip	nd/nd bud neck/bud enriched
Bud6p	Aip3p	Actin filament organisation at the bud tip Bud growth Establishment of cell polarity	Polarization and growth of the actin network Interacts with She5p (Two-hybrid and synthetic lethality)	No	C, bud tip	nd/nd bud enriched
Loc1p		RNA-binding rRNA processing	Binds <i>ASH1</i> mRNA zipcodes, general translation defect?	Yes (nucleus)	No	nd/13
Khd1p	Hek2p	RNA binding, KH domain	Involved in mRNA bud tip anchoring, translational repression	Yes	C	93/40
Puf5p	Mpt5p, Htr1p, Uth4p	Translational regulation mRNA Stability	Involved in mRNA bud tip anchoring Translational regulation?	No	nd	83/22
Scp160p		RNA binding, KH domain ER polysomes binding	Involved in mRNA bud tip anchoring Translational regulation?	No	C	84/23

C, Cytoplasmic; N, Nuclear; No, nucleolar; deletion phenotype is shown as: percentage of cells showing daughter cell localization of *ASH1* mRNA/percentage of cells showing daughter cell bud tip localization of *ASH1* mRNA. The wild type strain shows a phenotype of 99/98.

Table 2 | List of proteins that are involved in *ASH1* mRNA localization. Table modified from Darzacq X. *et al.*, 2011.

Besides the core locasome three other proteins namely Khd1p, Puf6p and Loc1p are necessary for the *ASH1* mRNA localization efficiency and the translational silencing of the mRNA in yeast (Irie K. *et al.*, 2002; Gu W. *et al.*, 2004; Paquin N. *et al.*, 2007).

Loc1p is a nuclear protein that associates with *ASH1* mRNA and thus is involved in the *ASH1* mRNA localization and early *ASH1* mRNP formation (Darzacq X. *et al.*, 2011). It is additionally involved in export and assembly of ribosomes. It has been shown that Loc1p is required for the binding between *ASH1* mRNA and She2p and therefore Loc1p belongs to a class of proteins which affect the recruitment of a RNA-binding protein in the nucleus (Long R.M. *et al.*, 2001; Martin K.C. and Ephrussi A., 2009). Identified as a protein that is in case of its deletion affecting *ASH1* mRNA Loc1p is able to bind to E3 and E1 zipcodes. In a $\Delta loc1$ strain the *ASH1* mRNA could not be correctly localized. Additionally, the restricted Ash1p localization in the daughter cell nucleus was strongly affected (Long R.M. *et al.*, 2001). However, it is yet unknown if the delocalized phenotype of *ASH1* mRNA is directly caused by loss of Loc1p or if it is caused by a translational defect (Darzacq X. *et al.*, 2011).

Puf6p (Pumilio-homology domain protein) is a protein that binds to the 3'UTR of the *ASH1* mRNA and represses its translation. This repression is required for the proper asymmetric *ASH1* mRNA localization and the daughter specific translation (Gu W. *et al.*, 2004; Li Z. *et al.*, 2009). Because of the fact that Puf6p is detected in the nucleus it might also associate with the *ASH1* mRNA already in the nucleus (Shav-Tal, Y. and Singer R.H. *et al.*, 2005).

Khd1p belongs to the locasome and is the only of these three proteins that co-localizes with the *ASH1* mRNA to the bud tip. Thus, it might have a direct role in the localization of mRNA (Irie K. *et al.*, 2002). During this transport it inhibits translation of the localized mRNA. Previous studies have shown that Khd1p interacts with the E1 zipcode (Paquin N. *et al.*, 2007) of *ASH1* mRNA explaining the observed co-localization with the locasome. Additionally, it has been reported that Khd1p is affecting the anchoring of the *ASH1* mRNA to the distal tip and experiments with overexpressed Khd1p lead to a reduction of the cellular amounts of the Ash1p protein and thus might decrease its translation (Irie K. *et al.*, 2002). Thus, Khd1p might have a more specific role at the bud tip (Darzacq X. *et al.*, 2011).

Altogether these proteins are important for the correct *ASH1* mRNA trafficking and translational silencing during the transport of localized mRNAs.

1.5 Inheritance of cortical endoplasmic reticulum in *S. cerevisiae*

Interestingly, the Myo4p-She3p co-complex that is an important part of the core locosome and thus essential for the mRNA localization machinery is also involved in a second transport procedure that is directed towards the bud namely the inheritance of cortical ER (cER; Estrada P. *Et al.*, 2003).

1.5.1 Function of the ER

The sustainment of the complex architecture in eukaryotic cells needs e.g. newly synthesized proteins that are delivered to their definite locations (Hugh R.B. *et al.*, 1988). In eukaryotic cells like the yeast *S. cerevisiae* the cellular functionalities are compartmentalized into organelles that are bound to membranes (Lowe M. and Barr F.A. 2007). Because of different morphology and function the ER can be divided into three distinct sub-domains: smooth ER (sER), rough ER (rER) and translational ER (tER) that altogether represent a variety of functions (Estrada de Martin P. *et al.*, 2005; Voeltz G.K. *et al.*, 2007). While the sER is characterized by biosynthesis of phospholipids, steroids and cholesterol and the absence of membrane-associated ribosomes, the tER is a particular type of the sER that is characterized by vesicle budding and packaging of cargoes (Baumann O. *et al.*, 2001; Estrada de Martin P. *et al.*). The rER is distinguished by ribosomes associated with its cytoplasmic face. The rER is also characterized by the fact that it is in charge of all processes that are linked to membrane proteins and the biogenesis of secretory proteins.

Altogether, the ER contains regions that are characterized by forming a highly organized system of tubules, interconnected cisternae and fenestrations. For generating and maintaining these structures as well as those of other organelles like the Golgi complex special mechanisms are required.

The ER and most membrane-bound organelles are characterized by their complex and dynamic shape that often include regions of various morphologies (Munro S. 2004; Voeltz G.K. *et al.*, 2007). Their membranes are characterized by parameters like membrane thickness, fluidity, surface charge and their ability to bend and curve.

To generate and maintain these structures and abilities, various mechanisms have been proposed like proteins that are required to stabilize highly curved membranes. Thus, curvature is required to maintain different shapes like tubules, cisternae and others (Voeltz G.K. *et al.*, 2007) and will therefore be described in more detail in the next section.

The curvature within the ER membranes can be generated by three mechanisms (Figure 9).

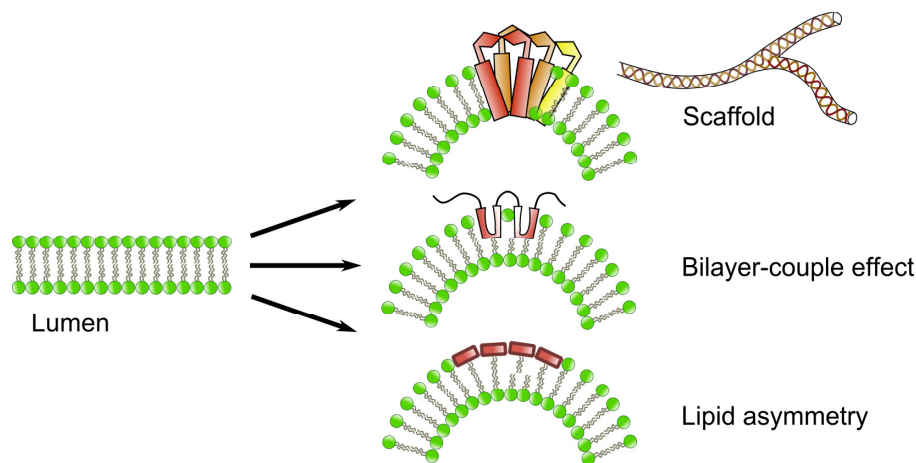


Figure 9 | Three mechanisms to generate high membrane curvature. This scheme of generating high curvature of organelle membranes in general is showing the three possible mechanisms; scaffolding, bilayer-couple effect and lipid asymmetry. For more detailed information see text. Figure adapted from Voeltz G.K. *et al.*, 2007.

First, integral membrane proteins are inserted with their transmembrane domains into the membrane bilayer. Oligomerizing and the formation of a protein scaffold which has an angle of curvature results in bending the membrane. Secondly, a protein might integrate into one layer only which results in a larger outer leaflet than the inner leaflet. This will curve the bilayer caused by the so-called bilayer-couple effect. This phenomenon describes the possibility that the hydrophobic interactions between two leaflets tend to keep coupled. This second mechanism might result in introducing the curvature in ER tubules by proteins of the reticulon (Rtn) family. Finally, the curvature can be generated by the asymmetric distribution of lipids that are located between the leaflets of the membrane bilayer (Voeltz G.K. *et al.*, 2007).

The ER can additionally be divided into two classes of ER structures namely the perinuclear ER and the peripheral ER (Rose M.D. *et al.*, 1989; Preuss D.J. *et al.*, 1992). While the perinuclear ER is identical with the nuclear envelope (NE), the

cortical ER forms a highly dynamic network consisting of interconnected tubules that forms the periphery (Figure 10).

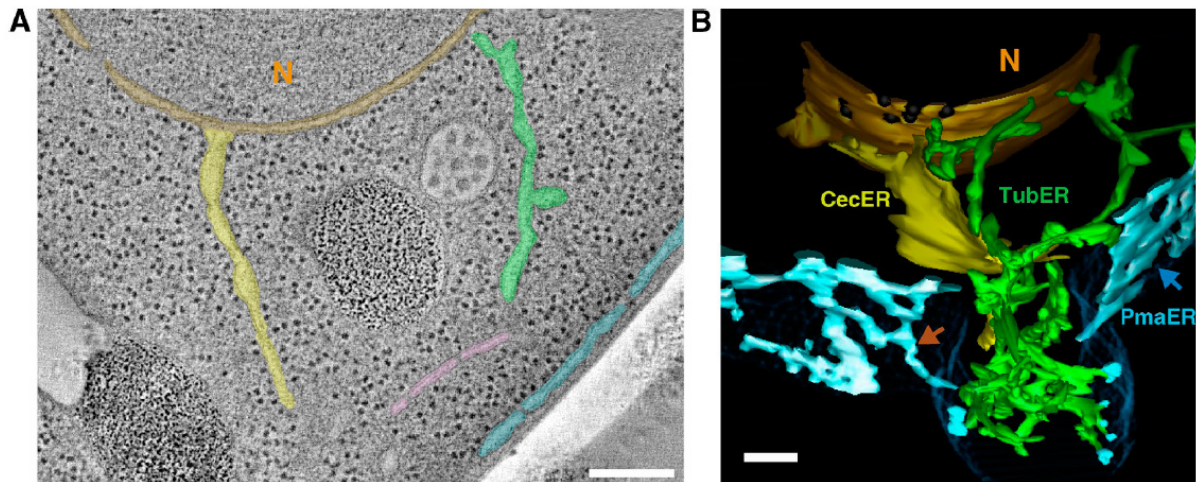


Figure 10 | 3D structural analysis of ER morphology. (A and B) 2D tomography derived from a 200 nm thick section shows the NE (orange), pmaER (plasma membrane associated ER), cecER (central cisternal ER), tubER (tubular ER) and Golgi (pink; A) and corresponding 3D model (of A) shows all ER domains in a wild type yeast cell (bud size = 665 nm; B). The blue shade is the PM. N is the nucleus. Black holes on the NE are nuclear pores. The orange arrow points to a more tubular pmaER structure, whereas the blue arrow points to a fenestrated cisternal pmaER. Bars: (A) 200 nm; (B) 100 nm. Figure adapted and text modified from West M. *et al.*, 2011.

Some individual large tubules are stretched across the cytoplasm and therefore connect the peripheral ER with the perinuclear ER (Voeltz G.K. *et al.*, 2002). This highly dynamic network is similar to higher eukaryotes but positioned underneath the cell cortex (Prinz W.A. *et al.*, 2000) and thus also named cortical ER. It is also characterized by the fact that it undergoes frequent tubule branching movements and ring closures of an ER loop to a single tubule.

1.5.2 Inheritance of the ER

In budding yeast the largest sub-domain of the ER is a network of cortical ER (cER) that associates to the plasma membrane (Loewen J.R.C. *et al.*, 2007). Since ER cannot be synthesized *de novo* during cell division, but has to be assigned from the mother to the daughter (Du Y. *et al.*, 2004) the mother cell undergoes a so-called closed mitosis. This means that the nucleus-surrounding ER and the NE itself remains intact. During this closed M-phase the microtubule cytoskeleton transports one nucleus together with its perinuclear ER to the daughter cell (Fagarasanu A. *et al.*, 2007; Lowe M. *et al.*, 2007). Besides the perinuclear ER that is essential for the

ER inheritance the cortical ER also plays an important role during cell division. While the perinuclear ER is partitioned in M-phase to the daughter cell, the cortical ER inheritance occurs earlier and starts during the process of budding (Loewen J.R.C. *et al.*, 2007). This process facilitates the local synthesis of the bud and therefore initiates ER inheritance. In the following these processes are described in detail.

The inheritance of the ER in *S. cerevisiae* is a multi step mechanism that is temporarily ordered (Figure 11). The delivery of cER from mother cells to buds, termed cER inheritance, occurs as a process early in budding (Loewen J.R.C *et al.*, 2007) and is dependent on actin cables (Estrada P. *et al.*, 2003). The segregation of ER occurs when tubular structures effuse from the perinuclear ER and move towards the bud in a Myo4p-She3p-dependent manner. This movement starts at S-phase (Du Y. *et al.*, 2004; West M. *et al.*, 2011). The first cER elements that can be observed are cytoplasmic ER tubules that are oriented along the axis between mother and bud (Du Y. *et al.*, 2001). These tubules can either associate with the pre-bud site and thus be passively pulled into the bud during bud growth (Fehrenbacher K.L. *et al.*, 2002) or can migrate into the daughter cell after bud emergence (Du Y. *et al.*, 2001). The tubular formation and their alignment along the mother-bud axis implicate that this orientation is dependent on a polarized structure like the actin cytoskeleton. In case of actin filaments the actin is required for the ER dynamics and motility and in case of other organelles for its inheritance (Catlett N.L. *et al.*, 2000; Prinz W.A. *et al.*, 2000; Fehrenbacher K.L. *et al.*, 2002; Wöllert T. *et al.*, 2002).

The ER inheritance itself can be divided into three distinct phases (Figure 11).

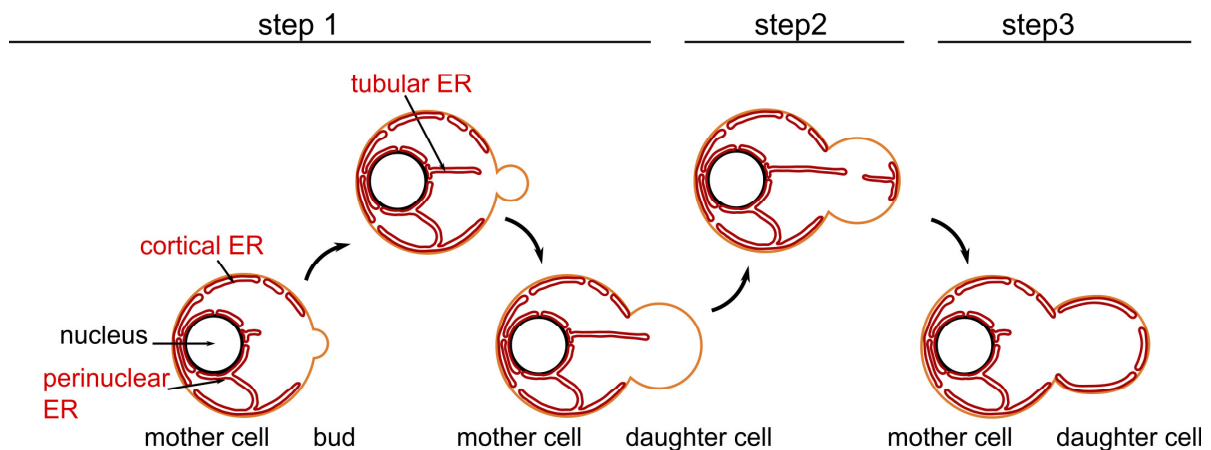


Figure 11 | The three steps of the ER inheritance in *S. cerevisiae*. The Schematic drawing shows the ER inheritance in yeast *S. cerevisiae* that can be divided into three steps; First, cytoplasmic ER tubules are moving from the mother cell towards the small bud along actin cables over the relatively long distance of the mother-bud axis. After reaching the bud the second step occurs; the first domain of cER associates to the plasma membrane at the bud tip (Loewen J.R.C *et al.*, 2007). Finally, in the third step the cER spreads around the entire bud and forms a polygonal tubular network (Fehrenbacher K.L. *et al.*, 2002; Du Y. *et al.*, 2006).

First, cytoplasmic ER tubules move from the mother cell towards the small bud along actin cables over the relatively long distance of the mother-bud axis. After reaching the bud the first domain of cER is associated to the plasma membrane (Loewen J.R.C *et al.*, 2007). The associational step itself might be facilitated by interactions of reticulons (Rtn1p, Rtn2p and Yop1p: see below) with components of the translocon machinery (Sbh1p and Sbh2p) and the exocyst complex (Sec3p, Sec6p and Sec8p). This suggestion was supported by experiments where these components were deleted leading to delayed ER inheritance (Wiederkehr A.Y. *et al.*, 2003; Reinke C.A. *et al.*, 2004; De Craene J.O. *et al.*, 2006). In a final step the cER spreads around the entire bud and forms a polygonal tubular network (Fehrenbacher K.L. *et al.*, 2002; Du Y. *et al.*, 2006).

Besides the aforementioned factors, a large number of additional proteins are required for proper cER segregation. Ypt11p is a member of the Rab protein family and interacts with the C-terminal tail domain of Myo2p. The Rab family consists of peripheral membrane proteins that are anchored to a membrane by the lipid prenyl group that is covalently linked to two cysteines in the C-terminus. It was reported that Rab11p is located on the ER and that it is enriched in the peripheral ER of the daughter cell indicating that it also plays a possible role during ER inheritance (Buvelot Frei S. *et al.*, 2006).

Ice2p is an integral ER membrane protein consisting of type-III transmembrane domains. Mutations of Ice2p are causing morphology defects of the cortical ER in mother and daughter cell suggesting a role in ER inheritance (Estrada de Martin P. *et al.*, 2005)

Swa2p (Aux1p) is also implicated to have a role during ER inheritance. The protein Auxilin is also known as DnaJ family member because of its J-domain that is critical for its interaction with Hsc70 (Hennessy F. *et al.*, 2005). Auxilin was first identified in mammals (Ungewickell E. *et al.*, 1995) and is a co-factor in the Hsc70-mediated disassembly. Auxilin is required for uncoating of clathrin vesicles and thus for the clathrin recycling in cells (Gall W.E. *et al.*, 2000). Aux1p is an auxilin-like protein that localizes to ER membranes. Besides its function in uncoating of clathrin it is also known to be required for cER inheritance (Du Y. *et al.*, 2001; Du Y. *et al.*, 2010).

Nbp2p and Ptc1p that are both regulators of the mitogen-activated protein kinase (MAPK) signaling pathway, it has been shown to function during cER inheritance. Ptc1p is a serine/threonine phosphatase that regulates cell wall integrity (CWI) MAPK pathway and as most important for this study Ptc1p is known for having a role during late steps of cER segregation by regulating the cER inheritance via Slt2p (Du Y. *et al.*, 2006).

Additionally, Scs2p is a highly conserved integral ER membrane protein that regulates phospholipid metabolism. It was shown that Scs2p is required for cER inheritance (Kagiwada S. *et al.*, 1998; Loewen C.J.R. *et al.*, 2005 and 2007). If cells lack Scs2p a strong defect in ER segregation can be observed (Estrada P. *et al.*, 2003).

Finally, as I already mentioned the myosin V motor protein Myo4p and its adaptor She3p that are carrying ER tubules into the budding cell are playing an important role during ER inheritance (Estrada P. *et al.*, 2003).

1.6 Reticulons

The reticulons are a family of proteins that are present in all eukaryotic organisms like *X. laevis*, *D. rerio*, *D. melanogaster*, *C. elegans* and *S. cerevisiae* but not in bacteria or archaea (Moreira E.F. *et al.*, 1999; Oertle T. *et al.*, 2003; Diekmann H. *et al.*, 2005; Voeltz G.K. *et al.*, 2006; Wakefield S. *et al.*, 2006; Nziengui H. *et al.*, 2007). This observation indicates that the evolutionary evolution of reticulons is closely associated with that of the ER or endomembrane system of eukaryotes. Structurally, all family members contain a reticulon homology domain (RHD) that is a conserved region at the carboxy-terminal end and consist of two hydrophobic regions flanking a hydrophilic loop. However, the amino acid sequence identity of the RHDs between e.g. *C. elegans* and *S. cerevisiae* is about only 15-50% (Yang Y.S. and Strittmatter S.M., 2007). This RHD region could both be detected intracellular and on the surface of cells. This suggests that the RHD hydrophobic regions are able to completely span the plasma or ER membrane (Oertle T. *et al.*, 2003).

Reticulons may play a role in nuclear pore complex and vesicle formation (Yang B.C. *et al.*, 2007), but in addition they are necessary for bending and shaping ER tubules by generating the high curvature that is required to form tubular membrane structures. For ER segregation not only their role in tubule formation, but also during the association phase has been reported (Wiederkehr A.Y. *et al.*, 2003; Reinke C.A. *et al.*, 2004; De Craene J.O. *et al.*, 2006). Additionally, reticulons are involved in apoptosis and the transport of cargoes from the ER to the Golgi system (Voeltz G.K. *et al.*, 2006; Yang Y.S. and Strittmatter S.M., 2007).

In baker's yeast two reticulons do exist, Rtn1p and Rtn2p. Rtn1p is a member of the reticulon-like A (RTNLA) family interacting with Sey1p to maintain ER morphology and also interacting with the exocyst subunit Sec6p, Sbh1p and with Yip3p. Sec6p is an essential protein of the exocyst complex (TerBush D.R. and Novick P. 1995), while Sbh1p is involved in protein translocation into the ER (Toikkanen J.H. *et al.*, 2003). It interacts with Rtn1p and with the exocyst complex (Feng D. *et al.*, 2007). Yip3p is a protein that is proposed to be involved in ER to Golgi transport. It also interacts with Rtn1p and members of the aforementioned Rab family (Otte S. *et al.*, 2001; Calero M and Collins R.N. 2002). In case of null mutants of Sec6p, Sbh1p or Yip3p an altered ER morphology was observed (Oertle T. *et al.*, 2003; Geng J. *et al.*, 2005; De Craene J.O. *et al.*, 2006; Feng D. *et al.*, 2007; Hu J. *et al.*, 2009). Rtn2p is

a protein with a yet unknown function but has similarity to mammalian reticulons and is also a member of the RTNLA subfamily (Oertle T. *et al.*, 2003). Both Rtn1p and Rtn2p interact with DP1/Yop1p. Yop1p is a membrane protein that interacts with Yip1p to mediate membrane traffic and that interacts with Sey1p to maintain ER morphology (Voeltz G.K. *et al.*, 2006). Yop1p helps to generate the high curvature that is important for the tubular formation of membrane structures with 50 nm diameters in mammals and 30 nm in yeast (Hu J. *et al.*, 2008).

Previous studies have shown that in case of triple knock out mutants of Rtn1p, Rtn2p and Yop1p the ER shape changes dramatically (West M. *et al.*, 2011; Figure 12). In contrast a single knockout of Rtn1p results in the reorganization of the cER from a highly reticulated to a cisternal structure but without any significant changes in the total membrane surface of the ER (De Craene J.O. *et al.*, 2006; Figure 13; Yang Y.S. and Strittmatter S.M., 2007).

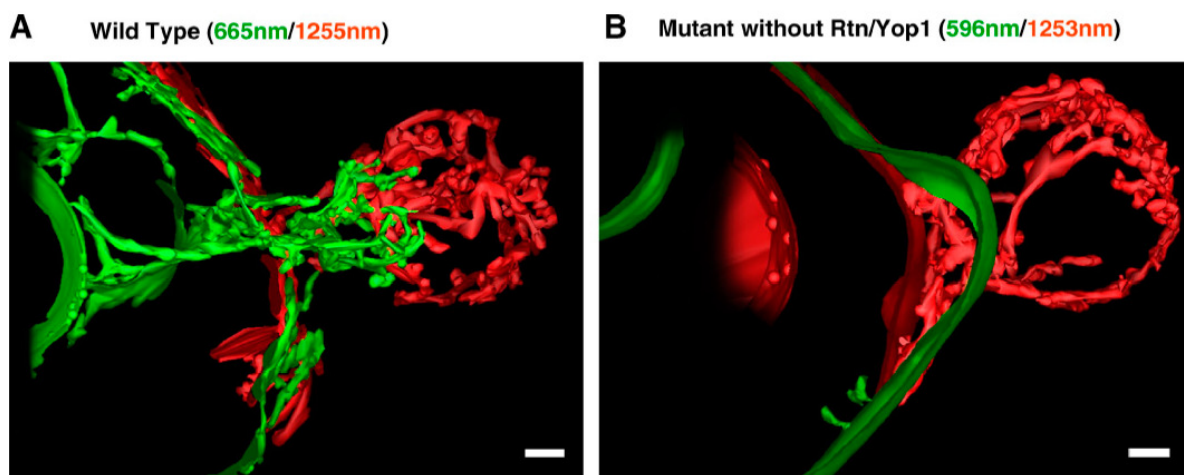


Figure 12 | Dramatic changes in ER shape and curvature occur in the absence of Rtns/Yop1p. (A) 3D model of ER in a wild type cell with a 665-nm bud and a 1,255-nm bud that were overlaid to show the transition of ER domains into the bud. (B) As in A for corresponding mutant cells. Note the loss of membrane curvature throughout the mother of both mutant cells. However, the ER is still inherited by an Rtns/Yop1p-independent process into the bud. Bars: 200 nm. Figure and text adapted from West M. *et al.*, 2011.

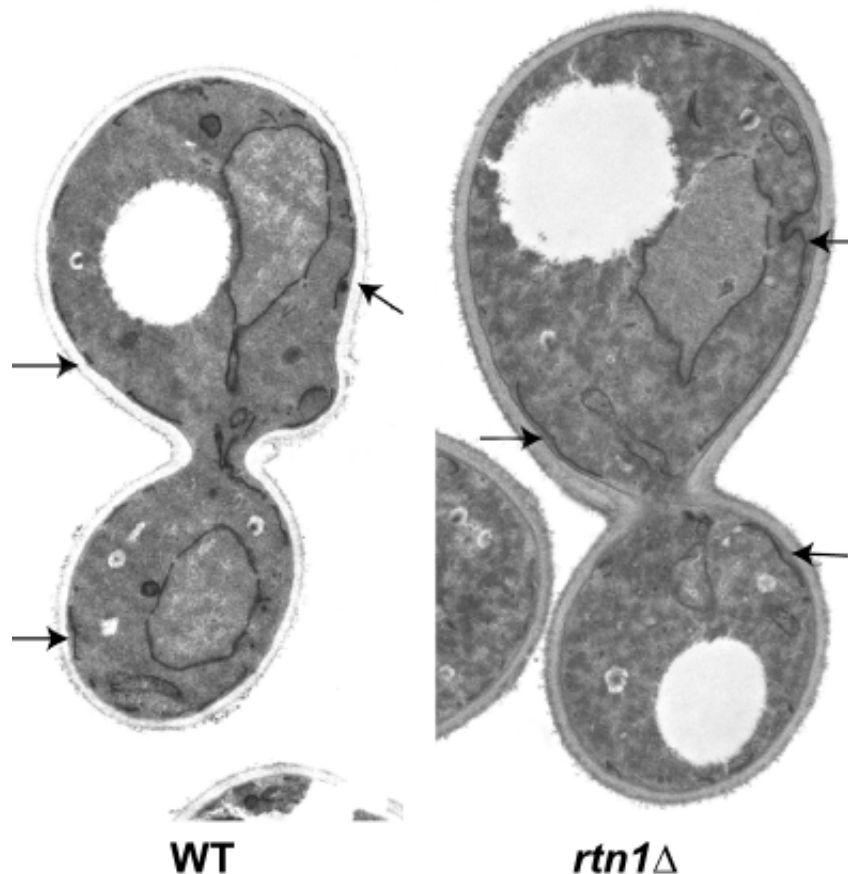


Figure 13 | Rtn1p is required for the structure of the ER. Thin section electron microscopy micrographs of wild type (NY1210) and *rtn1* Δ (NY2651) cells. Arrows point to ER membrane stretches. Magnification: 4700 x. Figure and text adapted from De Craene J.O. *et al.*, 2006.

Reticulons are interacting with proteins that are involved in vesicular formation and fusion like soluble N-ethylmaleimide-sensitive-factor attachment receptors (SNAREs) and synaptosomal-associated proteins (SNAPs). Reticulons also play a role in ER morphogenesis.

1.7 Indications for the co-transport of mRNA and ER in *S. cerevisiae*

As aforementioned, Myo4p and She3p are key components of the core locosome and as a complex are essential for transporting localized mRNAs towards the bud tip. Additionally, this Myo4p-She3p co-complex is also required for the proper localization of cortical ER (Estrada P. *Et al.*, 2003).

The transport of localized mRNA in form of an mRNP complex driven by a motor protein in the core locosome on the one hand and the Myo4p-She3p assisted transport of ER tubules on the other hand imply a connection between the mRNP

trafficking and ER transport. This leads to the question if this connection is direct, specific, if this is the basis of a coordinated co-transport and finally, if these two transport mechanisms are irremediable linked to each other.

During previous studies this idea was supported by an experiment designed to follow the trafficking of both ER and mRNPs (Schmid M. *et al.*, 2006; Figure 14).

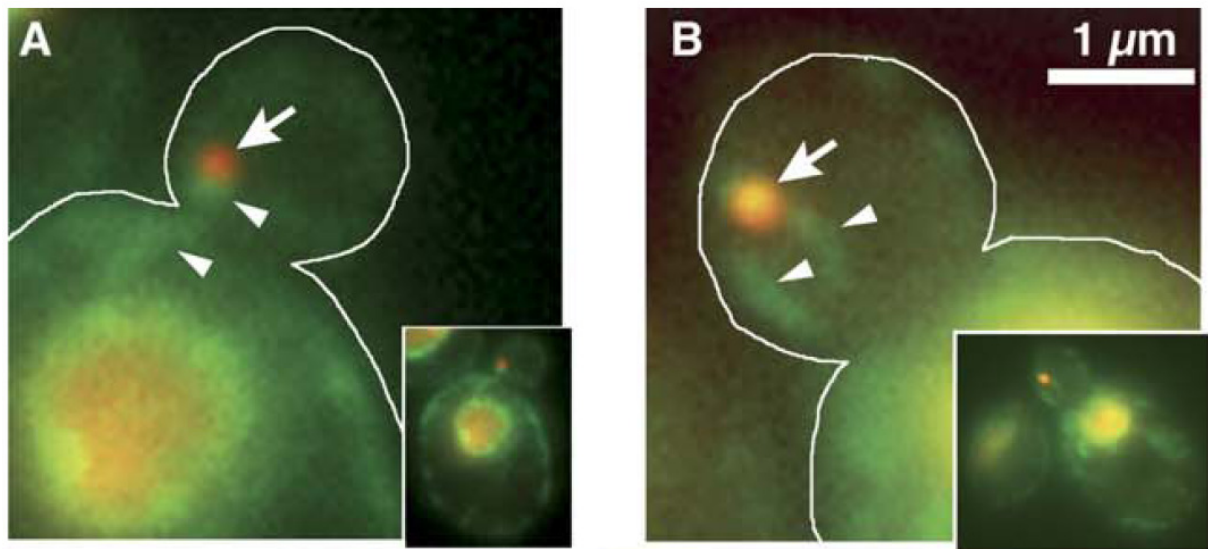


Figure 14 | Co-localization of *ASH1-MS2* mRNP particles with tubular ER in the bud. (A and B) Representative examples of cells from strain RJY2339 with *ASH1-MS2* mRNP particles (arrows) labeled by MS2-RedStar fusion protein and ER tubules (arrowheads) labeled by Hmg1p-GFP fusion protein. *ASH1-MS2* particles (red) co-localize with the tip of ER tubules (green) in the bud. Figure and text adapted from Schmid M. *et al.*, 2006.

For these experiments a tagged *ASH1* mRNA was used containing six MS2 binding sites in its 3' UTR. *ASH1* mRNA was chosen because it is well studied, dependent on Myo4p and She3p, and if expressed at any selected stage of the cell cycle localizes efficiently to the bud (Long R.M. *et al.*, 1997). Expressed from a *GAL1* promoter this *ASH1-MS2* mRNA was then visualized by the co-expression of the MS2 coat protein (MS2-CP) that was fused to RedStar, a red fluorescence protein. To allow a better visualization of RNP complexes in the cytoplasm the MS2-CP-RedStar fusion contains a nuclear localization signal for targeting unbound protein to the nucleus (Bertrand E. *et al.*, 1998). ER tubules were visualized by a fusion of hydroxymethylglutaryl-coenzyme A reductase (Hmg1p) with GFP. Hmg1p is required for ergosterol synthesis and is characterized as an ER-resident protein. GFP fused to Hmg1p is both present in cER and perinuclear ER and in motile ER tubules (Estrada P. *Et al.*, 2003).

During these observations it was also shown that *ASH1* mRNP binds to the tip of ER membrane tubules suggesting that the correct curvature of the ER tubules is important for the correct transport of *ASH1-MS2* mRNPs.

An additional experiment showed that the *ASH1-MS2* mRNP binding to the ER tubule is independent on the Myo4p-She3p co-complex since deletion of *MYO4* did not disturb RNP-tubule association (Figure 15). However, in contrast to the wild type no *ASH1-MS2* particles were visible in the bud and the labeled tubule does not show directional movement towards the bud.

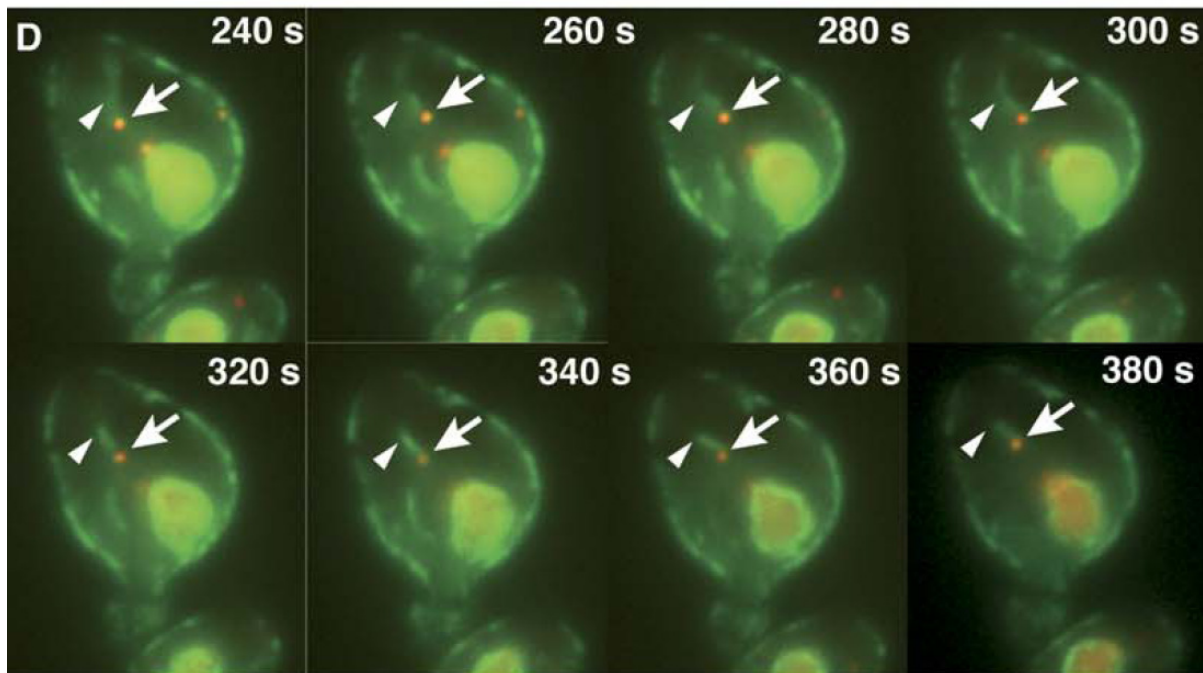


Figure 15 | Co-localization of *ASH1-MS2* mRNP particles with tubular ER in the bud. (D) Co-localization of *ASH1-MS2* mRNP with ER tubules in the absence of Myo4p. Individual images from a time-lapse series of strain RJY2372 showing MS2-RedStar labeled *ASH1-MS2* mRNP particle (red, arrow) associated with tubular ER structures (green, arrowhead) in the mother cell. In contrast to wild type cells, the marked tubule does not show directional movement to the bud and that no *ASH1-MS2* particles are visible in the bud (at the bottom of the cell). Figure adapted and text modified from Schmid M. *et al.*, 2006.

These findings match previous data indicating that Myo4p-dependent tubule transport might not be the only mechanism to segregate ER tubules into the bud (Reinke C.A. *et al.*, 2004).

In vitro experiments with recombinant She2p in a sucrose velocity gradient centrifugation supported the assumption of it being a candidate for the association of specific mRNAs to ER tubules (Schmid M., Dissertation 2008). In these experiments

bacterially expressed and purified She2p was incubated with a cell extract of a yeast strain lacking She2p. These results show that She2p co-migrates with ER also supported by previous experiments done by Schmid M. *et al.*, 2006 and Aronov S. *et al.*, 2007 with She2p which binds to localized mRNAs and co-fractionates with the ER even after mRNA degradation or polysomal disruption.

Besides yeast, evidence for a link between ER and mRNPs also exists in other organisms. One example is *X. laevis*. The aforementioned *Vg1* mRNA that is bound to the RNA-binding Vera protein associates with ER membranes. Although not understood in much detail ER transport is also proposed to have a function during the localization of *Vg1* mRNA (Deshler J.O. *et al.*, 1997).

Altogether, the yeast studies suggest that *ASH1-MS2* mRNPs are moving together with ER tubules in a coordinated manner suggesting a coordination of cER distribution and mRNA localization (Figure 16).

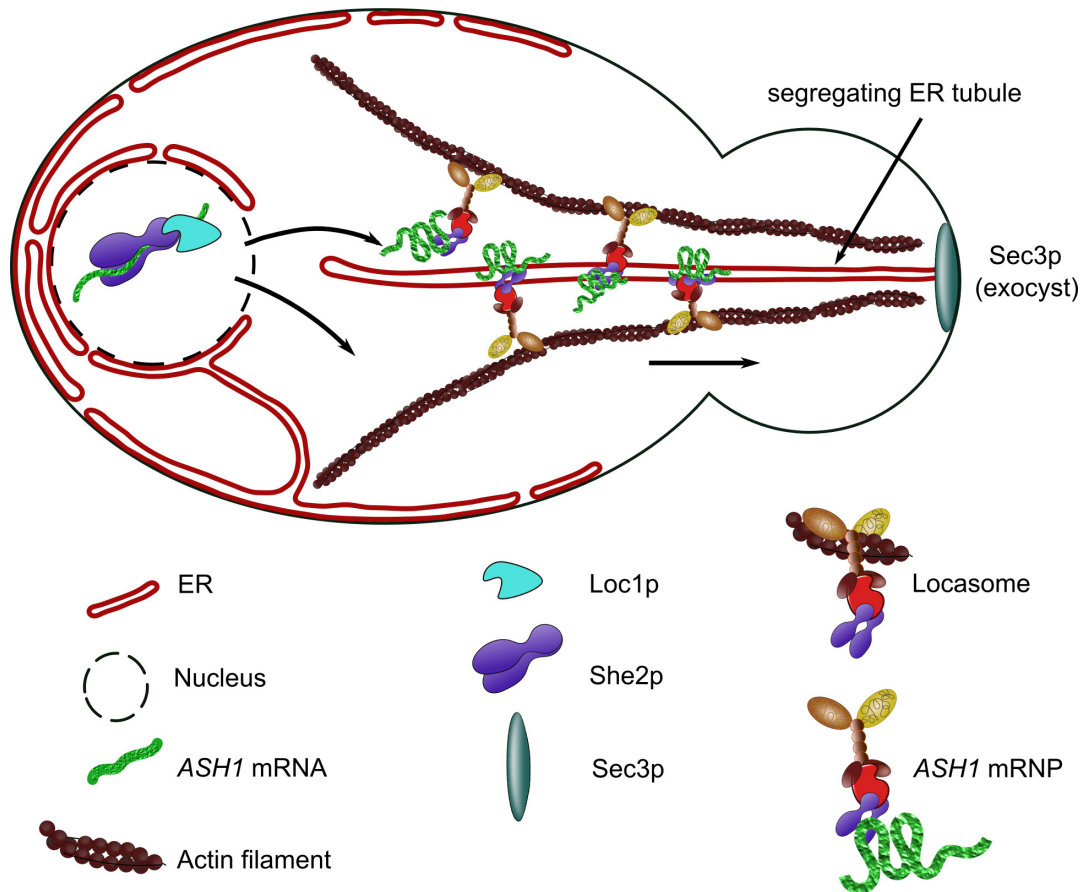


Figure 16 | Model for the mRNA localization in *S. cerevisiae*. Schematic drawing shows the dependency of the mRNA localization in *S. cerevisiae* on the Myo4p motor protein. The mother cell is shown on the left side while the growing bud is shown on the right side. After transcription in the nucleus the *ASH1* mRNA is recognized by the RNA-binding protein She2p. Then Loc1p is interacting with She2p and the complex is joined by Puf6p and Khd1p (not shown for reasons of simplicity). By passing through the nucleus the complex is exported into the cytoplasm. In the cytoplasm the core locasome is formed by a ternary interaction of She2p, the adapter protein She3p and the motor protein Myo4p. Together with the *ASH1* mRNA the *ASH1* mRNP is transported towards the bud. During the transport the translation is repressed by Puf6p. Additionally, the Myo4p-She3p co-complex is required for the translocation of cortical ER and thus is attached to ER tubular structures. The complex is transported along actin cables consisting of actin filaments and then reaches the bud tip where Sec3p is located. Sec3p is responsible for the stabilization of the cortical association of ER tubules that are delivered into the bud. The *ASH1* mRNA gets anchored and translated and the Ash1p protein gets produced.

1.8 Aim of this work including experimental background

mRNA localization and inheritance of cER are two transport mechanisms that appear to be highly coordinated for the reproduction not only in yeast cells. As shown in section 1.7 first evidence for a link between the ER inheritance and mRNA transport does exist.

The main aim of this work was to find additional evidence for the link between mRNA localization and ER inheritance in budding yeast *S. cerevisiae*. As aforementioned

(1.4), most of the localized mRNAs in yeast are encoding for secreted or membrane proteins. So it could be more efficient if these mRNAs were pre-assembled and transported together with the organelle (i.e. ER) where they are translated and then processed.

To test this hypothesis *in vivo* different mRNAs were chosen that have different roles at different stages of cell growth (section 1.8.2). To recapitulate first evidence for the co-localization of ER and mRNA, as shown in section 1.7 and to improve this *in vitro*, sucrose velocity gradient centrifugation and She2p binding experiments were performed. This was done by using recombinant mutant versions of She2p protein incubated together with purified membranes of strains lacking the recombinant She2p and further processed in a sucrose velocity gradient centrifugation on the one hand or by using a pelleting assay with increasing amounts of recombinant She2p together with purified ER microsomes on the other hand. With this experiments *in vitro* the binding of She2p to the ER has to be characterized and thus to find evidence if this binding is direct and specific or if other binding partners are involved. Additionally, the *in vitro* methods all together will narrow down potential ER-mRNA linker to specific candidates.

1.8.1 Visualization of mRNPs

To visualize the localization of endogenous mRNAs of interest *in vivo* the method introduced by Haim L. *et al.*, 2007 was used. In principle, using a PCR based genomic integration method based on homologous recombination a DNA sequence coding for 12xMS2 stem loops (12xMS2L) of the MS2 phage are introduced into the 3'UTR of the corresponding gene of interest. Co-expression of the MS2-CP that is fused to three copies of fluorescent protein GFP enables visualization of the tagged mRNA by live cell imaging.

1.8.2 mRNAs of interest

For the *in vivo* experiments the mRNAs *EAR1*, *IST2*, *SRL1*, *MID2*, *WSC2* and *ASH1* were chosen and then visualized using the MS2-tagging system (Haim L. *et al.*, 2007). Besides *ASH1* these mRNAs are expressed during S-phase or between G1- and G2-phase (Shepard K.A. *et al.*, 2003) and thus allows testing whether mRNAs present at different stages of the cell cycle are transported in different ways (Table 3). By using ER markers together with the MS2-tagged versions of the mRNAs and

observing the mRNP transport by live cell imaging this additionally would allow a deeper insight into the transport mechanism of mRNPs and the dependency on ER inheritance. This would show whether the transport of mRNAs and the segregation of ER occurs chronologically or simultaneously.

mRNA	expressed during cell cycle	RNP distribution (WT)
<i>IST2</i>	always	
<i>EAR1</i>	always	
<i>MID2</i>	always	
<i>ASH1</i>	M phase	
<i>SRL1</i>	G1 phase	
<i>WSC2</i>	S phase	

Table 3 | Expected distribution of localized mRNPs at different cell stages of WT yeast cells. This table shows the expected distribution of localized mRNPs during different stages of the cell cycle in wild type (WT) cells of *S. cerevisiae*. Cells expressing a tagged mRNA visualized by MS2-CP-GFP(x3) are shown. The GFP fused mRNP is shown as green dots. The nuclear shape is shown in the middle of the cell.

EAR1 mRNA encodes an endosomal specificity factor required for the ubiquitination and sorting of cargo proteins at the multivesicular body (Giaever G. *et al.*, 2002; Terashima H. *et al.*, 2002; Leon S. *et al.*, 2008). *MID2* mRNA is known to encode a cell wall sensor (Philip B. and Levine D.E., 2001; Green R. *et al.*, 2003) and *IST2* mRNA is coding for a plasma membrane protein that may be involved in osmotolerance (Takizawa P.A. *et al.* 2000; Seedorf M. *et al.*, 2009). While *WSC2* mRNA encodes a sensor-transducer of a stress activated signaling pathway involved in maintenance of cell wall integrity (Verna J. *et al.*, 1997), *SRL1* mRNA encodes a

cell wall mannoprotein that is required for cell wall stability (Terashima H. *et al.*, 2002; Hagen I. *et al.*, 2004).

Thus, the main aim of this work was to find additional evidence for a link between ER inheritance and mRNP localization in yeast. Via biochemical approaches molecular characteristics of the ER and mRNP that ensure the transport mechanism should be identified, including potential candidates and their molecular characteristics essential for the mRNA transport and linkage to ER.

2 Results

2.1 ER morphology of yeast mutants

During the course of this work several mutants described to affect ER segregation or morphology should be inspected for their function in RNA localization. In order to verify the observed defects of the mutants on ER segregation in the strain background used in this study, I initially visualized the ER labeled with a marker protein (Scs2-TMD) fused to the red fluorescence protein DsRed (Loewen C.J.R., *et al.*, 2007). Therefore, different deletion mutants were generated and transformed with the ER marker plasmid RPJ1686 as described in Methods, 5.8.

For this experiment the following proteins were deleted: Aux1p, Myo4p, Ptc1p, Rtn1p, Scs2p, Sec3p, Sey1p, Slt2p and Yop1p.

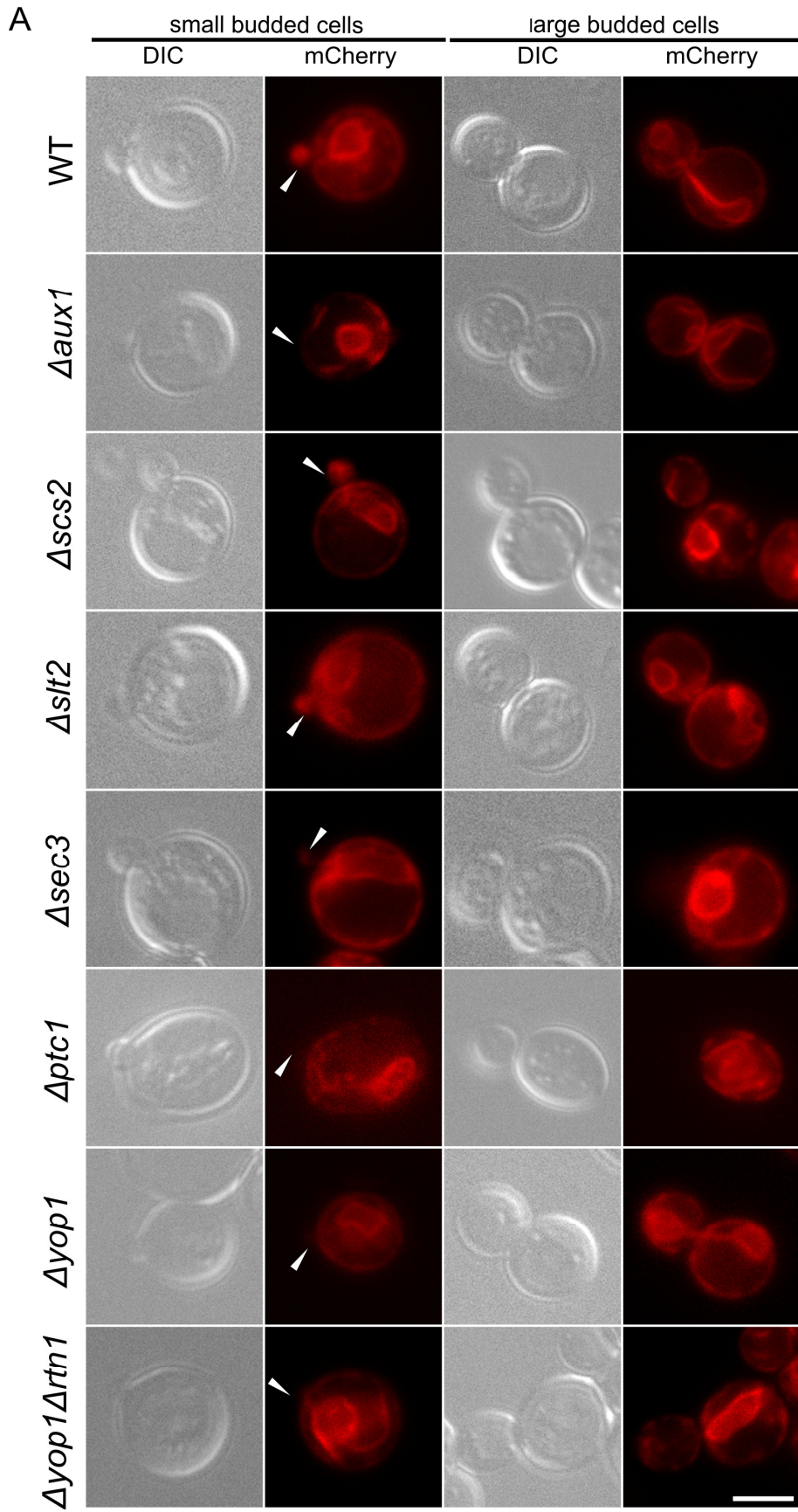
For Aux1p also known as Swa2p it is known that this protein is an auxilin-like protein that localizes to ER membranes and is required for cER inheritance (Du Y. *et al.*, 2010). Additionally, the COOH terminus of Aux1p contains a so-called J-domain. The J-domain is a motif of 70 aa conserved in Hsp40 family members and other Hsp70-binding co-chaperones (Kelley W.L. *et al.*, 1998). It is also known, that the J-domain has a copious sequence similarity to a subfamily of J-domains related to the J-domain of auxilin (Holstein S.E. *et al.*, 1996). Deletion of the J-domain of Aux1p results in the accumulation of clathrin-coated vesicles (Pishvae B. *et al.*, 2000). Other studies suggest that the J-domain of Aux1p combined with the NH₂-terminal clathrin binding domain (1-287 aa, Gall W.E. *et al.*, 2000) may act as an auxillin-related co-chaperone in the uncoating of clathrin-coated vesicles. Since deletion of the J-domain of Aux1p results in membrane accumulation and vacuole fragmentation but has no effect on the migration of peripheral ER, Aux1p may be a bi-functional protein with independent roles in cortical ER inheritance and membrane traffic (Du Y. *et al.*, 2001).

Myo4p is one of the type V myosin motors (Haarer B.K. *et al.*, 1994) and in case of the Myo4p-She3p co-complex it is also involved in cER inheritance (Schmid M. *et al.*, 2006). For Ptc1p it is known, that it has a function during late steps of cER segregation by regulating cER inheritance via Slt2p (Du Y. *et al.*, 2006). The deletion of Ptc1p affects precursor tRNA splicing, mitochondrial inheritance and sporulation

(Maeda T. *et al.*, 1993; Warmka J. *et al.*, 2001). Rtn1p is an ER membrane protein (see chapter 1.6) that interacts with Sey1p to maintain ER morphology (De Craene J.O. *et al.*, 2006) whereas Sey1p is a GTPase interacting genetically and physically with Yop1p and Rtn1p (Brands A. and Ho TH., 2002; Hu J. *et al.*, 2009). The ER membrane protein Yop1p helps to generate the high curvature that is necessary for the formation of tubular membrane structures in yeast (Hu J. *et al.*, 2008).

Scs2p is a highly conserved integral ER membrane protein that regulates phospholipid metabolism and is required for cER inheritance (Kagiwada S. *et al.*, 1998; Loewen C.J.R. *et al.*, 2005 and 2007). Slit2p is a serine/threonine MAP kinase which is involved in regulating maintenance of cell wall integrity (Du Y. *et al.*, 2006; Novick P. *et al.*, 2010; Mao K. *et al.*, 2011). Finally, Sec3p is a subunit of the exocyst complex (He B. and Guo W., 2009) and is suggested to be required for cortical ER inheritance (Reinke C.A. *et al.*, 2004; Wiederkehr A. *et al.*, 2003).

The results of the ER visualization experiments are shown in Figure 17. To check the morphology of the ER small budded S-phase cells and large budded G1-phase cells were observed in double blind experiments. Variations in structure like disorganization, cortical dysfunction or, if no ER signal appears, in either the mother cell or the bud were counted. The results are shown in two graphs according to the different cell sizes. For $\Delta slit2$ and $\Delta sey1$ strains no differences in structure and signal intensity were observed in comparison to the wild type strain which correlates with the literature (Novick P. *et al.*, 2006; Novick P. *et al.*, 2010; Niwa N. *et al.*, 2010; Hu J. *et al.*, 2009). For $\Delta aux1$ cells it is known that they are defective in cER segregation. The ER structures in case of *AUX1* deletion show the same pattern as shown before by Estrada P. *et al.*, 2003 and Schmid M. *et al.*, 2006. In more than 70% of both mother and budded yeast cells of different sizes the observed ER structure was disrupted. In case of $\Delta scs2$ more than 86% of the cells show a disrupted ER structure pattern. In comparison to the wild type the signal was very weak and the pattern seemed to be punctual or even not existing. Previous studies have shown that in case of this deletion the cortical ER was reduced in the bud and mother cell and the cER was disrupted by the loss of Scs2p (Loewen C.J.R. *et al.*, 2007). For $\Delta myo4$, $\Delta sec3$ and $\Delta ptc1$ no ER signal in the bud was detected in $\geq 84\%$ of the counted cells.



B

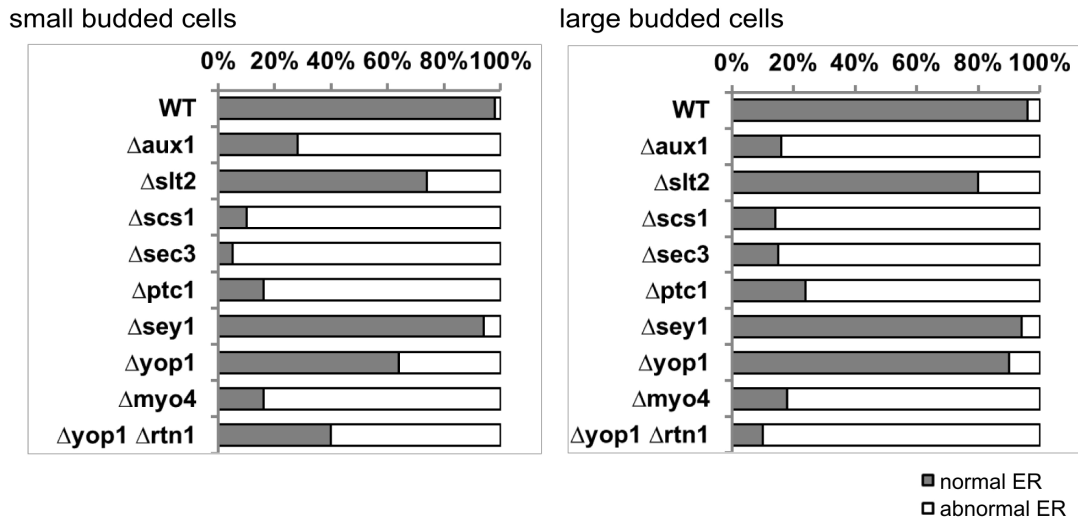


Figure 17 | ER morphology of yeast mutants tested for mRNA localization defects. (A) Representative images of cells expressing the ER marker plasmid RPJ1686 (SCS2-TMD-2xRFP). The left panel shows small budded and the right panel large budded yeast cells of wild type cells (RJY3994) in the first row and following mutations in the rows beneath; $\Delta aux1$ (RJY3995), $\Delta scs2$ (RJY3996), $\Delta slt2$ (RJY3997), $\Delta sec3$ (RJY3998), $\Delta ptc1$ (RJY4001), $\Delta yop1$ (RJY4002) and the double mutant $\Delta yop1 \Delta rtn1$ (RJY4005). No images are shown for the $\Delta sey1$ (RJY4000), $\Delta myo4$ (RJY4011), $\Delta yop1 \Delta sey1$ (RJY4003) and $\Delta yop1 \Delta ptc1$ (RJY4005) strains. As reported by other studies (Brands A. and Ho TH., 2002; Hu J. et al., 2009) wild type as well as $\Delta ptc1$ and $\Delta yop1$ cells contain cER in small buds. No cER is present in small buds of $\Delta aux1$, $\Delta sec3$, $\Delta scs2$ and $\Delta rtn1 \Delta yop1$. The Figure (A) shows images taken from the DIC and mCherry channels. Small buds are indicated by arrowheads. White bar corresponds to 4 μ m. (B) Quantification of either wild type like ER structures and ER structure abnormality. The counting of $n > 50$ small budded cells and $n > 100$ large budded cells was repeated two times in independent experiments. White bars indicate cells with ER morphology differing from the wild type situation while normal ER structures are represented by grey bars. The experiment was done by double blind experiments.

These results are supported by previous studies of Novick P. *et al.*, 2003, 2004 and 2006. Finally, in case of the double mutant $\Delta yop1 \Delta rtn1$ a disorganization in large budded cells or even no ER signal in small budded cells was observed in more than 82% of all counted cells. Interestingly, in the single mutant $\Delta yop1$ only 36% of the small budded cells show no signal. In large budded cells a normal pattern compared to the wild type of the ER structure was observed in 90% of the counted cells. These results are supported by the previous work of West M. *et al.*, 2011.

2.2 Myo4p as control protein used for studying mutants affecting mRNP transport

Previous studies have shown that Myo4p is essential for the transport of mRNPs to the bud tip by acting as the motor element (Bertrand E. *et al.*, 1998; Long R.M. *et al.*, 1997). Additionally, it is known that the Myo4p-She3p co-complex is also involved in cER inheritance (Schmid M. *et al.*, 2006). Both processes appear to be linked since *ASH1* mRNA particles bind to the tip of ER-tubular membrane structures.

To recapitulate the influence of Myo4p for the transport process of mRNPs and to set a standard for the anticipated effects of other mutants, I repeated the experiments with MS2-tagged mRNAs in $\Delta myo4$ strains. I defined two classes of cells with small and large buds to differentiate between early and late transport mechanisms. The definition of the two classes was made according to Figure 18.

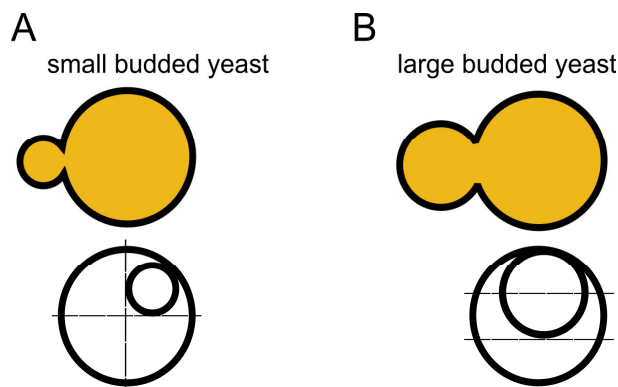


Figure 18 | Definition for small and large budded yeast cells. Scheme of the bud size definition for differentiating between small and large budded yeast cells is shown. The bud size was defined according to the size of the mother cell for each budded cell. (A) Small buds correlating at most to $\frac{1}{4}$ of mother cell size or (B) large buds correlating at most to $\frac{2}{3}$ of mother cell size.

The results of counting mRNPs in both small and large budded cells are shown in Figure 19. In wild type cells more than 84% of all cases of these MS2-tagged mRNPs localize to the bud of small budded S-phase and large budded wild type cells of the G2 cell cycle (Figure 19, wild type). In contrast, in cells lacking Myo4p the mRNP localization drops to less than 29% (Figure 19, $\Delta myo4$). Therefore, the loss of the class V myosin Myo4p disrupts localization of all five tested mRNAs to a similar degree.

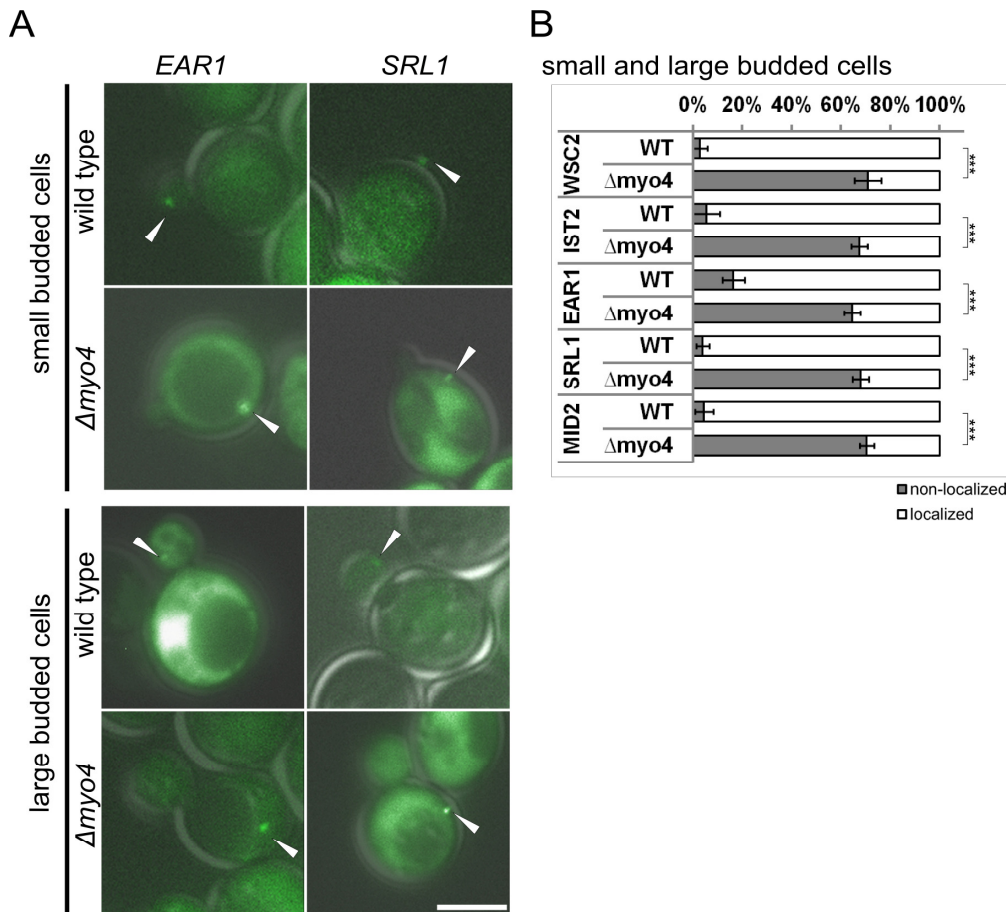


Figure 19 | Deletion of *Myo4* affects localization of *EAR1*, *MID2*, *IST2*, *SRL1* and *WSC2* mRNA. (A) Representative images of cells expressing MS2-tagged *EAR1* and *SRL1* mRNA. The first and third row show wild type cells (RJY3622 and RJY3630). The second and fourth row show $\Delta myo4$ cells (RJY4006 and RJY4010). The upper two panels show small budded and the lower two panels large budded yeast cells. Images show an overlay of DIC and GFP channels. White arrowheads indicate cytoplasmic mRNPs with tagged *WSC2* and *EAR1* mRNA (images of MS2-tagged *IST2*, *MID2* and *WSC2* mRNA are not shown). White bar corresponds to 4 μ m. (B) Quantification of mRNP localization of MS2-tagged *WSC2*, *IST2*, *EAR1*, *SRL1* and *MID2* mRNA to the bud in wild type cells (RJY3626, RJY3783, RJY3622, RJY3630 and RJY3634) and $\Delta myo4$ cells (RJY4008, RJY4007, RJY4006, RJY4009 and RJY4010). The first row shows the quantification graph of small budded cells and the second row shows the quantification graph of large budded cells. The counting of $n > 100$ small S-phase budded cells and $n > 100$ large budded cells was repeated four times in independent experiments. White bars indicate cells with bud-localized mRNPs, not localized mRNPs are represented by grey bars. Error bars assign two standard deviations. The confidence interval was determined assuming random sampling and using the normal approximation for a binomial distribution. *** Indicates a statistical significance of $P < 0.001$ in a one-tailed two-proportion t-test.

The results of the $\Delta myo4$ experiments verify the already known effect of this mutant on mRNP localization. They are also useful in setting the threshold of localization defects in other mutants, i.e. the percentage of cells with mislocalized mRNAs that allow me to classify a mutant as a mislocalization mutant or not.

For a significant mislocalization the effect of localized mRNPs between the wild type situation and the mutant has to be assessed from independent experiments by counting cells with localized vs. non-localized mRNAs. Statistical evaluation is ensured by including standard deviations and statistical significance (p-value) in a one-tailed two-proportion test. Three different mRNP localization classes can be defined. First, if the standard deviations of wild type and mutant would overlap each other no effect on mRNP localization would occur. Therefore, the p-value would be higher than 0.1. Second, if the standard deviations did not overlap each other and the p-value is lower than 0.001 an extensive significance and therefore a strong effect on the mRNP localization can be defined. And third, a p-value <0.1 would define a low effect on mRNP localization comparing to the wild type.

Samples of the significant mislocalization of mRNPs and its definition are shown in Figure 20.

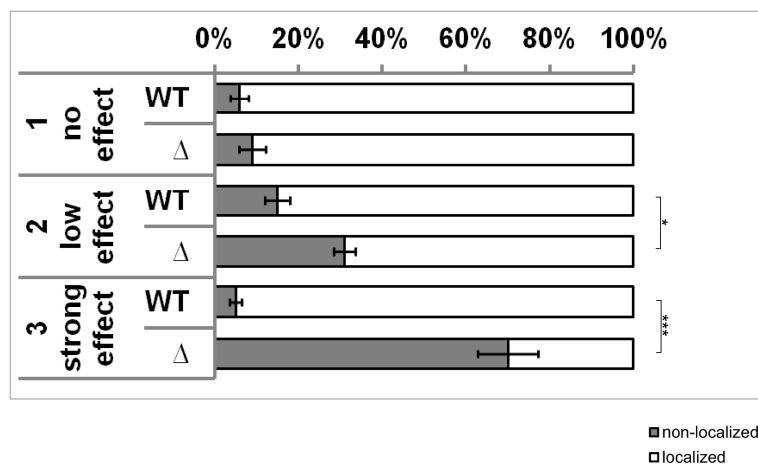


Figure 20 | Model scheme for defining mRNP localization effects. First example on top shows no significant mRNP localization effect and therefore is defined as no significance. The p-value is < 0.1 and the standard deviations of both WT and mutant cover each other. Second row shows the low effect by not covering its standard deviations but having a p-value <0.001 that indicates a low statistical significance. Finally, the third row shows an example of a strong effect defined by its p-value and standard deviations of both WT and mutant strain. White bars indicate cells with bud-localized mRNPs, not localized mRNPs are represented by grey bars. Error bars assign two standard deviations. The confidence interval was determined assuming random sampling and using the normal approximation for a binomial distribution. * Indicates a statistical significance of $P < 0.1$ in a one-tailed two-proportion test. *** Indicates a statistical significance of $P < 0.001$ in a one-tailed two-proportion t-test.

2.3 Deletion of *AUX1* affects localization of *WSC2*, *IST2*, *SRL1* and *EAR1* mRNAs but not *ASH1* mRNA

Previous studies (Schmid M. *et al.*, 2006) of live cell imaging experiments in yeast using the MS2 system suggest a coordination of cER distribution and mRNA localization.

Additionally, it is known that bud-localized mRNAs like *ASH1* mRNA were found to co-fractionate with ER microsomes dependent on She2p and Sec3p. Therefore, cortical inheritance and asymmetric mRNA transport are connected processes in yeast (Schmid M. *et al.*, 2006; Aronov S. *et al.*, 2007).

One possibility to test the link between the mRNP transport and ER inheritance would be to knock out several genes that are required for ER inheritance (e.g. Aux1p) and check how or if the mRNP localization is affected.

ASH1-MS2-tagged mRNA that is expressed in large budded anaphase cells associates with the tip of already assembled ER-membrane tubular structures and co-migrates to the bud tip (Schmid M. *et al.*, 2006). MS2-tagged *ASH1* mRNA expressed from a *GAL1* promoter was detected in different stages of the growing cell whereas in an $\Delta aux1$ mutant which is known to be defective in cER segregation the localization did not occur (Estrada P. *et al.*, 2003; Schmid M. *et al.*, 2006). It should also be mentioned that the expression level of *ASH1* from the *GAL1* promoter induced by galactose and repressed by growth on glucose (Flick J. S. and Johnston M., 1990) does not represent naturally occurring expression levels.

To verify the hypothesis of a link between mRNA localization and ER inheritance further experiments were performed in a modified way using the MS2-system by epitope-tag *ASH1* mRNA at its genomic locus (*ASH1-MS2*) and therefore expressed from its endogenous promoter (Haim L. *et al.*, 2007). Haim L. *et al.*, 2007 showed that *ASH1-MS2* tagged mRNAs were detected during the pre-mitotic (G2) and mitotic (M) phase (Haim L. *et al.*, 2007). Interestingly, in case of the experiments recapitulated in this work, the deletion of *AUX1* had no effect on the localization of the mRNA particles (Figure 21).

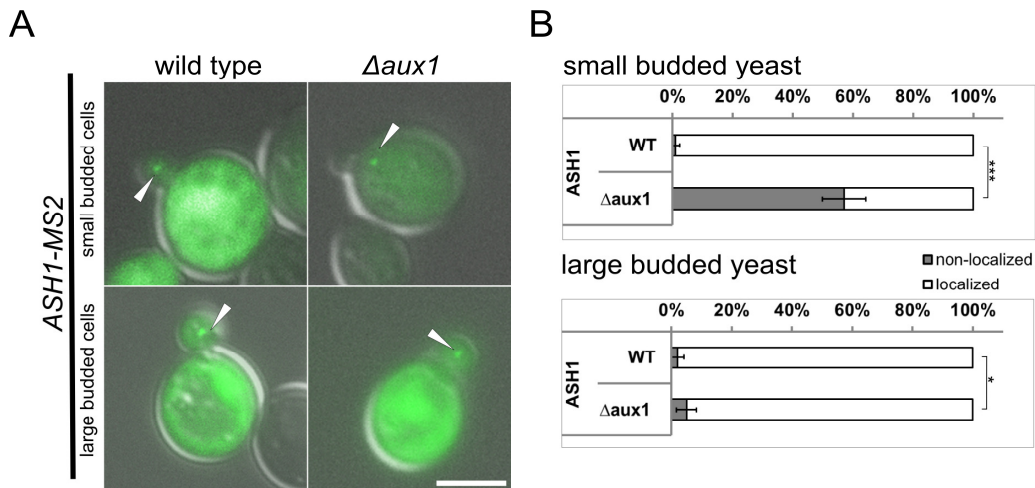


Figure 21 | Deletion of *Aux1p* does not affect distribution of endogenous expressed *ASH1* mRNA. (A) Representative images of cells expressing MS2-tagged *ASH1* mRNA in (left) wild type (RJY3525) and (right) $\Delta aux1$ (RJY3782) cells. The upper panel shows small budded and the lower panel large budded yeast cells. Images show an overlay of DIC and GFP channels. White arrowheads indicate RNPs. White bar corresponds to 4 μ m. (B) Quantification of mRNA localization to the bud. The counting of $n > 100$ small and large budded cells was repeated four times in independent experiments. White bars indicate cells with bud-localized mRNPs, not localized mRNPs are represented by grey bars. Error bars assign two standard deviations. The confidence interval was determined assuming random sampling and using the normal approximation for a binomial distribution. * Indicates a statistical significance of $P < 0.1$ in a one-tailed two-proportion test. *** Indicates a statistical significance of $P < 0.001$ in a one-tailed two-proportion t-test.

My results show that in case of large budded cells about 2% of wild type cells and 5% of $\Delta aux1$ cells contain MS2-tagged mRNPs of *ASH1* mRNA in the mother, i.e. show mislocalization. Therefore, no effect caused by the loss of *Aux1p* was observed. Interestingly, in case of the mRNA localization in small budded $\Delta aux1$ cells 57% of all cells contain MS2-tagged mRNPs of *ASH1* mRNA while in the wild type only 1% of all cells contain mRNPs of *ASH1* mRNA in the mother. The presence of mRNPs in small budded cells could be explained by the fact that MS2-tagged mRNA molecules are more stable and therefore survive G1-phase in which the *ASH1* mRNA is normally degraded. It has been demonstrated that MS2-tagged *ASH1* mRNA behaves like untagged mRNA in terms of localization (Bertrand E. *et al.*, 1998; Haim L. *et al.*, 2007) and MS2 tags might influence the regulated degradation of *ASH1* mRNA during G1-phase. Thus unlike in case of *ASH1* expressing cells, in some cells expressing *ASH1-MS2* the mRNA might still be present during the following S-phase when directed RNA transport re-starts.

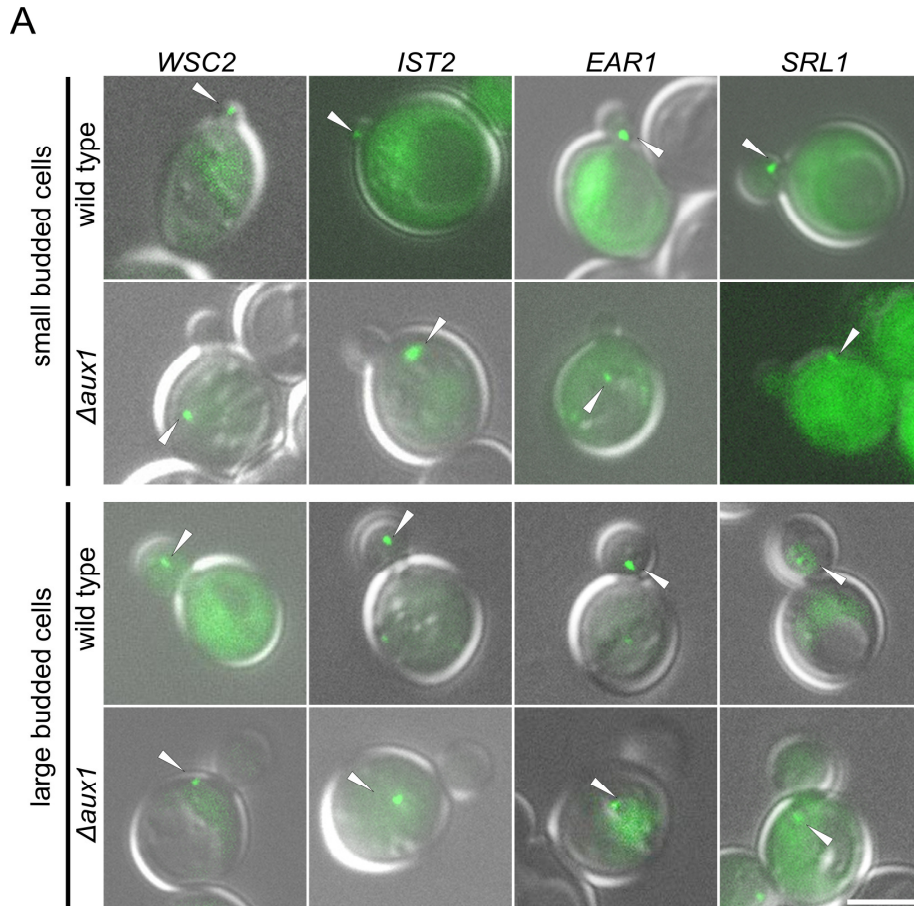
This can be explained by the fact that the previous observed mRNA localization in case of *ASH1* mRNA (Schmid M. *et al.*, 2006) does not represent endogenous

expression levels. Schmid M. *et al.*, 2006 used the expression from a *GAL1* promoter. The promoter leads to a galactose-regulated genetic transcription that is induced after adding galactose to the media and thus the protein expression occurs later than under natural conditions. This might have consequences on the transport mechanism. The endogenous promoter that I used in my study ensures natural expression levels and behavior of the transport machinery of localized mRNAs.

This suggests that the independence of *ASH1* mRNA on *AUX1* function is probably related to M-phase specific expression of *ASH1*. Next I focused on other localized mRNAs that are expressed in S-phase or between G1- and G2-phase (Shepard K.A. *et al.*, 2003). For detailed information of the mRNP expression see Table 3. These mRNAs include *EAR1*, *MID2*, *IST2*, *SLR1* and *WSC2*. *EAR1* encodes an endosomal specificity factor required for Rsp5p-dependent ubiquitination and sorting of specific cargo proteins at the multivesicular body (Giaever G. *et al.*, 2002; Terashima H. *et al.*, 2002; Leon S. *et al.*, 2008). It is known that *EAR1* mRNA is targeted to the bud via the She2p-dependent mRNA transport system. *MID2* encodes an O-glycosylated plasma membrane protein that acts as a sensor for the cell wall and interacts with another cell wall integrity protein, Zeo1p (Philip B. and Levine D.E., 2001; Green R. *et al.*, 2003). *IST2* is coding for a plasma membrane protein that may be involved in osmotolerance. It is also already known that mRNPs localize to the mother cell in small-budded cells and to the bud in medium- and large-budded cells while its transport to the bud-tip occurs via an actomyosin-driven process (Takizawa P.A. *et al.* 2000; Seedorf M. *et al.*, 2009). For *SRL1* mRNA it is known that it encodes a cell wall mannoprotein that is required for cell wall stability (Terashima H. *et al.*, 2002; Hagen I. *et al.*, 2004). Finally, *WSC2* mRNA encodes a sensor-transducer of the stress-activated *PKC1-MPK1 (SLT2)* signaling pathway which is involved in the maintenance of cell wall integrity and recovery from heat shock. Wsc2p is also required for the arrest of secretion response (Verna J. *et al.*, 1997; Imazu H. and Sakurai H., 2005; Nanduri J. and Tartakoff A.M., 2001).

In a wild type strain more than 90% of all cells contain MS2-tagged mRNPs of the aforementioned mRNAs in the bud of small budded S-phase cells which agrees with data shown by Haim L. *et al.*, 2007. In large budded wild type cells of the G2 cell cycle, more than 76% of the mRNPs were localized to the bud (Figure 22, wild type). In contrast, in cells lacking Aux1p the mRNP localization to the bud drops to less

than 15% (Figure 22, $\Delta aux1$) in all counted cells. For *WSC2* a smaller effect was observed. About 45% of mRNPs were localized to the bud in cells lacking Aux1p.



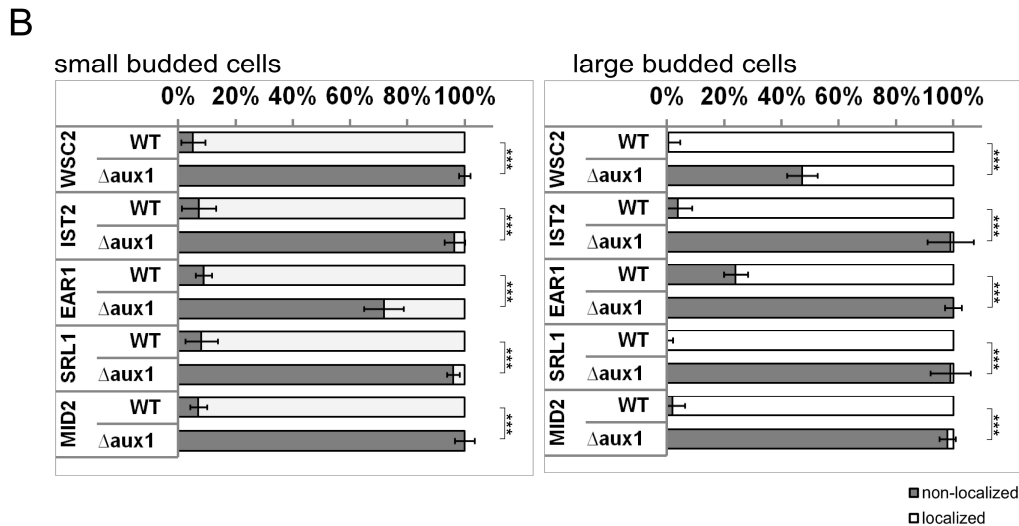


Figure 22 | Deletion of *AUX1* affects localization of *EAR1*, *MID2*, *IST2*, *SRL1* and *WSC2* mRNA. (A) Representative images of cells expressing MS2-tagged *WSC2*, *IST2*, *EAR1* and *SRL1* mRNA. The first and third row show wild type cells (RJY3626, RJY3783, RJY3622 and RJY3630). The second and fourth row show $\Delta aux1$ cells (RJY3754, RJY3761, RJY3752 and RJY3756). The upper two panels show small budded and the lower two panels large budded yeast cells. Images show an overlay of DIC and GFP channels. White arrowheads indicate cytoplasmic mRNPs with tagged *WSC2*, *IST2*, *EAR1* and *SRL1* mRNA (images of MS2-tagged *MID2* mRNA are not shown). White bar corresponds to 4 μ m. (B) Quantification of mRNP localization of MS2-tagged *WSC2*, *IST2*, *EAR1*, *SRL1* and *MID2* mRNA to the bud in wild type cells (RJY3626, RJY3783, RJY3622, RJY3630 and RJY3634) and $\Delta aux1$ cells (RJY3754, RJY3761, RJY3752, RJY3756 and RJY3758). The counting of $n > 100$ small budded cells and $n > 100$ large budded cells was repeated four times in independent experiments. White bars indicate cells with bud-localized mRNPs, not localized mRNPs are represented by grey bars. Error bars assign two standard deviations. The confidence interval was determined assuming random sampling and using the normal approximation for a binomial distribution. *** Indicates a statistical significance of $P < 0.001$ in a one-tailed two-proportion t-test.

To ensure that the observed mRNP mislocalization caused by the *AUX1* deletion is not strain-specific, all these experiments were repeated using four strains with the following different mating types and backgrounds (see 4.8 for detailed information): W303a (RJY358), W303 α (RJY359), BY4741 (RJY2049) and BY4742 (RJY2050). The observed distribution of mRNPs in either wild type cells or mutated cells was the same like shown in Figure 22. The following experiments were done using the formerly used W303 mating type and background.

Another indispensable evidence for the mRNP localization effects are time lapse experiments in both wild type cells and cells lacking Aux1p. These experiments were done as described in 5.5.4.

The results are shown in Figure 23. In case of the wild type situation the localization of both *IST2* mRNA and *EAR1* mRNA, which is expressed during all stages of the cell cycle, occurs in about 18 seconds to one minute in small budded or large budded yeast cells. The RNP contains either *IST2* or *EAR1* mRNA that travels from the mother cell through the bud neck to the bud of the daughter cell. In case of *Aux1p* mutants of MS2-tagged *EAR1*, *IST2* and *WSC2* mRNA the observation was performed for more than two minutes. Even until the GFP signal was bleached after four or five minutes no mRNP localization was observed. The particle only moved randomly in the cytoplasm of the mother but did not travel to the budded cell.

For every experiment a minimum of ten movies was generated. While previous studies suggested a slow-down or delay of the mRNP transport in $\Delta aux1$ mutants (Du Y. *et al.*, 2001; Loewen C.J.R. *et al.* 2007) my results support a complete failure of the transporting process.

The results of the *AUX1* deletion strains suggest that in contrast to *ASH1* mRNA the localization of mRNAs that are expressed during early stages of the cell cycle like S-phase requires a functional *Aux1p*. This suggests that the expression time of mRNAs for whose localization functional *Aux1p* is required correlates with the timing of transport and anchoring of the ER to the bud. This further indicates a dependency of these mRNAs on the transport of ER tubules to the bud.

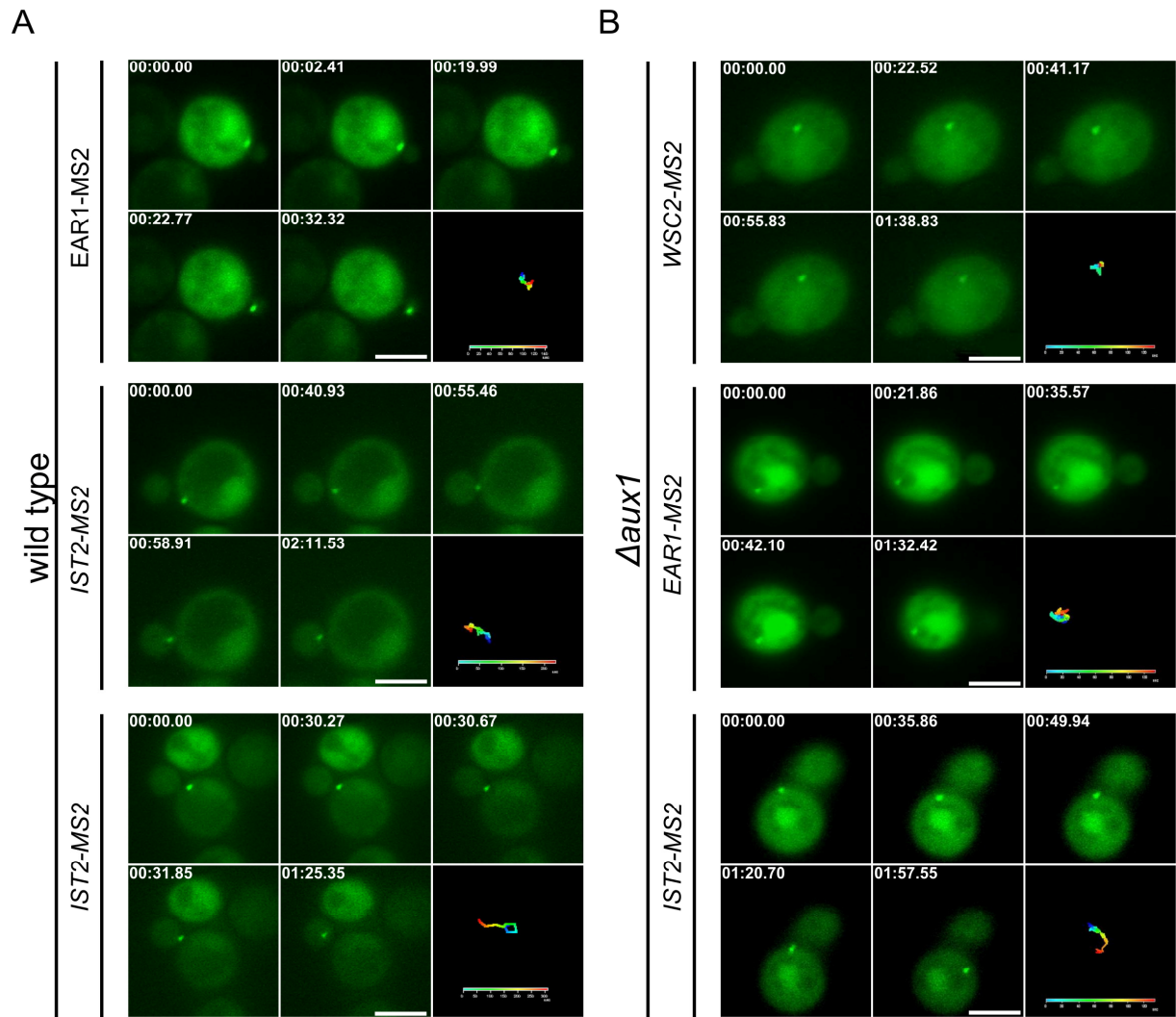


Figure 23 | *EAR1*, *IST2* and *WSC2-MS2* mRNP movement to the bud requires *AUX1* function. Time lapse experiments in living wild type and $\Delta aux1$ yeast cells are shown. (A) Representative images of wild type cells expressing MS2-tagged *EAR1* and *IST2* mRNA. First row shows the movement of a RNP containing *EAR1* mRNA (RJY3622) with 12xMS2L in small budded cells. Second and third row show a RNP containing *IST2* mRNA (RJY3783) with 12xMS2L in medium and large budded cells. The particle travels from the mother cell to the bud neck and from there to the bud of the daughter cell. (B) Representative images of $\Delta aux1$ cells expressing MS2-tagged *WSC2* (RJY3754), *EAR1* (RJY3752) and *IST2* (RJY3761) mRNA. First and second row show the distribution of a RNP containing *WSC2* and *EAR1* mRNA in case of small budded cells. Third row shows the distribution of *IST2* mRNA in large budded cells. The time points shown in the first five images of each row were generated by using AxioVision (ZEISS). Every last image of each row shows the colored tracking of one mRNP and its time bar, generated by using the tracking application. Each image represents a wide-field slice of the same image plane. The elapsed time (minutes, seconds and milliseconds) is shown in the upper left corner. The white bar corresponds to 4-4.5 μm .

2.4 Deletion of J-domain of Aux1p affects mRNP localization

Besides the results of the mRNP localization in case of the Aux1p deletion, I wanted to test whether the aforementioned J-domain of Aux1p may cause the effect in case of $\Delta aux1$ cells. Relating to previous studies the J-domain correlates to the last 168 aa of Aux1p (Figure 24). As I already mentioned the deletion of the J-domain results in membrane accumulation and vacuole fragmentation but has no effect on the migration of peripheral ER into daughter cells. This suggests that Aux1p may be a bi-functional protein with roles in cortical ER inheritance and membrane traffic (Du Y. *et al.*, 2001).



Figure 24 | Scheme of Aux1p (Swa2p) containing a J-domain at the COOH terminus. BLAST search done by Du *et al.*, 2001 reveals the presence of a possible J-domain at the COOH terminus and three potential tetratricopeptide (TPR) motifs in the centre (374-500 aa) portion of Aux1p. Figure modified from Du *et al.*, 2001.

To test whether the J-domain causes the aforementioned effects of Aux1p, strains without the J-domain were generated by replacing this domain via homologous recombination by integrating a marker sequence. Therefore, $\Delta J\text{-domain}$ strains were generated and the mRNP distribution was determined to assess the role of this sequence during the localization process. The results of this experiment are shown in Figure 25.

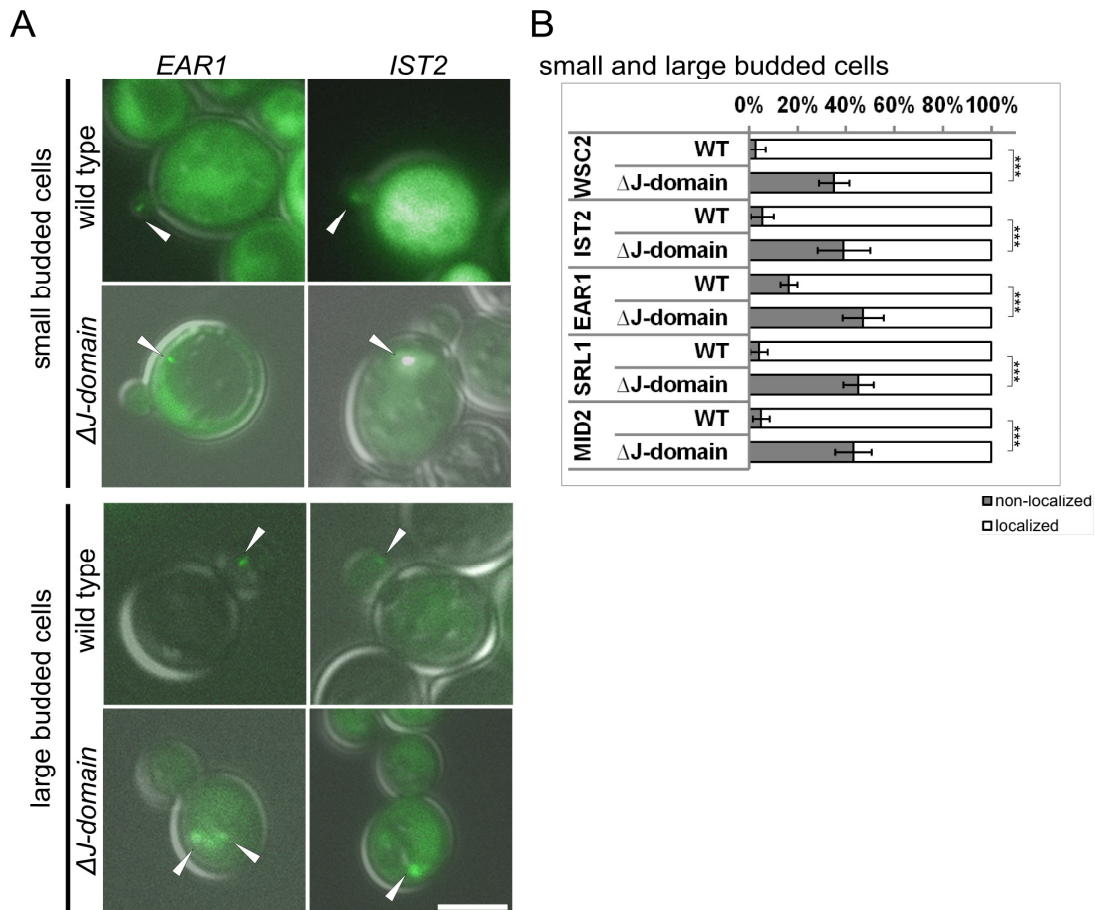


Figure 25 | Deletion of J-domain of Aux1p affects localization of *EAR1*, *MID2*, *IST2*, *SRL1* and *WSC2* mRNA. (A) Representative images of cells expressing MS2-tagged *EAR1* and *IST2* mRNA. First and third row show wild type cells (RJY3622 and RJY3783). The second and fourth row show ΔJ -domain cells (RJY4084 and RJY4085). The upper two panels show small budded and the lower two panels large budded yeast cells. Images show an overlay of DIC and GFP channels. White arrowheads indicate cytoplasmic mRNPs with tagged *EAR1* and *IST2* mRNA (images of MS2-tagged *WSC2*, *SRL1* and *MID2* mRNA are not shown). White bar corresponds to 4 μ m. (B) Quantification of mRNA localization of MS2-tagged *WSC2*, *IST2*, *EAR1*, *SRL1* and *MID2* mRNA to the bud in wild type cells (RJY3626, RJY3783, RJY3622, RJY3630 and RJY3634) and ΔJ -domain cells (RJY4087, RJY4085, RJY4084, RJY4089 and RJY4086). The counting of $n > 50$ small budded cells and $n > 50$ large budded cells was repeated two times in independent experiments. White bars indicate cells with bud-localized mRNPs, not localized mRNPs are represented by grey bars. Error bars assign two standard deviations. The confidence interval was determined assuming random sampling and using the normal approximation for a binomial distribution. *** Indicates a statistical significance of $P < 0.001$ in a one-tailed two-proportion t-test.

In case of the wild type 84%-97% of all cells contain MS2-tagged mRNPs of the *WSC2* (97%), *IST2* (95%), *EAR1* (84%), *SRL1* (96%) or *MID2* (95%) mRNA in the bud of small and large budded cells. In contrast, in cells lacking the J-domain of Aux1p 35%-47% of all cells contain MS2-tagged mRNPs of *WSC2* (35%), *IST2* (39%), *EAR1* (47%), *SRL1* (45%) and *MID2* (43%) mRNA in the mother cell.

According to our model the observed mislocalization defect by the deletion of the J-domain has to be defined as a middle-to-strong effect. By comparison to the strong effect caused by the deletion of total *AUX1* it seems that in addition to the J-domain other parts of the protein are involved in RNA localization.

In order to visualize whether the deletion of the J-domain of Aux1p influences ER segregation or morphology the $\Delta J\text{-domain}$ strains were transformed with the ER marker plasmid RPJ1686 as described in Methods, 5.8. Images of the ER in case of wild type cells, $\Delta aux1$ and of cells lacking the J-domain of Aux1p are shown in Figure 26.

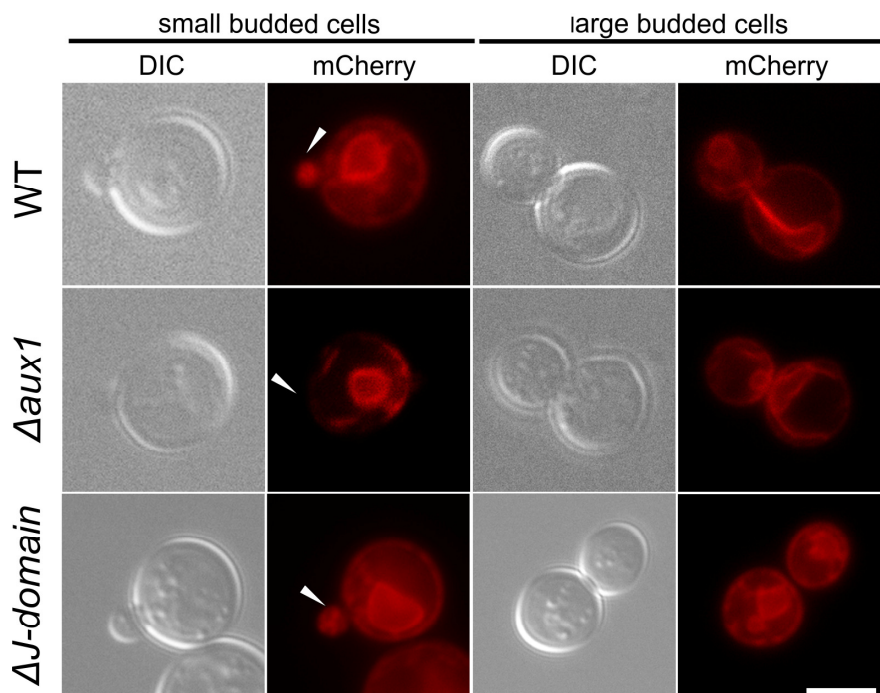


Figure 26 | Deletion of J-domain of Aux1p does not lead to abnormal ER structure. Representative images of cells expressing the ER marker Plasmid RPJ1686 (SCS2-TMD-2xRFP) are shown. The left panel shows small budded and the right panel large budded yeast cells of wild type cells in the first row, $\Delta aux1$ in the second and $\Delta J\text{-domain}$ of Aux1p in the third row. Images show DIC and mCherry channel images. Small buds are indicated by arrowheads. White bar corresponds to 4 μm .

Comparing the ER morphology of the wild type strain with cells lacking Aux1p that is defective in cER segregation show the same pattern as demonstrated before by Estrada P. *et al.*, 2003 and Schmid M. *et al.*, 2006. In case of cells lacking the J-domain of Aux1p no differences to the wild type were observed. Both small budded cells as well as large budded cells showed the same ER pattern as the wild type

strain reported by Du Y. *et al.*, 2001. Therefore, the ER structure is not affected by the lack of the J-domain.

First experiments (which need further validation) indicate that the J-domain of Aux1p might be involved in the correct transport of the chosen MS2-tagged mRNAs. This would confirm the predicted bi-functional characteristics of the J-domain.

2.5 Deletion of Slt2p and Scs2p only perturbs localization of a subset of mRNAs

To test if other proteins with a function in ER segregation may play a role during mRNP localization two other proteins, Scs2p and Slt2p (Mpk1p) were tested. Both are known to have an important role during late steps of cER inheritance. While Aux1p is involved in tubular ER movement to the bud (Du Y. *et al.*, 2004; Du Y. *et al.*, 2001), I tested whether mutants blocked at later steps of cER segregation also inhibit mRNP localization.

SCS2 mRNA encodes a highly conserved integral ER membrane protein that regulates phospholipid metabolism. It is also required for the second step of the cER inheritance: the correct association of cortical ER to the plasma membrane at the bud tip (Kagiwada S. *et al.*, 1998; Loewen C.J.R. *et al.*, 2005 and 2007). *SLT2* mRNA encodes a serine/threonine mitogen-activated protein kinase (MAPK) which is involved in regulating maintenance of cell wall integrity (CWI; Novick P. *et al.*, 2010; Mao K. *et al.*, 2011). It is also known that Slt2p is required for the late step of cER inheritance (Du Y. *et al.*, 2006) consisting of the spreading of cER tubules around the entire bud to form a polygonal tubular network.

The results of observed mRNP localization for the *SCS2* and *SLT2* deletion strains are shown in Figure 27 and 28. In case of the wild type 84%-97% of all cells contain MS2-tagged mRNPs of *WSC2* (97%), *IST2* (95%), *EAR1* (84%), *SRL1* (96%) or *MID2* (95%) mRNA while in $\Delta scs2$ cells 73%-91% of all cells contain MS2-tagged mRNPs of the aforementioned mRNAs in the bud. This means in case of *EAR1* 80% and in case of *IST2* 86%, *MID2* 73%, *SRL1* 91% and *WSC2* 80% of all cells contain mRNPs in the bud. Only small differences of 84%-97% in wild type and 73%-91% in $\Delta scs2$ cells were observed. In cells lacking Scs2p the results are comparable to the wild type. Thus, only a small effect caused by *SCS2* deletion was observed.

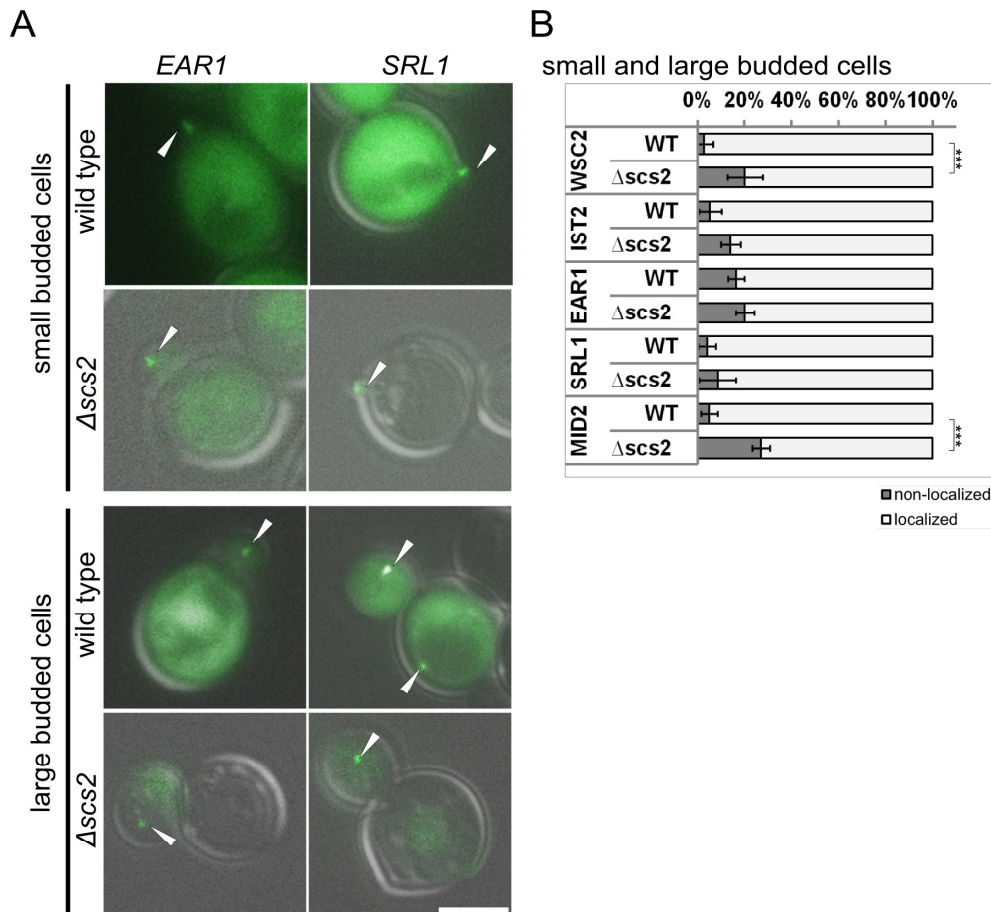


Figure 27 | Effects of *SCS2* deletion on localization of *EAR1*, *MID2*, *IST2*, *SRL1* and *WSC2* mRNA. (A) Representative images of cells expressing MS2-tagged *EAR1* and *SRL1* mRNA. First and third row show wild type cells (RJY3622 and RJY3630). The second and fourth row show $\Delta scs2$ cells (RJY3764 and RJY3770). The upper two panels show small budded and the lower two panels large budded yeast cells. Images show an overlay of DIC and GFP channels. White arrowheads indicate cytoplasmic mRNPs with tagged *EAR1* and *SRL1* mRNA (images of MS2-tagged *MID2*, *IST2* and *WSC2* mRNA not shown). White bar corresponds to 4 μ m. (B) Quantification of mRNP localization of MS2-tagged *WSC2*, *IST2*, *EAR1*, *SRL1* and *MID2* mRNA to the bud in wild type cells (RJY3626, RJY3783, RJY3622, RJY3630 and RJY3634) and $\Delta scs2$ cells (RJY3768, RJY3772, RJY3764, RJY3770 and RJY3766). The counting of $n > 100$ small budded cells and $n > 100$ large budded cells was repeated four times in independent experiments. White bars indicate cells with bud-localized mRNPs, not localized mRNPs are represented by grey bars. Error bars assign two standard deviations. The confidence interval was determined assuming random sampling and using the normal approximation for a binomial distribution. * Indicates statistical significance $P < 0.1$. *** Indicates a statistical significance of $P < 0.001$ in a one-tailed two-proportion t-test.

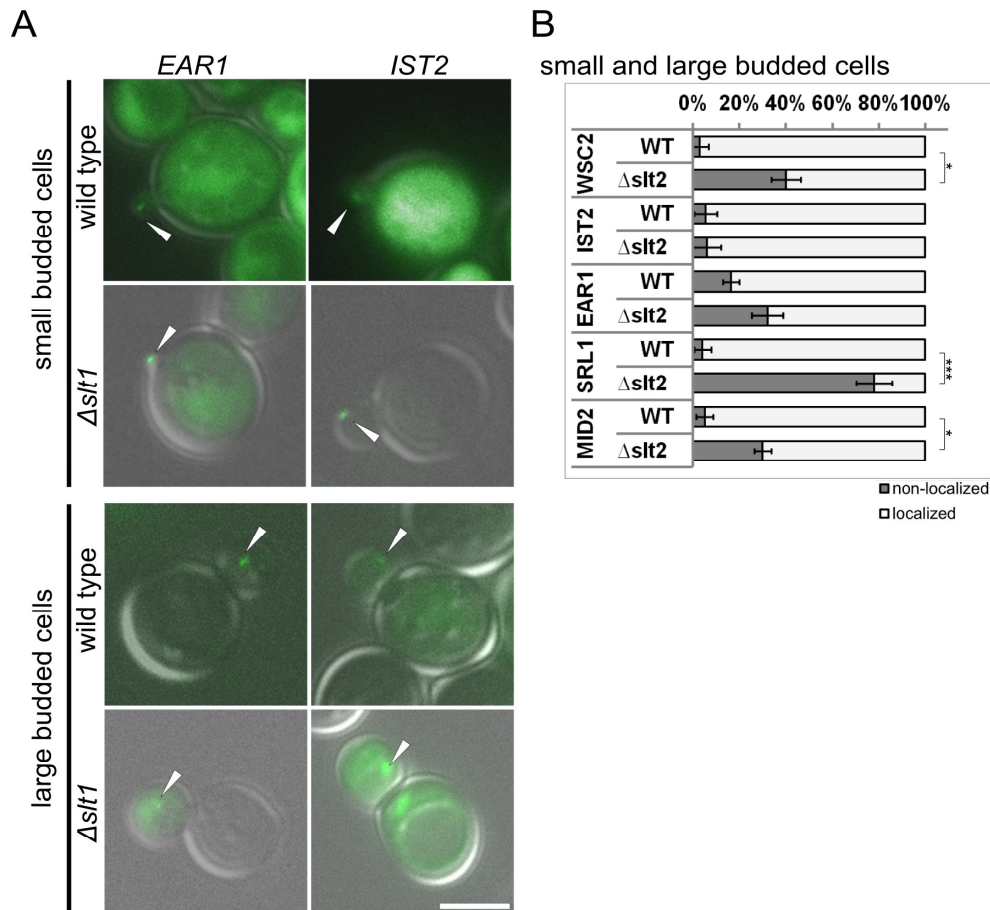


Figure 28 | Effects of *SLT2* deletion on localization of *EAR1*, *MID2*, *IST2*, *SRL1* and *WSC2* mRNA. (A) Representative images of cells expressing MS2-tagged *EAR1* and *IST2* mRNA. First and third row show wild type cells (RJY3622 and RJY3783). The second and fourth row show Δ *slt2* cells (RJY3763 and RJY3771). The upper two panels show small budded and the lower two panels large budded yeast cells. Images show an overlay of DIC and GFP channels. White arrowheads indicate cytoplasmic mRNPs with tagged *EAR1* and *IST2* mRNA (images of MS2-tagged *IST2*, *MID2* and *WSC2* mRNA not shown). White bar corresponds to 4 μ m. (B) Quantification of mRNP localization of MS2-tagged *WSC2*, *IST2*, *EAR1*, *SRL1* and *MID2* mRNA to the bud in wild type cells (RJY3626, RJY3783, RJY3622, RJY3630 and RJY3634) and Δ *slt2* cells (RJY3767, RJY3771, RJY3763, RJY3769 and RJY3765). The counting of $n > 100$ small budded cells and $n > 100$ large budded cells was repeated four times in independent experiments. White bars indicate cells with bud-localized mRNPs, not localized mRNPs are represented by grey bars. Error bars assign two standard deviations. The confidence interval was determined assuming random sampling and using the normal approximation for a binomial distribution. * Indicates statistical significance $P < 0.1$. *** Indicates a statistical significance of $P < 0.001$ in a one-tailed two-proportion t-test.

Interestingly, in case of Δ *slt2* the effect differs between the observed mRNAs. For *EAR1*, *IST2*, *MID2* and *WSC2* mRNA 68%, 94%, 70% or 60% of all cells contain mRNPs which can be defined as no or only low effects. But in case of the MS2-tagged *SRL1* mRNA a strong effect of only 22% of cells containing mRNPs due to the *SLT2* deletion was observed.

This data suggests that in case of all aforementioned mRNAs besides *SRL1* the mRNP localization is not affected either by *SCS* or *SLT2* deletion. In case of *SRL1* mRNA the localization might occur later than for the other mRNAs which therefore results in an effect of the deleted protein Slt2p that is known to be sufficient for the spreading of cER tubules around the entire bud to form a polygonal tubular network. The fact that *SRL1* mRNA encodes a mannoprotein that has tight associations with the cell wall and is required for its stability (Hagen I. *et al.*, 2004), and that the deletion of *SLT2* occurs in temperature-dependent cell lysis pre-initiating cell stress (Levin D.E. *et al.*, 2005), could be another reason why the mRNP localization was affected.

No mislocalization effect of the mRNPs of the aforementioned mRNAs was detected in case of $\Delta scs2$ strains. These results can be explained by the fact that the mRNPs are already localized to the bud before the process affected by the mutation occurs. In case of *SLT2* deletions a strong effect of mislocalization for *SRL1* mRNA was observed. For *WSC2*, *EAR1* and *MID2* mRNA a low effect on mRNP localization caused by the deletion of Slt2p was observed. In case of the cell wall integrity regulator Srl1p the mislocalization can be explained in two ways. Under stress conditions, triggered by deletion of the cell wall maintenance involved protein Slt2p, the RNA localization is affected anyhow. And/or the *SRL1* mRNA is transported later than the other aforementioned mRNAs which occurs in affected mRNP localization. Therefore, these proteins significantly involved in late steps of cER segregation (like association to cortical plasma membrane or spreading of cortical ER along the cortex) are not required for proper mRNA localization of *EAR1*, *MID2*, *IST2* and *WSC2*.

2.6 Deletion of Ptc1p has no effect in mRNP localization of *EAR1*, *IST2*, *MID2*, *SRL1* and *WSC2* mRNA

The protein Ptc1p was chosen because its mRNA encodes a phosphatase that acts during late steps of cER segregation and its deletion affects precursor tRNA splicing, mitochondrial inheritance and sporulation (Maeda T. *et al.*, 1993; Warmka J. *et al.*, 2001). Previous studies (Du Y. *et al.*, 2006) indicate that Ptc1p and Nbb2p regulate ER inheritance through cell wall integrity (CWI) via mitogen-activated protein kinase (MAPK) pathway by modulating the MAPK Slt2p.

The experiments previously done by Du Y. *et al.*, 2006 were recapitulated and the results are shown in Figure 29.

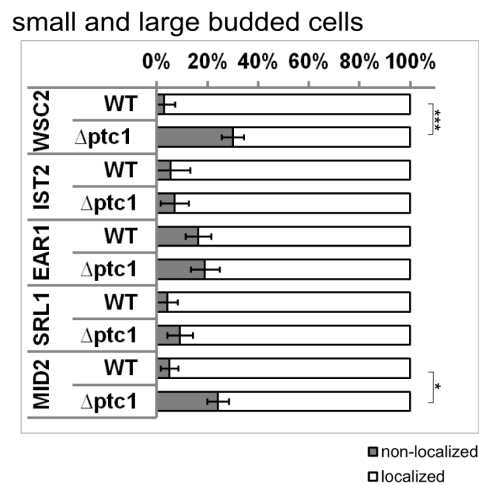


Figure 29 | Deletion of *PTC1* has no effect on localization of *EAR1*, *MID2*, *IST2*, *SRL1* and *WSC2* mRNA. Quantification of mRNP localization of MS2-tagged *WSC2*, *IST2*, *EAR1*, *SRL1* and *MID2* mRNA to the bud in wild type cells (RJY3626, RJY3783, RJY3622, RJY3630 and RJY3634) and $\Delta ptc1$ cells (RJY3887, RJY3885, RJY3888, RJY3886 and RJY4069). The counting of $n > 100$ small budded cells and $n > 100$ large budded cells was repeated four times in independent experiments. White bars indicate cells with bud-localized mRNPs, not localized mRNPs are represented by grey bars. Error bars assign two standard deviations. The confidence interval was determined assuming random sampling and using the normal approximation for a binomial distribution. * Indicates statistical significance $P < 0.1$. *** Indicates a statistical significance of $P < 0.001$ in a one-tailed two-proportion t-test.

With 81%-94% the distribution of localized MS2-tagged mRNAs in the $\Delta ptc1$ strain looks almost the same as under wild type conditions, with the exception of *MID2* and *WSC2*. In case of *MID2* 76% and in case of *WSC2* 70% of mRNPs were localized to the bud. Therefore the effect of the deletion was not significant enough to mention it as mRNP mislocalization or transport failure.

2.7 Localization of early expressed mRNAs requires tubular ER transport and the exocyst component Sec3p

Next I focused on another possible protein for the linkage between cER inheritance and mRNP localization. Sec3p is a subunit of the exocyst complex acting as spatial landmark for polarized secretion (He B. and Guo W., 2009). It has also been suggested that Sec3p is required to facilitate docking of ER tubules at the tip or cortex of the bud and might therefore be required for cortical ER inheritance (Reinke C.A. *et al.*, 2004; Wiederkehr A. *et al.*, 2003).

It is also known that bud-localized mRNAs including *ASH1* were found to co-fractionate with ER microsomes in a She2p- and Sec3p-dependent manner. Therefore asymmetric mRNA transport and cortical ER inheritance are connected processes in yeast (Aronov S. *et al.*, 2007).

In wild type cells more than 84% of cells localize *ASH1* (98%), *EAR1* (84%), *IST2* (95%), *MID2* (95%), *SRL1* (96%) and *WSC2* (97%) MS2-tagged mRNAs to the bud of small budded S-phase cells and large budded wild type cells of the G2 cell cycle (Figure 30, wild type) while in contrast in cells lacking Sec3p the mRNP localization drops to 25% or less (Figure 30, $\Delta sec3$). In case of *ASH1* mRNA 25% of all cells contain mRNPs in the bud while in case of *EAR1* only 6%, *IST2* 11%, *MID2* 10%, *SRL1* 6% and *WSC2* 15% of all cells contain mRNPs in the bud.

These results show that $\Delta sec3$ cells have an aberrant localization of all tested mRNPs to an extent that is similar to $\Delta aux1$ mutants besides *WSC2* mRNA. As mentioned above, in case of $\Delta aux1$ cells the mRNP localization drops to less than 15% of all aforementioned mRNAs while in case of *WSC2* 45% of mRNPs were still localized to the bud. In case of cells lacking Sec3p no differences between *WSC2* mRNA and the other mRNAs were observed. This could be explained by the fact that Sec3p is a protein that is a spatial landmark for secretion (He B. and Guo W., 2009) while Wsc2p is known to be a protein required for the arrest of secretion response (Ng D.T., 2001). Therefore the deletion of Sec3p directly affects *WSC2* mRNA localization.

In contrast to cells lacking Aux1p or Sec3p in $\Delta scs2$ cells no significant change of the mRNP distribution compared to the wild type was observed. In case of wild type cells 84%-97% and in $\Delta scs2$ cells 73%-91% contain MS2-tagged mRNPs of the aforementioned mRNAs.

Interestingly, the effect of mRNP localization to the bud differs in cells lacking Slt2p. While in case of *EAR1* (68%), *IST2* (94%), *MID2* (70%) and *WSC2* (60%) mRNA more than 68% of all cells contain mRNPs, in cells with MS2-tagged *SLT2* mRNA only 22% contain mRNPs in the bud.

As mentioned before, in the $\Delta ptc1$ strain 81%-94% of all counted cells contain localized mRNAs similar to the wild type, with the exception of *MID2* and *WSC2* mRNA. In case of *MID2* 76% and in case of *WSC2* 70% of mRNPs were localized to

the bud. Applying the formerly mentioned definition of (mis)localization the distribution of *WSC2* mRNA is affected middle-strongly. *MID2* is moderately affected and all the other mRNAs are not influenced by the loss of Ptc1p.

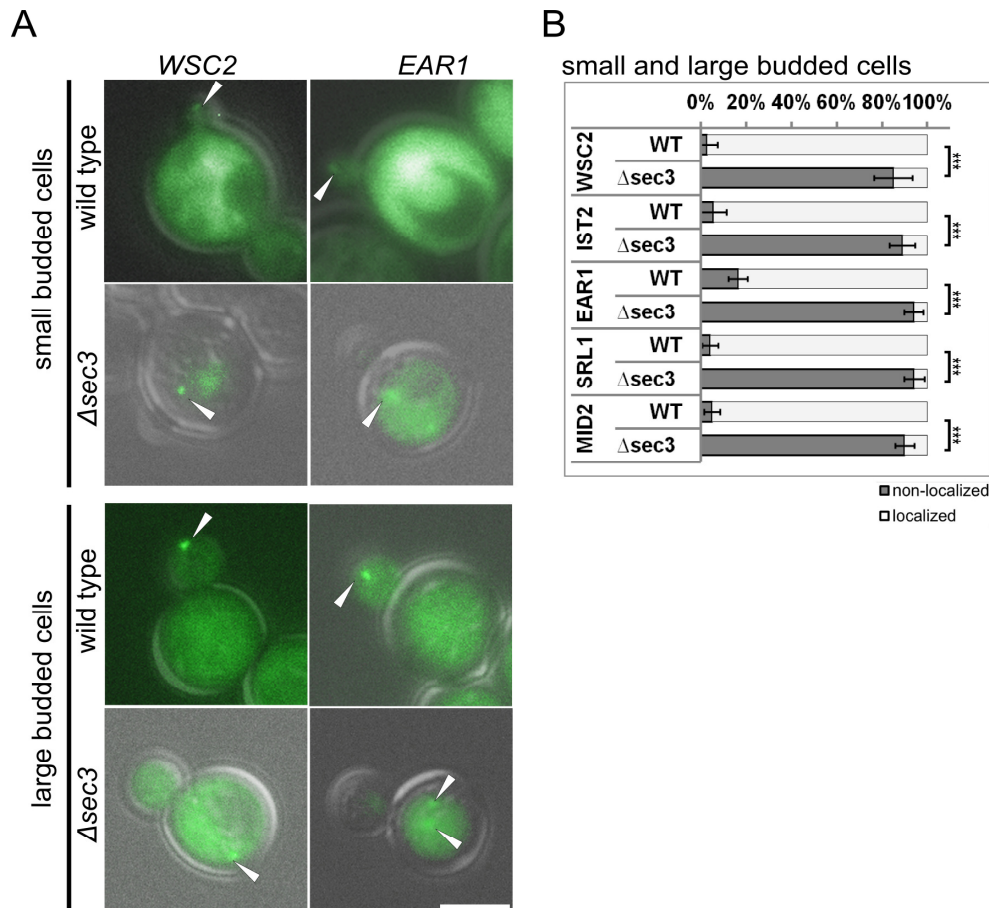


Figure 30 | Deletion of *SEC3* affects localization of *EAR1*, *MID2*, *IST2*, *SRL1* and *WSC2* mRNA. (A) Representative images of cells expressing MS2-tagged *WSC2* and *EAR1* mRNA. First and third row show wild type cells (RJY3626 and RJY3622). The second and fourth row show $\Delta sec3$ cells (RJY3853 and RJY3854). The upper two panels show small budded and the lower two panels large budded yeast cells. Images show an overlay of DIC and GFP channels. White arrowheads indicate cytoplasmic mRNPs with tagged *WSC2* and *EAR1* mRNA (images of MS2- tagged *ASH1*, *IST2*, *MID2* and *SRL1* mRNA not shown). White bar corresponds to 4 μ m. (B) Quantification of mRNP localization of MS2-tagged *WSC2*, *IST2*, *EAR1*, *SRL1*, *MID2* and *ASH1* mRNA to the bud in wild type cells (RJY3626, RJY3783, RJY3622, RJY3630, RJY3634 and RJY3525) and $\Delta sec3$ cells (RJY3853, RJY3850, RJY3854, RJY3851, RJY3849 and RJY3852). The counting of $n > 100$ small budded cells and $n > 100$ large budded cells was repeated four times in independent experiments. White bars indicate cells with bud-localized mRNPs, not localized mRNPs are represented by grey bars. Error bars assign two standard deviations. The confidence interval was determined assuming random sampling and using the normal approximation for a binomial distribution. *** Indicates a statistical significance of $P < 0.001$ in a one-tailed two-proportion t-test.

2.8 Knockout of *YOP1* together with *RTN1* or *SEY1* leads to affected RNP transport while single knockout has no effect

Besides proteins that are required for the inheritance of the cortical ER (e.g. Sec3p and Aux1p) it is also necessary to have a look at proteins which are necessary for the shape and formation of cER tubular structures. Because of the fact that ER tubules are the elements that are required for the segregation and transport of mRNAs which takes place before inheritance of cortical ER would occur, it was also important to have a closer look at the tubular structures of the ER. So another group of proteins became interesting; a group of evolutionary conservative proteins residing predominantly in ER and playing a role in promoting membrane curvature to form tubular structures (Voeltz G.K. *et al.*, 2006; Hu J. *et al.*, 2008). The so-called reticulons may also play a role in nuclear pore complex formation and vesicle formation (Yang B.C. *et al.*, 2007).

Shaping of ER tubules involves two protein families the reticulons (Rtns) and DP1/Yop1p to generate the high curvature required to form tubular membrane structures. Previous studies show that the localized *ASH1* mRNA binds to the tip of ER-membrane tubules (Schmid M. *et al.*, 2006). Yop1p is a membrane protein that interacts with Yip1p to mediate membrane traffic. Its overexpression leads to cell death and accumulation of internal cell membranes (Calero M. *et al.*, 2001; Brands A. and Ho T.H., 2002; Hu J. *et al.*, 2009). As mentioned above, this protein helps to generate the high curvature which is necessary for tubular formation of membrane structures with a diameter of 30 nm in yeast (Hu J. *et al.*, 2008).

Previous studies show a dramatic change in ER shape and curvature by generating triple knockout strains ($\Delta rtn1\Delta rtn2\Delta yop1$) of *RTN1*, *RTN2* and *YOP1*. Interestingly, the ER is still inherited by a Rtn/Yop1-independent process into the bud suggesting that these proteins maintain rather than generate the curvature of the membrane at all peripheral ER domains (West M. *et al.*, 2011).

To test the influence of this protein family and proteins which are interacting with the reticulons and the process of mRNP localization, I first generated single knockouts of Sey1p and Rtn1p.

Rtn1p is an ER membrane protein that interacts with Sey1p to maintain ER morphology. The null mutant shows an altered ER morphology (De Craene J.O. *et al.*, 2006 and Hu J. *et al.* 2009). Sey1p is a GTPase with a role in ER morphology and interacts genetically and physically with Yop1p and Rtn1p (Brands A. and Ho T.H., 2002; Hu J. *et al.*, 2009).

The results of the single knockouts of Sey1p or Rtn1p (Figure 31) support the mRNP localization that is comparable to the wild type. In detail, in $\Delta rtn1$ cells 82% of all counted cells contain MS2-tagged *EAR1* mRNA 83% *IST2*, 82% *MID2*, 88% *SRL1* and 68% *WSC2* mRNA in the bud. In $\Delta sey1$ cells 84% of all counted cells contain MS2-tagged 84% *EAR1* mRNA 95% *IST2*, 85% *MID2*, 89% *SRL1* and 69% *WSC2* mRNA in the bud.

The Results in case of Rtn1p were expected due to the fact that it is known that the single deletion of the *RTN1* gene results in a re-organization of the cER structure with no significant changes in the total membrane surface area of the ER (Novick P. *et al.*, 2006).

As mentioned before, in case of the triple knockout of Rtn1p together with Rtn2p and Yop1p a dramatic change of the ER shape and curvature was observed by West M. *et al.*, 2011 while the results of the single mutants of Sey1p and Rtn1p did not show significant changes in ER structure and distribution.

Thus, I tested whether Yop1p together with Sey1p and Rtn1p would cause these effects on ER structure and would occur in a change of localizing mRNPs to the bud in yeast cells. So strains with either $\Delta sey1\Delta yop1$ or $\Delta rtn1\Delta yop1$ were generated.

The results of the mRNP distribution of MS2-tagged *WSC2*, *EAR1*, *IST2*, *SRL1* and *MID2* mRNAs in the $\Delta sey1\Delta yop1$ and $\Delta rtn1\Delta yop1$ double knockouts are shown in Figure 31 (B).

In contrast to the wild type, cells with deletions of both Rtn1p and Yop1p show a loss of mRNP localization to the bud in about 63%-81% of all counted cells. In detail, this means in case of the double mutant $\Delta sey1\Delta yop1$ no mRNP localization was observed in 63%-69% and in case of $\Delta rtn1\Delta yop1$ in 72%-81% of all counted cells.

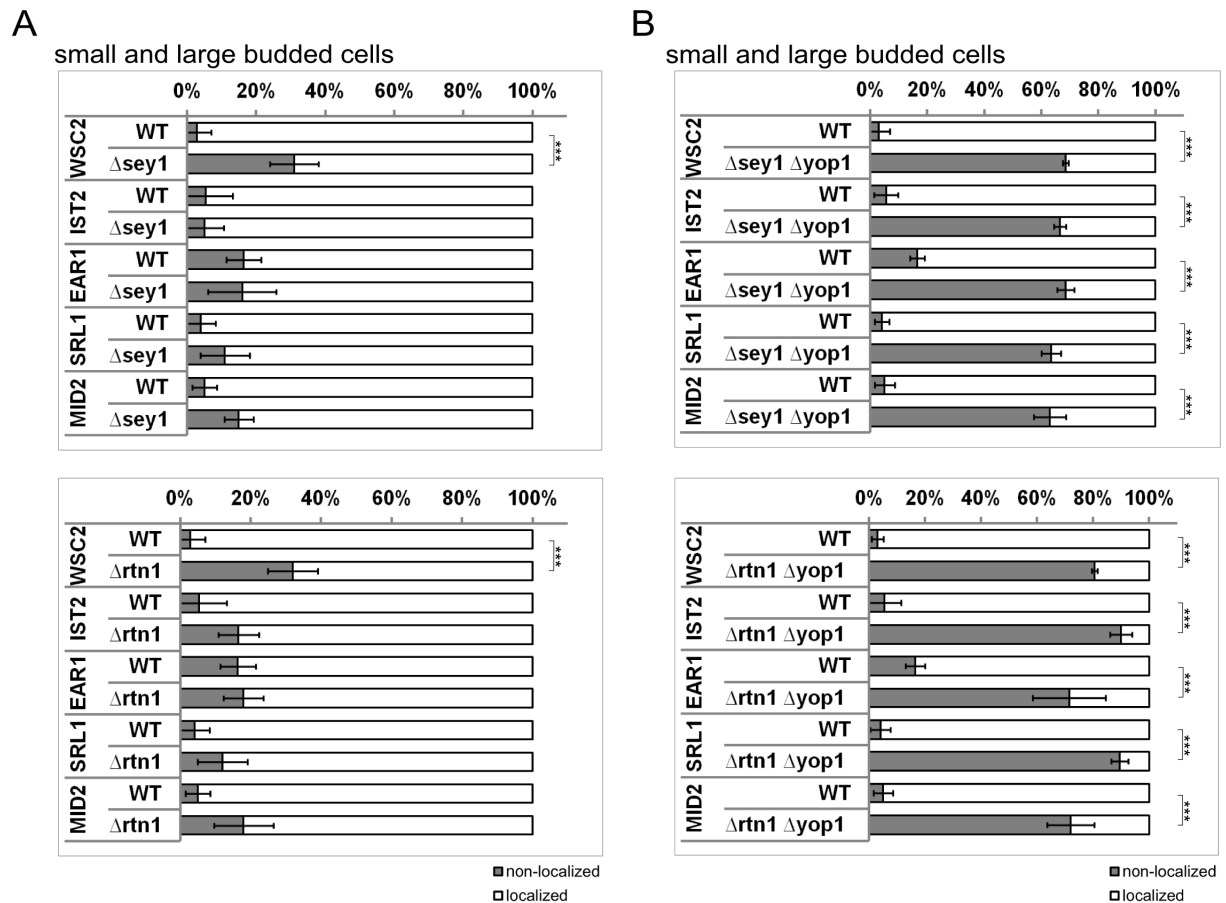


Figure 31 | Tubular ER is required for mRNA localization. Quantification of mRNP localization of MS2-tagged *WSC2*, *IST2*, *EAR1*, *SRL1* and *MID2* mRNA in wild type cells (RJY3626, RJY3783, RJY3622, RJY3630 and RJY3634) and different mutants is shown. (A) In the first row the quantification results of Δ *sey1* (RJY3883, RJY3881, RJY3884, RJY3882 and RJY4070) and in the second row the quantification results of Δ *rtn1* (RJY3876, RJY3877, RJY3880, RJY3879 and RJY4071) are shown. (B) In the first row the quantification results of Δ *sey1* Δ *yop1* cells (RJY3906, RJY3904, RJY3907, RJY3905 and RJY4073) and in the second row the quantification results of Δ *rtn1* Δ *yop1* cells (RJY3900, RJY3901, RJY3903, RJY3902 and RJY4074) are shown. The counting of $n > 100$ small budded cells and $n > 100$ large budded cells was repeated four times in independent experiments. White bars indicate cells with bud-localized mRNPs, not localized mRNPs are represented by grey bars. Error bars assign two standard deviations. The confidence interval was determined assuming random sampling and using the normal approximation for a binomial distribution. * Indicates a statistical significance $P < 0.1$. *** Indicates a statistical significance of $P < 0.001$ in a one-tailed two-proportion t-test.

2.9 Loss of Yop1p alters RNP localization efficiency at early stages of cell growth

Based on the fact that the single knockouts of Sey1p and Rtn1p show wild type-like mRNP distribution levels and together with the deletion of Yop1p the localization drops down dramatically it seems that Yop1p might have a more pronounced function for the correct transport process of the chosen MS2-tagged mRNAs, e.g. by providing the correct development of tubular structures and curvatures of the

membranes. Therefore single $\Delta yop1$ strains were generated and the mRNP distribution was observed to determine the role of this protein during the localization process. The results are shown in Figure 32.

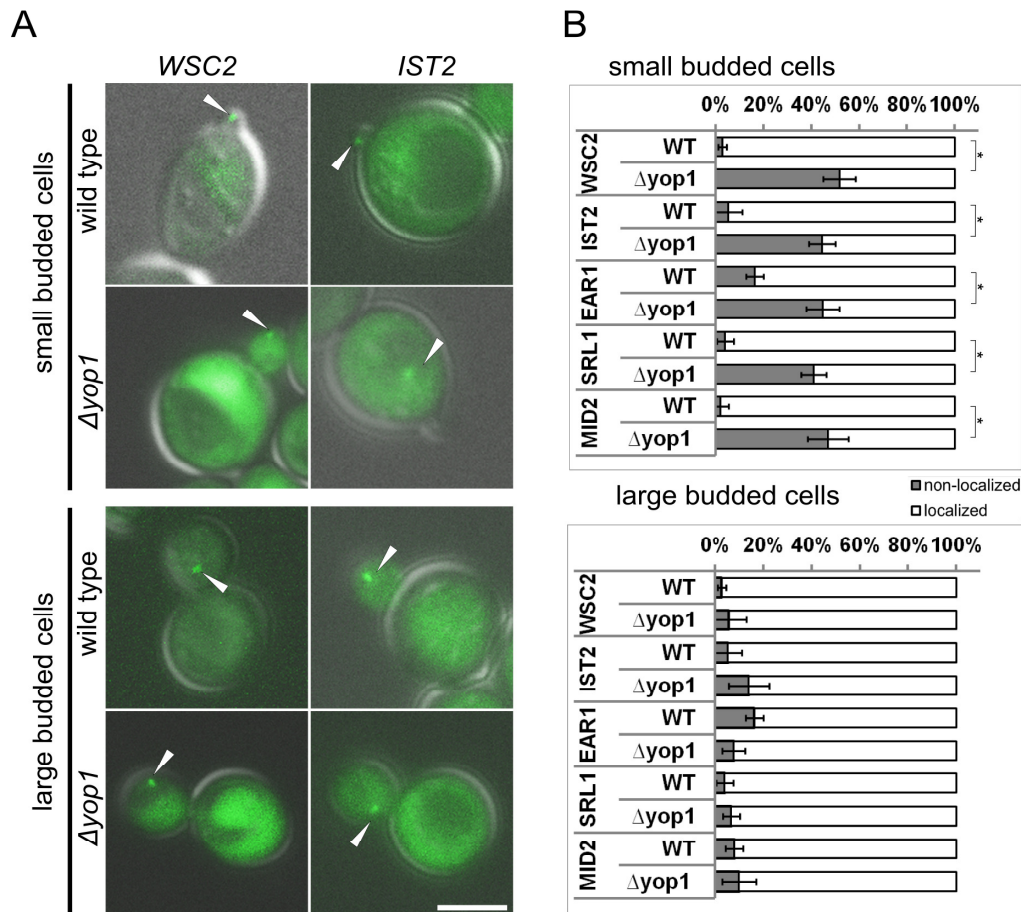


Figure 32 | Deletion of *YOP1* perturbs localization of *EAR1*, *MID2*, *IST2*, *SRL1* and *WSC2* mRNA. (A) Representative images of cells expressing MS2-tagged *WSC2* and *IST2* mRNA. First and third row show wild type cells (RJY3626 and RJY3783). The second and fourth row show $\Delta yop1$ cells (RJY3992 and RJY3991). The upper two panels show small budded and the lower two panels large budded yeast cells. Images show an overlay of DIC and GFP channels. White arrowheads indicate cytoplasmic mRNPs with tagged *WSC2* and *EAR1* mRNA (images of MS2-tagged *EAR1*, *MID2* and *SRL1* mRNA not shown). White bar corresponds to 4 μ m. (B) Quantification of mRNP localization of MS2-tagged *WSC2*, *IST2*, *EAR1*, *SRL1* and *MID2* mRNA to the bud in wild type cells (RJY3626, RJY3783, RJY3622, RJY3630 and RJY3634) and $\Delta yop1$ cells (RJY3992, RJY3991, RJY3990, RJY3993 and RJY4075). First row shows quantification graph of small budded S-phase cells and second row shows quantification graph of large budded G2-phase cells. The counting of $n > 100$ small budded cells and $n > 100$ large budded cells was repeated four times in independent experiments. White bars indicate cells with bud-localized mRNPs, not localized mRNPs are represented by grey bars. Error bars assign two standard deviations. The confidence interval was determined assuming random sampling and using the normal approximation for a binomial distribution. * Indicates a statistical significance of $P < 0.1$ in a one-tailed two-proportion t-test.

Interestingly, an effect on mRNP localization was observed only during early stages of the cell cycle. In comparison to wild type cells 41%-52% of the MS2-tagged

mRNPs remained in the mother cell of small budded S-phase cells (Figure 32, small budded cells). In large budded cells of the G2 cell cycle $\geq 86\%$ of the mRNPs were localized to the bud (Figure 32, large budded cells).

2.10 Co-visualization of ER structures and mRNPs

To underline the linked process of mRNPs together with cortical ER structures different strains with both markers for RNPs (GFP) and ER (mCherry) were used in time lapse combined z-stack experiments as described in 5.5.4 and 5.5.6.

Therefore the MS2-tagged strains, generated as described in 5.4 were transformed with the ER marker SCS2-TMD-2xRFP (5.8). Time lapse series were taken in different foci of small budded S1-phase and large budded G1-phase cells. Three dimensional (3D) images were prepared according to the manufacturer's manual (Figure 33, 34 and 35).

The Figures 33, 34 and 35 are showing evidence for the link between localized mRNPs and cER tubular structures. In both cases the localized mRNP complexes are tightly associated to ER tubular structures. The distance defined by AxioVision software between the mRNPs and the ER was too short to be calculated.

Unfortunately, statistical validation of the distance measurement between the mRNP and ER is hindered by the low signal intensity of both ER and GFP markers. However, the 3D reconstruction images shown below demonstrate a direct contiguousness between cER and mRNPs.

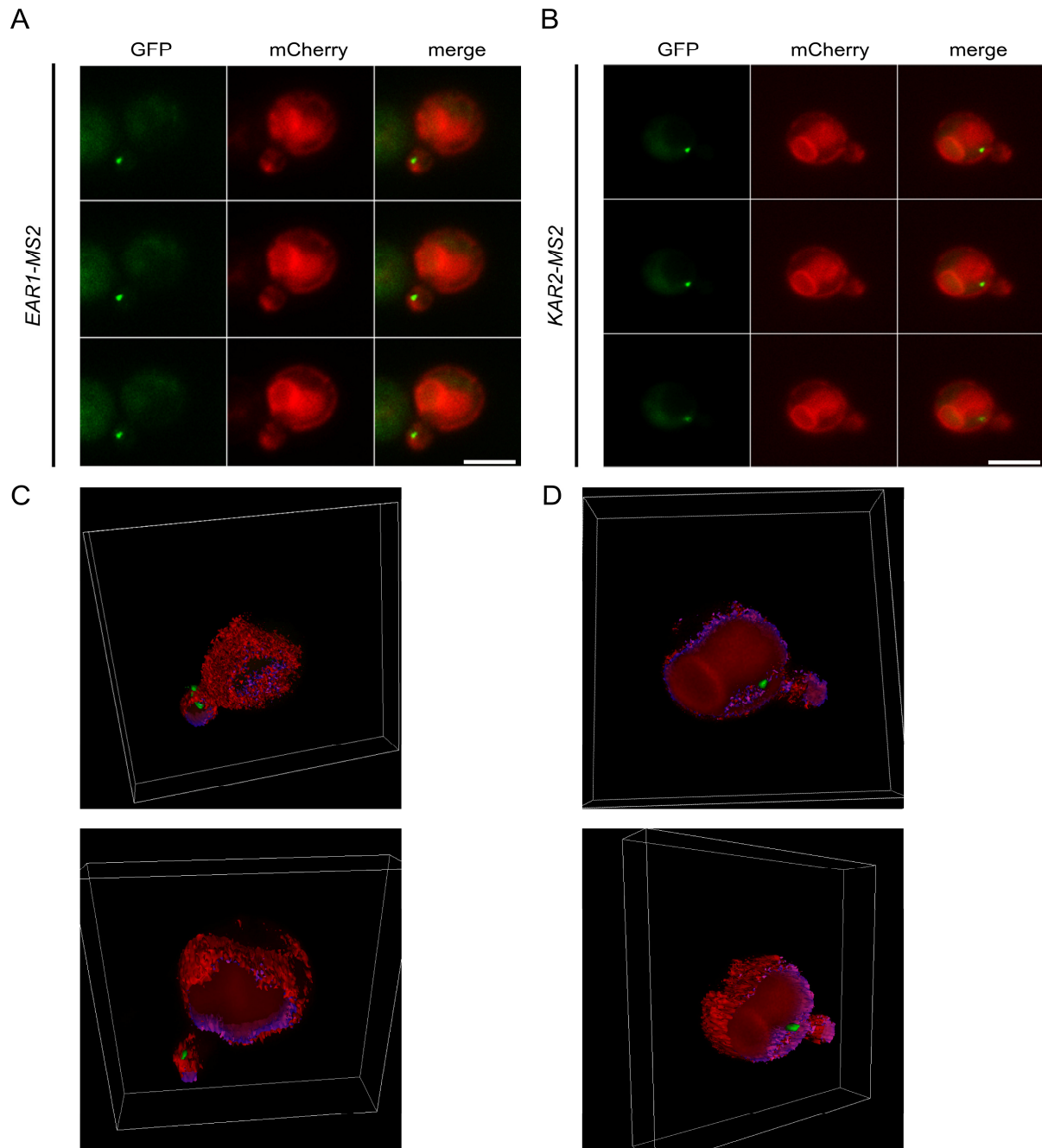


Figure 33 | Examples of co-localization in small budded cells in case of *EAR1* and *KAR2* mRNA. (A/B) Representative images of cells expressing MS2-tagged *EAR1* (RJY3622; A) and *KAR2* mRNA (RJY3780; B) in small budded cells are shown. The images (A and B) represent a time lapse gallery of GFP, mCherry and merged channels. White bars correspond to 4 μm . (C/D) Show corresponding 3D images of calculated ER structures together with the mRNP complex.

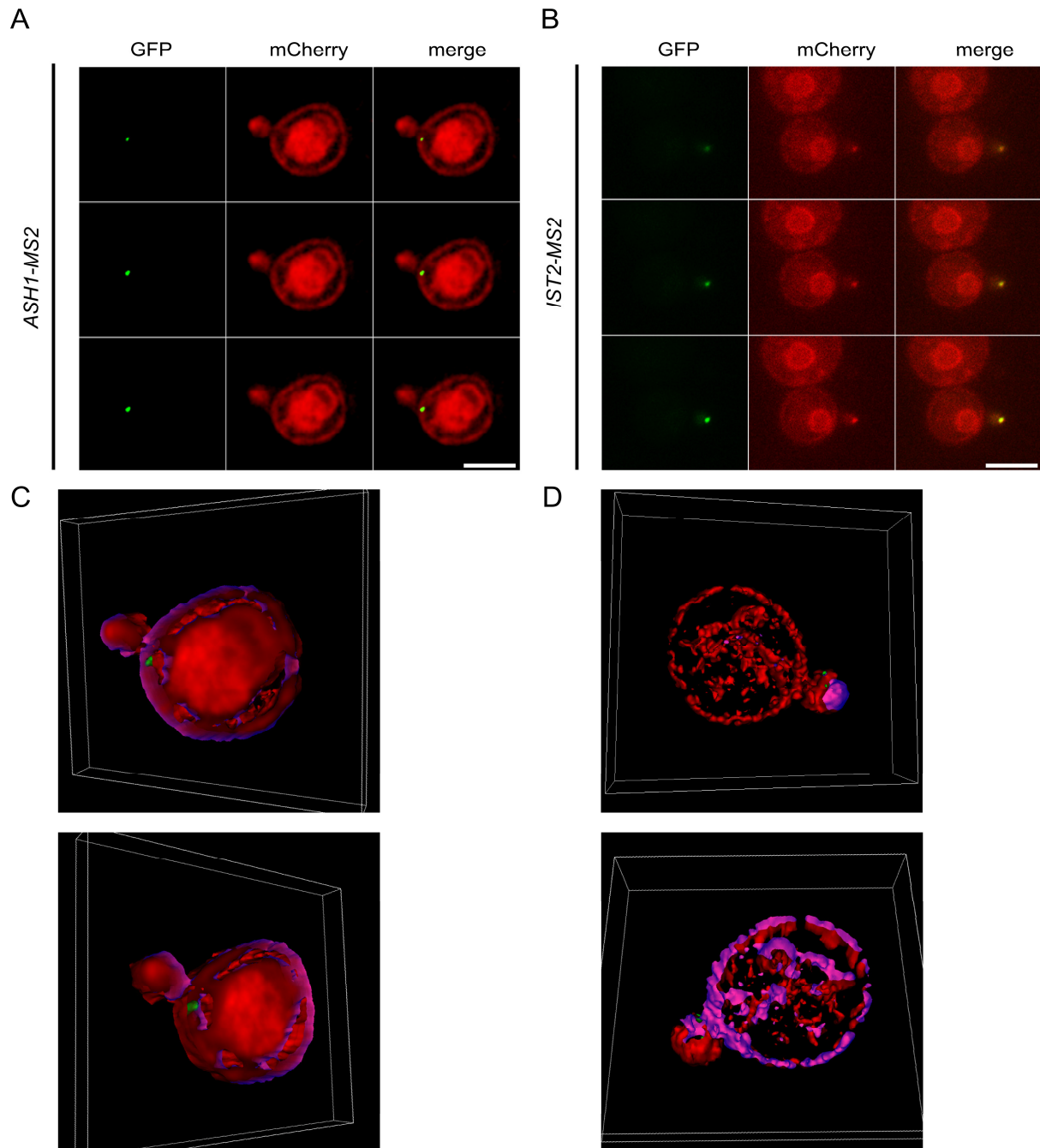


Figure 34 | Examples of co-localization in small budded cells in case of *ASH1* and *IST2* mRNA. (A/B) Representative images of cells expressing MS2-tagged *ASH1* (RJY3525; A) and *IST2* mRNA (RJY3783; B) in small budded cells are shown. The images represent a time lapse gallery of GFP, mCherry and merged channels. White bars correspond to 4 μ m. (C/D) Show corresponding 3D images of calculated ER structures together with the mRNP complex.

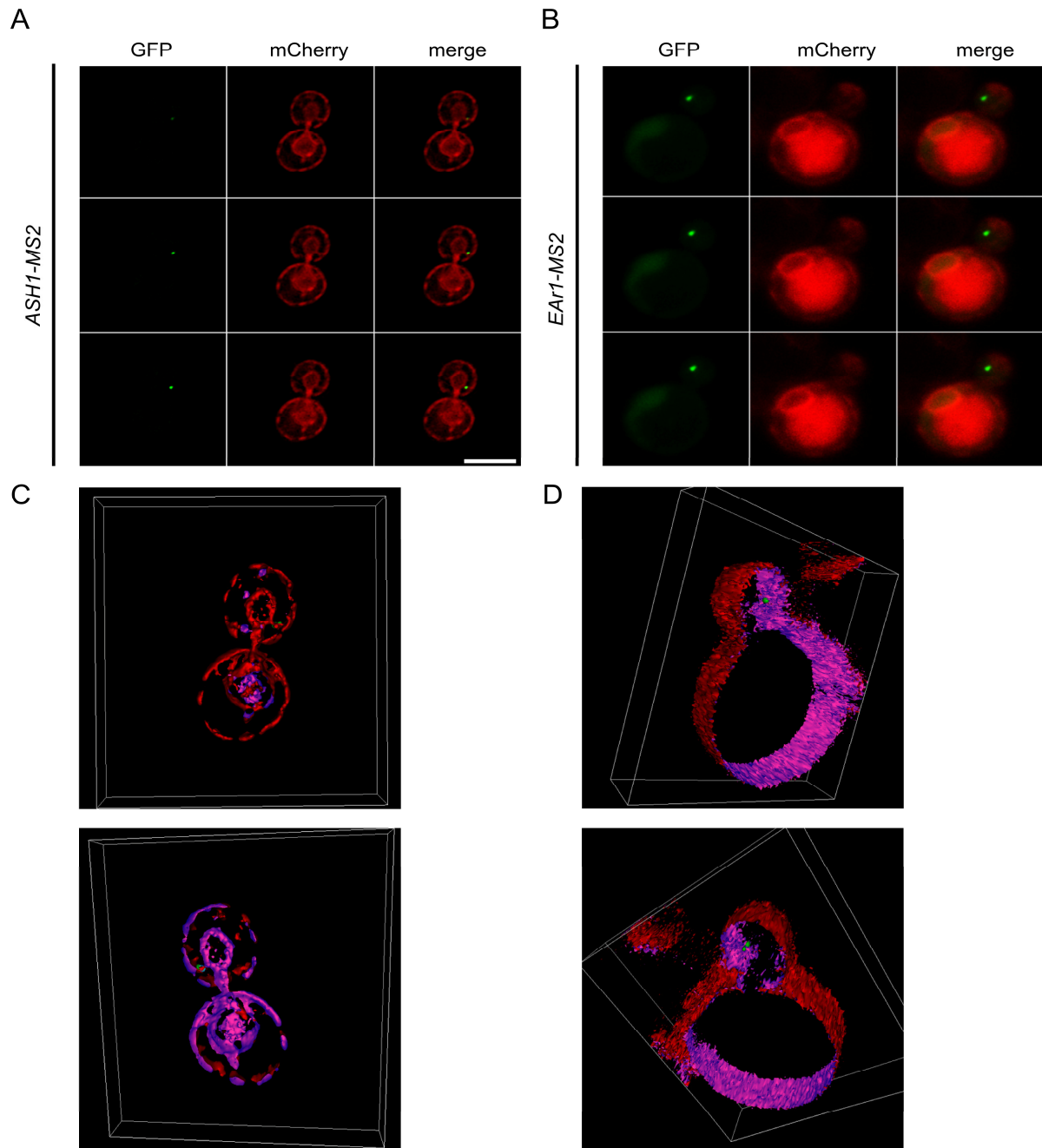


Figure 35 | Examples of co-localization in large budded cells in case of *ASH1* and *EAR1* mRNA. (A/B) Representative images of cells expressing MS2-tagged *ASH1* (RJY3525; A) and *EAR1* mRNA (RJY3622; B) in large budded cells are shown. The images represent a time lapse gallery of GFP, mCherry and merged channels. White bars correspond to 4 μ m. (C/D) Show corresponding 3D images of calculated ER structures together with the mRNP complex.

2.11 RNP particle localization of *WSC2* is independent of its translation

To test whether a co-translational insertion of the encoded protein causes the link between the analyzed mRNAs and ER tubular movement and docking, the importance of the signal peptide has to be clarified.

Because the protein Ist2p has no signal peptide whereas Srl1p (20 aa) and Wsc2p (24 aa) contain an N-terminal signal sequence, I decided to use *WSC2* mRNA to test if the co-translational ER translocation would be caused by its full length protein. This would clarify whether the signal peptide of the protein is essential for the mRNA localization and its connection to the segregation of cER.

Therefore I generated a mutated version of MS2-tagged *WSC2* that carries an AUG->UUG mutation as described in 5.7. This point mutation results in an out of frame translation of *WSC2* that starts 111 nucleotides after the original start codon.

The mutated and wild type MS2-tagged *WSC2* mRNA was expressed both in wild type and $\Delta aux1$ mutant cells from plasmids using the endogenous promoter and carrying either the AUG->UUG mutation or the original start codon. As shown in Figure 36 wild type cells, either expressed with *WSC2-MS2* or *WSC2(-AUG)-MS2* behave identical. In more than 90% of all counted cells the mRNPs were localized to the bud. The same behavior of expressed mRNPs was observed in the appropriate mutated $\Delta aux1$ strains for both *WSC2-MS2* and *WSC2(-AUG)-MS2* expressed mRNAs. In both cases more than 85% of mRNPs remain in the mother cell. These results show that the N-terminal located signal peptide of Wsc2p is not necessary or essential for *WSC2* mRNA localization. This indicates that the localization process of mRNAs does not involve co-translational mRNA targeting.

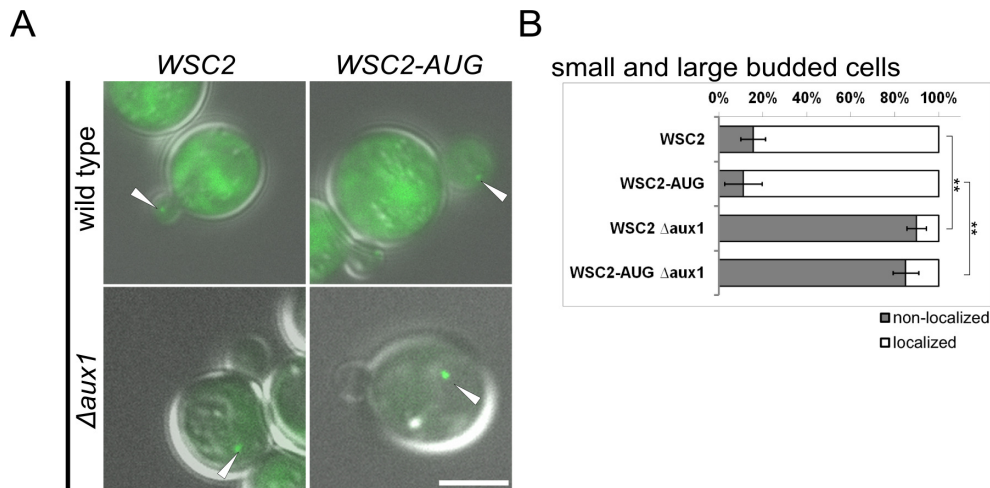


Figure 36 |mRNP localization of WSC2 mRNA is translational independent. (A) Representative images of cells expressing MS2-tagged *WSC2* mRNA. The upper panel shows wild type cells expressing *WSC2-MS2* mRNA (RJY3872) on the left side and wild type cells expressing *WSC2-MS2* mRNA (RJY3873) with an AUG→UUG mutation of the start codon AUG carried by a plasmid on the right side. The lower panel shows $\Delta aux1$ cells expressing *WSC2-MS2* mRNA (RJY3874) on the left side and $\Delta aux1$ cells expressing *WSC2-MS2* mRNA (RJY3875) with an AUG→UUG mutation on the right side. Images show an overlay of DIC and GFP channels. White arrowheads indicate mRNPs with tagged *WSC2* mRNA. White bar corresponds to 4 μm . (B) Quantification of mRNP localization of MS2-tagged *WSC2* mRNA to the bud. The counting of $n > 100$ budded cells was repeated four times in independent experiments. White bars indicate cells with bud-localized mRNPs, not localized mRNPs are represented by grey bars. Error bars assign two standard deviations. The confidence interval was determined assuming random sampling and using the normal approximation for a binomial distribution. *** Indicates a statistical significance of $P < 0.001$ in a one-tailed two-proportion t-test.

2.12 Biochemical analysis

2.12.1 Oligomerization of She2p is required for ER association

The results of the experiment described in 2.11 indicate that localization of mRNAs is independent of co-translational targeting but depends on functional segregation of cER. Previous studies have shown that the attachment of the localized mRNAs to the ER via the RNA binding protein She2p might be essential for its localization (Shepard K.A. *et al.*, 2003) and that She2p co-migrates with ER-derived vesicles *in vivo* (Schmid M. *et al.*, 2006). Because of the fact that the binding capacity of ER to She2p was not influenced by disruption of the RNA-binding features of She2p (Schmid M. *et al.*, 2006) the whole process of binding between ER and She2p seems to be more obscure. How She2p binds to the ER and how the transport of its complex takes place has not yet been completely understood. To better understand these processes several mutations of She2p were generated and tested in the last

years. The research of these processes is hindered by the fact that the expression of these mutated protein versions *in vivo* results in the prevention of shuttling She2p to the nucleus or nucleolus. Nevertheless, the nucleolar transit of She2p is essential for the correct assembling (Du T. *et al.*, 2008) of the transport complex. It was also shown that She2p has a non-classical nuclear localization signal (NLS) which is essential for its nuclear import. The Exclusion of the She2p protein by generating a mutated NLS results in localization defects of *ASH1* mRNA (Shen Z. *et al.*, 2009).

However, to illuminate this field the identification of new potential binding sites in She2p came into focus of the following experiments. Therefore, She2p mutants that were already known to have mRNA localization defects were used in *in vitro* assays.

First of all the co-migration of endogenous She2p with ER markers was recapitulated as done before by Schmid M. (Dissertation, 2008). Thus, cell extracts were prepared as described in 5.8 and 5.9 and shown in Figure 37.

By separating the cell extracts on a 18%-60% sucrose gradient including the pellet, 13 fractions were collected and tested by Western blotting using She2p and ER markers (Sec61p) shown in Figure 38 (A). The ER marker Sec61p which is known to be an essential subunit of the translocon in yeast (Romisch K. *et al.*, 1999) migrates close to the bottom of the high-density fractions of the linear gradient. The RNA-binding She2p shows a similar fractionation pattern like Sec61p which was the first evidence for a direct physical association between ER and She2p. Due to the quantification of Western blots, prepared out of ≥ 3 independent experiments, the percental distribution of She2p and Sec61p was detected. Interestingly, She2p was also detected in the top fraction ($21\% \pm 1.5\%$ of total She2p present in all fractions) in contrast to Sec61p. This suggests that not all of the endogenous She2p is associated to the ER.

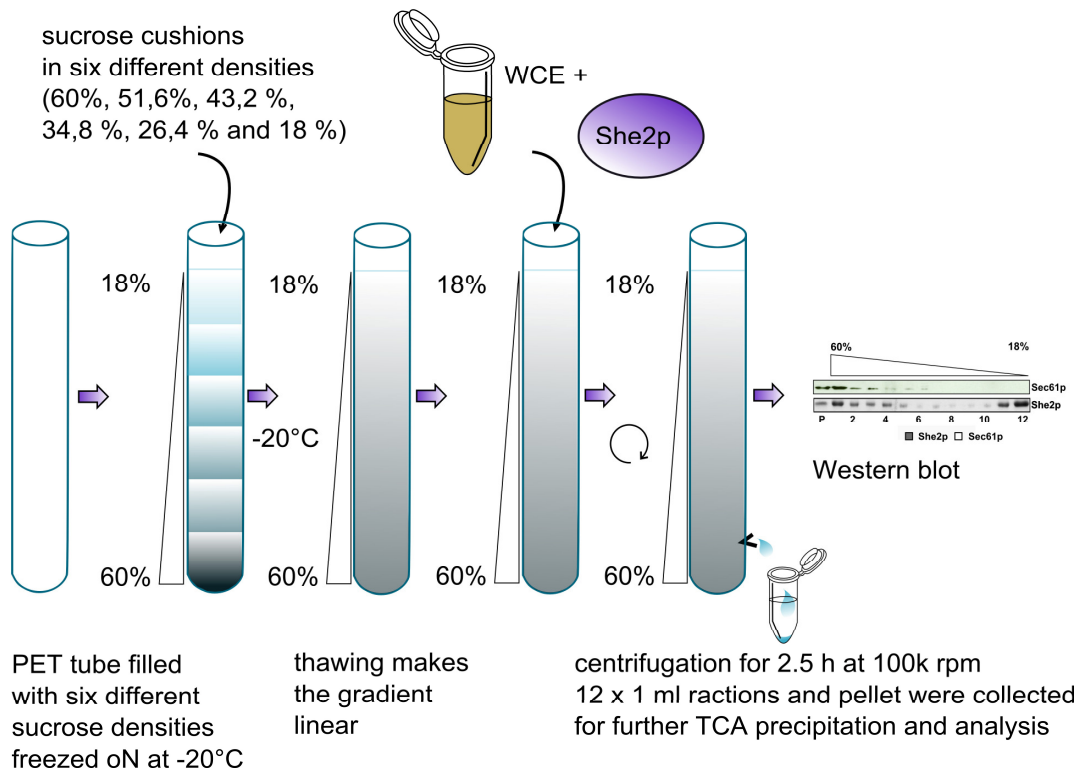
in vitro sucrose gradient centrifugation

Figure 37 | Experimental approach of sucrose velocity gradient centrifugation. Schematic overview of the *in vitro* assay is shown. Endogenous She2p (purified from RJY358), recombinant She2p (bacterially expressed; RJB441), or mutated She2p (She2p-L130Y from RJB445; She2p-S120Y from RJB444; She2p Δ helix E from RJB480/481) was either directly used for centrifugation in case of endogenous She2p, or incubated with WCE from a Δ she2 strain (RJY2053). The mixture was loaded on top of previously prepared 18%-60% linear sucrose gradients and centrifuged. After preparing fractions of similar amounts the samples were TCA precipitated and used for Western blotting analyses.

The fractionation of recombinant She2p was tested (Figure 38, B). The lysate of a Δ she2 yeast strain (RJY2053) was added to bacterially expressed wild type She2p and processed like described in 5.9. As shown before with endogenous She2p, the co-fractionation pattern between Sec61p and the previously added recombinant She2p looks similar. In this case the amount of She2p which was detected in the top fractions was slightly less ($16\% \pm 1.5\%$) compared to endogenous conditions. Nevertheless, the results of bacterially expressed She2p are very similar to endogenous expressed She2p which indicates that posttranslational modifications like phosphorylation are not required for the association between ER and She2p. It also suggests that recombinant She2p maintains the capacity to associate with microsomes.

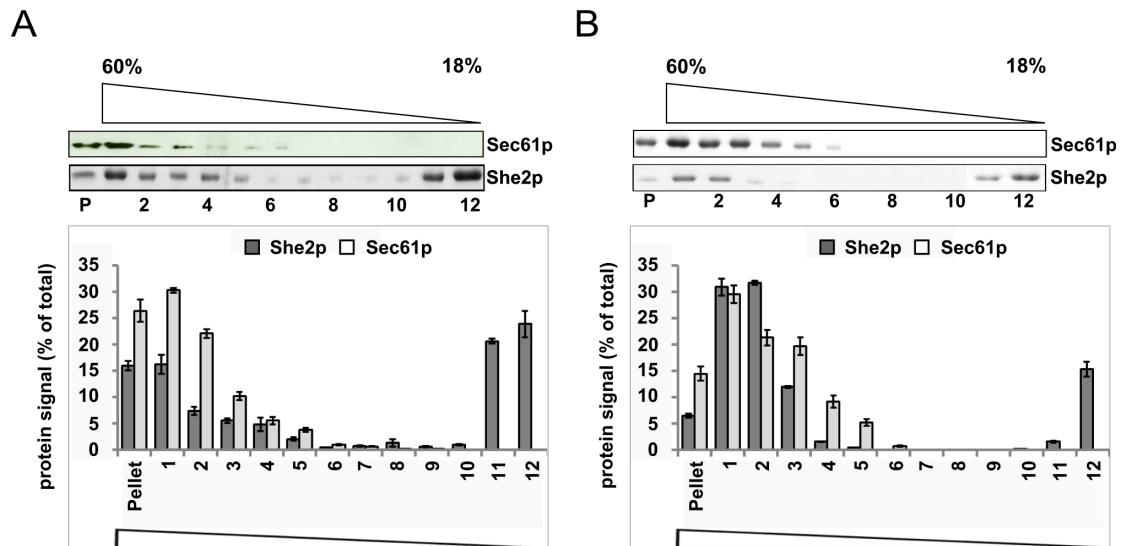


Figure 38 | Endogenous and recombinant She2p co-migrates with ER marker proteins in sucrose velocity gradient centrifugation. (A) Upper panel shows cell extracts from wild type She2p (RJY358) separated on a linear sucrose gradient and treated as described above. Aliquots of 12 fractions (1 as the bottom and 12 as top fraction) and the pellet were analyzed by Western blotting against Sec61p and She2p. Representative images of Western blots are shown. The Lower panel shows the relative amounts of She2p and Sec61p in the corresponding fractions in % of total She2p or Sec61p detected in all fractions. The quantification was done using the ImageJ Software by analyzing \geq three independently generated Western blots. (B) Recombinant She2p co-migrates with ER in sucrose velocity gradient centrifugation. Upper panel shows cell extracts from $\Delta she2$ (RJY2053) incubated with bacterially expressed and purified recombinant She2p (RJB441), separated on a linear sucrose gradient and treated as described above. Aliquots of 12 fractions (1 as the bottom and 12 as top fraction) and the pellet were analyzed by Western blotting against Sec61p and She2p. Representative images of Western blots are shown. The Lower panel shows the relative amounts of She2p and Sec61p in the corresponding fractions in % of total She2p or Sec61p detected in all fractions. Average values and standard deviation from \geq three experiments are displayed.

Next, I tested different She2p mutants for their co-fractionation (Figure 39). The first mutant was She2p-L130->Y (B) which seems to be affected in its ability to bind to the adapter protein She3p (Schmid M. *et al.*, 2006; Gonsalvez G.B. *et al.*, 2003) and is impaired in tetramerization of She2p. While tetramerization is essential for the targeting of RNAs it does not reduce general RNA binding processes (Müller M. *et al.*, 2009).

Compared to the co-fractionation of recombinant She2p which was similar to the wild type situation, shown in Figure 39 (A), the L130->Y (B) mutant showed a reduced co-fractionation with the ER marker Sec61p. Only 20.3% of total She2p L130->Y was detected in the first three fractions containing Sec61p while about 40% of She2p L130->Y was detected in the top two fractions and 28% in the pellet. These results suggest that She2p L130->Y aggregates partially (Müller M. *et al.*, 2009).

The second tested mutant was She2p-S120->Y (Figure 39, C). This mutant has a defect in its homodimerization capability and loss of binding activity to the *ASH1* E3 element and failure for the correct localization of *ASH1* mRNA *in vivo* shown by Niessing D. *et al.*, 2004. These previous experiments suggest that the dimerization of She2p is necessary for the binding of She2p to RNA.

The co-fractionation experiments I did also show a reduction of the She2p ER co-fractionation as published by Niessing D. *et al.*, 2004. In this case 20% of total She2p S120->Y was detected in the first three fractions containing Sec61p. The detected co-fractionation of She2p and ER was observed in more fractions than for the She2p L130->Y mutant. While in contrast to the She2p L130->Y mutant where 40% accumulated in the top two fractions and 28% in the pellet in this mutant only 22% of the total She2p was detected in the top two fractions and 24% in the pellet. The dispersion of ER and She2p was more spreaded in the linear sucrose gradient. Saying in other words the decrement of the co-fractionation between ER and She2p for She2p S120->Y was not as strong as for the She2p L130->Y mutant.

Finally, I tested She2p with a deletion of helix E which was identified by Müller M. from the Niessing Lab. The helix E is involved in targeting mRNA selection. This mutant has a deletion of the α -helix which sticks out from both sides orthogonally at the middle of the dimer of She2p. It is also known that this mutant is impaired in binding of the *ASH1* E3 element (Schmid M., Dissertation 2008).

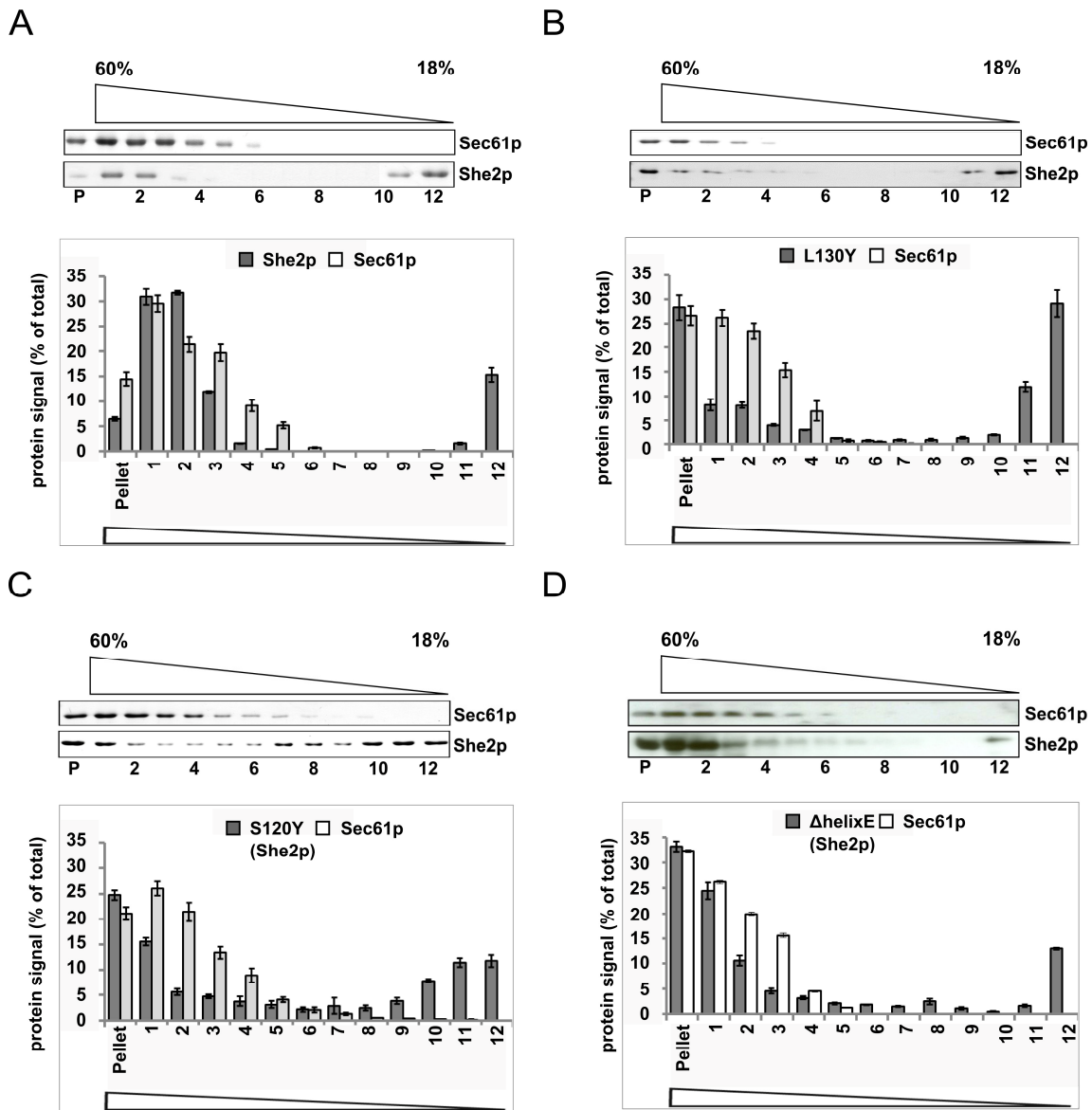


Figure 39 | Tetramerization but not RNA binding of She2p is required for ER association.

(A) Recombinant She2p co-migrates with ER in sucrose velocity gradient centrifugation. Upper panel shows cell extracts from $\Delta she2$ (RJY2053) incubated with bacterially expressed and purified recombinant She2p (RJB441) and separated on a linear sucrose gradient. Aliquots of 12 fractions (1 as the bottom and 12 as top fraction) and the pellet were analyzed by Western blotting against Sec61p and She2p. Representative images of Western blots are shown. The Lower panel shows the relative amounts of She2p and Sec61p in the corresponding fractions in % of total She2p or Sec61p detected in all fractions. (B) Reduced co-migration with ER of the tetramerization mutant She2p-L130Y. Upper panel shows cell extracts from $\Delta she2$ (RJY2053) incubated with bacterially expressed and purified recombinant She2p-L130Y (RJB445). Western blots against recombinant She2p-L130Y and Sec61p after gradient centrifugation are shown. Lower panel displays the quantification as described for (A). (C) Co-fractionation of She2p-S120Y together with ER. Upper panel shows cell extracts from $\Delta she2$ (RJY2053) incubated with bacterially expressed and purified recombinant She2p-S120Y (RJB444). Western blots against recombinant She2p-S120Y and Sec61p after gradient centrifugation are shown. Lower panel displays the quantification as described for (A). (D) Co-migration of She2p $\Delta helix E$ (RJB480/481) incubated with RJY2053 in the upper panel. Lower panel displays the quantification as described for (A). Average values and standard deviation from ≥ 3 experiments are displayed.

Interestingly, this mutant does not affect the She2p ER co-localization significantly and shows a co-fractionation pattern comparable to the wild type She2p. As shown in Figure 39 (D) about 40% of total She2p Δ helix E was detected in the first three fractions of high sucrose density containing Sec61p. While only 14% accumulates in the top two fractions 33% of She2p Δ helix E was detected in the pellet. A similar effect was shown for the She2p N36->S/R63->K mutant by Du T. *et al.*, 2008; Müller M. *et al.*, 2009 and Schmid M. *et al.* 2006. This mutant has two point mutations (N36S and R63K) which disrupt RNA binding (Gonsalvez G.B. *et al.*, 2003).

The results of these studies, especially the quantification of the detected amounts of She2p and Sec61p, suggest that the RNA binding capability is not required for its association of She2p to the ER while the correct tertiary structure is.

2.12.2 Characterization of the association of She2p and ER

As mentioned above, the co-fractionation experiments indicate that not all of the endogenous or recombinant She2p associates to the ER. Thus, it was necessary to investigate if the association of She2p to ER tubular structures requires another factor, maybe an ER-bound protein and if the binding itself is specific and direct.

Previous studies of pelleting assays of recombinant She2p or GST and purified ER microsomes indicate that pelleting of She2p with microsomes is specific (Schmid M., Dissertation 2008). GST was used as a control for She2p because it has similar characteristics in certain cases. With 26 kDa GST has nearly the same molecular weight as She2p (26 kDa) and like She2p (Niessing D. *et al.*, 2004) GST also forms dimers (Ji X. *et al.*, 1992).

While in contrast to She2p which pellets together with ER microsomes, GST can not penetrate through the sucrose gradient in the presence of purified membranes, even though it has a smaller size. Therefore these experiments suggest another protein characteristic which made the binding of She2p to ER structures specific. As mentioned above, another possibility would be that the binding between She2p and ER depends on another protein or protein-like structure.

Previous studies show (Genz C., Diploma Thesis 2009) that She2p preferentially binds to smaller protein-free liposomes indicating a preferential binding to high-

curvature membranes. This also indicates that no other protein would distinguish between binding or not binding of She2p and ER.

In the next experiment I wanted to clarify whether the binding itself is terminated by She2p. Therefore, I used different amounts of She2p and pre-incubated these with purified microsomes as described in Methods, 5.10.4 and shown in Figure 40 and 41.

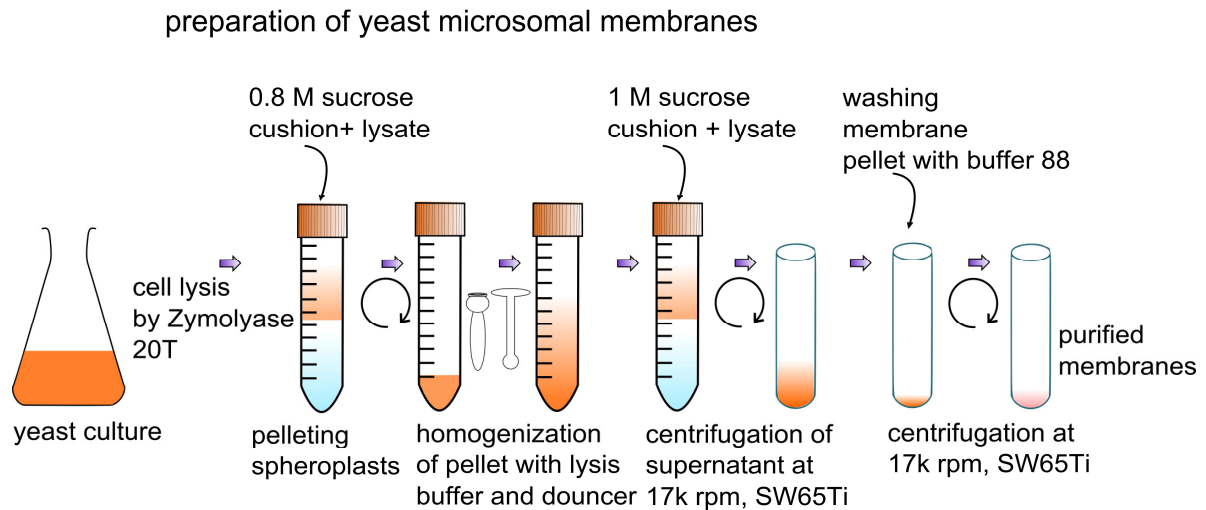


Figure 40 | Experimental approach of preparation of yeast microsomal Membranes (YMRs). Schematic overview of the preparation of YMRs according to Brodsky J.L. *et al.*, 1993; Rothblatt J.A. and Meyer D.I., 1986 and Schmid M. *et al.*, 2006. The strain was inoculated in 2 l YPD media starting at OD_{600} 0.2. The cells were harvested at OD_{600} 1.0-2.0 and lysed gently by Zymolyase® 20T. After centrifugation of the spheroplast suspension through a 0.8 M sucrose cushion, the spheroplast pellet was homogenized and lysed by using a dounce homogenizer. The cell debris was separated from the suspension by centrifugation through a 1 M sucrose cushion. By washing and repeated centrifugation the membranes were separated and therefore purified in a first approach. For more detailed information see method section 5.10.1.

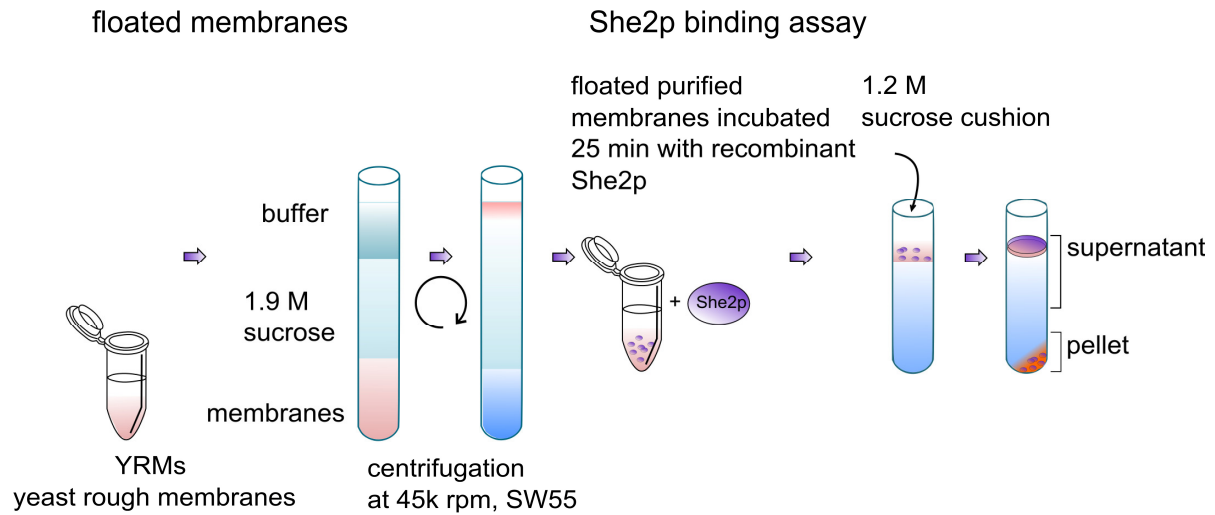


Figure 41 | Experimental approach of She2p binding assay. Schematic overview of purifying membranes by floatation and She2p binding assay according to Brodsky J.L. *et al.*, 1993; Rothblatt J.A. and Meyer D.I., 1986 and Schmid M. *et al.*, 2006. The membranes were purified again by using the floatation assay through a 1.9 M sucrose cushion. By centrifugation the membranes floated on top of the buffer. Different She2p amounts were added to the purified membranes and incubated for 10 min at RT and 15 min on ice. The *in vitro* mix was layered onto a 1.2 M sucrose cushion and centrifuged at 100.000 rpm for 1 h at 4°C. The supernatant and pellet were collected. Before precipitating the proteins by using TCA (5.13.3.) aliquots of both supernatant and pellet were used as control for SDS-PAGE and Western blotting. For more detailed information see method section 5.14.

Indicated amounts of She2p (starting with 0 to 282.35 pmol She2p) were incubated with 40 µg of purified microsomes, layered on top of a sucrose cushion and were centrifuged. The supernatant and the lowest fraction was collected and analyzed by quantitative Western blot. Input and bound She2p was analyzed by the ratio of bound She2p vs. the signal strength of the input shown in Figure 42 (A). By adding increasing amounts of She2p to purified membranes I observed that with amounts of She2p higher than 105.88 pmol the ratio between bound She2p and input started to decrease. Therefore, the membranes were saturated of She2p. This strongly indicates that the binding itself is saturable and therefore might involve a binding partner on the membrane.

As mentioned above, other studies suggest that no other protein would be necessary for the binding of She2p to ER. Therefore, a protein component could be the yet unknown factor. To test this I recapitulated experiments done previously by Schmid M. (Dissertation, 2008) in which the membranes first were treated with Pronase E and Proteinase K before adding to She2p. This treatment done by Schmid M. did not lead to a clear result. Thus, I repeated this experiment by first using the same amounts of Pronase A and Proteinase K (Figure 42, B). In this case the protein

treatment results in the removal of the cytoplasmic epitope which was tested by the ER marker Sec61p resulting in the successful proteolysis. By increasing the amounts of Pronase E and Proteinase K from 0.05 mg up to 2 mg (Figure 42, C) the portion of She2p that co-pellets with the membranes was reduced but did not mitigate it suggesting that maybe other protein adapters on the ER are involved in the interaction between ER and mRNPs. The results also show that $55\% \pm 2\%$ were still detected in the pellet fraction. To test whether these results are caused by the ability of She2p forming multimers *in vivo* (Müller M. *et al.*, 2009) She2p was mixed with the supernatant of a cell lysate (S100). This lysate was centrifuged at 100.000 rpm using a TLA 120.2 rotor to reduce the membrane contingent. In these cases only very small amounts of She2p were pelleted (Figure 42, B) indicating that pelleting would not result in formation of large She2p multimers.

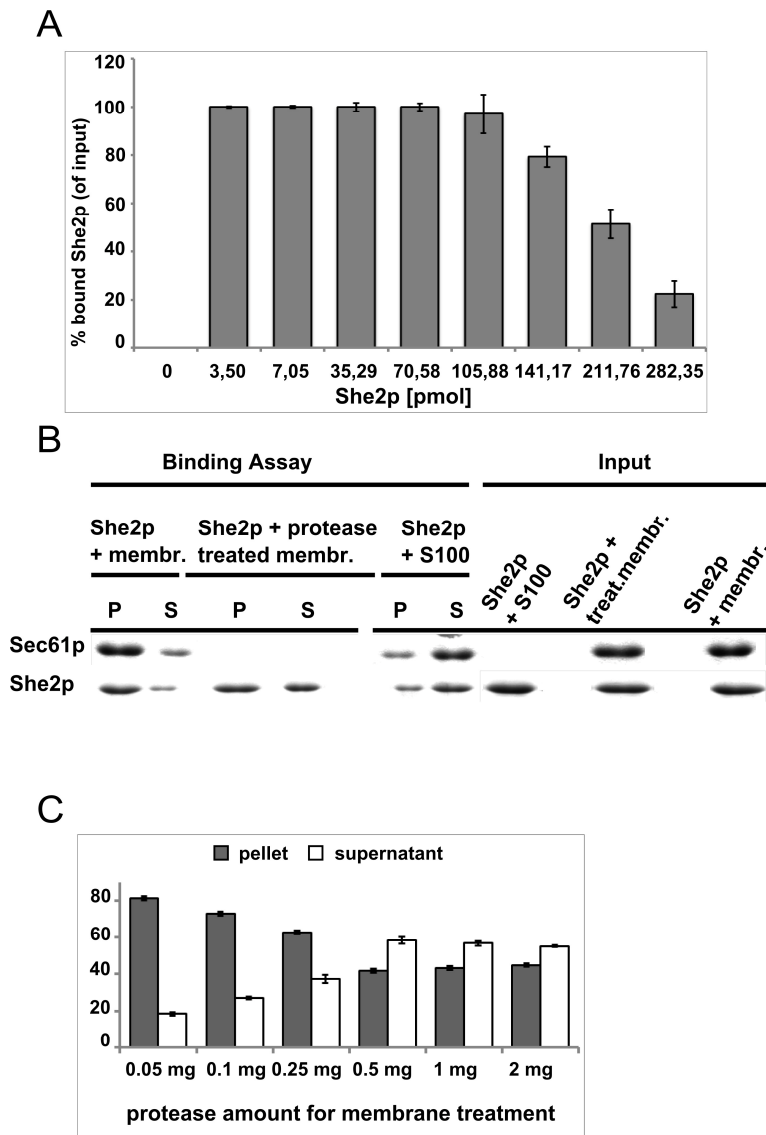


Figure 42 | She2p is saturable and binds to purified microsomes *in vitro*. (A) Binding of She2p to membranes is saturable. Indicated amounts of She2p were incubated with 40 μ l microsomes (corresponding to 40 μ g of membrane-associated protein). Input and bound She2p were analyzed by quantitative Western blotting and the ratio of bound She2p signal versus input was quantified. Average ratio (in %) and standard deviation of n=3 experiments is displayed. (B) Pelleting assay of recombinant She2p and protease-treated microsomes. She2p was either incubated with membranes, membranes treated with a combination of Pronase E and Proteinase K or a supernatant depleted of membranes (S100). After the binding reaction, all samples were analyzed by Western blotting against She2p or Sec61p. (C) Protease treatment of microsomes results in only partial loss of She2p binding capacity. Identical quantities of microsomes as in (B) were treated with increasing protease amounts before addition of She2p and membrane pelleting. Even at high protease concentration of >40% She2p can be pelleted. Bars indicate average values from n=4 experiments.

3 Discussion

The endoplasmic reticulum (ER) is possibly the most multifunctional and extensive organelle in eukaryotic cells and characterized by its complex structure with an extremely large surface area (Voeltz G.K. *et al.*, 2002). Proteins that are translocated across the membrane of the ER are subsequently folded and modified before they are passing through the secretory pathway. Besides its role in protein synthesis the ER also plays a central role in processes like signaling, Ca^{2+} -segregation and lipid synthesis (Du Y. *et al.*, 2004).

Like all organelles the ER has to be inherited from the mother to the daughter cells. In budding yeast the segregation pathway of cER is initiated by the development of tubular ER structures pointed towards the newly formed bud (Du Y. *et al.*, 2004; West M. *et al.*, 2011). The movement of these tubules requires the Myo4p-She3p co-complex which consists of the myosin motor protein Myo4p and its adapter protein She3p. She3p is known for its function as a connector between Myo4p and specific mRNAs that are localized during mRNP transport (Estrada P. *et al.*, 2003). The Myo4p-She3p co-complex is crucial for at least 24 mRNAs that have to be localized from the mother cell to the bud (Shepard K.A. *et al.*, 2003). The role of Myo4p in mRNA localization is confirmed in this work (section 2.2). MS2-tagged mRNAs (*EAR1*, *MID2*, *IST2*, *SRL1* and *WSC2* mRNA) in $\Delta myo4$ strains (Figure 19) were compared to the same MS2-tagged mRNAs in wild type cells related to their mRNP distribution. In wild type cells more than 84% of all cases of these MS2-tagged mRNPs localized to the bud of small budded S-phase and large budded wild type cells of the G2 cell cycle (Figure 19, wild type) while in contrast in cells lacking Myo4p the mRNP localization drops to less than 29% (Figure 19, $\Delta myo4$). This demonstrates that the loss of the class V myosin Myo4p disrupts localization of all five tested mRNAs.

Previous studies suggested that the transport of mRNAs and ER structures as tubules could occur in two different ways. Either transport of ER and mRNA occurs independently of each other (Estrada P. *et al.*, 2003) or via the attachment of mRNAs to ER tubules as suggested by studies on *ASH1* mRNA. The latter case would mean that both processes happen in a coordinated way (Schmid M. *et al.*, 2006).

In case of the *ASH1* mRNA experiments (done by Schmid M. *et al.*, 2006), the *ASH1* mRNA was expressed from an inducible, heterologous *GAL1* promoter. The cells were observed in S-phase whereas the expression of *ASH1* mRNA occurs during late M-Phase (Bobola N. *et al.*, 1996). During the late mitotic phase the segregation of cortical ER is already completed and thus the cER inheritance has to be studied during S- and G1-phase, when cER segregation occurs, to investigate if mRNA localization dependent on tubular ER is rather relevant for mRNAs in earlier phases of reproduction during budding. It is already known that many localized mRNAs encode secreted or membrane proteins and therefore it could be favorable if these mRNAs were pre-assembled and co-transported with the ER where they are translated (Shepard P. *et al.*, 2003). Thus, the following mRNAs namely *EAR1*, *MID2*, *IST2*, *SRL1* and *WSC2*, which all code for membrane or secreted proteins were used in this study. All mRNAs are also expressed early during S- and G2-phase of the yeast cell cycle. In this phase of ER inheritance the ER tubules are moving towards the bud and associate to the plasma membrane (Loewen C.J.R. *et al.*, 2007) at the bud tip. This part of the three phases of the ER inheritance is described in detail in section 1.5.2. During the association step the interactions of reticulons (Rtn1p, Rtn2p and Yop1p) with components of the translocon (Sbh1p and Sbh2p) and with components of the exocyst (Sec3p, Sec6p and Sec8p) are supposed to support this phase of cER inheritance (Wiederkehr A.Y. *et al.*, 2003; Reinke C.A. *et al.*, 2004; De Craene J.O. *et al.*, 2006).

My work shows that the segregation of cER is required for the proper localization of the five tested mRNAs. Knocking out genes that are encoding proteins necessary during the early steps of cER inheritance leads to marked defects in the localization of mRNAs used in this study. Deletion of *AUX1* (section 2.3), a gene that is known to be required similar to She3p and Myo4p during early steps of ER inheritance (Du Y. *et al.*, 2001) leads to localization defects for all the five aforementioned mRNAs. At the same time, (section 2.1) $\Delta aux1$ cells show the same pattern of disrupted ER signals in more than 70% of mother and daughter cells in comparison to wild type cells as it was published previously (Estrada P. *et al.*, 2003 and Schmid M. *et al.*, 2006). This direct connection between mRNA localization failure and disrupted ER structure underlines the link between these two different pathways. Nevertheless, the molecular function of Aux1p during early cER segregation remains unclear (Du Y. *et al.*, 2001; Du Y. *et al.*, 2004). The suggested bi-functionality of Aux1p regarding to

roles in cortical ER inheritance and membrane traffic (Du Y. *et al.*, 2001) is also supported by this study. Deletion of the J-domain (section 2.4) of Aux1p affects mRNA localization but has no effect on the migration of peripheral ER into daughter cells (Du Y. *et al.*, 2001) while the full length deletion of *AUX1* leads to defects in both ER inheritance and mRNA localization. This indicates that the J-domain only together with other sequential parts of the *AUX1* gene is required for proper ER inheritance coupled with the localization of mRNAs. This is also supported by the results which show that in case of ΔJ -domain cells the mislocalization of mRNAs was less strong than in case of $\Delta aux1$ cells.

Similar observations as shown for $\Delta aux1$ cells were made in case of *SEC3* (section 2.7) deletion mutants. Sec3p is a protein that encodes together with Sec6p and Sec8p the exocyst complex and plays a role during the previously mentioned association phase of cER inheritance by supporting the docking of tubular ER to the bud cortex (Wiederkehr A. *et al.*, 2003; Reinke C.A. *et al.*, 2004). Its deletion leads to similar strong effects on mRNA localization as shown for $\Delta aux1$ with a dramatic reduction of mRNP localization to less than 16% of all counted MS2-tagged mRNAs (Figure 30, $\Delta sec3$). In case of the visualized ER structure no signal in the bud was detected in $\geq 84\%$ of the counted cells similar to observations in the case of $\Delta myo4$ and $\Delta ptc1$ cells. These observations support the previous studies done by Novick P. *et al.*, 2003, 2004 and 2006.

In contrast to $\Delta aux1$ or $\Delta sec3$ the deletion of either *PTC1* (section 2.6) or *SLT2* (section 2.5) did not affect mRNA localization. *PTC1* encodes a phosphatase that acts during late steps of cER segregation (Maeda T. *et al.*, 1993; Warmka J. *et al.*, 2001; Du Y. *et al.*, 2006) whereas *SLT2* codes for a kinase (Novick P. *et al.*, 2010; Mao K. *et al.*, 2011) that is known to be required for the last step of ER inheritance by spreading cER tubules around the entire bud to form a polygonal tubular network (Du Y. *et al.*, 2006). Only the localization of *SRL1* mRNA (section 2.5, Figure 30) was affected in $\Delta slt2$ cells where only 22% of all counted cells contained MS2-tagged *SRL1* mRNA in the bud. *SRL1* mRNA encodes a mannoprotein that has tight associations with the cell wall and is also required for the cell wall stability (Hagen I. *et al.*, 2004). In addition, the deletion of Slt2p leads to temperature-dependent cell lysis pre-initiating cell stress (Levin D.E. *et al.*, 2005). This would also explain the mislocalization defect in $\Delta srl1$ cells.

ER structures observed in $\Delta slt2$ cells showed the same pattern as wild type cells. Thus, no effect on ER morphology was observed. In support of the hypothesis for a link between ER inheritance and mRNA localization this explains why the mRNA localization in small budded cells was not affected and therefore the movement of ER tubules into the bud was followed by the docking at the bud cortex.

Scs2p encodes (section 2.5) an integral ER membrane protein that is required for the second step of the cER inheritance: the correct association of cortical ER to the plasma membrane at the bud tip (Kagiyada S. *et al.*, 1998; Loewen C.J.R. *et al.*, 2005 and 2007). Its deletion has no effect on the localization of the five tested mRNAs to the bud. In case of the ER structure more than 86% of the cells show a disrupted ER structure pattern with a weak punctual or even not existing ER signal comparing to the wild type confirmed by previous studies (Loewen C.J.R. *et al.*, 2007). This can be explained by the fact that the aforementioned mRNAs are already localized to the bud before the loss of Scs2p affects the late steps in ER segregation.

Together with the findings on $\Delta slt2$ and $\Delta ptc1$ these results lead to the conclusion that the transport and docking of tubular ER is required in order to localize mRNAs to small buds and thus underlines the thesis of this work.

As mentioned above, the reticulons (Rtns) Rtn1p, Rtn2p and DP1/Yop1p (section 2.8.) are required for the shaping of ER tubules and generating the high curvature to form tubular structures (Calero M. *et al.*, 2001; Brands A. and Ho T.H., 2002; Hu J. *et al.*, 2009). In addition, they also play a role during the association step of cortical ER inheritance (Wiederkehr A.Y. *et al.*, 2003; Reinke C.A. *et al.*, 2004; De Craene J.O. *et al.*, 2006).

In the $\Delta rtn1$ mutant no defect of *EAR1*, *MID2*, *IST2* and *SRL1* mRNA localization was observed. Previous studies showed that the deletion of the *RTN1* gene results in an altered ER morphology where the cortical ER becomes more cisternal but with no significant changes in the total membrane surface area of the ER (De Craene J.O. *et al.*, 2006). Together this indicates that in case of a link between ER inheritance and mRNA localization the altered ER morphology caused by the single knockout of *RTN1* might not be significant enough to affect the mRNA localization. In case of Sey1p which is a GTPase that interacts genetically with Rtn1p and Yop1p and is known to have a role in ER morphology (Brands A. and Ho T.H., 2002; Hu J. *et al.*,

2009), also little to none effects on mRNA localization were observed. However, in both cases ($\Delta rtn1$ and $\Delta sey1$) a small effect on localization for the MS2-tagged *WSC2* mRNA was observed. While in the wild type cells 97% of all counted cells contain MS2-tagged *WSC2* mRNA in the bud, in $\Delta rtn1$ only 68% and in $\Delta sey1$ only 69% of all counted cells contain *WSC2* mRNA. Nevertheless, this effect has to be classified as a small effect of mRNP mislocalization.

In case of the double knockouts $\Delta rtn1\Delta yop1$ and $\Delta sey1\Delta yop1$ the ER morphology as well as mRNA localization was affected. In $\Delta rtn1\Delta yop1$ cells no mRNP localization to the bud was observed in 72%-81% of all counted cells and in case of $\Delta sey1\Delta yop1$ in about 63%-69%. The ER morphology of $\Delta rtn1\Delta yop1$ cells (section 2.1) was characterized by disorganization in large budded cells or no ER signal in small budded cells in about 82% of cells. The changes in ER morphology are consistent with previous studies (West M. *et al.*, 2011) where a dramatic change in ER shape and curvature by generating triple knockout strains ($\Delta rtn1\Delta rtn2\Delta yop1$) of *RTN1*, *RTN2* and *YOP1* was observed.

Surprisingly, the single *YOP1* (section 2.9) knockout showed different results for early stages and later stages of the cell growth. While in case of small budded cells 41%-52% of MS2-tagged mRNAs remained in the mother cells, in large budded cells more than 86% were localized into the bud. By having a closer look at the ER morphology in these cells (section 2.1) it was evident that no ER signal was seen in buds of about 36% of small budded cells while in large budded cells in about 90% the ER morphology was normal. These results are supported by the previous work of West M. *et al.*, 2011 suggesting a direct connection between mRNA localization in small and large budded cells and a correct ER morphology. An overview of the proteins that are known to be involved in ER inheritance is shown in Figure 43.

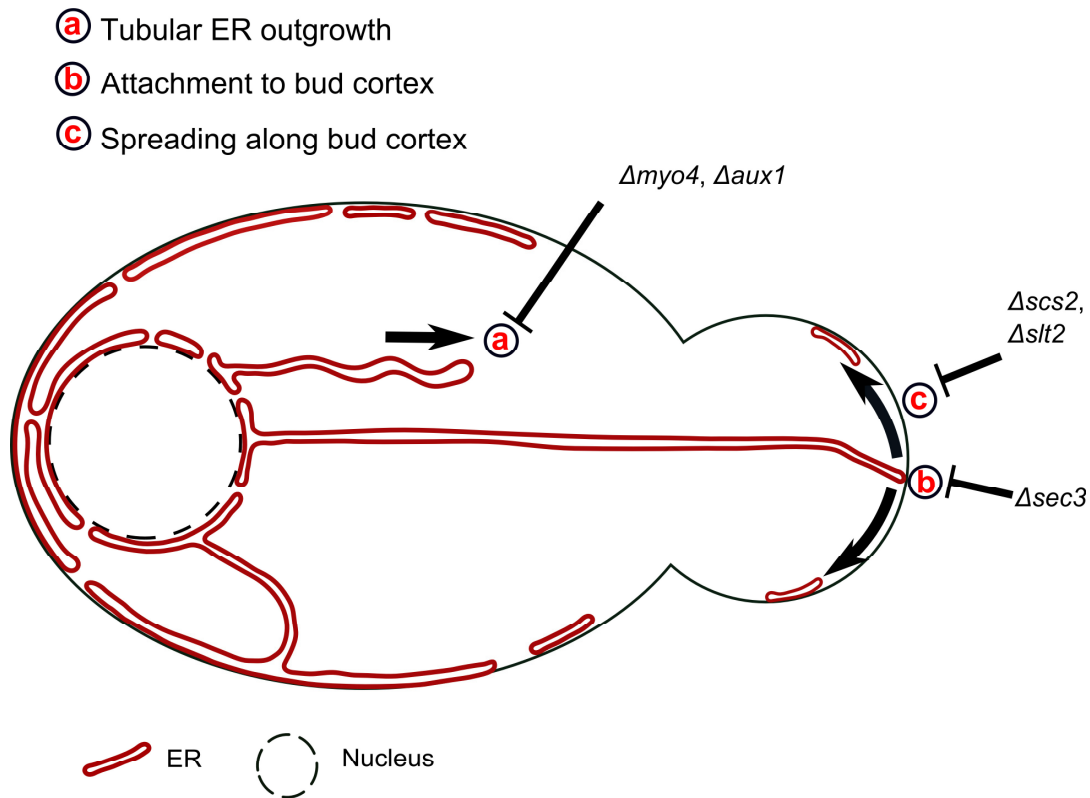


Figure 43 | ER inheritance is affected by a subset of mutants that are known to be involved in cER inheritance. The ER Inheritance can be classified by three main steps. First (a) ER tubules are moving from the mother cell into the bud; second (b) ER tubules are anchoring at the bud tip and finally (c); arrows indicate the spreading of cortical ER along the bud cortex forming a polygonal tubular network (Fehrenbacher K.L. *et al.*, 2002; Du Y. *et al.*, 2006). Mutations of indicated genes are blocking the specified steps of inheritance. While $\Delta myo4$ and $\Delta aux1$ is blocking the first step of cER inheritance, $\Delta sec3$ blocks the attachment of ER tubules to the bud tip. Finally, $\Delta scs2$ and $\Delta slt2$ are blocking independently the spreading of the cER tubules through the bud periphery.

All previously mentioned experiments were done using the aforementioned five MS2-tagged mRNAs *EAR1*, *IST2*, *MID2*, *SRL1* and *WSC2*. Additional experiments with MS2-tagged *ASH1* mRNA indicated that *ASH1* mRNA is not affected by the loss of *AUX1*. This was also shown by previous studies using genetic screens for genes that affect *ASH1* mRNA localization in which no genes were detected that are involved in ER segregation or physiology (Bobola N. *et al.*, 1996; Long R.M. *et al.*, 2001; Irie K. *et al.*, 2002).

As I already mentioned in the results section (section 2.3), in case of cells lacking Aux1p the localization of *ASH1* mRNA was comparable to wild type strains. In detail, in large budded cells (M-phase) 98% of wild type and 95% of $\Delta aux1$ cells the *ASH1* mRNPs were localized to the bud whereas in small budded cells (S- and G1-phase) 99% of wild type and only 43% of $\Delta aux1$ cells showed a localization of *ASH1* mRNPs

to the bud. This can be explained by the fact that in case of $\Delta aux1$ cells the MS2-tagged mRNA molecules are more stable in small budded cells. The previous experiments (Haim L. *et al.*, 2007) show another mRNP distribution in case of *ASH1* mRNA that did not represent the natural case by using an expression from a *GAL1* promoter. In contrast, in this study the endogenous promoter was used suggesting that the *ASH1* mRNA in *AUX1* function is related to M-phase specific expression of *ASH1* mRNA.

All five tested mRNAs (*EAR1*, *IST2*, *MID2*, *SRL1* and *WSC2* mRNA) encode membrane or extracellular proteins. With the exception of Ist2p (Jüschke C. *et al.*, 2004) these proteins have an N-terminal signal sequence that allows protein translocation into the ER. However, in this study (section 2.11) it was shown that the translation of the signal sequence is not required for the successful localization of *WSC2* mRNA suggesting that the localization process of mRNAs does not involve co-translational mRNA targeting.

This is not surprising because it was also shown in human cell lines that mRNAs do exist that are encoding proteins that do not have a signal sequence or in case of cytosolic proteins that have been detected on ER-bound polyribosomes. This suggests that another yet unknown factor is responsible for the targeting mechanism of mRNAs and thus the partition of mRNAs between ER compartments and the cytosol (Lerner R.S. and Nicchitta C.V. 2006; Pyhtila B. *et al.*, 2008).

A recent paper (Cui X.A. *et al.*, 2012) show that in metazoans a subset of mRNAs encoding secreted proteins are containing information for targeting and anchoring these mRNAs to the ER in an ribosomal- and translational-independent manner. This indicates the existence of an alternative pathway for targeting and maintaining secretory mRNAs at the ER.

Normally, the process of localizing mRNAs occurs by utilizing *trans*-recognition factors, *cis*-targeting elements to guide the organization of translational suppressed mRNAs. In contrast to this mechanism the localization of mRNAs to the ER occurs via a co-translational mechanism that is dependent on a signal sequence/signal recognition particle (SRP; Shan S.O. and Walter P., 2005).

In a previous study with human cells (Lerner R.S. and Nicchitta C.V. 2006) a Coxsackie B virus (CBV) infection was used as a tool to inactivate polysomes and

translation initiation to show that the RNA-ER association is independent of translation. The CBV infection results in the efficient cleavage of the eukaryotic translation initiation factor 4 gamma (eIF4G) and the Poly(A)-binding protein (PABP). This cleavage results in the breakdown of polyribosomes at the ER and in the cytosol and thus suppresses translation. In another study with human cell lines (Pyhtila B. *et al.*, 2008) it was shown that an ER-directed mRNA localization pathway exists that is independent on the signal recognition particle (SRP)-pathway and signal sequence, respectively.

Finally, these publications suggest that the mRNA and ribosome release from the ER was regulated translational independent and thus identified the ER as a privileged site to synthesize proteins (Lerner R.S. and Nicchitta C.V. 2006; Pyhtila B. *et al.*, 2008). Thus, the yet unknown factor for targeting and partitioning mRNAs between ER and cytosol could also involve proteins that bind to the RNA and facilitate the link between the ER and the mRNA.

Besides the PABPs in human cells RNA-binding proteins that are involved in targeting the mRNA or associated to the ER also exist in prokaryotes as well as metazoans and yeasts (Kraut-Cohen J. and Gerst J.E. 2010).

In case of the budding yeast several RNA-binding proteins that are associated to the ER does exist, like Whi3p (Colomina N. *et al.*, 2008) a cell fate and cell size regulating protein (Nash R.S. *et al.*, 2001), Bfr1p (Lang B.D. *et al.*, 2001) a protein that is implicated in nuclear segregation and secretion (Jackson C.L. and Kepes F. 1994), Scp160p (Frey S. *et al.*, 2001) a component of cortical actin cytoskeleton that binds and cross-links actin filaments (Goodman A. *et al.*, 2003) and She2p that is a component of the core locosome and restricts the accumulation of certain proteins to the bud (Long R.M. *et al.*, 2000; Bohl F. *et al.*, 2000; Shepard K.A. *et al.*, 2003). These proteins are known to co-fractionate or co-localize with ER. In case of Bfr1p and Scp160p the co-localization with ER is dependent on translation (Frey S. *et al.*, 2001; Lang B.D. *et al.*, 2001) while in case of Whi3p the mechanisms how the ER is associated to Whi3p are unknown. She2p co-fractionates with ER even after the polysomes were disrupted or the mRNA was degraded (Schmid M. *et al.*, 2006; Aronov S. *et al.*, 2007; this study section 2.12.2). Thus, She2p might be a candidate for the specific and direct association of mRNAs to ER tubules. The co-fractionation experiments (section 2.12.1) suggest that the RNA-binding capability is not required

for the association of She2p to ER while its correct tertiary structure in form of the oligomerization is. Because the co-fractionation experiments (section 2.12.1) show that not all of the endogenous or recombinant She2p associates with the ER, indicate that maybe another factor like an ER-bound protein is involved (section 2.12.2). Another explanation can be that not all of the She2p was bound to the membranes or its binding to the ER membranes was specific but not strong enough resulting in the release of She2p during the experiment. To test whether a protein factor is required for the binding of She2p to ER membranes, these membranes were treated with Pronase E and Proteinase K before addition of She2p. The rationale was that by this treatment a potential cytoplasmic epitope of such a factor is removed. The results of this *in vitro* assay show that the portion of She2p that was pelleting together with the purified ER membranes was reduced after increasing the protease treatment but did not diminish it. This was not caused by the ability of She2p of forming multimers *in vivo* (Figure 42, B). The *in vitro* experiments also show that She2p can bind at the same time to ER membranes and to an RNA localization element and thus support the idea that She2p is a likely candidate for association specific mRNAs to the ER.

Two features are necessary for the specific binding of She2p to mRNA. On the one hand the tetramerization of She2p (Müller M. *et al.*, 2009) is required for the specific RNA binding and on the other hand the basic helical hairpin motif and the helix E (Niessing D. *et al.*, 2004; Müller M. *et al.*, 2011). In detail, endogenous and recombinant She2p as well as mutated She2p in form of She2p-S120Y that has a defect in its homodimerization interface (Niessing D. *et al.*, 2004) and She2p Δ helix E co-migrates with ER (section 2.12.1) as indicated by the ER marker Sec61p, whereas the tetramerization-deficient mutant She2p-L130Y does not associate with ER. She2p is not only a dimer that was shown before in crystallography experiments done by Niessing D. *et al.*, 2004 but has a tetrameric structure in solution shown by Müller M. *et al.*, 2009 and Kremmentsova E.B. *et al.*, 2011.

Thus, the tetrameric structure appears to function in membrane and RNA-binding while the helix motif on She2p seems to be responsible for the binding between She2p and She3p (Müller M. *et al.*, 2011; Kremmentsova E.B. *et al.*, 2011). Therefore, tetramerization of She2p would also be more efficient for the trafficking mechanism by providing a larger interaction interface for membrane and RNA-binding than a dimeric structure. This is also consistent with previous studies (Kremmentsova E.B. *et*

al., 2011; Figure 5) that show by using EM images that a tetrameric She2p recruits two Myo4p-She3p co-complexes making the trafficking mechanism more stable and energetically balanced.

She2p is able to interact with synthetic membranes in form of protein-free liposomes without specific negatively charged phospholipids like phosphatidylinositol (PI) and phosphatidylserine (PS; Schmid M. Dissertation, 2008) that are known to be primary binding targets of globular domains like C2 domains and pleckstrin (Lemmon M.A., 2008). This leads to the conclusion that the binding itself is not depending on membranes composed of special lipids. This was also shown by other experiments using protein-free liposomes. Interestingly, the binding of She2p to protein-free lipids of different diameter tested by an *in vitro* floatation assay (Figure 44) showed that She2p preferentially binds to lipids with the smallest diameter, in this case 30 nm (Genz C., Diploma Thesis 2009). In detail, purified liposomes with diameters of 30 nm, 80 nm, 200 nm and 400 nm were mixed with She2p and incubated. After centrifugation the liposome-containing interface was harvested and analyzed for presence of She2p. The result is shown in Figure 44 (with the permission of Genz C., IFIB, Tübingen University).

The fact that She2p preferentially binds to smaller protein-free liposomes indicate a preferential binding to high-curvature membranes. Thus, lipid curvature might be one of the limiting and necessary factors that ensure binding of She2p to tubular ER membranes. This is consistent with the fact that in yeast cells mRNP complexes contain She2p protein that co-localize with tubular ER structures (Schmid M. *et al.*, 2006; Aronov S. *et al.*, 2008) that have a diameter of 38 nm (West M. *et al.*, 2011).

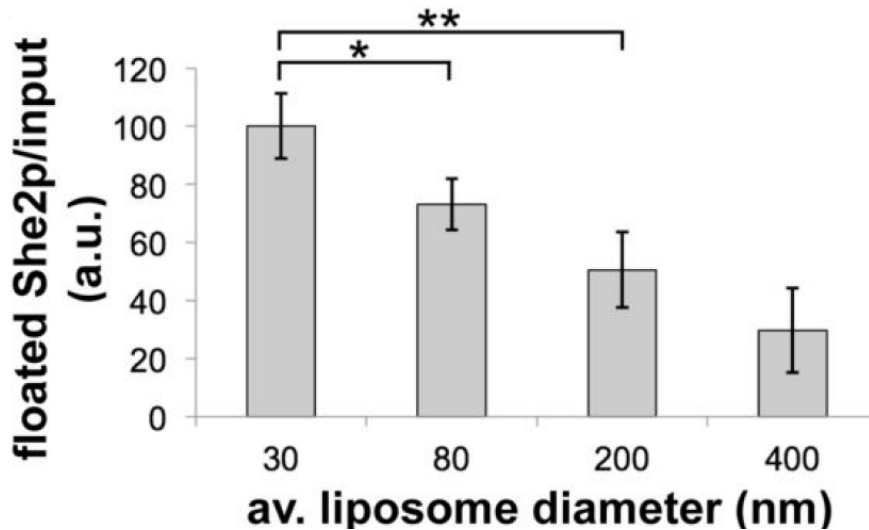


Figure 44 | She2p preferentially binds to 30 nm liposomes. The result in form of the Western blot quantification of the liposome-She2p co-floitation assay using liposomes with different diameters (30 nm, 80 nm, 200 nm and 400 nm) is shown. 50 pmol She2p was pre-incubated for 15 min on RT and additional 10 min on ice with 100 μ l artificial liposomes were mixed with 50 pmol She2p in 140 μ l binding buffer (50 mM Hepes/KOH, 150 mM K-acetate, 1 mM Mg-acetate, 1 mM EDTA, 1 mM DTT). 40 μ l of sample were kept as input control. 200 μ l were mixed with 3 ml binding buffer containing 70% sucrose and added to the bottom of a SW40 polycarbonate tube. The sample was then covered with three cushions of 3 ml binding buffer containing 50%, 40% and 0% sucrose. After centrifugation to equilibrium (22.000 rpm for 16 h at 4 $^{\circ}$ C) the liposome-containing interface between the 40% and 0% sucrose cushions was harvested, precipitated by TCA, dissolved in 45 μ l SDS sample buffer and used for immunoblotting analysis using antibodies against She2p. The bars are displaying average ratio of floated She2p versus input in artificial units (a.u.) resulting from quantification of three independent flotation experiments (* $p < 0.01$; ** $p < 0.002$). Figure adapted and text modified with the permission of Genz C.

This strongly suggests that She2p has an unexpected membrane binding property that is consistent with its association to ER and localized mRNAs. The molecular basis of this association has to be identified. Additionally, direct evidence for the proposed direct linkage of specific mRNAs to membranes via the mRNA-binding protein She2p has to be gathered. The same holds true for other cases where RNA-binding proteins were proposed to act as a direct link between RNA and ER like Vg1RBP (Vera) from *X. laevis* (Dreshler J.O. *et al.*, 1997).

As I already mentioned above, the double mutant $\Delta rtn1\Delta yop1$ was deficient in both ER as well as mRNA localization. In these mutant cells the ER tubules look expanded and have an increased diameter (West M. *et al.*, 2011) that strongly supports the importance of the curvature of ER tubules. Interestingly, this tubular ER shape caused by the mutation of both Rtn1p and Yop1p was no obstacle for the segregation of these tubules into the bud (West M. *et al.*, 2011). However, since

mRNA localization was dramatically affected it is tempting to speculate that the mRNP complexes containing She2p do not associate well to these bloated ER tubules. Because She2p lacks known motifs for membrane curvature sensing or binding (Madsen K.L. *et al.*, 2010) it is possible that the second RNA-binding protein of the locosome complex, She3p also contributes to ER membrane association. This is consistent with the observation that She3p together with Myo4p co-localizes with ER membranes also in the absence of She2p (Estrada P. *et al.*, 2003).

Not only ER tubules but also other ER structures like plasma membrane associated ER and central cisternal ER (Shibata Y. *et al.*, 2010; West M. *et al.*, 2011) and in addition other membranous structures like vesicles do offer possible interaction sites characterized by a high membrane curvature. In order to fully explain ER specific binding of She2p one also has to include (an) unknown protein adapter(s) on the ER. This is supported by the protease treatment experiments (section 2.12.2) showing that extensive treatment of ER membranes with proteases reduces the portion of She2p that co-pellets with the membranes (Figure 42).

Recent studies (Cui X.A. *et al.*, 2012) identified a subset of putative mRNA receptors that physically interact with the ER by using sub-fractionating cell experiments. A putative receptor, FKBP-25 was identified that has homologies with the *FKBP* gene family of which one member is present in *S. cerevisiae*. This indicates similarities of the alternative pathway for targeting and maintains secretory mRNA at the ER also in other organisms as postulated by Cui X.A. *et al.*, 2012. One member of this family, *FKB1* interacts genetically with an RNA-binding protein (Rrp5p; Wilmes G.M. *et al.*, 2008) and with an ER membrane protein (Csg2p; Tanida I. *et al.*, 1996). It was also identified to interact physically with an RNA-binding protein (Slf1p) that associates with polysomes (Schenk L. *et al.*, 2012).

3.1 New model for mRNP trafficking in yeast - early versus late transport strategies

Regarding to the link between ER inheritance and mRNA localization, the transport properties itself has to be characterized in more detail to ensure a most efficient transport of cargo. The most time-efficient and energetically-exploited strategy for a cell that has to be able to respond to environmental conditions as fast as possible

and thus initiating reproduction is by coupling pathways that are necessary for growth and budding.

This is reflected by coupling of mRNA localization via the locosome and their key players She2p, She3p and Myo4p and ER inheritance that is linked to each other in case of early expressed mRNAs to the movement of tubular ER. This is in contrast to mRNAs expressed during later stages of the cell cycle, when the peripheral ER already spreads through the bud cortex after ER tubules have already moved to the bud. In this case the transport of mRNAs is not associated to ER inheritance indicating the existence of two independent strategies: the early and late pathway for transporting mRNAs in yeast. The current evidence for this is a recent demonstration that MS2-tagged *ASH1* mRNA - a typical late expressed mRNA - is localized to the bud in cells lacking *SCS2*, *PTC1*, *YOP1* together with *RTN1* or *YOP1* (data not shown).

Based on the observations by Kremontsova E.B. *et al.*, 2011 that only two Myo4p-She3p motors are required to support the transport over long distances in yeast can imply that the She2p-mRNA complex should be able to recruit two Myo4p-She3p motors with each zipcode of localized mRNA. This ability of associating to the motor complex only if She2p is bound to an mRNA would ensure that the transport machinery would not occur “empty” and only complexes that are containing mRNA would be transported. This is supported by the fact that the She2p-mRNA complex is formed only in the presence of She3p (Müller M. *et al.*, 2011) which is located in the cytoplasm and thus ensures the following transport to the point of its destination.

Other quality checkpoints for the transport machinery ensuring a most exploited procedure *in vivo* are that on the one hand mRNPs are containing multiple copies of one mRNA (Lange S. *et al.*, 2008) that also facilitates the transport process and its intracellular cargo arrangement and on the other hand many mRNAs like *ASH1* mRNA are containing more than one zipcode and thus are able to bind to multiple Myo4p-She3p motor complexes. This would also increase the efficiency of the transport itself (Chung S. and Takizawa P.A: 2010). While one single Myo4p-She3p motor complex that is required for the ER inheritance (Estrada P. *et al.*, 2003) is able to transport the mRNA over a distance of a micrometer, multiple motor complexes recruited by more than one zipcode (e.g. four zipcodes in case of *ASH1* mRNA)

would improve the run-length of the transport and may overcome a resistance caused by the cargo (Krementsova E.B. *et al.*, 2011).

The fact that the ER inheritance would occur at the same time as the early mRNA localization would simplify many time-based interactions during the establishment of a new generation, whereas the late pathway represents the localization of late expressed mRNAs.

Based on the results of this study a new model of the mRNA localization in yeast *S. cerevisiae* can be established (Figure 45). The mRNP localization of mRNAs that are expressed in G1- or S-phase and thus occurs early during the cell cycle is differing with observations of localized mRNAs that are expressed late during M-phase. The localization is split in this new model into two temporally independent pathways. As mentioned before (section 1.7), the mRNA localization process starts with the nuclear transcription of the mRNA that is then recognized by the RNA-binding protein She2p. By passing through the nucleus the complex is exported into the cytoplasm. In the cytoplasm the core locosome is formed by a ternary interaction containing of She2p, the adapter protein She3p and the motor protein Myo4p. This is occurring identical either for the early or the late localization mechanism. Together with the mRNA the mRNP is transported into the bud. In case of the early pathway that is representative for mRNAs that are expressed during G1- or S-phase (e.g. *WCS2* and *SRL1* mRNA) She2p directly associates with the tubular ER while the Myo4p-She3p co-complex is attached to actin filaments. The movement towards the bud results in the driven force of the motor protein Myo4p and thus is Myo4p-dependent. During this transport the translation is repressed by Puf6p. The complex is transported along actin cables consisting of actin filaments and then reaches the bud tip where Sec3p is located and responsible for the stabilization of the cortical association of ER tubules that are delivered into the bud.

- (a) "early pathway" (e.g. *WSC2*)
 (b) "late pathway" (e.g. *ASH1*)

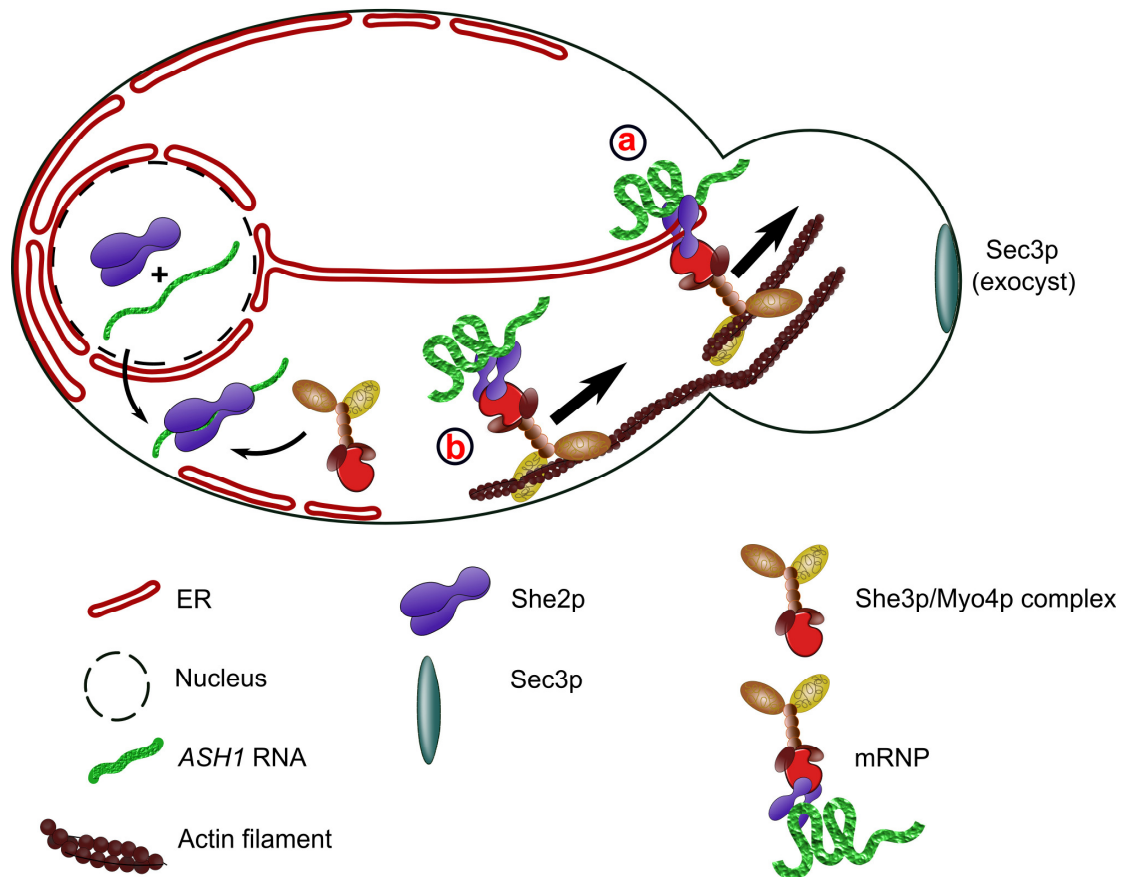


Figure 45 | New model for the mRNA localization in *S. cerevisiae*. The new model distinguishes between an early (a) and late (b) localization pathway. The mother cell is shown on the left side while the growing bud is shown on the right side. The RNA-binding protein She2p binds to the mRNA that is transcribed in the nucleus. After passing through the nucleus the complex is exported into the cytoplasm and then forms the core locosome consisting of She2p, She3p and Myo4p. In case of the early pathway (a), representative for mRNAs that are expressed during G1- or S-phase (e.g. *WSC2* and *SRL1* mRNA) She2p directly associates with the tubular ER while the Myo4p-She3p co-complex is attached to actin filaments. The movement towards the bud results in the driven force of the motor protein Myo4p and thus is Myo4p-dependent. The late pathway (b) represents mRNAs that are expressed late like the mitotic expressed *ASH1* mRNA. The locosome associates to the actin filaments that are bud-associated and expanding into the mother cell. The complex is transported along actin cables and then reaches the bud tip where Sec3p is located and responsible for the stabilization of the cortical association of ER tubules that are delivered into the bud. The *ASH1* mRNA gets anchored and translated and thus the Ash1p protein gets produced.

The mRNA gets anchored and translated and thus the protein gets produced. The late pathway represents mRNAs that are expressed late like the mitotic expressed *ASH1* mRNA. As mentioned above, *ASH1* mRNPs are localized towards the bud tip independently on the loss of a subset of genes like *AUX1*, *SCS2*, *RTN1* and *YOP1* (also in combination of *RTN1* and *YOP1*) representing ER morphology proteins. This is another hint for the existence of two independent pathways.

In this case the locosome associates to the actin filaments that are bud-associated and expands into the mother cell. This is consistent with previous studies (Yang H.C. and Pon L.A. 2002) that show that two different actin cables do exist. The first group of actin cables is described as bud-associated cables and the second group as randomly associated cables. The fact that the bud-associated cables are extended from the bud along the mother-bud axis and thus are spreading in the opposite direction of the mRNA localization that is orientated towards the bud makes it more likely that this group of actin is involved in the late localization pathway. In contrast to bud-associated cables the randomly associated cables are very short. This is making the transport mechanisms itself more complicated if not impossible by interrupting the transport mechanism due to the shortness of the cables. Another, but temporally unlikely possibility would be that after each short cable the locosome is falling off and has to be associated again to another short cable that is located closer to the bud. However this might explain the characteristically zigzag movement of mRNPs towards the bud tip.

To find more evidence for this new model of chronologically different mRNA transport mechanisms other mRNAs that are expressed early in budding of *S. cerevisiae* should be tested for their co-localization with ER. One set of mRNAs are the *POL* mRNAs. These bud mRNAs encode secretion and polarity factors in yeast and were identified (Aronov S. *et al.*, 2007) to be localized asymmetrically only with their association to She2p and the presence of cortical ER towards the tip of the emerging bud early in cellular growth.

Additionally, a search for putative mRNA receptors on the ER in yeast could be started as done by Cui X.A. *et al.*, 2012. In parallel *in vivo* studies with better marker proteins (e.g. reticulons) of the cortical or tubular ER and localizing mRNPs could be initiated to continue observations of ER morphology as done in this study. In late stages of cell growth other, only late localized mRNAs like *ASH1* mRNA in yeast should be observed together with tagged ER genes. Additional co-localization experiments of MS2-tagged mRNPs with tubular ER labeled with either Hmg1p-GFP (Schmid M. *et al.*, 2006) or ER structures, visible by using the ER marker Sec61p (this study), should be further processed.

A model of early and late mRNA localization pathways and their linkage to ER transport was also implied from studies in *X. laevis* oocytes. In this case localized

RNAs that accumulate at the vegetal cortex of the oocyte follow two distinct pathways and arrive at the cortex of the oocytes at different phases of oogenesis.

Early mRNAs (like *Xdaz1* and *Xcat2*) are using a so-called messenger transport organizer (METRO) structure to be localized towards the vegetal pole. These early mRNAs localize to the so-called mitochondrial cloud (MC) next to the vegetal side of the oocytes nucleus. Late mRNAs like the aforementioned *Vg1* mRNA only localizes when the MC already arrives the vegetal cortex and after early RNAs associated with the vegetal cortex. Then the late mRNAs are directly co-localizing with the ER after it is formed in a zone between the vegetale pole and the oocytes nucleus (Mowry K.L. and Cote C.A. 1999; King M.L. *et al.*, 2005)

Thus, *X. laevis* is one example of different and individual pathways with co-localized ER and mRNAs depending on the temporal formation of ER structures.

In summary, I have identified an mRNA transport mechanism in yeast that distinguishes between an early and late pathway as shown for *X. laevis* oocytes. Such a mechanism would make the transport of cargoes more efficient. For yeast this guarantees a fast environmental adaptation and reproduction depending on the nutrient supply. However, as She2p only exists in yeasts the relevance of this co-localization and coordinated transport mechanisms remains to be shown in other organisms. It is possible that other proteins with similar abilities as She2p or the other components of the core locosome have taken over this function.

The methods established in this thesis are also useful for further research in the field of mRNA transport mechanisms and should bring forward the search for other potential factors of this transport machinery also in higher eukaryotes. This would lead to a better understanding in the transport mechanism in general and might finally cumulate in projects leading to e.g. medical applications that are resorting to the transport machinery and mechanism such as direct targeting of mRNAs to a specific location of a cell, tissue or cell-compartment. This could enhance the effect of drugs and treatments and could make therapy more efficient.

4 Materials

4.1 Chemicals

Chemicals and Consumables used in this study:

ACROS ORGANICS	D-Glucose monohydrate
AppliChem	Bacto peptone Bacto yeast extract Ethylene Glycol Tetraacetic acid (EGTA)
biomol	Salmon sperm DNA (ssDNA)
Carl Roth®	Acetic Acid Agarose Amino acids Ammonium persulfate (APS) Bacto agar D-Galactose Dithiothreitol (DTT) Ethylene Diamine Tetraacetic acid (EDTA) Isopropyl-β-D-thiogalactopyranosid (IPTG) Lithium acetate dihydrate (LiOAc) Phenylmethylsulfonyl fluorid (PMSF) Polyethylene glycol 4000 (PEG) Potassium Acetate (KOAc) Potassium dihydrogen phosphate KH_2PO_4 Potassium phosphate K_2HPO_4 Sodium dodecyl sulfate (SDS) Sorbitol Sucrose Tris base TritonX-100
Fermentas	Deoxynucleotide triphosphate Mix (dNTPs)
Fluca™	Nucleic acids
FORMEDIUM™	Yeast nitrogen base
GENAXXON	GelRed
MERCK	Imidazol Magnesium acetate (MgOAc_2) Sodium hydroxide (NaOH)

Materials

Riedel-de Haën®	Hydrochloric acid (HCL)
Roche	Nonidet P-40 (NP40)
Sigma-Aldrich®	Chloroform Ethanol absolute (ETOH) Isopropyl alcohol β-mercaptoethanol (β-ME) Methanol (METOH) Sodium chloride (NaCl) Trichloroacetic acid (TCA)
Serva	Coomassie Brilliant Blue R-250

Consumables:

BECKMAN COULTER	Thinwall Ultra-Clear™ Thinwall Polyallomer Tubes Thickwall Ultra-Clear™
BIO-RAD	Poly-Prep® Chromatography Columns
Carl Roth® GmbH & Co.KG	cover slips object slides glass beads (diff. sizes) Rotilabo® - disposable cuvettes
Clontech	TALON® metal affinity beads
GE Healthcare	Amersham Hybond™ PVDF Transfer Membrane Amersham Hyperfilm™ ECL Gluthation Sepharose Fast Flow beads
KGW-Isotherm GmbH	Dewar Flasks cylindrical Type C
KONTES Glass Co., NJ	Dounce Homogenizer 40 ml
MoBiTec GmbH	Mobicol "F"
MILLIPORE™	Immobilon-FL Transfer Membrane
Pechiney Plastic Packaging	PM966-Parafilm M®
SARSTEDT AG & Co.	Centrifuge tube 50 ml, 15 ml CryoPure Storage Systems High quality pipette tips High quality serological pipettes Micro Tubes SafeSeal 2 ml, 1.5 ml PCR reaction tubes
Thermo Scientific	Menzel-Gläser® Diagnostika

	Pierce ECL Western blotting Substrate
WHEATON Industries Inc., USA	Dounce Homogenizer 7 ml
Hellma®	quarz cuvettes

4.2 Equipment

Alpha Innotec	FluorChem® FC2
analyticjena	FlexCycler
Bandelin	SONOREX Super RK 100
BECKMAN COULTER	Ultracentrifuge L8-70 Ultracentrifuge rotor SW 40 Ti Ultracentrifuge rotor TLA-120.2
BIO ER	ThermoCell Mixing Block MB-102
BIO-RAD	Mini-PROTEAN® Tetra Electrophoresis System PowerPac™ HC Power Supply Trans-Blot® SD Semi-Dry Electrophoretic Transfer Cell
BRANSON	Sonifier® S-250A
Eppendorf	Centrifuge 5415R Centrifuge 5702 Centrifuge 5810R Pipettes P1000, P200, P20, P10
GE Healthcare	GeneQuant™ 100 Spectrophotometer
IBS- INTEGRA Biosciences	Pipetboy acu
IKA®	RH basic 2 Vibrax® VXR basic
INFORS HT	Minitron
KERN	ABT PLS 2100-2
LI-COR Biosciences	Odyssey® Infrared Imaging System
LIEBHERR	Premium NoFrost
MILLIPORE™	SNAP i.d.™
Retsch®	Mixer Mill MM400
Sartorius	arium® 611 UV
Scientific Industries, Inc.	Vortex-Genie® 2
Stuart® Scientific	Gyro rocker
Thermo Scientific	Forma 900 Series

	GENESYS 10 Bio UV-Vis Spectrophotometer Sorvall® Discovery M120 SE Micro-Ultracentrifuge Sorvall® RC-6 PLUS Sorvall® TH-641 swing bucket centrifuge rotor
VWR®	INCU-Line Digital Mini-Incubator
ZEISS	Cellobserver Z1

4.3 Commercially available kits

QIAGEN	QIAquick Gel Extraction Kit QIAquick PCR Purification Kit QIAprep Spin Miniprep Kit
Invitrogen™	SilverQuest™ Silver Staining Kit
Promega	Wizard® SV Gel and PCR Clean-Up System

4.4 Enzymes

Agilent Technologies	Herculase® II Fusion DNA Polymerase
ambio®	Zymolyase® 20T, Zymolyase® 100T
Axon	Taq Polymerase
Biomol®	Lysozyme
Fermentas	Calf Intestine Alkaline Phosphatase (CIP) conventional restriction enzymes FastDigest® restriction enzymes PageRuler™ Prestained Protein Ladder RiboLock™ RNase Inhibitor RNase A T4 DNA Ligase T4 DNA Polymerase

4.5 Oligonucleotides

RJO	Name	Sequence	purpose
2003	She2_S120Y_for	CTGAACTATTATCTAACGCAGTACTTACAAA GGAAATTTTATCTAAAACCTTTGAACG	site directed mutagenesis
2004	She2_S120Y_rev	CGTTCAAAGTTTTAGATAAAAATTCCTTTTGT AAGTACTGCGTTAGATAATAGTTCAG	site directed mutagenesis
2033	MS22_She2_L130Y_f	CAAAAGGAAATTTTATCTAAAACCTTCGAACG	site directed

Materials

		AGGACCTAACGCTAAC	mutagenesis
2034	MS23_She2_L130Y_r	GTTAGCGTTAGGTCCTCGTTCTGAAGTTTTAG ATAAAATTTCTTTTTG	site directed mutagenesis
2147	AUX1_KO_F	AACCTATTCCTGTGCTTCTGGAAAGGACGCA GCCTGCAAGAAACAGTCAACATCACGTACG CTGCAGGTCGAC	gene deletion
2149	AUX1_KO_R	ATTTGTATAAAGTACATATCAAAAACAAC TGAGCGAAGCAGGCACACAAGGGAAAA TCGATGAATTCGAGCTCG	gene deletion
2367	YOP1_KO_F	GCAATTGGTAGTGAAAACAATAAACAAAGA CATAACCGCACTCCAATCCGTACGCTGCAG GTCGAC	gene deletion
2368	YOP1_KO_R	CAAAGAGAACAAAAACGAGAGTTTGATTTGA GGATATAGGTGAGTTGCCTCATCGATGAATT CGAGCTCG	gene deletion
2371	RTN1_KO_F	CCTACCCGCAAGCGTATATATATAATATAT ATTCACACACGCAAATCGTACGCTGCAGGTC GAC	gene deletion
2370	RTN1_KO_R	ATAAAGAGACAAAAGTTAGCTATTCTTGTTG AAATGAAAAAAGCACATCGATGAATT CGAGCTCG	gene deletion
2598	SEC3_KO_F	GCCAGATATCTCCAGCTAGGTAACAAGGCTA CGCAATTTATTCTATATTCGTACGCTGCAGG TCGAC	gene deletion
2599	SEC3_KO_R	CTTAATTAGTCTAAATATGTAATATGAAGCGA CAATGCAGAGGTTACATCGATGAATTCGAGC TCG	gene deletion
3434	ASH1-DET R	CTCCATGCATTGTTGG	tagging
3435	IST2-TAG F	CATAAAAAGGGGCTATTGCATAAGCTGAAAA AGAAGCTTTAAAACGCTGCAGGTCGACAAC CC	tagging
3436	IST2-Tag R	CCATATTATAAAAATAAAATTTGTTATCGTCC TAGCTTTTTTTTAGCATAGGCCACTAGTGGA TC	tagging
3444	ASH1-DET F	CGTGGTCCCAAGAAAGCA	tagging
3449	EAR1-Tag F	CGAACAATTTTCAGAATTTGATGATTACGAAA GCAGGATGCATGGCATATAAACGCTGCAG GTCGACAACCC	tagging
3450	EAR1-Tag R	GATAACTGACCGGGGCTAGTGTTTCAGCCTT ACTATCTCATGCATTTTCGTATTAGCATAGG CCACTAGTGGATC	tagging
3451	WSC2-Tag F	GATTACGATGATGCAAAGGATTCCAATAATA GTTCTTTGCGCTGAAACGCTGCAGGTCGAC AACCC	tagging
3452	WSC2-TagR	GTCTTTGATATGAATATGTAGTGTTGGTATCT AAACCTAGTCAGCATAGGCCACTAGTGGATC	tagging
3453	SRL1-Tag F	GGTACAACACCACTTCGATTACTAATTCGAC CAGTTGGTGAAACGCTGCAGGTCGACAACC C	tagging
3454	SRL1-Tag R	CAAAAAGAACTTAAAAGGACACGTTTGAAC CATAATTCAGCATAGGCCACTAGTGGATC	tagging
3455	MID2-Tag F	CTATGATGAACAAGGTAACGAATTATACCA CGAAATTATTAACGCTGCAGGTCGACAAC CC	tagging
3456	MID2-Tag R	AAAAGTAGCCATAAGCACTAAATGATATGAA TGGATATGATTAGCATAGGCCACTAGTGGAT C	tagging
3457	EAR1-Det F	CCAAAGGACTGGTGCCTA	tagging
3458	EAR1-Det R	CAGCCTTACTATCTCATG	tagging
3459	WSC2-Det F	GCTGTTCCGTTATAGGAC	tagging

Materials

3460	WSC2-Det R	CGTGCAATAATCGTCGGC	tagging
3461	SRL1-Det F	CCATTAATAGGTCTCGTC	tagging
3462	SRL1-Det R	GGTAGCAGAAGGATAGAG	tagging
3463	MID2-Det F	CACGAAGACGCCTCTGCC	tagging
3464	MID2-Det R	CTAATGAAGTCCACCTAC	tagging
3465	His3-Det R	GACTGTCAAGGAGGGTATTCTG	tagging
3551	ASH1-TAG F	GAAGGGTACCGTTGCTTATTTTGTAAATTACA TAACTGAGACAGTAGAGAATTGAAACGCTGC AGGTGCGACAACCC	tagging
3552	ASH1-TAG R	GAAGGGTACCGTTGCTTATTTTGTAAATTACA TAACTGAGACAGTAGAGAATTGAAACGCTGC AGGTGCGACAACCC	tagging
3554	MID2-TAGLFOR	GAAAAATTCTATGATGAACAAGGTAACGAAT TATCACCACGAAATTATTAACGCTGCAGG TCGACAACCC	tagging
3555	MID2_TAGLREV	GGAATGAAAAGTAGCCATAAGCACTAAATGA TATGAATGGATATGATTAGCATAGGCCACTA GTGGATC	tagging
3556	SRL1-TAGLFOR	CGTACAATGGTACAACACCACTTCGATTACT AATTCGACCAGTTGGTCAAACGCTGCAGGT CGACAACCC	tagging
3557	SRL1-TAGLREV	CAAAAAAGAAACAAAAAGAAGTAAAGGAC ACGTTTGAAGTATAATTGAGCATAGGCCAC TAGTGGATC	tagging
3569	IST2-DET F	GCAGCTATTATTGACTTC	tagging
3570	IST2-DET R	GCTGTGACTCCTCTCGAACG	tagging
3612	KAR2_TAG_F	CAAGAGTAGTCTCAAGGGAAAAAGCGTATCA AACATACCATGAACGCTGCAGGTGCGAAC CC	tagging
3613	KAR2_TAG_R	CCTTGAAGCTTCCAGCAGCAAAAATTTTTAA CTATTTTATCTAGCATAGGCCACTAGTGGAT C	tagging
3614	KAR2_DET_F	GGCGCGGCACCCGAGGAAC	tagging
3615	KAR2_DET_R	CTGGGGTTAAGGTAAGTCTCAG	tagging
3620	SLT2_For	CGAACTGTGCATTGAGTACAGC	colony PCR
3621	SLT2_Rev	GCGGAGTACGATTAAGATAAGC	colony PCR
3622	SCS2_For	GCCAGGATACCAGCACCG	colony PCR
3623	SCS2_Rev	CGTTCACTATGAGACCTAGC	colony PCR
3624	AUX1_For	AACACACCTCCCTCGGCTCT	colony PCR
3625	AUX1_PCR_R	CGTTGTCTTCTTCTTAACGGGC	colony PCR
3677	SCS_KO_F	GCAGAAGGGTATTCTACAATCTCCGCGAAC CTAAGTCGTACGCTGCAGGTGCGAC	knockout
3678	SCS_KO_R	GAATACAGCTATATCCTCAATCTCCCTAATC GATGAATTCGAGCTCG	knockout
3680	SLT2_KO_F	GCTATCAAATAGTAGAAATAATTGAAGGGC GTGTATAACAATTCTGGGAGCGTACGCTGCA GGTCGAC	knockout
3681	SLT2_KO_R	GCTTACATCTATGGTGATTCTATACTTCCCC GGTTACTTATAGTTTTTTGTGCATCGATGAATT CGAGCTCG	knockout
3759	deltaJFOR	GCAAGATTTGGTTATGCCCGTACGCTGCGAG GTCGAC	knockout
3760	deltaJRev	GCAGGCACACAAGGGAAAATCGATGAATTC GAGCTCG	knockout
3761	WSC2 FsphI	TACTGCATGCTCCAGCGACTGCTTTATACC	site directed mutagenesis
3762	WSC2 RsbI	AGTACCTGCAGGGGTAACATGCCTGATGG TG	site directed mutagenesis
3791	AUX1KOcheckR	CCATACTTTTTCTAACGCGC	colony PCR
3792	JKOcheckF	GCCCGTTAAGAAGAAGACAACG	colony PCR

Materials

3793	JKOcheckR	GCAGTTTGAACCTTATCCCAAGC	colony PCR
3837	deltaJ_2_FOR	GGTGCAATTGGAAGGATGTCTCTATGCAAGA TTTGGTTATGCCCGTACGCTGCAGGTCGAC	knockout
3838	deltaJ_2_REV	GTACATATCAAAAACAACCTGAGCGAAGCAGG CACACAAGGGAAAATCGATGAATTCGAGCTC G	knockout
4041	SEY1_KO_F	GACTTATTTCAACAAACGGGCTACTAACTCA CTCGACGGTTGACATACTTTAGTCCGTACGC TGCAGGTCGAC	knockout
4042	SEY1_KO_R	GTAACACGGTAAATTGAAATAAATTATTCTGA TCAAAAATATTTTCATAATCGATGAATTCGA GCTCG	knockout
4043	PTC1_KO_F	CATATATCATTTAGGCACTGCATTTATCTTTT AAAAATCATTATACGTACGCTGCAGGTCGAC	knockout
4044	PTC1_KO_R	GCATATCTCTATGTCTATGCATAATTTTTCGC CGGTTTATAACGGATCCTTCATCGATGAATT CGAGCTCG	knockout
4072	WSC2_SD_C	GCATTATAGAAGTGGAAATTTGCACCTAGAT	site directed mutagenesis
4073	WSC2_SD_B	GTGTATGAGATCTAGGTGCAAATTCCTACTT	site directed mutagenesis
4074	SEY1KOcheckF	GTTACCTTAACGAAGAGCGACAAAAC	colony PCR
4075	Sey1KOcheckR	CAACACACAGACACGTTAGGAGAACAG	colony PCR
4076	Ptc1KOcheckF	CCATTCTATACCGAGTATACGAGATTTTGC	colony PCR
4077	Ptc1KOcheckR	GATGCATGCAAATAGATTTGGTACG	colony PCR
4078	YOP1KOcheckR	CGATATATAACAACCTAATAACATATGTAC	colony PCR
4195	Myo4_FW	CGAAAATATCTCGAAGTTTAGCAGTAGTAG	knockout
4196	Myo4_epi	GCCGATAACCTAGCGGTCTCAGCCCAAGGC	knockout

4.6 Plasmids

Name	Short description	Origin
pRJ88	YEplac181- <i>ASH1</i>	Long R.M. <i>et al.</i> , 1997
pRJ139	YCplac33	Gietz R.D. and Sugino A., 1988
pRJ277	pYM3	Knop M. <i>et al.</i> , 1999
pRJ630	pGEX-GST-TEV- <i>SHE2</i>	AG Jansen, Ferring D.
pRJ1213	pFA6a-natNT2	Janke C. <i>et al.</i> , 2004
pRJ1347	pFA6a-KanMX6	Wach A. <i>et al.</i> , 1994
pRJ1386	pGEX-GST-TEV- <i>SHE2-S120Y</i>	Niessing D. <i>et al.</i> , 2004
pRJ1387	pGEX-GST-TEV- <i>SHE2-L130Y</i>	Gonsalvez G.B. <i>et al.</i> , 2003
pRJ1485	ploxP-HIS5-12xMS2L	Haim L. <i>et al.</i> , 2007
pRJ1486	pCP-MS2-GFPx3	Haim L. <i>et al.</i> , 2007
pRJ1686	SCS-TMD-2xRFP	Loewen C.J.R. <i>et al.</i> , 2007
pRJ1789	pGEX-MM-6P-1-She2p (<i>She2p Δhelix E</i>)	Müller M. <i>et al.</i> , 2009
pRJ1790	YEplac33-WSC2-WT	this work
pRJ1791	YEplac33-WSC2-atg->uug	this work

4.7 *Escherichia coli* (*E. coli*) strains

Strain	Essential genotype
TOP10 cells	F ⁻ <i>mcrA</i> Δ (<i>mrr-hsdRMS-mcrBC</i>) ϕ 80 <i>lacZ</i> Δ M15 Δ <i>lacX74</i> <i>recA1</i> <i>araD139</i> Δ (<i>ara-leu</i>) 7697 <i>galU</i> <i>galK</i> <i>rpsL</i> (StrR) <i>endA1</i> <i>nupG</i> (Invitrogen™)
BL21 (DE3)/RIL	B F ⁻ <i>ompT</i> <i>hsdS</i> (rB mB ⁻) <i>dcm</i> ⁺ <i>Tet</i> ^r <i>gal</i> λ (DE3) <i>EndA</i> <i>Hte</i> [<i>argU</i> <i>ileY</i> <i>leuW</i> <i>Cam</i> ^r] (Stratagene)

RJB	Transformed bacterial strain	+ pRJ	Plasmid name
48	BL21(DE3) pLsyS	361	His6 -TEV expression vector (pET9-TEV)
441	BL21(DE3)pRIL	630	pGEX-GST-TEV-She2p
444	BL21(DE3)pRIL	1386	pGEX-GST-TEV-She2p S120Y
445	BL21(DE3)pRIL	1387	pGEX-GST-TEV-She2p L130S
480	TOP10	1789	MM_pGex_6P_1_She2p (She2p Δ <i>helix E</i>)
481	BL21(DE3)	1789	MM_pGex_6P_1_She2p (She2p Δ <i>helix E</i>)
482	BL21(DE3)	1790	WSC2_WT
483	BL21(DE3)	1791	WSC2 atg->ttg SD
484	TOP10	1790	WSC2_WT
485	TOP10	1791	WSC2 atg->ttg SD

4.8 Yeast strains

Name	Relevant genotype	Source
W303a RJY358	<i>MATa</i> , <i>ade2-1</i> , <i>trp1-1</i> , <i>can1-100</i> , <i>leu2-3,112</i> , <i>his3-11,15</i> , <i>ura3</i> , <i>GAL</i> , <i>psi+</i>	Rothstein and Sherman, 1980
W303 α RJY359	<i>MATα</i> , <i>ade2-1</i> , <i>trp1-1</i> , <i>can1-100</i> , <i>leu2-3,112</i> , <i>his3-11,15</i> , <i>ura3</i> , <i>GAL</i> , <i>psi+</i>	Rothstein and Sherman, 1980
RJY870	<i>MATa</i> ; <i>trp1-901</i> ; <i>leu2-3,112</i> ; <i>ura3-52</i> ; <i>his3-200</i> ; <i>gal4Δ</i> ; <i>gal80Δ</i> ; <i>GAL2-ADE2</i> ; <i>LYS2::GAL1-HIS3</i> ; <i>met2::GAL7-lacz</i> , <i>myo4::TRP</i>	Claudia Kruse AG Jansen
RJY2049 BY4741	<i>MATa</i> ; <i>his3Δ1</i> ; <i>leu2Δ0</i> ; <i>met15Δ0</i> ; <i>ura3Δ0</i>	EUROSCARF collection

Materials

RJY2050 BY4742	<i>MATα</i> ; <i>his3_1</i> ; <i>leu2_0</i> ; <i>ura3_0</i>	EUROSCARF collection
RJY2053 BY14980	<i>MATα</i> , <i>his3D1</i> ; <i>leu2D0</i> ; <i>lys2D0</i> ; <i>ura3D0</i> ; <i>she2::kanMX4</i>	EUROSCARF collection
RJY2339	<i>Mat a</i> , <i>his3</i> , <i>leu2</i> , <i>TRP1</i> , <i>HMG1-GFP::URA3</i> , <i>pG14-MS2-DSRed</i> , <i>pRS313-pGAL1-ASH1-MS2(6)</i>	Schmid M. <i>et al.</i> , 2006
RJY2370	<i>MATa</i> , <i>his3</i> , <i>TRP1</i> , <i>she2::KAN</i> , <i>HMG1-GFP::URA3</i> , <i>YEplac181-ASH1</i> , <i>plasmid #88</i>	Andreas Jaedicke AG Jansen
RJY2400	<i>MATa</i> , <i>his3D1</i> ; <i>leu2D0</i> ; <i>met15D0</i> ; <i>ura3D0</i> , <i>plasmid #1097</i>	EUROSCARF collection
RJY2794	<i>Mat a</i> , <i>his3</i> , <i>leu2</i> , <i>TRP1</i> , <i>HMG1-GFP::URA</i> , <i>aux1D::KAN</i> , <i>pG14-MS2-DSRed</i> , <i>pRS313-pGAL1-ASH1-MS2(6)</i>	Schmid M. <i>et al.</i> , 2006
RJY3525	<i>Mat a</i> , <i>his3</i> , <i>leu2</i> , <i>TRP1</i> , <i>HMG1-GFP::URA</i> , <i>ASH1-12xMS2L (pCP-MS2-GFPx3 HIS)</i>	this work
RJY3622	<i>MATa</i> , <i>ade2-1</i> , <i>trp1-1</i> , <i>can1-100</i> , <i>leu2-3,112</i> , <i>his3-11,15</i> , <i>ura3</i> , <i>GAL</i> , <i>psi+</i> , <i>EAR1-12xMS2L (pCP-MS2-GFPx3 HIS)</i>	this work
RJY3623	<i>Mat α</i> , <i>ade2-1</i> , <i>trp1-1</i> , <i>can1-100</i> , <i>leu2-3,112</i> , <i>his3-11,15</i> , <i>ura3</i> , <i>GAL</i> , <i>psi+</i> , <i>EAR1-12xMS2L (pCP-MS2-GFPx3 HIS)</i>	this work
RJY3624	<i>MATa</i> , <i>his3</i> , <i>leu2</i> , <i>TRP1</i> , <i>HMG1-GFP::URA</i> , <i>EAR1-12xMS2L (pCP-MS2-GFPx3 HIS)</i>	this work
RJY3625	<i>MATα</i> , <i>his3D1</i> ; <i>leu2D0</i> ; <i>lys2D0</i> ; <i>ura3D0</i> ; <i>EAR1-12xMS2L (pCP-MS2-GFPx3 HIS)</i>	this work
RJY3626	<i>MATa</i> , <i>ade2-1</i> , <i>trp1-1</i> , <i>can1-100</i> , <i>leu2-3,112</i> , <i>his3-11,15</i> , <i>ura3</i> , <i>GAL</i> , <i>psi+</i> , <i>WSC2-12xMS2L (pCP-MS2-GFPx3 HIS)</i>	this work
RJY3627	<i>Mat α</i> , <i>ade2-1</i> , <i>trp1-1</i> , <i>can1-100</i> , <i>leu2-3,112</i> , <i>his3-11,15</i> , <i>ura3</i> , <i>GAL</i> , <i>psi+</i> , <i>WSC2-12xMS2L (pCP-MS2-GFPx3 HIS)</i>	this work
RJY3628	<i>MATα</i> , <i>his3D1</i> ; <i>leu2D0</i> ; <i>lys2D0</i> ; <i>ura3D0</i> ; <i>WSC2-12xMS2L (pCP-MS2-GFPx3 HIS)</i>	this work
RJY3629	<i>MATa</i> , <i>his3</i> , <i>leu2</i> , <i>TRP1</i> , <i>HMG1-GFP::URA</i> , <i>WSC2-12xMS2L (pCP-MS2-GFPx3 HIS)</i>	this work
RJY3630	<i>MATa</i> , <i>ade2-1</i> , <i>trp1-1</i> , <i>can1-100</i> , <i>leu2-3,112</i> , <i>his3-11,15</i> , <i>ura3</i> , <i>GAL</i> , <i>psi+</i> , <i>SRL1-12xMS2L (pCP-MS2-GFPx3 HIS)</i>	this work
RJY3631	<i>Mat α</i> , <i>ade2-1</i> , <i>trp1-1</i> , <i>can1-100</i> , <i>leu2-3,112</i> , <i>his3-11,15</i> , <i>ura3</i> , <i>GAL</i> , <i>psi+</i> , <i>SRL1-12xMS2L (pCP-MS2-GFPx3 HIS)</i>	this work
RJY3632	<i>MATa</i> , <i>his3</i> , <i>leu2</i> , <i>TRP1</i> , <i>HMG1-GFP::URA</i> , <i>SRL1-12xMS2L (pCP-MS2-GFPx3 HIS)</i>	this work
RJY3633	<i>MATα</i> , <i>his3D1</i> ; <i>leu2D0</i> ; <i>lys2D0</i> ; <i>ura3D0</i> ; <i>SRL1-12xMS2L (pCP-MS2-GFPx3 HIS)</i>	this work

Materials

RJY3634	<i>MATa</i> , <i>ade2-1</i> , <i>trp1-1</i> , <i>can1-100</i> , <i>leu2-3,112</i> , <i>his3-11,15</i> , <i>ura3</i> , <i>GAL</i> , <i>psi+</i> , MID2-12xMS2L (pCP-MS2-GFPx3 HIS)	this work
RJY3635	<i>Mat α</i> , <i>ade2-1</i> , <i>trp1-1</i> , <i>can1-100</i> , <i>leu2-3,112</i> , <i>his3-11,15</i> , <i>ura3</i> , <i>GAL</i> , <i>psi+</i> , MID2-12xMS2L (pCP-MS2-GFPx3 HIS)	this work
RJY3636	<i>MATα</i> , <i>his3D1</i> ; <i>leu2D0</i> ; <i>lys2D0</i> ; <i>ura3D0</i> ; MID2-12xMS2L (pCP-MS2-GFPx3 HIS)	this work
RJY3752	<i>MATa</i> , EAR1-12xMS2L (pCP-MS2-GFPx3 HIS), <i>aux1::kanMX6</i>	this work
RJY3753	<i>Mat α</i> , EAR1-12xMS2L (pCP-MS2-GFPx3 HIS), <i>aux1::kanMX6</i>	this work
RJY3754	<i>MATa</i> , WSC2-12xMS2L (pCP-MS2-GFPx3 HIS), <i>aux1::kanMX6</i>	this work
RJY3755	<i>Mat α</i> , WSC2-12xMS2L (pCP-MS2-GFPx3 HIS), <i>aux1::kanMX6</i>	this work
RJY3756	<i>MATa</i> , SRL1-12xMS2L (pCP-MS2-GFPx3 HIS), <i>aux1::kanMX6</i>	this work
RJY3757	<i>Mat α</i> , SRL1-12xMS2L (pCP-MS2-GFPx3 HIS), <i>aux1::kanMX6</i>	this work
RJY3758	<i>MATa</i> , MID2-12xMS2L (pCP-MS2-GFPx3 HIS), <i>aux1::kanMX6</i>	this work
RJY3759	<i>Mat α</i> , MID2-12xMS2L (pCP-MS2-GFPx3 HIS), <i>aux1::kanMX6</i>	this work
RJY3761	<i>MATa</i> , IST2-12xMS2L (pCP-MS2-GFPx3 HIS), <i>aux1::kanMX6</i>	this work
RJY3763	<i>MATa</i> , EAR1-12xMS2L (pCP-MS2-GFPx3 HIS), <i>slt2::kanMX6</i>	this work
RJY3764	<i>MATa</i> , EAR1-12xMS2L (pCP-MS2-GFPx3 HIS), <i>scs2::kanMX6</i>	this work
RJY3765	<i>MATa</i> , MID2-12xMS2L (pCP-MS2-GFPx3 HIS), <i>slt2::kanMX6</i>	this work
RJY3766	<i>MATa</i> , MID2-12xMS2L (pCP-MS2-GFPx3 HIS), <i>scs2::kanMX6</i>	this work
RJY3767	<i>MATa</i> , WSC2-12xMS2L (pCP-MS2-GFPx3 HIS), <i>slt2::kanMX6</i>	this work
RJY3768	<i>MATa</i> , WSC2-12xMS2L (pCP-MS2-GFPx3 HIS), <i>scs2::kanMX6</i>	this work
RJY3769	<i>MATa</i> , SRL1-12xMS2L (pCP-MS2-GFPx3 HIS), <i>slt2::kanMX6</i>	this work
RJY3770	<i>MATa</i> , SRL1-12xMS2L (pCP-MS2-GFPx3 HIS), <i>scs2::kanMX6</i>	this work
RJY3771	<i>MATa</i> , IST2-12xMS2L (pCP-MS2-GFPx3 HIS), <i>slt2::kanMX6</i>	this work

Materials

RJY3772	<i>MATa</i> , IST2-12xMS2L (pCP-MS2-GFPx3 HIS), <i>scs2::kanMX6</i>	this work
RJY3778	<i>MATa</i> , ASH1-12xMS2L (pCP-MS2-GFPx3 HIS), <i>slt2::kanMX6</i>	this work
RJY3779	<i>MATa</i> , ASH1-12xMS2L (pCP-MS2-GFPx3 HIS), <i>scs2::kanMX6</i>	this work
RJY3780	<i>MATa</i> , KAR2-12xMS2L (pCP-MS2-GFPx3 HIS), pRJ1686 (SCS-TMD-2xRFP)	this work
RJY3782	<i>MATa</i> , ASH1-12xMS2L (pCP-MS2-GFPx3 HIS), pRJ1686 (SCS-TMD-2xRFP)	this work
RJY3783	<i>MATa</i> , <i>ade2-1, trp1-1, can1-100, leu2-3,112, his3-11,15, ura3</i> , IST2-12xMS2L (pCP-MS2-GFPx3 HIS), pRJ1686 (SCS-TMD-2xRFP)	this work
RJY3784	<i>MATa</i> , <i>ade2-1, trp1-1, can1-100, leu2-3,112, his3-11,15, ura3, GAL, psi+</i> , IST1-12xMS2L (pCP-MS2-GFPx3 HIS)	this work
RJY3785	<i>MATa</i> , <i>ade2-1, trp1-1, can1-100, leu2-3,112, his3-11,15, ura3, GAL, psi+</i> , EAR1-12xMS2L (pCP-MS2-GFPx3 HIS), pRJ1686 (SCS-TMD-2xRFP)	this work
RJY3786	<i>MATa</i> , <i>ade2-1, trp1-1, can1-100, leu2-3,112, his3-11,15, ura3, GAL, psi+</i> , WSC2-12xMS2L (pCP-MS2-GFPx3 HIS), pRJ1686 (SCS-TMD-2xRFP)	this work
RJY3787	<i>MATa</i> , <i>ade2-1, trp1-1, can1-100, leu2-3,112, his3-11,15, ura3, GAL, psi+</i> , PGK1-12xMS2L (pCP-MS2-GFPx3 HIS), pRJ1686 (SCS-TMD-2xRFP)	this work
RJY3788	<i>MATa</i> , <i>ade2-1, trp1-1, can1-100, leu2-3,112, his3-11,15, ura3, GAL, psi+</i> , ASH1-12xMS2L (pCP-MS2-GFPx3 HIS), pRJ1686 (SCS-TMD-2xRFP)	this work
RJY3809	<i>MATa</i> , <i>ade2-1, trp1-1, can1-100, leu2-3,112, his3-11,15, ura3, GAL, psi+</i> , MID2-12xMS2L (pCP-MS2-GFPx3 HIS), pRJ1686 (SCS-TMD-2xRFP)	this work
RJY3810	<i>MATa</i> , <i>his3D1; leu2D0; lys2D0; ura3D0; MID2-12xMS2L</i> (pCP-MS2-GFPx3 HIS), pRJ1686 (SCS-TMD-2xRFP)	this work
RJY3811	<i>MATa</i> , <i>his3D1; leu2D0; lys2D0; ura3D0; IST2-12xMS2L</i> (pCP-MS2-GFPx3 HIS), pRJ1686 (SCS-TMD-2xRFP)	this work
RJY3849	<i>MATa</i> , MID2-12xMS2L (pCP-MS2-GFPx3 HIS), <i>sec3::kanMX6</i>	this work
RJY3850	<i>MATa</i> , IST2-12xMS2L (pCP-MS2-GFPx3 HIS), <i>sec3::kanMX6</i>	this work
RJY3851	<i>MATa</i> , SRL1-12xMS2L (pCP-MS2-GFPx3 HIS), <i>sec3::kanMX6</i>	this work
RJY3852	<i>MATa</i> , ASH1-12xMS2L (pCP-MS2-GFPx3 HIS), <i>sec3::kanMX6</i>	this work

Materials

RJY3853	<i>MATa</i> , WSC2-12xMS2L (pCP-MS2-GFPx3 HIS), <i>sec3::kanMX6</i>	this work
RJY3854	<i>MATa</i> , EAR1-12xMS2L (pCP-MS2-GFPx3 HIS), <i>sec3::kanMX6</i>	this work
RJY3855	<i>MATa</i> , MID2-12xMS2L (pCP-MS2-GFPx3 HIS), <i>sec3::kanMX6</i> , pRJ1686 (SCS-TMD-2xRFP)	this work
RJY3856	<i>MATa</i> , IST2-12xMS2L (pCP-MS2-GFPx3 HIS), <i>sec3::kanMX6</i> , pRJ1686 (SCS-TMD-2xRFP)	this work
RJY3871	<i>MATa</i> , his3D1; leu2D0; lys2D0; ura3D0; IST2- 12xMS2L (pCP-MS2-GFPx3 HIS), <i>aux1::kanMX6</i>	this work
RJY3872	<i>MATa</i> , WSC2-12xMS2L (pCP-MS2-GFPx3 HIS), plasmid #1790	this work
RJY3873	<i>MATa</i> , WSC2-12xMS2L (pCP-MS2-GFPx3 HIS), plasmid #1791(WSC2 ATG->TTG)	this work
RJY3874	<i>MATa</i> , WSC2-12xMS2L (pCP-MS2-GFPx3 HIS), <i>aux1::kanMX6</i> , plasmid #1790	this work
RJY3875	<i>MATa</i> , WSC2-12xMS2L (pCP-MS2-GFPx3 HIS), <i>aux1::kanMX6</i> , plasmid #1791(WSC2 ATG->TTG)	this work
RJY3876	<i>MATa</i> , WSC2-12xMS2L (pCP-MS2-GFPx3 HIS), <i>rtn1::kanMX6</i>	this work
RJY3877	<i>MATa</i> , IST2-12xMS2L (pCP-MS2-GFPx3 HIS), <i>rtn1::kanMX6</i>	this work
RJY3879	<i>MATa</i> , SRL1-12xMS2L (pCP-MS2-GFPx3 HIS), <i>rtn1::kanMX6</i>	this work
RJY3880	<i>MATa</i> , EAR1-12xMS2L (pCP-MS2-GFPx3 HIS), <i>rtn1::kanMX6</i>	this work
RJY3881	<i>MATa</i> , IST2-12xMS2L (pCP-MS2-GFPx3 HIS), <i>sey1::kanMX6</i>	this work
RJY3882	<i>MATa</i> , SRL1-12xMS2L (pCP-MS2-GFPx3 HIS), <i>sey1::kanMX6</i>	this work
RJY3883	<i>MATa</i> , WSC2-12xMS2L (pCP-MS2-GFPx3 HIS), <i>sey1::kanMX6</i>	this work
RJY3884	<i>MATa</i> , EAR1-12xMS2L (pCP-MS2-GFPx3 HIS), <i>sey1::kanMX6</i>	this work
RJY3885	<i>MATa</i> , IST2-12xMS2L (pCP-MS2-GFPx3 HIS), <i>ptc1::kanMX6</i>	this work
RJY3886	<i>MATa</i> , SRL1-12xMS2L (pCP-MS2-GFPx3 HIS), <i>ptc1::kanMX6</i>	this work
RJY3887	<i>MATa</i> , WSC2-12xMS2L (pCP-MS2-GFPx3 HIS), <i>ptc1::kanMX6</i>	this work
RJY3888	<i>MATa</i> , EAR1-12xMS2L (pCP-MS2-GFPx3 HIS), <i>ptc1::kanMX6</i>	this work
RJY3900	<i>MATa</i> , WSC2-12xMS2L (pCP-MS2-GFPx3 HIS), <i>rtn1::kanMX6</i> , <i>yop1::natNT2</i>	this work

Materials

RJY3901	<i>MATa</i> , IST2-12xMS2L (pCP-MS2-GFPx3 HIS), <i>rtn1::kanMX6, yop1::natNT2</i>	this work
RJY3902	<i>MATa</i> , SRL1-12xMS2L (pCP-MS2-GFPx3 HIS), <i>rtn1::kanMX6, yop1::natNT2</i>	this work
RJY3903	<i>MATa</i> , EAR1-12xMS2L (pCP-MS2-GFPx3 HIS), <i>rtn1::kanMX6, yop1::natNT2</i>	this work
RJY3904	<i>MATa</i> , IST2-12xMS2L (pCP-MS2-GFPx3 HIS), <i>sey1::kanMX6, yop1::natNT2</i>	this work
RJY3905	<i>MATa</i> , SRL1-12xMS2L (pCP-MS2-GFPx3 HIS), <i>sey1::kanMX6, yop1::natNT2</i>	this work
RJY3906	<i>MATa</i> , WSC2-12xMS2L (pCP-MS2-GFPx3 HIS), <i>sey1::kanMX6, yop1::natNT2</i>	this work
RJY3907	<i>MATa</i> , EAR1-12xMS2L (pCP-MS2-GFPx3 HIS), <i>sey1::kanMX6, yop1::natNT2</i>	this work
RJY3967	<i>MATα</i> , <i>ura3delta5, his, leu2-3,112, pra1-1, prb1-1,</i> <i>prc1-1, cps1-3, pRJ1713</i>	this work
RJY3968	<i>MATα</i> , <i>ura3delta5, his, leu2-3,112, pra1-1, prb1-1,</i> <i>prc1-1, cps1-3, pRJ1686 (SCS-TMD-2xRFP)</i>	this work
RJY3969	<i>MATa</i> , EAR1-12xMS2L (pCP-MS2-GFPx3 HIS), <i>ptc1::kanMX6, yop1::natNT2</i>	this work
RJY3970	<i>MATa</i> , IST1-12xMS2L (pCP-MS2-GFPx3 HIS), <i>ptc1::kanMX6, yop1::natNT2</i>	this work
RJY3971	<i>MATa</i> , WSC2-12xMS2L (pCP-MS2-GFPx3 HIS), <i>ptc1::kanMX6, yop1::natNT2</i>	this work
RJY3972	<i>MATa</i> , SRL1-12xMS2L (pCP-MS2-GFPx3 HIS), <i>ptc1::kanMX6, yop1::natNT2</i>	this work
RJY3990	<i>MATa</i> , EAR1-12xMS2L (pCP-MS2-GFPx3 HIS), <i>yop1::natNT2</i>	this work
RJY3991	<i>MATa</i> , IST1-12xMS2L (pCP-MS2-GFPx3 HIS), <i>yop1::natNT2</i>	this work
RJY3992	<i>MATa</i> , WSC2-12xMS2L (pCP-MS2-GFPx3 HIS), <i>yop1::natNT2</i>	this work
RJY3993	<i>MATa</i> , SRL1-12xMS2L (pCP-MS2-GFPx3 HIS), <i>yop1::natNT2</i>	this work
RJY3994	<i>MATa</i> , pRJ1686 (SCS-TMD-2xRFP)	this work
RJY3995	<i>MATa, aux1::kanMX6, pRJ1686 (SCS-TMD-2xRFP)</i>	this work
RJY3996	<i>MATa, scs2::kanMX6, pRJ1686 (SCS-TMD-2xRFP)</i>	this work
RJY3997	<i>MATa, slt2::kanMX6, pRJ1686 (SCS-TMD-2xRFP)</i>	this work
RJY3998	<i>MATa, sec3::kanMX6, pRJ1686 (SCS-TMD-2xRFP)</i>	this work
RJY3999	<i>MATa, rtn1::kanMX6, pRJ1686 (SCS-TMD-2xRFP)</i>	this work
RJY4000	<i>MATa, sey1::kanMX6, pRJ1686 (SCS-TMD-2xRFP)</i>	this work
RJY4001	<i>MATa, ptc1::kanMX6, pRJ1686 (SCS-TMD-2xRFP)</i>	this work
RJY4011	<i>MATa, myo4::TRP, pRJ1686 (SCS-TMD-2xRFP)</i>	this work
RJY4002	<i>MATa, yop1::kanMX6, pRJ1686 (SCS-TMD-2xRFP)</i>	this work
RJY4003	<i>MATa, sey1::kanMX6, yop1::natNT2, pRJ1686 (SCS-</i> <i>TMD-2xRFP)</i>	this work

Materials

RJY4004	<i>MATa</i> , <i>ptc1::kanMX6</i> , <i>yop1::natNT2</i> , pRJ1686 (SCS-TMD-2xRFP)	this work
RJY4005	<i>MATa</i> , <i>rtn1::kanMX6</i> , <i>yop1::natNT2</i> , pRJ1686 (SCS-TMD-2xRFP)	this work
RJY4006	<i>MATa</i> , EAR1-12xMS2L (pCP-MS2-GFPx3 HIS), <i>myo4::TRP</i>	this work
RJY4007	<i>MATa</i> , IST1-12xMS2L (pCP-MS2-GFPx3 HIS), <i>myo4::TRP</i>	this work
RJY4008	<i>MATa</i> , WSC2-12xMS2L (pCP-MS2-GFPx3 HIS), <i>myo4::TRP</i>	this work
RJY4009	<i>MATa</i> , MID2-12xMS2L (pCP-MS2-GFPx3 HIS), <i>myo4::TRP</i>	this work
RJY4010	<i>MATa</i> , SRL1-12xMS2L (pCP-MS2-GFPx3 HIS), <i>myo4::TRP</i>	this work
RJY4069	<i>MATa</i> , MID2-12xMS2L (pCP-MS2-GFPx3 HIS), <i>ptc1::kanMX6</i>	this work
RJY4070	<i>MATa</i> , MID2-12xMS2L (pCP-MS2-GFPx3 HIS), <i>sey1::kanMX6</i>	this work
RJY4071	<i>MATa</i> , MID2-12xMS2L (pCP-MS2-GFPx3 HIS), <i>rtn1::kanMX6</i>	this work
RJY4072	<i>MATa</i> , MID2-12xMS2L (pCP-MS2-GFPx3 HIS), <i>ptc1::kanMX6</i> , <i>yop1::natNT2</i>	this work
RJY4073	<i>MATa</i> , MID2-12xMS2L (pCP-MS2-GFPx3 HIS), <i>sey1::kanMX6</i> , <i>yop1::natNT2</i>	this work
RJY4074	<i>MATa</i> , MID2-12xMS2L (pCP-MS2-GFPx3 HIS), <i>rtn1::kanMX6</i> , <i>yop1::natNT2</i>	this work
RJY4075	<i>MATa</i> , MID2-12xMS2L (pCP-MS2-GFPx3 HIS), <i>yop1::natNT2</i>	this work
RJY4084	<i>MATa</i> , EAR1-12xMS2L (pCP-MS2-GFPx3 HIS), ΔJ - <i>domain::TRP1</i>	this work
RJY4085	<i>MATa</i> , IST2-12xMS2L (pCP-MS2-GFPx3 HIS), ΔJ - <i>domain::TRP1</i>	this work
RJY4086	<i>MATa</i> , MID2-12xMS2L (pCP-MS2-GFPx3 HIS), ΔJ - <i>domain::TRP1</i>	this work
RJY4087	<i>MATa</i> , WSC2-12xMS2L (pCP-MS2-GFPx3 HIS), ΔJ - <i>domain::TRP1</i>	this work
RJY4089	<i>MATa</i> , SRL1-12xMS2L (pCP-MS2-GFPx3 HIS), ΔJ - <i>domain::TRP1</i>	this work

The strain RJY2053 was designated with the genotype *MATa* containing the following full genotype: *MATa*, *ade2-1*, *trp1-1*, *can1-100*, *leu2-3,112*, *his3-11,15*, *ura3*, *GAL*, *psi+*. All strains from RPY3622-3907 designated with the genotype *MATa* or *MATa* contains the genomic informations as listet in W303a or W303a.

4.9 Antibodies

Name	Source	Dilution	Company
<i>Primary antibodies</i>			
anti-HA 3F10	rat	1:5000 (Western)	Roche Diagnostics
anti-myc	mouse	1:2000 (Western)	Roche
anti-sec61p	rabbit	1:3000 (Western)	gift from M. Seedorf, Heidelberg
anti-she2p	rat	1:3000 (Western)	Jansen lab
<i>Secondary antibodies</i>			
anti-rat	rabbit	1:5000 (Western)	Dianova
anti-rabbit	donkey	1:5000 (Western)	Amersham
anti-mouse	sheep	1:5000 (Western)	Amersham

5 Methods

The following biochemical, microbiological and molecular biochemical techniques were done based on standard (Sambrook J. *et al.*, 2001) or yeast-specific techniques. Therefore only methods are listed, which are not standard protocols or were modified during experimental processes. Available commercial Kits were used as described by the manufacture's indication. For all processes sterile deionised water and material, like flasks, bottles and other consumables were used. Standard buffers (e.g. TAE pH 8.0, TE pH 7.5 and Tris-HCl pH 7.2-8.0) were prepared as described in Sambrook J. *et al.*, 2001.

5.1 Basic methods

5.1.1 Agarose gel electrophoresis and gel extraction

According to Sambrook J. and Russel D.W., 2001 the agarose gel electrophoresis was performed. Because of the unclear influence of ethidium bromide to the human body in case of contact, agarose gels contain 2-4 µl/150 ml 10.000x GelRed. The 1% gels were prepared using 0.1 g/10 ml agarose, added to 1xTAE and heated shortly until the agarose was completely dissolved. In case of fragment or PCR product purifications the bands were cut out using 70% intensity of the UV illumination at 365 nm. The gel extraction of the DNA was performed using the Promega Wizard Gel Extraction Kit by following the manufacture's manual.

5.1.2 Restriction digest and dephosphorylation

For the digestion of vector and insert DNA the following mixes were performed;

Insert DNA mix (20 µl):

2 µl (0.2-0.5 µg)

2 µl 10x buffer

1 µl Enzyme 1

1 µl Enzyme 2

14 µl distilled water

Vector DNA mix (30 µl):

2 µl (~1 µg)

2 µl 10x buffer

1 µl Enzyme 1

1 µl Enzyme 2

24 µl distilled water

The mixtures were then incubated at the temperature and time depending on the manufacture's manual (e.g. 37 °C, 1 h). Then 1 µl of alkaline phosphatase was

added to the vector mix and was incubated again (e.g. 37 °C, 1 h). The enzymatic activity was stopped by heating the mixtures (e.g. 65 °C, 10 min). After controlling by agarose electrophoresis and purification only 5 µl of the digested samples were used for ligation.

5.1.3 Blunting of DNA fragments

For blunting of DNA fragments after digestion, the T4 polymerase was used as provided by the manufacture's manual.

5.1.4 Ligation of DNA fragments

The molar ratio between vector and insert DNA should be 1:4 to 2:3 depending on the size of the insert and if the insert has blunt ends.

The ligation of digested DNA was performed as the following:

Ligation mix (20 µl):

10x Ligation buffer	3µl
T4 DNA Ligase	2 µl
DNA Vector	2 µl (~100-200 ng)
DNA Insert	7 µl (~450-600 ng)
Distilled water	6 µl

The ligation mix was incubated overnight at 4 °C and afterwards directly transformed into *E. coli* competent cells or stored at -20 °C.

5.2 *E. coli*-specific techniques

5.2.1 Preparation of chemical competent *E. coli* cells

To prepare chemical competent *E. coli* cells, the strain (*E. coli* top 10 or *E. coli* BL21) was grown in 50 ml Luria Bertani (LB) medium (0.8 g bacto peptone, 0.5 g yeast extract, 0.25 g NaCl pH 7.4) at 37 °C in a shaking incubator until the optical density of 0.4-0.6 at 600 nm was reached. Then the cells were chilled on ice for 15 min and harvested by centrifugation (10 min, 4.500 rpm, 4 °C). The pellet was resuspended in 1 ml ice-cold 50 mM calcium chloride solution. After spinning down the cells again the pellet was resuspended in 2 ml of ice cold calcium chloride solution. Finally the cells were pelleted and resuspended in a fourth of the volume of 0.1 M CaCl₂ with

10% glycerol. Aliquots of 50 µl were shock frozen in liquid Nitrogen (LN₂) and stored at -80 °C.

5.2.2 Preparation of plasmid-DNA

The preparation of highly pure bacterial plasmid DNA (e.g. for restriction analysis or further transformation into yeast cells) was performed with the Quiagen Miniprep Kit.

5.2.3 Transformation of competent *E. coli* cells

For the heat-shock transformation, chemically competent *E. coli* cells were thawed on ice for about 5 min minutes. Then the DNA (1-10 ng of plasmid DNA or 20 µl of the ligation mix) was added to 50 µl of cells and incubated on ice for 15 min. The heat-shock was performed at 42 °C for 30 sec. The mixture was then incubated on ice for 5 min and 600 µl pre-warmed LB medium was added. The cells were recovered for 1 h at 37 °C before 100-200 µl were plated on antibiotic containing LB agar plates and incubated at 37 °C overnight. After one day the grown bacterial colonies were picked and inoculated in 5 ml of LB media containing antibiotics (e.g. 10 µg/ml Chloramphenicol (CA) and 100 µg/ml Ampicillin Amp)) and grown for 6 h or overnight (37 °C, shaker) to perform a plasmid preparation (Miniprep).

5.2.4 Long term storage of bacteria

For the long term storage of bacteria, 500 µl of a cell suspension from an overnight culture were taken and mixed with 50% (w/v) glycerol to a final concentration of 15% (w/v) glycerol in cryo-tubes. The probes were shock-frozen with LN₂ and stored at -80 °C.

5.3 *S. cerevisiae*-specific techniques

5.3.1 Cell density of yeast cultures

The density of yeast cultures was defined with a spectrophotometer (GeneQuant™ 100 Spectrophotometer, GE Healthcare) at a wavelength of 600 nm against medium as blank value. The optical density at OD₆₀₀ = 1 correlates to a yeast amount of about 2.5 x 10⁷ cells.

5.3.2 Culture of *S. cerevisiae*

Yeast strains were cultured in either full medium or synthetic complete (SC) medium at 30 °C .In the case of temperature sensitive strains only 20-25 °C were performed for growing the cells.

The preparation of the media was as following:

Yeast extract peptone medium (YEP):

- 6.0 g yeast extract (AppliChem)
- 12.0 g peptone (AppliChem)
- 60 mg adenine hemisulphate (Carl Roth®)
- 600 ml distilled water

10 g bacto agar (Carl Roth®) in case of preparation of plates

Sterilized at 121 °C for 15 min by autoclaving.

For YEPD/YPD 2% of glucose and for YEPG/YPG 2% of galactose was added after cooling down the media.

Synthetic complete drop out (SC-drop out) media:

The following aa and nucleic acids were added to prepare synthetic drop out mixture;

- 1.0 g Adenine hemisulphate, 1.0 g Arginine HCl, 1.0 g Histidine HCl, 1.0 g Isoleucine, 2.0 g Leucine, 2.0 g Lysine HCl, 2.0 g Methionine, 1.5 g Phenylalanine, 1.0 g Serine, 1.0 g Threonine, 1.5 g Tryptophan, 1.0 g Tyrosine, 0.6 g Uracil, 4.5 g Valine.

For preparation of single drop out media (SC-His, SC-Leu, SC-Trp, SC-Ura or SC-Met), double drop-out media (e.g. SC-Leu/Trp) or triple drop-out media (e.g. SC-His/Leu/Ura) the drop out mix includes all essential amino and nucleic acids except the aa/s used as auxotrophy marker/s.

The media and plates were prepared as following:

- 4.0 g Yeast Nitrogen Base (w/o aa)
- 0.5 g Synthetic Complete Drop out mix (excluding aa used as marker) 600 ml distilled water
- 10 g bacto agar (Difco) in case of preparation of plates

Then the pH was adjusted to 5.6 with 10 N NaOH, which is important for the highest transformation efficiency and optimal growth. The media was sterilized (and in case of preparation of plates, the agar was melted) by autoclaving at 121 °C for 15 min.

For synthetic drop out complete media (SDC) 2% of glucose was added after cooling down the media.

For the preparation of clonNA_t (Werner Bio Agents), 5FOA (Apollo) or G418 (Invitrogen™) plates corresponding substance to a final concentration of 100 mg/l, 1 g/l or 360 mg/l was added.

5.3.3 Polymerase chain reaction

With the help of the polymerase chain reaction (PCR) copies of a particular DNA sequence can be amplified. The following different techniques were performed during several steps of experimental setups.

Two different polymerases were used. First, *Taq* Polymerase (Axon) which is very thermostable and second, for a most efficient and precise amplification (e.g. for subcloning and tagging) the Herculase® (Agilent Technologies) with its proof-reading ability were used. After PCR the products were purified directly using the Qiagen PCR purification Kit.

5.3.3.1 Standard analytical PCR

The standard analytical PCR reaction was prepared as the following:

<i>Reaction mixture (total volume 50 µl):</i>		<i>Program:</i>
10x Axon Taq buffer	5 µl	95 °C 2 min
dNTPs (10 mM)	2.5 µl	95 °C 1 min
MgCl ₂ (25 mM)	1 µl	50 °C 30 sec (depending on
Template (50-150 ng/µl)	1 µl	primer length and GC content)
Primer fwd (10 pmol/µl)	1 µl	72 °C 2 min (~1 kb product
Primer rev (10 pmol/µl)	1 µl	size/sec)
distilled water	37.5 µl	step 2-4 35x
Axon Taq Polymerase	1 µl	72 °C 10 min
		4 °C ∞

5.3.3.2 Tagging PCR

For the generation of linear inserts (e.g. for yeast transformation) the PCR was used with Herculase® as the following:

<i>Reaction mixture (total volume 50 µl):</i>		<i>Program:</i>
5x Herculase buffer	10 µl	95 °C 3 min
dNTPs (10 mM)	2 µl	95 °C 1 min
MgCl ₂ (25 mM)	1 µl	75 °C 1 min (depending on primer length and GC content)
Template (50-150 ng/µl)	1 µl	68 °C 2 min (~1 kb product size/sec)
Primer fwd (10 pmol/µl)	1 µl	step 2-4 40x
Primer rev (10 pmol/µl)	1 µl	68 °C 10 min
distilled water	33 µl	4 °C ∞
Herculase®	1 µl	

5.3.3.3 Yeast colony PCR

Yeast colony PCR was performed as the following; a small amount of a freshly plated single yeast colony was scraped off a plate and diluted in 100 µl of 200 mM LiOAc containing 1% SDS. The mixture was then incubated at 70 °C for 15 min. After adding 300 µl of 100% ethanol and vortexing the DNA was collected by centrifugation at 13.000 rpm for 3 min. The precipitated DNA was dissolved in 100 µl TE and cell debris were spun down briefly at 1.000 rpm for 1 min and 1 µl of the supernatant was used for PCR (Lööke M. *et al.*, 2011).

<i>Reaction mixture (total volume 50 µl):</i>		<i>Program:</i>
10x Axon Taq buffer	5 µl	95 °C 2 min
dNTPs (25 mM)	0.5 µl	95 °C 1 min
MgCl ₂ (25 mM)	2.5 µl	50 °C 30 sec (depending on primer length and GC content)
Template	1-10 µl	72 °C 2 min (~1 kb product size/sec)
Primer fwd (10 pmol/µl)	1 µl	step 2-4 35x
Primer rev (10 pmol/µl)	1 µl	72 °C 10 min
distilled water	38.5-28.5 µl	4 °C ∞
Axon Taq Polymerase	0.5 µl	

5.3.4 Transformation of yeast cell

5.3.4.1 One-step transformation with plasmids

For the transformation of yeast with plasmids the protocol described by Chen D.C. *et al.*, 1992 was used. Therefore the cells were inoculated in 5 ml of media and incubated overnight or used directly by scraping off a fresh plate (one big loop was dissolved in water or media). The cell suspension (1 ml) was pelleted by centrifugation and the pellet was resuspended by vortexing shortly in 100 μ l of one-step buffer (see recipe below). An aliquot of single stranded sperm DNA (ssDNA) was thawed on ice, heated for 5 min at 95 °C and directly cooled down on ice to make the DNA linear. The amount of 20 μ g ssDNA and 100 ng up to 500 ng plasmid DNA was added to the cell-buffer suspension and mixed by vortexing. Then the mixture was incubated for 30 min at 45 °C. After adding 1 ml YPD media the mixture was centrifuged at 10.000 rpm for 15 sec and the supernatant was discarded. The pellet was carefully resuspended in 1 ml YPD media and 100-200 μ l of the suspension was plated onto the corresponding selective plate. Colonies appeared after 2-3 days. In case of temperature sensitive constructs the plates were incubated at room temperature (RT) and light-sensitive plates (e.g. 5FOA) were placed in the dark.

One-step buffer:

0.2 M LiOAc, 40% PEG 4000, 100 mM DTT.

Dissolve LiOAc and PEG, then add DTT and filter sterilize. Aliquots of 1 ml were stored at -20 °C.

5.3.4.2 High efficiency yeast transformation

High efficiency yeast transformation was used when linear DNA fragments and PCR products (for genomic integration via homologous recombination) had to be transformed into yeast. The method was adapted from Gietz and Schiestl (Schiestl R.H. and Gietz R.D., 1989) and modified. The 50 ml YPD medium was inoculated with an overnight culture to an OD_{600} of 0.2-0.3. The cells were grown for two generations until OD_{600} reaches 1. The cells were then harvested in 50 ml falcon tubes at 2.500 rpm for 5 min. The supernatant was discarded, the cells were washed with 25 ml water using the same conditions as above and the pellet was

resuspended in 1 ml of freshly prepared 100 mM LiOAc (from a 1 M stock). After centrifugation at top speed for 30 sec the supernatant was removed and the cells were resuspended in 400-500 μ l of 100 mM LiOAc. An aliquot of ssDNA was thawed on ice, boiled for 5 min at 95 °C and quickly chilled on ice. For one transformation mix, 50 μ l of suspension was transferred into a new 1.5 ml reaction tube. After centrifugation and complete removing the LiOAc the transformation mix was added to the cell pellet as the following:

Transformation mix:

240 μ l PEG (50% w/v)

36 μ l 1 M LiOAc

25 μ l ssDNA (2 mg/ml)

50 μ l water with 0.1-5 μ g linear DNA

The mixture was vortexed vigorously until the pellet was completely mixed. The mixture was then incubated for 30 min to 1 h at 30 °C, heat-shocked for 20-25 min at 42 °C and centrifuged at 2.000 rpm for 30 sec. The transformation mix was removed briefly and 1 ml of water or media was added to resuspend the pellet. 100- 200 μ l of the suspension was plated onto the corresponding selective media.

In the case of problematic transformations (e.g. $\Delta aux1$, $\Delta sec3$) a recovery term of 2 h to overnight at 30 °C in 5 ml media was applied before plating. 1 ml of the culture was centrifuged at 2.000 rpm for 30 sec, 750 μ l of the supernatant removed and the pellet resuspended in the remaining 250 μ l. 100 μ l were plated. Colonies appeared after 2-3 days.

In case of temperature sensitive constructs the plates were incubated at RT and light-sensitive plates (e.g. 5FOA) were placed in the dark.

5.3.5 Preparation of genomic DNA from yeast

5.3.5.1 Mechanical lysis of yeast cells

In order to use genomic DNA as a template for sequential changes (e.g. tagging or knockout constructs) by PCR or for controlling the success of a transformation the DNA was extracted from yeast as the following. Either a 5 ml overnight culture or a small amount of the colony, which was scraped off the plate and resuspended in 1 ml water were centrifuged at 4 °C for 5 min at 1.000 rpm. Then the pellet was

resuspended in 200 µl of DEB (DNA extraction buffer, 1% SDS, 100 mM NaCl, 10 mM Tris-HCl pH 8.0, 1 mM EDTA pH 8.0 and 0.2% TritonX-100). 500 µl of acid washed glass beads (0.4 mm diameter) and 200 µl of Phenol/Chloroform/Isoamylalcohol (24:24:1) were added to the cells and vibraxed for 5 min (top speed, 4 °C). The lysate was mixed with 200 µl TE, vortexed 30 sec and centrifuged at RT for 10 min at 12.000 rpm. After transferring 200 µl of the supernatant to a new reaction tube filled with 750 µl of 100% ETOH and after vortexing the mixture, the genomic DNA was precipitated by centrifugation at RT for 10 min at 12.000 rpm. The Ethanol was removed by aspiration. The tube was centrifuged again to remove residual ethanol, again by aspiration. The pellet was dried for about 10 min by leaving the tube open and finally resuspended in 50 µl of TE buffer. The DNA was directly used for e.g. PCR or stored at -20 °C.

5.3.5.2 Chemical lysis of yeast cells

For the chemical lysis of yeast cells one loop of cells was mixed with 1 ml water, 150 µl 1.85 M NaOH and 7.5% β-Me-ETOH and chilled on ice for 15 min. After adding 150 µl 50% TCA the mixture was centrifuged 15 min at 4 °C and 14.000 rpm. The supernatant was discarded and 50 µl HU buffer (8 M urea, 5% SDS, 20 mM Tris pH 8.8, 1.5% DTT, bromphenolblue) was added to each pellet. The mixture was then shaken on a thermoblock for 10 min at 65 °C. After another step of centrifugation for 1 min at 14.000 rpm and 4 °C the supernatant can be used for further experiments (e.g. PCR).

5.3.6 Whole cell extracts

5.3.6.1 WCE preparation

For small scaled cell fractionation experiments the preparation of whole cell extracts (WCE) was used as the following. A stationary overnight culture was diluted to OD₆₀₀ 0.15 in 2 x 100 ml media. The cells were grown until OD₆₀₀ 0.5-0.6. Then 10 mg Cycloheximide (CHX) was added to each culture and incubated for 15 min at 30 °C. The cells were harvested and washed with distilled water containing 100 µg/ml CHX after transferring the pellet to a 2 ml reaction tube. The pellet was resuspended in 1 ml of LS-buffer (20 mM HEPES/KOH, pH 7.6, 100 mM KOAc, 5 mM MgAOc, 1 mM EDTA, 2 mM DTT, protease inhibitors, 100 µg/ml CHX) and two cell pellet volumes of glass beads were added. After breaking the cells by using the vibrax for 5 min at 4°C,

the cells were spun down for 2 min at 1.200 rpm. The supernatant was transferred into a fresh 1.5 ml reaction tube and 30 μ l were taken as WCE aliquot. The remaining WCE was centrifuged for 20 min at 4 °C and 7.600 rpm. After transferring the supernatant (SUP) to an ultracentrifugation tube, the pellet (PI) was rinsed twice with ice-cold water and resuspended in 150 μ l loading buffer. The SUP was spun for 20 min at 4°C and 15.700 rpm and the SUP was transferred in a new tube. The remaining pellet (PII) was rinsed twice as described above and resuspended in 100 μ l loading buffer. The remaining SUP was spun 75.000 rpm. A 50 μ l aliquot of the SUP was taken and the remaining pellet (PIII) was rinsed as described above and resuspended in 100 μ l loading buffer. 5 μ l loading buffer were added to 50 μ l of the SUP. All samples were boiled at 65 °C for 10 min while shaking and were stored at -20°C or used immediately.

5.3.6.2 WCE preparation using a Retsch® MM400 cell grinder

For not disrupting protein-protein interactions, the cells had to be broken very gently. Therefore the MM400 grinder from Retsch® was used with cell droplets or cell noodles as the following. Before starting, the jars, metal balls and the spoon had to be cleaned with ETOH and cooled down using LN₂. For up to 20 ml of cell droplets or noodles, the 50 ml jars were used. After switching on the machine, the same amounts of droplets or noodles were filled into the jars. The balls were added and the jars were closed after removing condensed water and fixed into the device. The programs were started and the cells were broken by using 1 cycle (3 min) at 20 Hz, 2 cycles at 14 Hz 3 cycles at 12 Hz. After each cycle the jars had to be removed and cooled down again in LN₂. After the whole procedure the jars were removed, cooled down and opened one after another. The broken cells were removed with the ice-cold spoon and stored in a 50 ml falcon at -80 °C.

5.4 Genomic tagging of mRNAs with MS2L

To visualize the localization of endogenous mRNAs *in vivo*, the protocol, published by Heim L. *et al.*, 2007 was used. This manual describes the m-TAG strategy: a PCR based genomic integration method by homologous recombination, which introduces 12xMS2L of the MS2 phage into the 3'UTR of a RNA of interest. The visualization of

the tagged mRNA by live cell imaging is possible by enabled co-expression of MS2-CP fused with a fluorescent protein (3x GFP).

All strains resulting from this procedure were derived from wild type W303a or W303 α cells.

For the mRNAs of interest (*ASH1*, *EAR1*, *IST2*, *MID2*, *SRL1* and *WSC2*) the tagging PCR (5.3.3.2.) was done using the following tagging primers; *ASH1* (RJO3551 and RJO3552), *EAR1* (RJO3449 and RJO3450), *IST2* (RJO3435 and RJO3436), *MID2* (RJO3554 and RJO3555), *SRL1* (3556 and RJO3557) and *WSC2* (RJO3451 and RJO3452) and the MS2-tagging cassette RJP1485. These primers contain a stop codon including sequence of 40 bp at the 3' terminus or a 40 bp sequence at the 3' terminus immediately starting after the stop codon. The tagging PCR was optimized in relation to the concentration of dNTPs and using MgCl₂. The first PCR results in a linear DNA fragment which was integrated into the genome by homologous recombination. The resulting clones, which appear after 2-3 days after transformation were checked by using the colony PCR (5.3.3.3.) using the following forward primers; *ASH1* (RJO3444), *EAR1* (RJO3457), *IST2* (RJO3569), *MID2* (RJO3463), *SRL1* (RJO3461) and *WSC2* (RJO3459), which anneals ~200 bp upstream of the termination codon of the open reading frame and the following reverse primer RJO3465 which anneals within the *HIS5* gene. The successful integration results in a 400-500 bp PCR product. Five colonies were chosen for the transformation with the plasmid RJP407 using the one-step transformation procedure (5.3.4.1.). This plasmid contains a CRE-recombinase which is galactose inducible and has an *ura3* marker. By growing the cells after transformation in 5 ml of SC-Ura media for 24-48 h, plating them on YPD and replica plating the colonies on SC-His plates, the His5 marker excision can be checked. Clones which were unable to grow on SC-His but on YPD were checked by colony PCR (5.3.3.3.) using the following primers; *ASH1* (RJO3444 and RJO3434), *EAR1* (RJO3457 and RJO3458), *IST2* (RJO3569 and RJO3570), *MID2* (RJO3463 and RJO3464), *SRL1* (RJO3461 and RJO3462) and *WSC2* (RJO3459 and RJO3460). Finally the MS2-tagged strains were transformed, using the one-step transformation strategy (5.3.4.1.), with RJP1486, which encodes for the MS2-CP and binds MS2L with three copies of the green fluorescent protein GFP. The strains were then checked using the fluorescent microscope Cellobserver Z1 (ZEISS) following the imaging strategy described below.

The procedure of the m-TAG strategy is shown in the following scheme (Heim L. *et al.*, 2007).

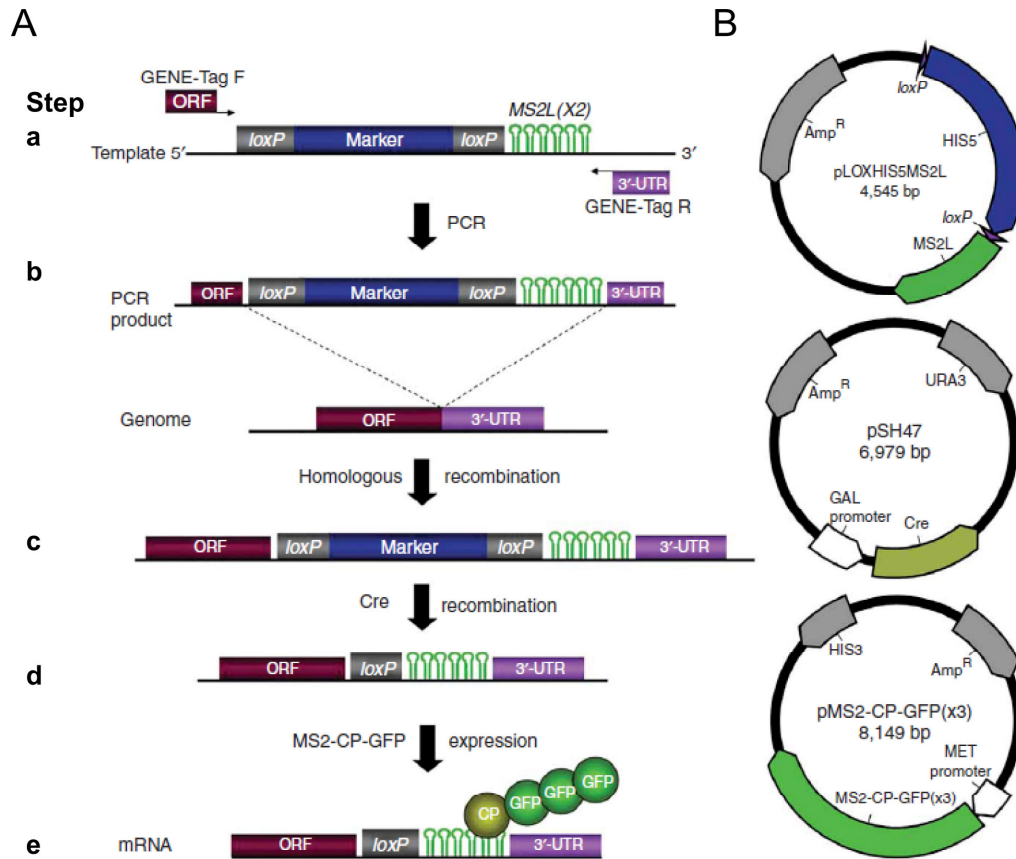


Figure 46 | m-TAG, a method for visualizing endogenous mRNAs in living yeast cells. (A) An overall schematic representation of the m-TAG procedure. Step (a), amplification of the template integration cassette by PCR, using forward and reverse primers having identity to the coding region (including stop codon) and 3'-UTR of a given gene (open reading frame; ORF), respectively. The template cassette contains 12xMS2L sequences, which are able to bind up to 12xMS2-CP dimers and a selectable marker (SpHis5+) flanked by loxP sites. Step (b) shows the transformation of the PCR amplification product into yeast cells. Step (c), integration of the template cassette by homologous recombination into the gene between the coding region and 3'-UTR. Step (d), excision of the selectable marker located between the loxP sites by the expression of Cre recombinase, leaving one loxP site and MS2L between the coding region and the 3'-UTR. Step (e), transformation of cells with a plasmid expressing MS2-CP-GFP(x3) from a methionine starvation inducible promoter in order to visualize mRNA localization (adapted from of Haim L. *et al.*, 2007) (B) Maps of plasmids used in the m-TAG procedure. Three plasmids are used: pLOXHIS5MS2L, pSH47 and pMS2-CP-GFP(x3). Coding regions (i.e., selection markers: *Saccharomyces pombe* his5+, Amp_R, URA3 and HIS3; and Cre recombinase, Cre), tagging regions (MS2L) and regulatory sequences (i.e., GAL and MET promoters) are represented by black arrows and indicate the direction of transcription. (Figure and text adapted from Gerst J.E. *et al.*, 2009).

5.5 Preparation for microscopy

For live cell imaging special microscope slides were used (Menzel-Gläser®, Thermo Scientific). These slides have an adhesive black Epoxy background with 10 outlined, not covered spots where the cells are dropped on.

5.5.1 Growth of yeast cells on plate

Using the MS2-tagged strains for live cell imaging, the yeast cells were incubated onto selective SC-His plates overnight. Only a very small amount of cells were scraped off the plate and resuspended in 10 μ l of medium or distilled water. The thin agarose layer was prepared by dissolving the agarose mixture (1% glucose, 0.2 g/10 ml agarose) in SC-complete media with reduced methionine concentration (44 mg/l) by heating. The mixture was dropped onto a microscope slide (Menzel-Gläser®, Diagnostika) and covered with another cover slide (Carl Roth®) until it was cooled down and polymerized. The cover plate was removed and 1 μ l of the cell suspension was dropped onto the layer and then covered with a cover slip (Figure 47).

preparation of microscope slides for live cell imaging

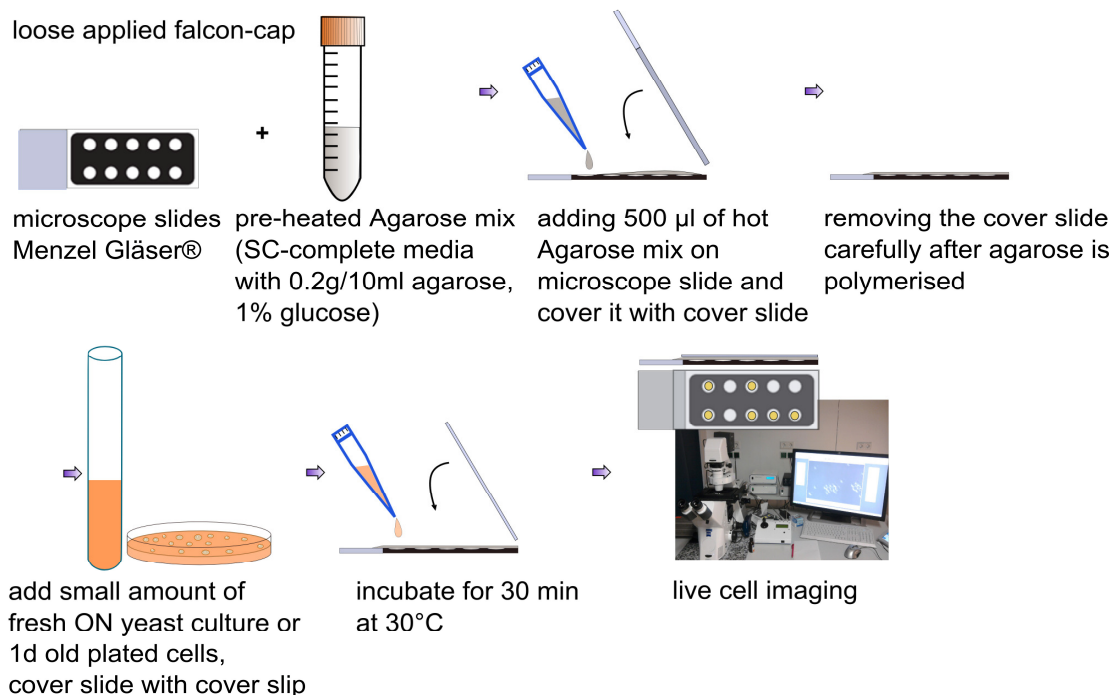


Figure 47 | Scheme of preparation of microscope slides for live cell imaging using yeast cells. An overall schematic representation of the preparation of microscope slides for live cell imaging. For detailed information see method section.

5.5.2 Growth of yeast cells in fresh liquid culture

To overcome the problems of faint and bleaching signals, for some strains ($\Delta aux1$, $\Delta slt2$) fresh liquid cultures were used. In this case a small amount of cells from a glycerol-stock (stored at $-80\text{ }^{\circ}\text{C}$) was inoculated into 5 ml of YPD media containing 2% glucose. The cells were incubated overnight at $30\text{ }^{\circ}\text{C}$ using a shaker. 10 μl were used and diluted in 1 ml of fresh media or distilled water. About 1 μl of this suspension was used and dropped onto the slides as described above (Figure 47).

5.5.3 Imaging

The agarose layer with the cell probes, prepared as described above, was covered with a cover slip. The cells were incubated at $30\text{ }^{\circ}\text{C}$ between 30 and 60 min (longer incubation times would result in dried out agarose layers). The Images were captured with the ZEISS CellObserver Z1 fluorescence microscope operated by AxioVision software (ZEISS). The imaging as itself was done using GFP and DIC filters (ZEISS) according to 130-150 ms of exposure time. Especially for the GFP filter it was necessary to use as short as possible exposure time to overcome the problem of overheating and bleaching the cells.

5.5.4 Time lapse experiments

For the real-time observation of RNPs in wild type and mutated cell lines, time lapse experiments were performed using the ZEISS microscope CellObserver Z1 and AxioVision software (ZEISS). By choosing a 6D experiment using the GFP channel, 500 or less images, each 200 ms with an exposure time of 150 ms were taken. For every experiment a minimum number of ten videos were generated and analyzed via tracking described below.

5.5.5 Tracking

Tracking of time lapse experimental results were performed using the AxioVision software from ZEISS. With this application you are able to define a structure, in this case a Particle (RNP) and track this structure during the time of recording. You can create a colored track view and a merged image of all detected structures, like particles. The tracking itself was done automatically or manual, due to the fact, that particles were moving through the whole 3D structure of both, mother cell and budded cell. The program itself is not able to re-find a missing structure by moving

through different areas. So the tracking was also performed by re-defining the structure for selected time points.

5.5.6 Z-stack experiments

So-called z-stack experiments were performed for generating time lapse experiments through different foci to generate 3D images and time line galleries. Therefore the ZEISS microscope CellObserver Z1 and AxioVision software (ZEISS) was used. First the multidimensional acquisition was chosen to acquire multicolor images through a 6D acquisition experiment by combining a z-stack experiment with time lapse series (or only z-stack experiments). By processing a z-stack image the different z-stacks can be processed later on to generate a 3D image. The number of z-stacks was chosen according to the cell thickness and the position of the mRNPs. The distance between different slices was about 0.25 μm .

Then by using the AxioVision software, the images were used for generating 3D images according to the manufacturers` manual.

5.5.7 Statistical procedures and measurements

To assess RNP particle distribution, more than 150 cells were counted per experiment per yeast strain. This was repeated for at least three times ($n > 450$) and only cells where mother/daughter pairs can be allocate in the DIC channel were considered. For distinguishing between small or large buds, the bud size was defined according to the size of the mother cell for each budded cell (small buds correlating at most to $\frac{1}{4}$ of mother cell size or large buds correlating maximal to $\frac{2}{3}$ size of mother cell size). Post-capture image processing (e.g. background subtraction, merging) was done using the ZEISS AxioVision software. Average values and standard deviation were calculated using Excel. Statistical analysis was done by calculating the p-values for a one-tailed two-proportion t-test using GraphPad (www.graphpad.com).

5.6 Genomic deletion via homologous recombination

The generation of deletions of *AUX1*, *PTC1*, *RTN1*, *SCS2*, *SEC3*, *SEY1*, *SLT2* and *YOP1* in cells expressing mRNAs tagged with MS2L mRNAs were performed by gene disruption using a KanMX4 (Wach A. *et al.*, 1994), KanMX6, or natNT2 marker

(Janke C. *et al.*, 2004). The oligonucleotides, used for tagging or gene disruption, are listed in 4.5. All gene knockouts were verified by colony PCR (5.3.3.3.)

For the generation of $\Delta myo4$ strains, the genomic backbone of a *myo4::TRP* strain (RJY870) was used. Therefore the region of the *myo4::TRP* sequence was amplified using Primers (RJO4195 CGAAAATATCTCGAAGTTTAGCAGTAGTAG and RJO4196 GCCGATAACCTAGCGGTCTCAGCCCAAGGC) which primes 300 bp up/downstream the sequence of interest. After PCR the insert was transformed into wild type strains of MS2-tagged mRNAs and selected by the used marker and tested by genomic PCR.

In order to generate an Aux1p version that lacks the C-terminal J domain, plasmid pRJ277 (6xHA, kITRP1) was used. The DNA used for deletion by homologous integration was generated using primers RJO3837 and RJO3838. The corresponding PCR product inserts before the coding part of the J domain and introduces a 6xHA tag with a stop codon. After transformation into the wild type strains of MS2-tagged mRNAs positive clones were selected by using the introduced marker TRP by plating the transformants onto SC-His-Trp plates.

5.7 Plasmid generation and site directed mutagenesis

The generation of the plasmid for expression of MS2L-tagged *WSC2* and the plasmid of tagged *WSC2* lacking an AUG was done by amplifying the *WSC2-MS2* by PCR from genomic DNA of RJY3626 using the primers RJO3761 and RJO3762. The PCR product was digested and ligated into YCPlac33 (Gietz R.D. and Sugino A., 1988) resulting in the plasmid pRJ1790. By using the mutagenic primers RJO4072 and RJO4073 and the flanking primers RJO3761 and RJO3762 a point mutation that modifies the ATG start codon into a TTG codon was introduced by site directed mutagenesis (Heckman K.L. and Pease L.R., 2007). The resulting PCR product was cloned into YPlac33 and checked by sequencing. The plasmids were finally transformed into the yeast strains RPY3626 and RPY3754.

5.8 ER visualization

For visualizing the ER, together with mRNA particles (RNPs), the RFP Plasmid pRJ1686 (red fluorescence) was used. This plasmid (SCS2-TMD-2xRFP) consists of a transmembrane domain (TMD) of the ER protein Scs2p fused to 2x RFP and Ura3 as a selectable marker. To avoid subsequent marker conflicts and to lose the plasmid

pRJ407 (Cre plasmid), the strains, tagged with MS2L as described above (5.4.) has to be grown overnight in 5 ml SC-His media, the selective media for the GFP plasmid. After preparing dilution series (1:10) 100 µl/clone were plated onto 5FOA plates (1 g/500 ml; Apollo). The yet grown clones had lost the Cre plasmid. To check if the GFP is still intact, the clones were plated onto SC-His. Two clones were picked, transformed (5.3.4.1) with the plasmid pRJ1686 and plated onto SC-His-Ura plates.

The imaging was done as described above using a mCherry filter.

For the single visualization of the ER (e.g. for wild type and $\Delta aux1$ strains), the MS2L-GFP Plasmid has to be removed. Therefore the strains were grown 4-5 times as day cultures in 5 ml YPD. A 1:1000 dilution of the cell suspension was prepared and 100 µl were plated onto a YPD plate. After one day the clones were replica plated on SC-His. Clones which only can grow on YPD but not on SC-His were used for the transformation (5.3.4.1.) with the plasmid pRJ1686 (URA3).

5.9 Sequencing and analysis

Sequencing was done by MWG Eurofins, Munich. The plasmids and primers were prepared and/or chosen as recommended by the company. The analysis of the sequences was done by using the software using the software *A Plasmid Editor* (Ape; <http://www.biology.utah.edu/jorgensen/wayned/ape/>).

5.10 Long term storage of yeast strains

For the long term storage of yeast, 500 µl of a cell suspension from an overnight culture were taken and mixed with 50% (w/v) glycerol to a final concentration of 25% (w/v) glycerol in cryo-tubes. The probes were shock-frozen with LN₂ and stored at -80 °C.

5.11 SDS-PAGE and Western blot

5.11.1 SDS-PAGE

The sodium dodecyl sulfate polyacrylamide gel electrophoresis (SDS-PAGE) was performed as described by Laemmli U.K., 1970 using Mini-Protean® Terra System (BIO-RAD).

With the help of the SDS-PAGE, protein extracts can be separated according to their molecular weight. The detergent SDS leads to a negative charge of the protein and by boiling the protein with β -ME it gets denatured. After preparation of a 12% agarose gel, existing of a stacking and a separating part, the probes were loaded and the proteins were separated first at 100 V for 20 min and afterwards for 200 V until the blue band reached the end of the gel. The gel was removed and either prepared for Staining or Western blotting.

5.11.2 Staining of polyacrylamid gels

5.11.2.1 Coomassie staining

For the staining of polyacrylamid gels using Coomassie Brilliant Blue R-250 the gel was stained for 30 min while shaking. The destaining (40% ETOH, 10% acetic acid) occurs until no background was visible.

5.11.2.2 Silver staining

The silver staining was performed using the silver staining kit from Invitrogen™.

5.11.3 Western blot

The protein transfer onto a polyvinylidene fluoride (PVDF; GE Healthcare) transfer membrane was performed using a semi-dry procedure with the Trans-Blot® SD Semi-Dry Transfer Cell (BIO-RAD). Both gel and whatman-paper slices were covered with 1x transfer buffer (10x; 0.25 M Tris, 1.92 M glycine, pH 8.6 \pm 0.2) for 20 min. The PVDF membrane was activated by shortly covering with METOH. The transfer sandwich was prepared (2 thin whatman-papers slices, membrane, gel, 2 thin whatman-papers slices) and the proteins were transferred 1 h at 15 V.

The membrane was blocked over night in 5% blocking buffer (5% milk powder in PBS-Tween(2%)) or 0.1% blocking buffer (0.1% milk powder in PBS-Tween(2%)) when directly using the SNAP i.d.™ system for immunoblotting. Before using the membrane, blocked with 5% milk, the membrane was washed 3 times with PBS-Tween to avoid clocking the membrane of the SNAP i.d.™ chambers.

The Immunoblotting procedure was done as described in the manufacturer's manual.

The antibodies are listed in 4.9.

For the indirect detection of the proteins by using light sensitive films (Amersham Hyperfilm™ ECL, GE Healthcare) or using the FluorChem® FC2 (Alpha Innotech) chemiluminescence imaging system. The Pierce® ECL-Kit (Thermo Scientific) was used as described in the manufactory's manual.

5.12 Purification of recombinant She2p and She2p mutants from *E. coli*

The Glutathione-S-Transferase (GST) was expressed and purified according to the manufacture's instructions (GE Healthcare). Wild type She2p and all She2p mutants were expressed as GST fusion proteins in *E. coli* BL21(DE3)/pRIL (Invitrogen™). The purification to >95% homogeneity was reached using standard chromatography techniques (Müller M. *et al.*, 2009; Niessing D. *et al.*, 2004). The GST tag was removed by cleavage with tobacco etch virus (TEV) protease (Invitrogen™) or in case of She2p Δ helix E, by cleavage using PreScission Protease (GE Healthcare). After addition of glycerol to 20%, She2p was frozen in LN₂ and stored at -80 °C. The detailed proceeding is shown below.

5.12.1 Purification of TEV protease

For the constructs beside RJB481, TEV protease has to be purified. Thus, the *E. coli* strain RJB48 was used. The cells were plated onto an LB media plate containing Kanamycine (KAN; 25 µg/ml) and Chloramphenicol (CA; 34 µg/ml) and grown for one day at 37 °C. The next day 2 ml of LB media (supplemented with antibiotics) were inoculated with a single colony and grown over day at 37°C. In the evening 50 ml of LB media were inoculated with the culture and grown at 37°C over night. The culture was then diluted into 0.8 l pre-warmed LB_{CA/KAN} to OD₆₀₀ 0.1-0.2. The cells were grown until the OD₆₀₀ 0.7 was reached, which took around 2 hours. The cells were cooled down by adding 200 ml cold LB_{CA/Kan} media and placing the flask on ice for a while. After removing a 1 ml (UI) aliquot as control, the cells were induced by adding 0.5 mM IPTG for 3 h at 24 °C. One aliquot (ind) was removed as induced control and the cells were collected by centrifugation at RT for 10 min and 5.000 rpm. The cells were resuspended in 25 ml TEV-buffer/250 ml culture (20 mM Tris-HCl pH 7.2, 150 mM NaCl, 2 mM β-ME, 20% glycerol, 0.03% NP40, 1 mM PMSF) and frozen. After thawing the cell-buffer suspension, the cells were broken by sonification (2 x 5 min, 40% duty cycle, 70% output) using the Sonifier 250 (Branson). The

homogenate was centrifuged for 15 min at 15.000 rpm at 4 °C, using the SS34 rotor. The supernatant was discarded (take a 200 µl aliquot (SUP)) and the pellet resuspended in the same volume as in the lysis step (200 µl aliquot (P)). The Talon-bead suspension (400 µl/250 ml culture) was equilibrated with 2 x 5 ml TEV-buffer by centrifugation at 4°C at 1.800 rpm and kept on ice. The lysate was batched together with the beads at 4°C for 2 h using a rotation wheel. After washing the beads 2 x with 5 ml TEV-buffer and 1 x with 5 ml TEV-buffer + 1 M NaCl, the elution was performed by using 2 x 1 ml TEV-buffer + 10 mM imidazole (E10), 2 x 1 ml TEV-buffer + 50 mM imidazole (E50), 2 x 1 ml TEV-buffer + 150 mM imidazole (E150-1) and 2 x 1 ml TEV-buffer + 150 imidazole (E150-2). The eluates and all other aliquots were checked by SDS-PAGE. The fractions containing mostly pure TEV protease (25 kDa) were dialysed over night at 4 °C in 1 l fresh dialysis-buffer (50% glycerol, 25 mM Tris-HCl pH 8.0, 150 mM NaCl, 5 mM DTT). Aliquots of 25-50 µl were frozen in LN₂ at -20 °C (ready to use) or stored for long term at -80 °C.

5.12.2 Recombinant expression in *E. coli*

The Expression of She2p fused to GST (Glutathione-S-Transferase) from RJB441 by using the plasmid pGEX-GST-TEV-SHE2 (pRJ630) and GST-She2p-Mutants in *E. coli* BI21(DE3)/RL(RJB343) from RJB444 (S120Y), RJB445 (L130S) or RJB481 (She2p *Δhelix E*) by using the plasmids pRJ1386 (pGEX-GST-TEV-She2p S120Y), pRJ1387 (pGEX-GST-TEV-She2p L130S) and pRJ1789 (MM_pGex_6P_1_She2p) was done as the following; 800 ml LB media (containing appropriate antibiotics) were inoculated with an overnight culture of the respective strain at OD₆₀₀ 0.2-0.3 and grown until OD₆₀₀ 0.8 at 37 °C. Before induction by adding 1 mM IPTG for 5-6 h at 25°C, 200 ml of cold LB was added to cool down the cells. The cells were harvested at 5.000 rpm for 15 min at RT and washed with 200 ml sterile water. Afterwards the cell pellet was shock frozen with LN₂ and stored at -20 °C.

5.12.3 Lysis of cells

The cells were resuspended in 30 ml lysis-buffer (25 mM Hepes/KOH, pH 7.5, 0.1 mM EDTA pH 8, 1 M NaCl, 2 mM DTT, 1x Protease Inhibitor) and lysed after adding 100 mg/l Lysozyme at 30 °C for 30 min on a rotating wheel. After thawing the cells in a water bath at 37 °C and freezing in LN₂ three times the cells were broken by sonifying (40%, 0.5 sec, 4 x 5 min, cooled down on ice after each 5 min) using the

Sonifier 250 (Branson). After adding 0.1% NP40 (Nonidet P-40), the cells were rotated for 30 min at 4 °C and afterwards centrifuged at 4 °C for 30 min and 15.000 rpm using the SS34 rotor. A 100 µl aliquot of pellet and supernatant was taken as control for the SDS-PAGE.

5.12.4 Affinity purification

The purification was done by using GST Fast Flow Sepharose beads (Amersham Biosciences). The beads were washed in 10 ml lysis-buffer and added to the lysate for batching for 1 h at 4 °C under rotation. The poly-prep chromatography column (BIO-RAD) was prepared by adding the suspension and the Flow-through was collected. The column was washed with 10 ml of washing buffer I (25 mM HEPES/KOH pH 7.5, 0.1 mM EDTA pH 8.0, 12.5 mM MgCl₂, 1 M NaCl, 0,1% NP40, 2 mM DTT, 1x Protease Inhibitor) and 10 ml of washing buffer II (25 mM HEPES/KOH pH 7.5, 0,1 mM EDTA pH 8.0, 12,5 mM MgCl₂, 0.7 M NaCl, 0.1% NP40, 1 mM DTT). Both fractions were collected.

The beads were then equilibrated by using 10 ml of TEV-buffer (50 mM Hepes/KOH pH 7.9, 150 mM KOAc, 0.1% NP-40, 0.5 mM EDTA, 1 mM DTT). The matrix was transferred onto a small Mobicol “F” column (MobiTec) by adding 500 µl to the beads.

The cleavage of the protein was performed by using 30 µl (500-600 ng) TEV-Protease under rotation for 1.5 h at 16 °C. The elution of She2p (and TEV) was done by centrifugation of the column, placed in a 2 ml reaction tube at 2.000 rpm for 2 min at 4 °C. One aliquot was prepared as control. About 200 µl of 3xTEV-buffer washed Ni-NTA beads were added to the eluate in a new column and incubated for 2 h at 4 °C to bind and therefore remove the TEV protease. After centrifugation at 2.000 rpm for 1 min, the pure She2p was collected.

In case of She2p *Δhelix E*, the cleavage was done by using PreScission Protease (GE Healthcare). After addition of glycerol to 20%, She2p was frozen in LN₂ and stored at -80 °C.

5.13 Subcellular fractionation experiments

5.13.1 Spheroplasting of yeast and cell lysis

For a gentle lysis of yeast, spheroplasts generated from strains BY4742 (*SHE2*) or RJY2053 (*Δshe2::kanMX4*) to maximally preserve subcellular integrity, e.g. protein

interaction studies, were prepared as described in Schmid M. *et al.*, 2006. Spheroplasts are artificial generated cells without a cell wall, which will lyse after transferring into a hypotonic solution. This was performed as the following. Up to 530 OD₆₀₀ cells were harvested and resuspended in 5 ml isotonic buffer SB (1.4 M sorbitol, 50 mM KPi pH 7.5, 10 mM NaN₃, 0.4% β-Me-EtOH). The cells were spheroplasted by adding 2 mg/ml Zymolyase® 20T and shaking gently for 1 h at 30°C. Intact spheroplasts were collected by pipetting carefully onto an 8 ml sorbitol cushion (1.7 M Sorbitol, 50 mM KPi pH 7.5) and centrifuged at 4 °C for 10 min at 1.730 rpm. The pellet was resuspended in 6 ml HEPES lysis-buffer (20 mM HEPES/KOH, 140 mM KOAc, 1 mM MgOAc₂, 1 mM EDTA, 100 U/ml RiboLock™ RNase Inhibitor (Thermo Scientific) and a protease inhibitor cocktail). The lysis was performed by using a 40 ml dounce homogenizer (Kontes Glass Co.) 30-40 times. The cell debris was pelleted by centrifugation 5 x 5 min at 1.400 rpm and the homogenate can be used freshly or after shock-freezing with LN₂ by thawing only one time.

5.13.2 Velocity gradient centrifugation on discontinuous sucrose gradients

The velocity gradient centrifugation of cell lysates on 18%-60% sucrose gradients was performed as described (Barrowman J. *et al.*, 2000; Estrada P. *et al.*, 2003; Schmid M. *et al.*, 2006). In brief, cells corresponding to 400 OD₆₀₀ units were harvested, spheroplasted, lysed with a needle and cleared from cell debris as described above (5.9.1.). 1 ml of the homogenate (corresponding to 66 OD₆₀₀ units) was loaded onto a linear 18%-60% gradient of sucrose in 20 mM HEPES/KOH pH 6.8, 140 mM KOAc, 1 mM MgOAc₂. After centrifugation in a SW40 swing-out rotor for 2.3 h at 17.350 rpm, 12 fractions, according to 1 ml were collected in 2 ml reaction-tubes starting close to the bottom of the gradient. Therefore the tube was penetrated by a needle. The remaining pellet was resuspended in 1 ml lysis-buffer (20 mM HEPES/KOH, 140 mM KOAc, 1 mM MgOAc₂, 1 mM EDTA, 100 U/ml RiboLock™ RNase Inhibitor (Thermo Scientific) and a protease inhibitor cocktail). Fractions were precipitated with trichloroacetic acid (TCA) as described in 5.9.3 and resuspended in 100 µl SDS sample buffer. 20 µl were used for Western blot analysis except for the top three fractions where only 7 µl were used in order to avoid overloading of the gel. Western blots were performed as described in 5.7.2 using enhanced

chemiluminescence (ECL). The blots were scanned and quantified by using Image J (Java based, Wayne Rasband NIH).

5.13.3 Protein precipitation by TCA from sugar containing samples

For the precipitation of sucrose containing protein-samples, TCA and insulin was used. The probes were diluted in 1 ml of sterile water before insulin (100 µg/2 ml) was added and vortexed carefully. TCA was added to the reaction-tubes to a final concentration of 10%-20%, inverted and stored overnight at 4 °C for precipitation. The next day the samples were centrifuged for 45 min at 13.000 rpm at 4 °C. The supernatant was removed carefully and 1 ml of ice-cold acetone was added. The tubes were inverted and centrifuged at 4 °C for 45 min and 13.000 rpm. The supernatant was removed again and the pellet was dried at 50 °C for 5 min. Then the pellet was resuspended in 100 µl 5 x sample buffer and boiled at 50 °C for 30 min while shaking. If the samples turned orange, the pH was adjusted by using 2 M Tris base. Furthermore the sonifier-bath SONOREX Super RK 100 (Bandelin) was used for 5 min and the samples were boiled 20 min at 60 °C while shaking.

The samples were then directly loaded onto the SDS-Gel after cooling down, or stored at 4 °C.

5.13.4 *In vitro* binding assay: Velocity gradient centrifugation with whole cell extracts and recombinant protein

In vitro binding experiments were performed by using a crude lysate of yeast cells. This lysate was prepared by spheroplasting and preclearing as described above but instead using a $\Delta she2$ (RJY2370) strain. Therefore 1 ml of the lysate (corresponding to 66 OD₆₀₀) was pre-incubated for 30 min on ice with recombinant She2p and She2p mutants in an amount of about 1.5 µg protein per reaction.

The suspension was carefully loaded on top of an 18%-60% linear gradient and centrifuged by using a SW40 rotor. The centrifugation and collection of the fractions and their further processing was done exactly as described earlier.

5.14 *In vitro* binding assay with flotation purified ER membranes

The *in vitro* binding assay with flotation purified ER membranes was performed according to Brodsky J.L. *et al.*, 1993; Rothblatt J.A. and Meyer D.I., 1986 and Schmid M. *et al.*, 2006.

5.14.1 Preparation of yeast microsomal membranes

For the preparation of yeast microsomal membranes (Brodsky J.L. *et al.*, 1993; Rothblatt J.A. and Meyer D.I., 1986, Schmid M. *et al.*, 2006), the according strain (e.g. RJY2053 ($\Delta she2$)) was inoculated in 2 l YPD media containing 2% glucose. After start at OD₆₀₀ 0.2, the cells were harvested at OD₆₀₀ 1.0-2.0 at RT for 5 min at 5.000 rpm. The pellet was washed in distilled water and the pellet was weighted and after centrifuged again, resuspended in 100 mM Tris-SO₄ pH 9.4, 10 mM DTT to a final concentration of 50 OD₆₀₀/ml. The cells were incubated at RT for 15 min and then washed with 15 ml 1.2 M sorbitol. The pellet was resuspended in 40 ml YPD containing 0.7 M sorbitol, 20 mM K_pi pH 7.4, Zymolase 20T with 2.5 mg/g cells and mixed by gentle shaking for 90 min at 30 °C to prepare spheroplasts. The spheroplast-suspension was layered on 25 ml cushion I (0.8 M sucrose, 1.5% Ficoll 400, 20 mM HEPES/KOH pH 7.4) and centrifuged at 3.000 rpm for 15 min at 4 °C. The supernatant was discarded and the spheroplasting pellet resuspended in 0.7 M sorbitol, 20 mM K_pi pH 7.4 to a final concentration of 1000 OD₆₀₀/ml. The samples were stored until usage at -80 °C after shock-freezing with LN₂.

The spheroplast-suspensions were thawed on ice and pelleted at 3.000 rpm for 15 min at 4 °C. After resuspended in ice-cold lysis-buffer (100 mM sorbitol, 50 mM KOAc pH 7.4, 2 mM EDTA pH 8.0, 20 mM HEPES/KOH pH 7.4, 1 mM DTT, 1 mM PMSF) to a final concentration of 200 OD₆₀₀/ml the cells were broken by using the 40 ml dounce homogenizer (Kontes Glass Co.) 30-40 times. The lysate was layered on 15 ml cushion II (1 M sucrose, 50 mM KOAc pH 7.4, 20 mM HEPES/KOH pH 7.4, 1 mM DTT) in conical 50 ml falcons and centrifuged 10 min at 4.000 rpm at 4 °C. The upper phase, enriched in microsomes (yeast rough membranes, YRM) was removed carefully and centrifuged again at 17.000 rpm for 10 min at 4 °C using the SW65 Ti swing-out rotor (to avoid collapsing of the tubes, they must be filled up to 2/3 of the tube size). The membrane pellet was then washed 2 times with 2 ml buffer 88 (20 mM HEPES/KOH pH 6.8, 150 mM KOAc pH 7.4, 250 mM sorbitol, 5 mM MgOAc₂) at

17.000 rpm at 4 °C for 10 min. The membranes were stored in buffer 88 after shock-freezing with LN₂, according to a final 10-12 mg/ml protein concentration.

5.14.2 Protease treatment of purified microsomal membranes

For protease treatment (according to Brodsky J.L. *et al.*, 1993; Rothblatt J.A. and Meyer D.I., 1986, Schmid M. *et al.*, 2006) the purified microsomes were adjusted to 10 mM CaCl₂ and treated with a combination of Proteinase K (20 mg/ml stock) and Pronase E (20 mg/ml stock) at 37°C before aliquoted and stored at -80 °C. To digest, the samples were then treated with excess EDTA and EGTA and 1 mM PMSF. To inactivate the protease activity, samples were incubated for 15 min at -80 °C. After washing 2 x with buffer 88 (20 mM Hepes/KOH pH 6.8, 150 mM KOAc pH 7.4, 250 mM sorbitol, 5 mM MgOAc₂), the pellets were resuspended in the original volume of buffer 88 and shock frozen with LN₂.

5.14.3 Flotation purification of ER membranes

For flotation of YRM (yeast rough membranes) 5-10 µl of microsomes were mixed with cushion III (2.3 M sucrose in 50 mM Hepes/KOH pH 7.5, 5 mM MgOAc₂, 150 mM KOAc, 1.5 mM DTT) and layered on the bottom of a thick-walled SW55 tube. Onto this layer 500 µl of cushion IV (1.9 M sucrose in 50 mM Hepes/KOH pH 7.5, 5 mM MgOAc₂, 150 mM KOAc, 1.5 mM DTT) and 200 µl of cushion V (50 mM Hepes/KOH pH 7.5, 5 mM MgOAc₂, 150 mM KOAc, 1.5 mM DTT) were added carefully. After centrifugation for 90 min at 45.000 rpm (SW55 Ti, Sorvall UZ) the membrane-fraction between cushion IV and V was removed. The membranes were resuspended in binding-assay-buffer (50 mM HEPES/KOH pH 7.5, 5 mM MgOAc₂, 150 mM KOAc, 1.5 mM DTT) and stored at -80 °C after using LN₂.

5.14.4 *In vitro* binding assay

For *in vitro* binding experiments, yeast lysate (corresponding to 66 OD₆₀₀) was prepared from the *Δshe2* strain RJY2053 and RJY2370 as described above. Four fractions of purified membranes, corresponding to 40 µg of protein were resuspended in binding-assay-buffer (50 mM Hepes/KOH pH 7.5, 5 mM MgOAc₂, 150 mM KOAc, 1.5 mM DTT) and pre-incubated with purified recombinant She2p or She2p mutant protein (50 pmol per binding reaction or different amounts for She2p saturation experiments) for 10 min at RT and 15 min on ice. The *in vitro* mix was layered onto

500 μ l cushion VI (1.2 M sucrose, 50 mM HEPES pH 7.5, 5 mM MgOAc₂, 150 mM KOAc, 1.5 mM DTT) and centrifuged at 100.000 rpm (TLA 120.2 rotor) for 1 h at 4 °C. The supernatant was collected and the lowest fraction was resuspended in 1 ml binding-assay-buffer (50 mM Hepes/KOH pH 7.5, 5 mM MgOAc₂, 150 mM KOAc, 1.5 mM DTT). Before precipitating the proteins by using TCA (5.9.3.), 20 μ l were used as a control for the SDS-PAGE and Western blotting.

6 Summary

The localization of mRNAs is a mechanism that is widely spread in most of the eukaryotic cells to spatially define protein synthesis and thus contributes to maintenance and generation of cellular asymmetry, neuronal function and embryonic development. In budding yeast localized mRNAs are forming RNA-protein (RNP) complexes with the mRNA-binding protein She2p, the adaptor protein She3p, that is also known to bind to mRNAs and the motor protein She1p (Myo4p). The mRNA binds to She2p by its *cis*-acting elements (zipcodes) and She2p is then associated to Myo4p via She3p that acts as an adapter. The Myo4p-She3p co-complex that is an important part of the core locosome and thus essential for the mRNA localization machinery is also involved in the inheritance of cortical ER (cER; Estrada P. *et al.*, 2003). The mRNP is transported towards the barbed ends of actin cables consisting of actin molecules and tropomyosin filaments located at the bud tip. The process by which the mRNAs are anchored at the bud tip is unknown (Jansen R.P. *et al.*, 1996; Gonsalvez G.B. *et al.*, 2005). This She1-3 machinery is known to localize about 24 mRNAs to the bud tip including 16 mRNAs that encode secreted or membrane proteins like the aforementioned *IST2* mRNA or the She2p transport-dependent *EAR1* mRNA (Giaever G. *et al.*, 2002; Terashima H. *et al.*, 2002; Leon S. *et al.*, 2008). RNP particles form the initial element for the segregation of cER. The fact that RNPs can localize together with tubular ER structures was also supported by the *ASH1* mRNA which binds to the tip of ER-membrane tubules (Schmid M. *et al.*, 2006) suggesting a coordination of mRNA localization and cER distribution.

This study demonstrates that mutants that are defective on ER segregation and morphology are at the same time affecting mRNA localization of early expressed mRNAs. This indicates a direct link between mRNA localization and ER inheritance. It was shown that the RNA-binding protein She2p associates independently of polysomes with ER membranes. This and the mRNP localization experiments with *WSC2* mRNA demonstrate that the mRNA localization occurs independent on its translation.

Based on this study it was shown that the proper segregation of cER is essential for the localization of a subset of mRNAs that are transported early during cell growth and then get expressed at the time of tubular ER movement into the bud. Thus, a new model of early and late mRNA localization pathways linked to ER inheritance

during the early stages of budding was established. mRNAs that are expressed early during the cell cycle are therefore co-localized with the ER, while late expressed mRNAs are localized towards the bud ER-independently. This temporally split mRNA localization represents the most time and energetically efficient transport mechanism during budding. Altogether, this study confirmed the hypothesis of a link between mRNA localization and ER transport.

Additionally, this study confirms that the tetramerization of She2p, the basic helical hairpin motif and the helix E (Niessing D. *et al.*, 2004; Müller M. *et al.*, 2011) are essential for the proper co-localization of tubular ER and RNPs that are depending on She2p. The mRNA-binding protein She2p can bind to artificial and protein-free liposomes depending on their curvature with a preference to a diameter of 30 nm comparable to the diameter of ER tubules in yeast. Because of the fact that the binding of She2p to membranes is saturable, She2p has an unexpected membrane binding property and thus is a likely candidate for the association of specific mRNAs to ER tubules.

She2p is therefore not only a protein that binds mRNA in the nucleus and thus initiates the mRNA transport mechanism but is also able to bind to liposomes and therefore can also be characterized as a lipid-binding protein that recognizes membrane curvature. So She2p is an ideal coordinator of mRNA transport and ER tubules.

7 References

- Aronov S., Gelin-Licht R., Zipor G., Haim L., Safran E., Gerst J.E. (2007). mRNAs encoding polarity and exocytosis factors are cotransported with the cortical endoplasmic reticulum to the incipient bud in *Saccharomyces cerevisiae*. *Molecular and Cellular Biology* 27: 3441-3455.
- Babour A., Bicknell A.A., Tourtellotte J. and Niwa M. (2010). A Surveillance Pathway Monitors the Fitness of the Endoplasmic Reticulum to Control Its Inheritance. *Cell*, Volume 142, Issue 2, 256-269, 08.
- Barrowman J., Sacher M., Ferro-Novick S. (2000). TRAPP stably associates with the Golgi and is required for vesicle docking. *The EMBO Journal* 19: 862-869.
- Bashirullah A., Cooperstock R.L., and Lipshitz H.D. (1998). RNA localization in development. *Annu. Rev. Biochem.* 67, 335–394.
- Baumann O. and Walz B. (2001). Endoplasmic reticulum of animal cells and its organization into structural and functional domains. *Int Rev Cytol*, 205, 149-214.
- Beach D.L., Salmon E.D., & Bloom K. (1999). Localization and anchoring of mRNA in budding yeast. *Curr Biol*, 9(11), 569-578.
- Bender A., Pringle J.R. (1989). Multicopy suppression of the *cdc24* budding defect in yeast by *CDC42* and three newly identified genes including the ras-related gene *RSR1*. *Proc. Natl. Acad. Sci. USA* 89:9976–80.
- Bertrand E., Chartrand P., Schaefer M., Shenoy S.M., Singer R.H., Long R.M. (1998). Localization of *ASH1* mRNA particles in living yeast. *Mol Cell* 2:437–445.
- Besse F., Ephrussi A. (2008). Translational control of localized mRNAs: restricting protein synthesis in space and time. *Nat Rev Mol Cell Biol* 9: 971-980.
- Bobola N., Jansen R.P., Shin T.H., Nasmyth K. (1996). Asymmetric accumulation of Ash1p in postanaphase nuclei depends on a myosin and restricts yeast mating-type switching to mother cells. *Cell* 84: 699-709.
- Böhl F., Kruse C., Frank A., Ferring D., & Jansen R. P. (2000). She2p, a novel RNA-binding protein tethers *ASH1* mRNA to the Myo4p myosin motor via She3p. *Embo J*,19(20), 5514-5524.
- Brands A. and Ho T.H. (2002). Function of a plant stress-induced gene, HVA22. Synthetic enhancement screen with its yeast homolog reveals its role in vesicular traffic. *Plant Physiol* 130(3):1121-31.
- Buvelot Frei S., Rahl P.B., Nussbaum M., Briggs B.J., Calero M., Janeczko S., Regan A.D., Chen C.Z., Barral Y., Whittaker G.R., and Collins R.N. (2006). Bioinformatic and comparative localization of rab proteins reveals functional insights into the uncharacterized GTPases Ypt10p and Ypt11p. *Mol. Cell. Biol.* 26:7299–7317.
- Calero M. and Collins R.N. (2002). *Saccharomyces cerevisiae* Pra1p/Yip3p interacts with Yip1p and Rab proteins. *Biochem Biophys Res Commun* 290(2):676-81.
- Calero M., Whittaker G.R., Collins R.N. (2001). Yop1p, the yeast homolog of the polyposis locus protein 1, interacts with Yip1p and negatively regulates cell growth. *J Biol Chem* 276(15):12100-12.
- Catlett N.L., and Weisman L.S. (2000). Divide and multiple: organelle partitioning in yeast. *Curr. Opin. Cell Biol.* 12:509–515.
- Chabanon H., Mickleburgh I., and Hesketh J. (2004). Zipcodes and postage stamps: mRNA localisation signals and their trans-acting binding proteins. *Brief Funct Genomic Proteomic*, 3(3), 240-256.
- Chant J.(1999). Cell polarity in yeast. *Annu. Rev. Cell Dev. Biol.* 15:365–391.
- Chant J., Herskowitz I. (1991). Genetic control of bud site selection in yeast by a set of gene products that constitute a morphogenetic pathway *Cell* 65:1213-24.
- Chartrand P., X.-H. Meng R. H. Singer and Long R.M. (1999). Structural elements required for the localization of *ASH1* mRNA and of a green fluorescent protein reporter particle *in vivo*. *Curr. Biol.* 9:333–336.
- Chartrand P., Singer R.H., Long R.M. (2001). RNP localization and transport in yeast. *Annu Rev Cell Dev Biol* 17: 297-310.

References

- Chen D. C., Yang B. C. and Kuo T. T. (1992). One-step transformation of yeast in stationary phase. *Curr Genet*, 21(1), 83-84.
- Chung S., and Takizawa P.A. (2010). Multiple Myo4 motors enhance *ASH1* mRNA transport in *Saccharomyces cerevisiae*. *J. Cell Biol.* 189:755–767.
- Colomina N., Ferrezuelo F., Wang H., Aldea M., Garí E. (2008). Whi3, a developmental regulator of budding yeast, binds a large set of mRNAs functionally related to the endoplasmic reticulum. *J Biol Chem* 283: 28670-28679.
- Cooper G.M. (2000). *The Cell - A Molecular Approach*. 2nd ed . Sunderland (MA): Sinauer Associates, Inc. 2000
- Cui X.A., Zhang H., Palazzo A.F. (2012). p180 Promotes the Ribosome-Independent Localization of a Subset of mRNA to the Endoplasmic Reticulum. *PLoS Biology*, Volume 10, Issue 5, e1001336.
- Darzacq, X., Powrie, E., Gu, W., Singer, R. H., & Zenklusen, D. (2003). RNA asymmetric distribution and daughter/mother differentiation in yeast. *Curr Opin Microbiol*, 6(6),614-620.
- De Craene J.O., Coleman J., Estrada de Martin P., Pypaert M., Anderson S., Yates J.R. , Ferro-Novick S., and Novick P. (2006). Rtn1p is involved in structuring the cortical ER. *Mol. Biol. Cell.* 17:3009–3020.
- Deshler J.O., Highett M.I., Schnapp B.J. (1997). Localization of *Xenopus Vg1* mRNA by Vera protein and the endoplasmic reticulum. *Science* 276: 1128-1131.
- DeRosier, D.J. and L.G. Tilney. (2000). F-actin bundles are derivatives of microvilli: what does this tell us about how bundles might form? *J. Cell Biol.* 148:1-6.
- Diekmann H., Klinger M., Oertle T., Heinz D., Pogoda H.M., Schwab M.E., Stuermer C.A. (2005). Analysis of the reticulon gene family demonstrates the absence of the neurite growth inhibitor Nogo-A in fish. *Mol Biol Evol*, 22:1635-1648.
- Du T.-G., Jellbauer S., Müller M., Schmid M., Niessing D., Jansen R.-P. (2008). Nuclear transit of the RNA-binding protein She2 is required for translational control of localized *ASH1* mRNA. *EMBO Rep* 9: 781-787.
- Du Y., Ferro-Novick S., Novick P. (2004). Dynamics and inheritance of the endoplasmic reticulum. *Journal of Cell Science* 117: 2871-2878.
- Du Y., Pypaert M., Novick P., and Ferro-Novick S. (2001). Aux1p/Swa2p is required for cortical endoplasmic reticulum inheritance in *Saccharomyces cerevisiae*. *Mol. Biol. Cell.* 12:2614–2628.
- Du Y., Walker L., Novick P., and Ferro-Novick S. (2006). Ptc1p regulates cortical ER inheritance via Sit2p. *EMBO J.* 25:4413–4422.
- Elson S.L., Noble S.M., Solis N.V., Filler S.G., Johnson A.D. (2009). An RNA Transport System in *Candida albicans* Regulates Hyphal Morphology and Invasive Growth. *PLOS genetics*, Volume 5, Issue 9, e1000664.
- Entian K.D. *et al.* (1999). Functional analysis of 150 deletion mutants in *Saccharomyces cerevisiae* by a systematic approach. *Mol Gen Genet* 262(4-5):683-702.
- Estrada de Martin P., Du Y., Novick P., and Ferro-Novick S. (2005). Ice2p is important for the distribution and structure of the cortical ER network in *Saccharomyces cerevisiae*. *J. Cell Sci.* 118:65–77.
- Estrada de Martin P., Novick P., Ferro-Novick S. (2005). The organization, structure, and inheritance of the ER in higher and lower eukaryotes. *Biochem Cell Biol*, 83(6), 752-761.
- Estrada P., Kim J., Coleman J., Walker L., Dunn B., Takizawa P., Novick,P. and Ferro-Novick S. (2003). Myo4p and She3p are required for cortical ER inheritance in *Saccharomyces cerevisiae*. *J. Cell Biol.* 163, 1255–1266.
- Fagarasanu A. and Rachubinski R. A. (2007). Orchestrating organelle inheritance in *Saccharomyces cerevisiae*. *Curr Opin Microbiol*, 10(6), 528-538.
- Fehrenbacher K.L., Davis D., Wu M., Boldogh I., and Pon L.A. (2002). Endoplasmic reticulum dynamics, inheritance, and cytoskeletal interactions in budding yeast. *Mol. Biol. Cell.* 13:854–865.
- Feng D., Zhao X., Soromani C., Toikkanen J., Römisch K., Vembar S.S., Brodsky J.L., Keränen S., Jääntti J. (2007). The transmembrane domain is sufficient for Sbh1p function, its association with the Sec61 complex, and interaction with Rtn1p. *J Biol Chem* 282(42):30618-28.

- Fischer M.A., Temmerman K., Ercan E., Nickel, W. and Seedorf M. (2009). Binding of the plasma membrane lipids recruits the yeast integral membrane protein Ist2 to the cortical ER. *Traffic*, 10, 1084-1097.
- Flick J.S. and Johnston M. (1990). Two systems of glucose repression of the GAL1 promoter in *Saccharomyces cerevisiae*. *Mol Cell Biol*. 1990 September; 10(9): 4757-4769.
- Frey S., Pool M., Seedorf M. (2001) .Scp160p, an RNA-binding, polysome-associated protein, localizes to the endoplasmic reticulum of *Saccharomyces cerevisiae* in a microtubule-dependent manner. *J Biol Chem* 276: 15905-15912.
- Fujita A., Oka C., Arikawa Y., Katagai T., Tonouchi A., Kuhara S., Misumi Y. (1994). A yeast gene necessary for bud-site selection encodes a protein similar to insulin-degrading enzymes. *Nature* 372:567-70.
- Gall W.E., Higginbotham M.A., Chen C.-Y., Ingram M.F., Cyr D.M., Graham T.R. (2000). The auxilin-like phosphoprotein Swa2p is required for clathrin function in yeast. *Curr Bio*, 10:1349-1358.
- Geng J., Shin M.E., Gilbert P.M., Collins R.N., Burd C.G. (2005). *Saccharomyces cerevisiae* Rab-GDI displacement factor ortholog Yip3p forms distinct complexes with the Ypt1 Rab GTPase and the reticulon Rtn1p. *Eukaryot Cell* 4(7):1166-74.
- Giaever G. *et al.* (2002). Functional profiling of the *Saccharomyces cerevisiae* genome. *Nature* 418(6896):387-91.
- Gietz R.D., Sugino A. (1988). New yeast-*Escherichia coli* shuttle vectors constructed with *in vitro* mutagenized yeast genes lacking six-base pair restriction sites. *Gene* 74: 527-534.
- Gonsalvez G.B., Lehmann K.A., Ho D.K., Stanitsa E.S., Williamson J.R., Long R.M. (2003). RNA-protein interactions promote asymmetric sorting of the ASH1 mRNA ribonucleoprotein complex. *RNA*, 9(11):1383-99.
- Gonsalvez G.B., Little J.L., Long R.M. (2004). ASH1 mRNA anchoring requires reorganization of the Myo4p-She3p-She2p transport complex. *J Biol Chem* 279:46286-46294.
- Gonsalvez G.B., Urbinati C.R., & Long R.M. (2005). RNA localization in yeast: moving towards a mechanism. *Biol Cell*, 97(1), 75-86.
- Goodman A., Goode B.L., Matsudaira P. and Fink G.R. (2003). The *Saccharomyces cerevisiae* calponin/transgelin homolog Scp1 functions with fimbrin to regulate stability and organization of the actin cytoskeleton. *Mol Biol Cell* 14(7):2617-29.
- Green R., Lesage G., Sdicu A.M., Ménard P., Bussey H. (2003). A synthetic analysis of the *Saccharomyces cerevisiae* stress sensor Mid2p, and identification of a Mid2p-interacting protein, Zeo1p, that modulates the PKC1-MPK1 cell integrity pathway. *Microbiology* 149(Pt 9):2487-99.
- Gu W., Deng Y., Zenklusen D., Singer R.H. (2004). A new yeast PUF family protein, Puf6p, represses ASH1 mRNA translation and is required for its localization. *Genes & Development* 18: 1452-1465.
- Gulli M.P., Peter M. (2001). Temporal and spatial regulation of Rho-type guanine-nucleotide exchange factors: the yeast perspective. *Genes Dev.*, 15 pp. 365-379.
- Hagen I., Ecker M., Lagorce A., Francois J.M., Sestak S., Rachel R., Grossmann G., Hauser N.C., Hoheisel J.D., Tanner W., Strahl S. (2004). Sed1p and Srl1p are required to compensate for cell wall instability in *Saccharomyces cerevisiae* mutants defective in multiple GPI-anchored mannoproteins. *Mol Microbiol* 52(5):1413-25.
- Haim L. and Gerst J.E. (2009). m-TAG: a PCR-based genomic integration method to visualize the localization of specific endogenous mRNAs *in vivo* in yeast. *Nature Protocols* 4, - 1274 - 1284.
- Halme, A., Michelitch M., Mitchell E.L., and Chant J. (1996). Bud10p directs axial cell polarization in budding yeast and resembles a transmembrane receptor. *Curr. Biol.* 6: 570-579.
- He B., Guo W. (2009). The exocyst complex in polarized exocytosis. *Current Opinion in Cell Biology* 21: 537-542.
- Heckman K.L., Pease L.R. (2007). Gene splicing and mutagenesis by PCR-driven overlap extension. *Nat Protoc* 2: 924-932.
- Hennessy F., Nicoll W.S., Zimmermann R., Cheetham M.E., Blatch G.L. (2005). Not all J domains are created equal: implications for the specificity of Hsp40-Hsp70 interactions. *Protein Sci* 14:1697-1709.

- Heuck A., Du T.G., Jellbauer S., Richter K., Kruse C., Jaklin S., Müller M., Buchner J., Jansen R.P., Niessing D. (2007). Monomeric myosin V uses two binding regions for the assembly of stable translocation complexes. *Proc Natl Acad Sci U S A*, 104(50), 19778-19783.
- Heuck A., Fetka I., Brewer D.N., Hüls D., Munson M., Jansen R.-P., Niessing D. (2010). The structure of the Myo4p globular tail and its function in *ASH1* mRNA localization. *The Journal of Cell Biology* 189: 497-510.
- Hodges A.R., Kremontsova E.B., Trybus K.M. (2008). She3p binds to the rod of yeast myosin V and prevents it from dimerizing, forming a single-headed motor complex. *J Biol Chem* 283: 6906-6914.
- Holstein S.E., Ungewickell H., and Ungewickell E. (1996). Mechanism of clathrin basket dissociation: separate functions of protein domains of the DnaJ homologue auxilin. *J. Cell Biol.* 135, 925–937.
- Hu J., Shibata Y., Voss C., Shemesh T., Li Z., Coughlin M., Kozlov M.M., Rapoport T.A., Prinz W.A. (2008). Membrane proteins of the endoplasmic reticulum induce high-curvature tubules. *Science* 319: 1247- 1250.
- Hu J., Shibata Y., Zhu P.P., Voss C., Rismanchi N., Prinz W.A., Rapoport T.A. and Blackstone C. (2009). A class of dynamin-like GTPases involved in the generation of the tubular ER network. *Cell* 138(3):549-61.
- Huh W.K., Falvo J.V., Gerke L.C., Carroll A.S., Howson R.W., Weissman J.S., O'Shea E.K. (2003). Global analysis of protein localization in budding yeast. *Nature* 425(6959):686-91.
- Imataka H., Gradi A. and Sonenberg N. (1998). A newly identified N-terminal amino acid sequence of human eIF4G binds poly(A)-binding protein and functions in poly(A)-dependent translation. *EMBO J.* 17: 7480–7489.
- Imazu H. and Sakurai H. (2005). *Saccharomyces cerevisiae* heat shock transcription factor regulates cell wall remodeling in response to heat shock. *Eukaryot Cell* 4(6):1050-6.
- Irie K., Tadauchi T., Takizawa P.A., Vale R.D., Matsumoto K., Herskowitz I. (2002). The Khd1 protein, which has three KH RNA-binding motifs, is required for proper localization of *ASH1* mRNA in yeast. *The EMBO Journal* 21: 1158-1167.
- Jackson R.J. (1993). Cytoplasmic: regulation of mRNA function: the importance of the 3' untranslated region. *Cell* 1993, 74;9-14.
- Jackson C.L. and Kepes F. (1994). BFR1, a multicopy suppressor of brefeldin A-induced lethality, is implicated in secretion and nuclear segregation in *Saccharomyces cerevisiae*. *Genetics* 137(2):423-37.
- Jambhekar A, Derisi J.L. (2007). Cis-acting determinants of asymmetric, cytoplasmic RNA transport. *RNA* (5):625-42.
- Janke C., Magiera M.M., Rathfelder N., Taxis C., Reber S., Maekawa H., Moreno-Borchart A., Doenges G., Schwob E., Schiebel E., Knop M. (2004). A versatile toolbox for PCR-based tagging of yeast genes: new fluorescent proteins, more markers and promoter substitution cassettes. *Yeast* 21: 947-962.
- Jansen R.P., Dowzer C., Michaelis C., Galova M., & Nasmyth K. (1996). Mother cellspecific HO expression in budding yeast depends on the unconventional myosin myo4p and other cytoplasmic proteins. *Cell*, 84(5), 687-697.
- Ji X., Zhang P., Armstrong R. N. and Gilliland G. L. (1992). The three-dimensional structure of a glutathione S-transferase from the mu gene class. Structural analysis of the binary complex of isoenzyme 3-3 and glutathione at 2.2-Å resolution. *Biochemistry*, 31(42), 10169-10184.
- Jüschke C., Ferring D., Jansen R.P., Seedorf M. (2004). A novel transport pathway for a yeast plasma membrane protein encoded by a localized mRNA. *Current Biology* 14: 406-411.
- Kagiwada S., Hosaka K., Murata M., Nikawa J. and Takatsuki A. (1998). The *Saccharomyces cerevisiae* SCS2 gene product, a homolog of a synaptobrevin-associated protein, is an integral membrane protein of the endoplasmic reticulum and is required for inositol metabolism. *J Bacteriol* 180(7):1700-8.
- Kelley W.L. (1998). The J-domain family and the recruitment of chaperone power. *Trends Biochem. Sci.* 23, 222–227.
- King M. L., Messitt T. J. and Mowry K. L. (2005). Putting RNAs in the right place at the right time: RNA localization in the frog oocyte. *Biol Cell*, 97(1), 19-33.

- Knop M., Siegers K., Pereira G., Zachariae W., Winsor B., Nasmyth K. (1999). Epitope tagging of yeast genes using a PCR-based strategy: more tags and improved practical routines. *Yeast*, 15(10B), 963-972.
- Kraut-Cohen J., Gerst J.E. (2010). Addressing mRNAs to the ER: cis sequences act up. *Trends Biochem Sci*; 35(8):459-69.
- Krementsova E.B., Hodges A.R., Bookwalter C.S., Sladewski T.E., Travaglia M., Sweeney H.L., Trybus K.M. (2011). Two single-headed myosin V motors bound to a tetrameric adapter protein form a processive complex. *J Cell Biol.*, 195(4):631-41.
- Laemmli U.K., Molbert E., Showe M., and Kelenberger E. (1970). Form-determining function of genes required for the assembly of the head of bacteriophage T4. *J. Mol. Biol.* 49: 99-113.
- Lang B.D., Am L., Black-Brewster H.D., Fridovich-Keil J.L. (2001). The brefeldin A resistance protein Bfr1p is a component of polyribosome-associated mRNP complexes in yeast. *Nucleic Acids Research* 29: 2567-2574.
- Lange S., Katayama Y., Schmid M., Burkacky O., Bräuchle C., Lamb D.C., and Jansen R.-P. (2008). Simultaneous transport of different localized mRNA species revealed by live-cell imaging. *Traffic* 9, 1256-1267.1.2.1.
- Lemmon M. A. (2008). Membrane recognition by phospholipid-binding domains. *Nat Rev Mol Cell Biol*, 9(2), 99-111.
- Leon S., Erpapazoglou Z., Haguenaer-Tsapiris R. (2008). Ear1p and ssh4p are new adaptors of the ubiquitin ligase rsp5p for cargo ubiquitylation and sorting at multivesicular bodies. *Mol Biol Cell* 19(6):2379-88.
- Lerner R.S., Nicchitta C.V. (2006). mRNA translation is compartmentalized to the endoplasmic reticulum following physiological inhibition of cap-dependent translation. *RNA* 12: 775-789.
- Levin D.E. (2005). Cell Wall Integrity Signaling in *Saccharomyces cerevisiae*. *Microbiol Mol Biol Rev.*, 69(2): 262–291.
- Li X., Du Y., Siegel S., Ferro-Novick S., Novick P. (2010). Activation of the mitogen-activated protein kinase, Slt2p, at bud tips blocks a late stage of endoplasmic reticulum inheritance in *Saccharomyces cerevisiae*. *Molecular Biology of the Cell* 21: 1772-1782.
- Li Z., Lee I., Moradi E., Hung N.J., Johnson A.W., Marcotte E.M. (2009). Rational extension of the ribosome biogenesis pathway using network-guided genetics. *PLoS Biol* 7(10):e1000213.
- Lodisch, H., Berk, A., Zipursky, S.L., Matsudaira, P., Baltimore, D., Darnell J. (2000). *Molecular Cell Biology*, 4th edition (New York, W.H: Freeman and Company)
- Loewen C.J.R., Young B.P., Tavassoli S., Levine T.P. (2007). Inheritance of cortical ER in yeast is required for normal septin organization. *JCB* vol. 179 no. 3 467-483.
- Loewen C.J. and Levine T.P. (2005.) A highly conserved binding site in vesicle-associated membrane protein-associated protein (VAP) for the FFAT motif of lipid-binding proteins. *J Biol Chem* 280(14):14097-104.
- Long R.M., Gonzales I., Singer R., Nasmyth K., and Jansen R.-P. (1997). Mating type switching in yeast controlled by asymmetric localization of *ASH1* mRNA. *Science* 277: 383-387.
- Long R.M., Gu W., Lorimer E., Singer R. H., & Chartrand P. (2000). She2p is a novel RNA-binding protein that recruits the Myo4p-She3p complex to *ASH1* mRNA. *Embo J*, 19(23), 6592-6601.
- Long R.M., Gu W., Meng X., Gonsalvez G., Singer R.H., Chartrand P. (2001). An exclusively nuclear RNA-binding protein affects asymmetric localization of *ASH1* mRNA and *Ash1p* in yeast. *The Journal of Cell Biology* 153: 307-318
- Löoke M., Kristjuhan K. and Kristjuhan A. (2011). Extraction of genomic DNA from yeasts for PCR-based applications. *BioTechniques* 50:325-328
- Lowe M. and Barr F. A. (2007). Inheritance and biogenesis of organelles in the secretory pathway. *Nat Rev Mol Cell Biol*, 8(6), 429-439.
- Madsen K.L., Bhatia V.K., Gether U., Stamou D. (2010). BAR domains, amphipathic helices and membrane-anchored proteins use the same mechanism to sense membrane curvature. *FEBS Lett* 584:1848-1855.
- Maeda T., Tsai A.Y., and Saito H. (1993). Mutations in a protein tyrosine phosphatase gene (PTP2) and a protein serine/threonine phosphatase gene (PTC1) cause a synthetic growth defect in *Saccharomyces cerevisiae*. *Mol Cell Biol* 13(9):5408-17.

References

- Mao K., Wang K., Zhao M., Xu T., Klionsky D.J. (2011). Two MAPK-signaling pathways are required for mitophagy in *Saccharomyces cerevisiae*. *J Cell Biol* 193(4):755-67.
- Martin K.C., Ephrussi A. (2009). mRNA localization: gene expression in the spatial dimension. *Cell* 136: 719-730.
- Moreira E.F., Jaworski C.J., Rodriguez I.R. (1999). Cloning of a novel member of the reticulon gene family (RTN3): gene structure and chromosomal localization to 11q13. *Genomics*, 58:73-81.
- Mowry K. L. and Cote C.A. (1999). RNA sorting in *Xenopus* oocytes and embryos. *Faseb J*, 13(3), 435-445.
- Müller M., Heuck A., Niessing D. (2007). Directional mRNA transport in eukaryotes: lessons from yeast. *Cell Mol Life Sci.*, 64(2):171-80.
- Müller M., Heym R.G., Mayer A., Kramer K., Schmid M., Cramer P., Urlaub H., Jansen R.P., Niessing D. (2011). A Cytoplasmic Complex Mediates Specific mRNA Recognition and Localization in Yeast. *Plos Biology*, Volume 9, Issue 4, e1000611.
- Müller M., Richter K., Heuck A., Kremmer E., Buchner J., Jansen R.P., Niessing D. (2009). Formation of She2p tetramers is required for mRNA binding, mRNP assembly, and localization. *RNA* 15: 2002-2012.
- Münchow S., Sauter C., Jansen R.P. (1999). Association of the class V myosin Myo4p with a localised messenger RNA in budding yeast depends on She proteins. *J Cell Sci* 112 (Pt 10):1511-8.
- Munro S. (2004). Organelle identity and the organization of membrane traffic. *Nat Cell Biol.* 2004 Jun;6(6):469-72.
- Nanduri J. and Tartakoff A.M. (2001). The arrest of secretion response in yeast: signaling from the secretory path to the nucleus via Wsc proteins and Pkc1p. *Mol Cell* 8(2):281-9.
- Nash R.S., Volpe T. and Futcher B. (2001). Isolation and characterization of WHI3, a size-control gene of *Saccharomyces cerevisiae*. *Genetics* 157(4):1469-80.
- Ng D.T. (2001). Interorganellar signal transduction: the arrest of secretion response. *Dev Cell* 1(3):319-20.
- Niessing D., Hüttelmaier S., Zenklusen D., Singer R.H., Burley S.K. (2004). She2p is a novel RNA binding protein with a basic helical hairpin motif. *Cell* 119: 491-502.
- Nziengui H., Bouhidel K., Pillon D., Der C., Marty F., Schoefs B. (2007). Reticulon- like proteins in *Arabidopsis thaliana*: structural organization and ER localization. *FEBS Lett*, 581:3356-3362.
- Oeffinger M., Wei K.E., Rogers R., DeGrasse J.A., Chait B.T., Aitchison J.D., Rout M.P. (2007). Comprehensive analysis of diverse ribonucleoprotein complexes. *Nat Meth* 4: 951-956.
- Oertle T., Klinger M., Stuermer C.A., Schwab M.E. (2003). A reticular rhapsody: phylogenic evolution and nomenclature of the RTN/Nogo gene family. *FASEB J* 17(10):1238-47.
- Olivier C., Poirier G., Gendron P., Boisgontier A., Major, F., and Chartrand P. (2005). Identification of a conserved RNA motif essential for She2p recognition and mRNA localization to the yeast bud. *Mol Cell Biol*, 25(11), 4752-4766.
- Otte S., Belden W.J., Heidtman M., Liu J., Jensen O.N., Barlowe C. (2001). Erv41p and Erv46p: new components of COPII vesicles involved in transport between the ER and Golgi complex. *J Cell Biol* 152(3):503-18.
- Paquin, N., & Chartrand, P. (2008). Local regulation of mRNA translation: new insights from the bud. *Trends Cell Biol*, 18(3), 105-111.
- Paquin N., Ménade M., Poirier G., Donato D., Drouet E., Chartrand P. (2007). Local activation of yeast ASH1 mRNA translation through phosphorylation of Khd1p by the casein kinase Yck1p. *Mol Cell* 26:795-809.
- Pelham H.R., Hardwick K.G., Lewis M.J. (1988). Sorting of soluble ER proteins in yeast. *The EMBO Journal* vol.7 no.6 pp. 1 757 – 1762.
- Philip B. and Levin D.E. (2001). Wsc1 and Mid2 are cell surface sensors for cell wall integrity signaling that act through Rom2, a guanine nucleotide exchange factor for Rho1. *Mol Cell Biol* 21(1):271-80.
- Pishvaee B., Costaguta G., Yeung B.G., Ryazantsev S., Greener T., Greene L.E., Eisenberg E., McCaffery J.M., Payne G.S. (2000). A yeast DNA J protein required for uncoating of clathrin-coated vesicles *in vivo*. *Nat Cell Biol* 2(12):958-63.

References

- Preuss D., Mulholland J., Franzusoff A., Segev N., and Botstein D. (1992). Characterization of the *Saccharomyces* Golgi complex through the cell cycle by immunoelectron microscopy. *Mol. Biol. Cell.* 3:789–803.
- Prinz W.A., Grzyb L., Veenhuis M., Kahana J.A., Silver P.A., and Rapoport T.A. (2000). Mutants affecting the structure of the cortical endoplasmic reticulum in *Saccharomyces cerevisiae*. *J. Cell Biol.* 150:461–474.
- Pruyne D., Bretscher A. (2000). Polarization of cell growth in yeast. I. Establishment and maintenance of polarity states. *J. Cell Sci.* 113:365–375.
- Pruyne D., Legesse-Miller A., Gao L., Dong Y., Bretscher A. (2004). Mechanisms of polarized growth and organelle segregation in yeast. *Annu Rev Cell Dev Biol* 20:559-91.
- Pyhtila B., Zheng T., Lager P.J., Keene J.D., Reedy M.C., Nicchitta C.V. (2008). Signal sequence- and translation-independent mRNA localization to the endoplasmic reticulum. *RNA* 14: 445-453.
- Reinke C.A., Kozik P. and Glick B.S. (2004). Golgi inheritance in small buds of *Saccharomyces cerevisiae* is linked to endoplasmic reticulum inheritance. *Proc. Natl. Acad. Sci. USA.* 101:18018–18023.
- Roemer T., Madden K., Chang J., and Snyder M. (1996). Selection of axial growth sites in yeast requires Axl2p, a novel plasma membrane glycoprotein. *Genes & Dev.* 10: 777–793.
- Romisch K. (1999). Surfing the Sec61 channel: bidirectional protein translocation across the ER membrane. *J Cell Sci* 112 (Pt 23):4185-91.
- Rose M.D., Misra L.M., and Vogel J.P. (1989). KAR2, a karyogamy gene, is the yeast homolog of the mammalian BiP/GRP78 gene. *Cell.* 57:1211–1221.
- Sambrook J., and Russel D. W. (2001). *Molecular Cloning. A Laboratory Manual.* (3rd ed.). Cold Spring Harbor, New York: Cold Spring Harbor Laboratory Press.
- Schenk L., Meinel D.M., Strasser K., Gerber A.P. (2012). La-motif-dependent mRNA association with Sif1 promotes copper detoxification in yeast. *RNA* (3):449-61.
- Schiestl R.H. and Gietz R.D. (1989). High efficiency transformation of intact yeast cells using single stranded nucleic acids as a carrier. *Current Genetics* 16, 339-346.
- Schmid M., Jaedicke A., Du T.G., Jansen R.P. (2006). Coordination of endoplasmic reticulum and mRNA localization to the yeast bud. *Current Biology* 16: 1538-1543.
- Shan S.O., Walter P. (2005). Co-translational protein targeting by the signal recognition particle. *FEBS.Lett* 579: 921-926.
- Shav-Tal Y., & Singer R. H. (2005). RNA localization. *J Cell Sci*, 118(Pt 18), 4077-4081.
- Shen Z., Paquin N., Forget A., Chartrand P. (2009). Nuclear shuttling of She2p couples *ASH1* mRNA localization to its translational repression by recruiting Loc1p and Puf6p. *Mol Biol Cell* 20: 2265-2275.
- Shen Z., St-Denis A., Chartrand P. (2010). Cotranscriptional recruitment of She2p by RNA pol II elongation factor Spt4-Spt5/DSIF promotes mRNA localization to the yeast bud. *Genes Dev.*, 24(17):1914-26.
- Shepard K.A., Gerber A.P., Jambhekar A., Takizawa P.A., Brown P.O., Herschlag D., DeRisi J. L. and Vale R. D. (2003). Widespread cytoplasmic mRNA transport in yeast: identification of 22 bud-localized transcripts using DNA microarray analysis. *Proc Natl Acad Sci U S A* 100(20):11429-34.
- Shibata Y., Shemesh T., Prinz W.A., Palazzo A.F., Kozlov M.M., Rapoport T.A. (2010). Mechanisms Determining the Morphology of the Peripheral ER. *Cell* 143: 774-788.
- Takizawa, P.A., DeRisi, J. L., Wilhelm, J. E., & Vale, R. D. (2000). Plasma membrane compartmentalization in yeast by messenger RNA transport and a septin diffusion barrier. *Science*, 290(5490), 341-344.
- Takizawa P.A., Sil A., Swedlow J.R., Herskowitz I., & Vale R.D. (1997). Actin-dependent localization of an RNA encoding a cell-fate determinant in yeast. *Nature*, 389(6646),90-93.
- Terashima H., Fukuchi S., Nakai K., Arisawa M., Hamada K., Yabuki N., Kitada K. (2002). Sequence-based approach for identification of cell wall proteins in *Saccharomyces cerevisiae*. *Curr Genet* 40(5):311-6.
- TerBush D.R. and Novick P. (1995). Sec6, Sec8, and Sec15 are components of a multisubunit complex which localizes to small bud tips in *Saccharomyces cerevisiae*. *J Cell Biol* 130(2):299-312.

- Tanida I., Takita Y., Hasegawa A., Ohya Y., Anraku Y. (1996). Yeast Cls2p/Csg2p localized on the endoplasmic reticulum membrane regulates a non-exchangeable intracellular Ca²⁺ pool cooperatively with calcineurin. *FEBS Lett* 379(1):38-42.
- Toikkanen J.H., Miller K.J., Söderlund H., Jääntti J., Keränen S. (2003). The beta subunit of the Sec61p endoplasmic reticulum translocon interacts with the exocyst complex in *Saccharomyces cerevisiae*. *J Biol Chem* 278(23):20946-53.
- Ungewickell E., Ungewickell H., Holstein S.E., Lindner R., Prasad K., Barouch W., Martin B., Greene L. E., Eisenberg E. (1995). Role of auxilin in uncoating clathrin-coated vesicles. *Nature* 378, 632-635.
- Verna J., Lodder A., Lee K., Vagts A. and Ballester R. (1997). A family of genes required for maintenance of cell wall integrity and for the stress response in *Saccharomyces cerevisiae*. *Proc Natl Acad Sci U S A* 94(25):13804-9.
- Voeltz G.K. and Prinz W.A. (2007). Sheets, ribbons and tubules - how organelles get their shape. *Nat Rev Mol Cell Biol*, 8(3), 258-264.
- Voeltz G.K., Prinz W.A., Shibata Y., Rist J.M., Rapoport T.A. (2006). A class of membrane proteins shaping the tubular endoplasmic reticulum. *Cell*, 124:573-586.
- Voeltz G. K., Rolls M. M. and Rapoport T. A. (2002). Structural organization of the endoplasmic reticulum. *EMBO Rep.* 3, 944-950.
- Wach A., Brachat A., Pöhlmann R., Philippsen P. (1994). New heterologous modules for classical or PCR-based gene disruptions in *Saccharomyces cerevisiae*. *Yeast* (Chichester, England) 10: 1793-1808.
- Wakefield S., Tear G. (2006). The *Drosophila* reticulon, Rtnl-1, has multiple differentially expressed isoforms that are associated with a sub-compartment of the endoplasmic reticulum. *Cell Mol Life Sci*, 63:2027-2038.
- Warmka J., Hanneman J., Lee J., Amin D., Ota I. (2001). Ptc1, a type 2C Ser/Thr phosphatase, inactivates the HOG pathway by dephosphorylating the mitogen-activated protein kinase Hog1. *Mol Cell Biol* 21(1):51-60.
- Weil T.T., Parton R., Davis I., and Gavis E.R. (2008). Changes in bicoid mRNA anchoring highlight conserved mechanisms during the oocyte-to-embryo transition. *Curr. Biol.* 18, 1055–1061.
- West M., Zurek N., Hoenger A., Voeltz G.K. (2011). A 3D analysis of yeast ER structure reveals how ER domains are organized by membrane curvature. *The Journal of Cell Biology* 193: 333-346.
- Wiederkehr A., De Craene J.O., Ferro-Novick S., and Novick P. (2004). Functional specialization within a vesicle tethering complex bypasses a subset of exocyst deletion mutants by Sec1p or Sec4p. *JCB* vol. 167 no. 5 875-887.
- Wiederkehr A., Du Y., Pypaert M., Ferro-Novick S., and Novick P. (2003). Sec3p is needed for the spatial regulation of secretion and for the inheritance of the cortical endoplasmic reticulum. *Mol. Biol. Cell.* 14:4770–4782.
- Wilmes G.M., Bergkessel M., Bandyopadhyay S., Shales M., Braberg H., Cagney G., Collins S.R., Whitworth G.B., Kress T.L., Weissman J.S., Ideker T., Guthrie C., Krogan N.J. (2008). A genetic interaction map of RNA-processing factors reveals links between Sem1/Dss1-containing complexes and mRNA export and splicing. *Mol Cell* 32(5):735-46.
- Wöllert T., Weiss D.G., Gerdes H.H., and Kuznetsov S.A. (2002). Activation of myosin V-based motility and F-actin-dependent network formation of endoplasmic reticulum during mitosis. *J. Cell Biol.* 159:571–577.
- Yang, H.C., and Pon L.A., (2002). Actin cable dynamics in budding yeast. *Proc. Natl. Acad. Sci. USA.* 99:751–756.
- Yang Y.S. and Strittmatter M. (2007). The reticulons: a family of proteins with diverse functions; *Genome Biology*, 8:234 doi:10.1186/gb-2007-8-12-234.
- Yisraeli J.K., Sokol S., and Melton D.A. (1990). A two-step model for the localization of maternal mRNA in *Xenopus oocytes*: involvement of microtubules and microfilaments in the translocation and anchoring of *Vg1* mRNA. *Development* 108, 289–298.
- Zahner J.E., Harkins H.A., and Pringle J.R. (1996). Genetic analysis of the bipolar pattern of bud site selection in the yeast *Saccharomyces cerevisiae*. *Mol. Cell. Biol.* 16: 1857–1870.

8 Abbreviations

2D/3D	two/three dimensional
aa	amino acid
Amp	ampicillin
APS	ammonium persulfate
ATP	adenosine triphosphate
β-ME	beta-mercaptoethanol
bp	base pair
°C	degree centigrade
CA	Chloramphenicol
<i>C. elegans</i>	<i>Caenorhabditis elegans</i>
CHX	Cycloheximide
CIP	calf intestine alkaline phosphatase
clonNAT	nourseothricin
C-terminal	carboxy terminal
Da	Dalton
DIC	Differential interference contrast
<i>D. melanogaster</i>	<i>Drosophila melanogaster</i>
DNA	deoxyribonucleic acid
DNase	deoxyribonuclease
dNTPs	deoxyribonucleosid triphosphate
<i>D. rerio</i>	<i>Danio rerio</i>
DsRed	<i>Discosoma sp.</i> red fluorescent protein
DTT	dithiothreitol
ECL	enhanced chemoluminiscence
EDTA	Ethylene Diamine Tetraacetic acid (EDTA)
e.g.	<i>exempli gratia</i> (Latin: for example)
EGTA	Ethylene Glycol Tetraacetic acid
ER	endoplasmic reticulum
<i>et al.</i>	<i>et alii</i> (Latin: and others)
5FOA	5-Fluoroorotic acid
FISH	fluorescent <i>in situ</i> hybridization
fwd	forward
g	gram
G418	geneticin
GAPs	GTPase activating proteins
GDI	guanine–nucleotide dissociation inhibitors
GEFs	guanine–nucleotide exchange factors
GFP	green fluorescent protein
GST	glutathione <i>S</i> -transferase
GTP	Guanosine-5'-triphosphate
h	hour
HA	hemagglutinin
HCl	Hydrochloric acid
His	Histidine
Hepes	4-(2-hydroxyethyl)-1-piperazineethanesulfonic acid
HO	endonuclease homothallic switching endonuclease
i.e.	<i>id est</i> (Latin: that is; this means)
IPTG	isopropyl-beta-D-thiogalactoside
K	kilo
KAN	Kanamycine
Kb	kilo basepairs
l	litre
LB	Luria Bertani

Abbreviations

LE	localization element
Leu	Leucine
LN2	liquid nitrogen
μ	micro
m	milli
M	molar
mA	milliampere
MAPK	mitogen-activated protein kinase
mCherry	red fluorophore
Met	Methionine
MgOAc ₂	Magnesium acetate
min	minutes
mRNA	messenger ribonucleic acid
ms	milliseconds
MS-CP	MS2 coat protein
MS2L	MS2 stem loops
n	nano
N	normal
NaCl	Sodium chloride
NE	nuclear envelope
NP-40	Nonidet P-40
nt	nucleotide
OD	optical density
oN	over night
ORF	open reading frame
P	p-value
PABP	poly(A)-binding protein
PAGE	polyacrylamide gelelectrophoresis
PBS	phosphate buffered saline
PCR	polymerase chain reaction
PEG	polyethylene glycol
pH	potential of hydrogen
PI	phosphatidylinositol
PMSF	phenylmethylsulfonyl fluorid
PS	phosphatidylserine
PVDF	polyvinylidene fluoride (membrane)
RBP	RNA binding protein
rev	reverse
RHD	Rel homology domain
RNA	ribonucleic acid
RNP	ribonucleoprotein
Rpm	revolutions per minute
RT	room temperature
SC	synthetic complete
SDS	sodium dodecyl sulfate
sec	second
SNAPs	synaptosomal-associated proteins
SNAREs	<i>N</i> -ethylmaleimide-sensitive-factor attachment receptors
TAE	Tris-acetate-EDTA
TCA	trichloroacetic acid
TE	Tris-EDTA
TEMED	Tetramethylethylenediamine
TEV	tobacco etch virus
TMD	Transmembrane domain
Tris	trishydroxymethylaminomethane

Abbreviations

Trp	Tryptophan
UTR	untranslated region
Ura	Uracil
UV	ultraviolet
V	volt
vs.	versus
WCE	whole cell extract
WT	wild type
w/v	weight per volume
<i>X. laevis</i>	<i>Xenopus laevis</i>
YEPD/YPD	yeast extract peptone with glucose
YEPG/YEP	yeast extract peptone with galactose
YRMs	yeast rough membranes

9 Acknowledgement

The data content of this present study was prepared in the working group of Prof. Dr. Ralf-Peter Jansen at the Interfaculty Institute of Biochemistry IFIB in Tübingen. At this point I want to thank all the people who have been involved in the success of this thesis and for the friendly and warm working atmosphere. First of all I would like to thank my supervisor Prof. Dr. Ralf-Peter Jansen for providing me this attractive and interesting topic, for the opportunity to be a part of his working group, the outstanding conditions for working scientifically and for giving me such excellent supervision. Additionally, I want to thank him for the possibility to present my work at conferences, his patience and for still having an open ear even when he had a lot on his plate-and this was, typically, always the case.

Further thanks to Prof. Dr. Doron Rapaport for being the second examiner of my thesis and his helpful and interesting advices and mentions during our shared lab meetings. A big thank you also goes to the whole Rapaport group for borrowing and donating antibodies.

Then I would like to thank my lab mates: Sylvia and Valerie for sharing first problems in getting the microscope and MS2-tagging strategy up and running, investigating better cloning strategies and yeast colony PCRs. Besides scientific work this great teamwork resulted in friendship which really enriches my life. Even if I am not that tall a special huge bear hug goes to Sylvia for talks about life in general, for together rolling eyes when the AxioSoftware acts crazy and of course for inviting me and Daniel to Barcelona every year-a great place to relax and getting other things in mind. Next I want to thank Hanna for her support in using the Odyssey and grinding device. Mrs. Pfeifer-Guglielmi I want to thank for her support and having a nice time during the gene expression practical course. Christian for paying attention on making lunch breaks when I was so busy I wasn't recognizing the time. Balaji for his interesting talks about Indian traditions and Orit for always being ready to listen, especially when gushing about Berlin, sharing a nice time during the gene-expression practical course, Wolf for having interesting talks about nearly everything even if they only started with a short question about lab methods and of course the possibility for sharing his post-it collection.

Acknowledgement

Ingrid, Ulrike, Ruth, Erika and Martina for preparing media, plates, cleaning up, oligo orders, midi preps and everything else to make the lab running. A special thank goes to Ingrid for her great Viennese recipes for desserts and cakes that I am now addicted to.

Claudia for organizing meetings and providing bureau material and finally a big thank to the whole Jansen group for having such a great time also besides scientific work especially the delicious BBQs.

I also want to thank the Dodt and Duszenko lab for being a contact in borrowing liquid nitrogen and ordering restriction enzymes.

Moreover the biggest thank goes to my parents by supporting me in every life decision, offering me so many opportunities and who made my education possible. Saskia, thanks for being the best sister in the world and for always putting a smile on my face. And of course I want to thank Daniel for his love, patience, for being such a great person and always supporting me even during the phase of writing this thesis.

10 Curriculum Vitae

Persönliche Daten:

Name: Julia Fundakowski
Diplom-Biologin
Geburtstag: 21.03.1983
Geburtsort: Karl-Marx-Stadt/Chemnitz
Nationalität: deutsch
Familienstand: ledig

Akademische Ausbildung:

Seit 03/2009 Promotion am Interfakultären Institut für Biochemie (IFIB) der Eberhard Karls Universität Tübingen

Thema: „Co-Transport of mRNA and ER in *Saccharomyces cerevisiae*”

06/2008-02/2009 Wissenschaftliche Mitarbeiterin am Universitätsklinikum Tübingen (AG Prof. Dr. Gerd Döring: Abteilung für Medizinische Mikrobiologie und Hygiene)

08/2008 Wissenschaftliche Mitarbeiterin an der UNIL Universität Lausanne (AG Prof. Dr. Dieter Haas)

03/2007-12/2007 Diplomarbeit an der Georg-August-Universität Göttingen (Prof. Dr. Wolfgang Liebl: Abteilung für Mikrobiologie)

10/2002-03/2008 Studium der Biologie (Diplom) an der Georg-August-Universität Göttingen

Schulbildung:

1993 – 2001 Samuel-von-Pufendorf-Gymnasium Flöha, Abschluss: Abitur

1989 – 1993 Grundschule Augustusburg (Sachsen)

11 Publication

Localization of a subset of yeast mRNAs depends on inheritance of endoplasmic reticulum.

Fundakowski J, Hermesh O, Jansen RP., Interfaculty Institute of Biochemistry, Eberhard-Karls-Universität Tübingen, 72076, Tübingen, Germany.

2012 Sep 20. doi: 10.1111/tra.12011. [Epub ahead of print]